Investigations on Diterpene Biosynthesis through Substrate and Protein Engineering

Kumulative Dissertation

zur

Erlangung Doktorgrades (Dr. rer. nat)

der

Mathematisch-Naturwissenschaftlichen Fakultät

der

Rheinischen Friedrich-Wilhelms-Universität Bonn

vorgelegt von

Heng Li

aus

Ping Yuan

Bonn, 2025

Angefertigt mit Genehmigung der Mathematisch-Naturwissenschaftlichen Fakultät der
Rheinischen Friedrich-Wilhelms-Universität Bonn

Gutachter /Betreuer: Prof. Dr. Jeroen S. Dickschat
Gutachter: Prof. Dr. Dick Menche
Tag der Promotion: 02.10.2025
Erscheinungsjahr: 2025

Acknowledgements

First of all, I am deeply grateful to Prof. Dr. Jeroen. Dickschat for his patient guidance, encouragement, and consistent support throughout my PhD study. He is a self-disciplined and hard-working scientist, from whom I learnt how to think thoroughly and how to act efficiently. I also appreciate the chance to work in AK dickschat group where I not only harvested fruitful research publications but also gained valuable knowledge. Jeroen, many thanks to you for being my supervisor, my life guider and my good friend. Time has truly flown by during these years of study. I will never forget the days when we had academic discussions on my running project, during which I learnt the importance of perseverance and focus. I will always remember our challenging cycling and hiking tours, during which I experienced the joy of pushing my limits. I will also cherish our party times in your home or during our trips, where I learnt a lot about wine, food, history from you.

I also want to thank Prof. Dr. Dirk Menche for taking the time to reading and evaluate my thesis. Thanks also to Prof. Dr. Robert Glaum and Prof. Dr. Maja Köhn for serving on my examination committee.

Many thanks to all my colleagues whom I spent most of my time. Especially I would like to say thank you to Dr. Zhiyang Quan for providing a lot of help at the beginning of my study. I would like to thank Dr. Lukas Lauterbach, Dr. Houchao Xu, Dr. Geng Li, Dr. Anuj Chhalodia, Dr. BinBin Gu, Dr. Anwei Hou, Dr. Linfu Liang, Dr. Zhiyong Yin, Kizerbo Taizoumbe, Alain Tumma, Dr. Georges Bellier Tabekoueng, Min Wang, Kexin Yang, Dr. Peng Zhao, Neran Reuber and Alina Oseguera Jaramillo for the times we shared in the laboratory.

I also express my gratitude to our collaboration partners: Prof. Dr. Bernd Goldfuss, Prof. Dr. Bernhard Hauer, Prof. Dr. Andreas Kirschning, Prof. Dr. Ming Ma, Prof. Dr. Michael Groll, and Prof. Dr. Robin Teufel.

In addition, I need to thank all the technical and analytical facilities at the chemical institutes, especially to the NMR department and to the MS department for measuring numerous samples efficiently.

Finally, I want to thank my parents and my wife for their big supports as always.

Preamble

This cumulative dissertation “The Investigations on Diterpene Biosynthesis through Substrate and Protein Engineering” contains 11 chapters. First of all, a general introduction to terpenes biosynthesis, terpene synthases, non-natural substrates and protein engineering is presented in Chapter 1. Chapters 2-8 list brief summaries of all publications in this thesis, and the corresponding publications are all attached in Appendices A-G. Chapter 9 provides a summary and outlook based on the projects I worked on.

Table of Contents

Chapter 1

1 Terpene biosynthesis

1.1 The history of terpenes in natural product chemistry

Natural products (NPs) represent a large family of diverse chemical entities, including primary and secondary metabolites from living organisms. The largest group of natural products are terpenes, also known as terpenoids or isoprenoids, which is made up by more than 80,000 structures identified[1]. The investigations on terpenes started in the 19th century. In 1832, Wöhler and Liebig made the first breakthrough on the analysis of vegetable oils where they discovered the aromatic origin of the bitter almonds. During that period, several nonaromatic oils such as orange-peel oils, turpentine oils and the oil from plants contain compounds that remained like liquids when the temperature is below room temperature, which were termed "terpenes"[2]. However, due to the difficulty of structure elucidations in the 19th century, certain compounds with the same structure were given different names, leading to an unclear situation in the terpene field. Later on, Wallach, the recipient of the Nobel Prize in Chemistry in 1910, entered into this field, and he found that many terpenes named differently were indeed identical in structure. In 1909, 12 different terpenes: pinene, limonene, terpinene, camphene, borneol, camphor, terpin, terpineol, cineole, pinol, dipentene and terpinolene were structurally clarified in Wallach's publication[3] "Die Terpene und Campher" where he also demonstrated the isoprene rule that all terpenes originate from the five-carbon isoprene units (**1**, Figure 1). This rule was further formulated by the chemist Leopold Ružička (he was honored with Nobel prize in 1939) in 1922[4]. According to the rule, terpenes possessing the basic sum formula $(C_5H_8)_n$ are divided into monoterpenes (two units), sesquiterpenes (three units), diterpenes (four units), sesterterpenes (five units), triterpenes (six uints), and polyterpenes (many units).

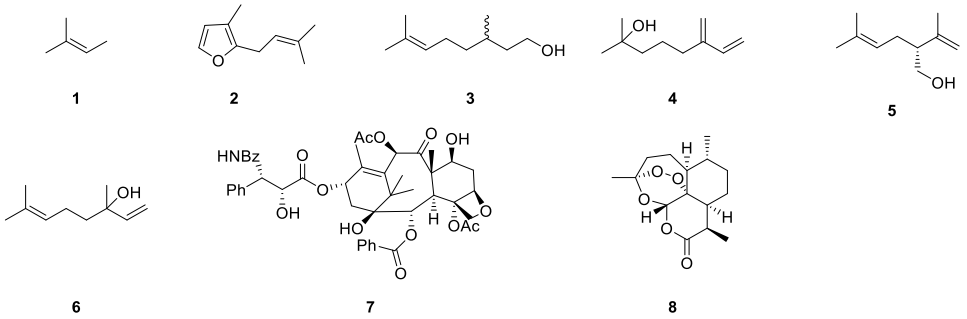

Figure 1. Structures of representative terpenes.

Historically, terpenes, such as rose furan (**2**), citronellol (**3**), myrcenol (**4**), lavandulol (**5**) and linalool (**6**, Figure 1), have widely been used in the perfume, fragrance and natural flavoring

industry due to their volatile nature and characteristic odor properties. Starting in the 1970s, terpenes are proven to have ecological roles in antagonistic or mutualistic interactions among organisms because of their function as toxins, repellents or attractants to other organisms[5]. For instance, the sesquiterpene (*E*)-β-farnesene (**7**, Figure 1) had been confirmed to be the principal attractive component of the volatiles that are released by the pine sawfly (*Diprion pini*) to attract the eulophid egg parasitoid *Chrysonotomyia ruforum* when it lays its eggs on pine twigs[6]. Apart from benefits to human daily life and ecology, some terpenes are also important drugs in the pharmaceutical area such as paclitaxel (**8**, Figure 1) used in cancer treatment[7] and artemisinin (**9**, Figure 1) applied to cure malaria[8].

1.2 Mevalonate pathway and non-mevalonate pathway

As indicated by the isoprene rule, terpenes share the same original biosynthetic pathway where two basic C_5 units, the electrophile dimethylallyl pyrophosphate (DMAPP) and the nucleophile isopentenyl pyrophosphate (IPP), are generated. Depending on the way of producing these two molecules, two distinct biosynthetic pathways are classified as mevalonate pathway (MVA pathway) and non-mevalonate pathway (MEP pathway, Scheme 1).

The MVA pathway is an essential metabolic pathway that exists in eukaryotes, archaea or some bacteria[9]. It starts from the condensation of two molecules of acetyl-CoA to yield acetoacetyl-CoA, which is catalyzed by acetyl-CoA thiolase. Subsequently, acetoacetyl-CoA is converted into 3-hydroxy-3-methylglutary-CoA (HMG-CoA) by an aldol addition catalyzed by HMG-CoA synthase, followed by a reduction with HMG-CoA reductase requiring the cofactor NADPH to result in (*R*)-mevalonic acid (mevalonate). At this stage with adenosine triphosphate (ATP) as the phosphate source, mevalonate undergoes two sequential phosphorylations catalyzed by mevalonate-5-kinase and phosphomevalonate kinase to reach mevalonate pyrophosphate. At the end, the product is decarboxylated to IPP by a corresponding decarboxylase, followed by the isomerization catalyzed by isopentenyl pyrophosphate isomerase (IDI) to yield DMAPP. In addition, an alternative pathway found in *Thermoplasma acidophilum*[10] can branche out from (*R*)-mevalonate to mevalonate-3,5-bisphosphate via two phosphorylations that are catalyzed by mevalonate-3-kinase and mevalonate-3-phosphate-5-kinase, respectively. The resulting 3,5-bisphosphate further proceeds with decarboxylation and phosphorylation to yield IPP (Scheme 1B). The third shunt pathway, which has been observed in some archaea, involves a single decarboxylation of mevalonate-5-phosphate to form isopentenyl phosphate (IP) which can subsequently be phosphorylated to yield isopentenyl diphosphate (IPP, Scheme 1C)[11]. Two types of IDI exist in nature and the isomerization step catalyzed by type I IDI has been studied

in depth since the 1970s, disclosing its stereochemical course[12]. Mechanistically, protonation on the *Re*-face at C2 of DMAPP initializes the isomerization to IPP, followed by a deprotonation from the (*E*)-methyl group. The reverse reaction starts from the protonation at C4 from the *Re*-face followed by an abstraction of the *pro-R* hydrogen at C2.

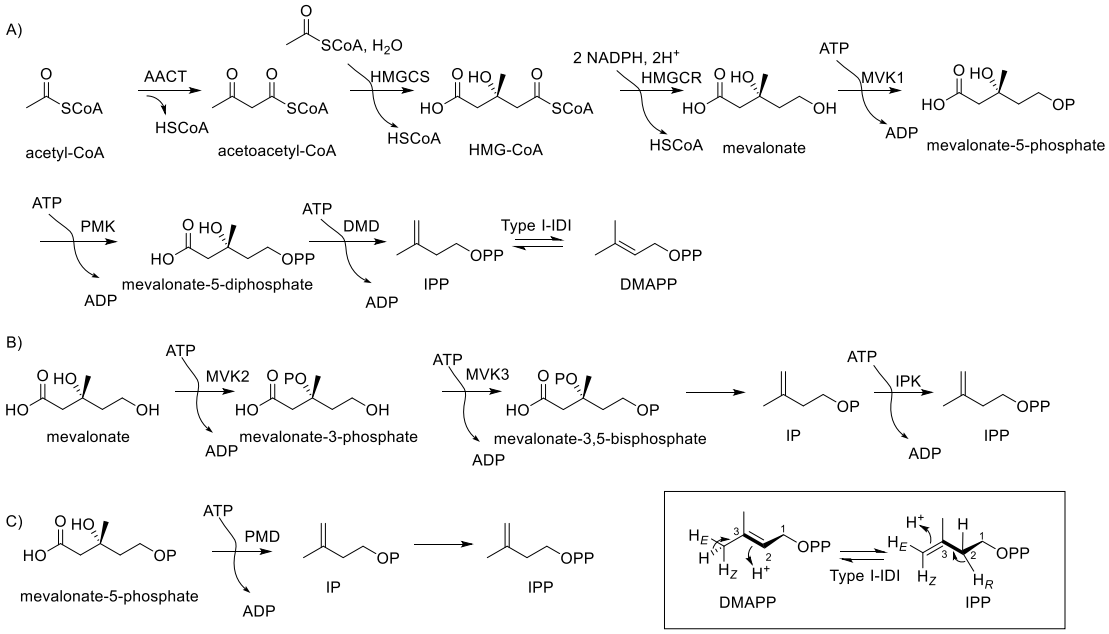

Scheme 1. Mevalonate pathway towards IPP and DMAPP. A) The classical MVA pathway. B) The branched MVA pathway found in *Thermoplasma acidophilum*. C) MVA pathway variant found in some archaea. The enzyme abbreviations used in this scheme are AACT: acetoacetyl-CoA synthase, HMGCS: HMG-CoA synthase, HMGCR: HMG-CoA reductase, MVK: mevalonate kinase, PMK: phosphomevalonate kinase, PMD: phosphomevalonate decarboxylase, IPK: isopentenyl pyrophosphate kinase, IDI: isopentenyl diphosphate isomerase. The stereochemical course of type I IDI catalyzed isomerization is shown in the bottom box.

Another pathway that yields IPP and DMAPP is the non-mevalonate pathway, also named as 2-C-methyl-D-erythritol 4-phosphate or 1-deoxy-D-xulylose 5-phosphate (MEP/DOXP) pathway (Scheme 2)[13]. First, pyruvate (**10**) and glyceraldehyde 3-phosphate (**11**) are fused to form 1-deoxy-D-xylulose 5-phosphate (**12**) by the thiamine pyrophosphate (TPP) dependent DXP synthase (DXPS). The bifunctional enzyme DXP reductoisomerase (DXR) subsequently catalyze the NADPH-dependent reduction and isomerization of **12** to yield 2-C-methylerythritol 4-phosphate (**13**). This compound is further converted to 4-diphosphocytidyl-2-C-methyl-D-erythritol (**14**) by 2-C-methyl-D-erythritol 4-phosphate cytidylyltransferase (CMS) with cytidine triphosphate (CTP) as the building block, followed by another phosphorylation at C2, resulting in the formation of 4-diphosphocytidyl-2-C-methyl-D-erythritol 2-phosphate (**15**). In the next

step, 2-C-methyl-D-erythritol 2,4-cyclodiphosphate synthase (MCS) catalyzes an intermolecular ring closure, leading to the formation of 2-C-methyl-D-erythritol 2,4-cyclodiphosphate (**16**) with the loss of a CMP unit. Compound **16** now can undergo a reductive elimination of water with the assistance of HMB-PP synthase (HDS) and ferredoxin to install the double bond between C2 and C3 of (*E*)-4-hydroxy-3-methyl-but-2-enyl pyrophosphate (**17**). At the final stage, HMB-PP reductase (HDR) selectively reduces the allylic alcohol **17** to yield IPP and DMAPP in a fixed ratio of 5:1. In plant cells, the MVA pathway takes place in the cytoplasm, while the MEP pathway located in plastids[14]. In addition, this pathway is also observed in some pathogenic bacteria and malaria parasites like *Mycobacterium tuberculosis*[15] and *Plasmodium falciparum*[16], respectively, while it is not found in humans. The investigation on related enzymes involved in the MEP pathway hereby is of high interest to discover new antimicrobial drugs.

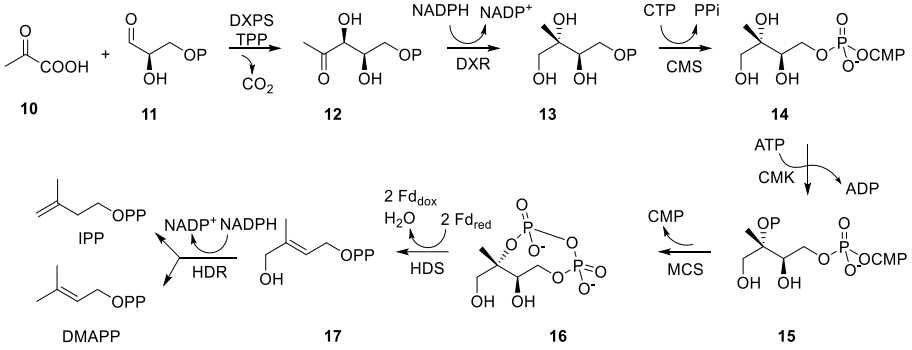

Scheme 2. Non-mevalonate pathway to yield IPP and DMAPP. The enzyme abbreviations are DXPS: thiamine pyrophosphate (TPP) dependent DXP synthase, DXP: reductoisomerase, CMS: 2-C-methyl-D-erythritol 4-phosphate cytidylyltransferase, MCS: 2-C-methyl-D-erythritol 2,4-cyclodiphosphate synthase, HDS: HMB-PP synthase, HMB-PP reductase.

1.3 Prenyltransferases

Prenyltransferases (PTs) are a group of enzymes that can catalyze the condensation of IPP and an allylic diphosphate to form C_{5n} (n = 2, 3, etc.) isoprenoid diphosphates[17,18] which serve as precursors of diverse terpenes. The reaction follows a sequential assembly line in which a DMAPP and an IPP molecule are fused to yield geranyl diphosphate (GPP, C_{10}), a precursor of monoterpenes, to which a second IPP is coupled, generating farnesyl diphosphate (FPP, C_{15}) for sesquiterpenes. Successive elongation with another molecule of IPP can create geranylgeranyl diphosphate (GGPP, C_{20}), a basis for the formation of diterpenes. GGPP can undergo further couplings to reach geranylfarnesyl diphosphate (GFPP, C_{25}) for sesterterpenes, farnesylfarnesyl diphosphate (FFPP, C_{30}) for triterpenes and diphosphates with even longer

chains for various terpenes. According to the length of chain elongated, diverse PTs are specifically named GPPS, FPPS, GGPPS, GFPPS, FFPPS and so on. The oligoprenyl diphosphates usually feature (*E*)-configured double bonds as a consequence of the coupling reaction catalyzed by *trans*-prenyltransferases (TPTs), a family of enzymes that can utilize (*E*)-configured precursors. In contrast, the structurally distinct *cis*-prenyltransferases (CPTs) allow infusion of preassembled oligomers in both (*E*)- and (*Z*)-configurations[19,20]. One representative TPT is avian FPPS featuring a homodimeric structure composed of 10 α-helices arranged in an antiparallel topology. Each subunit contains two aspartate-rich metal ion binding motifs DDXXD located on helices D and H (Figure 2)[21].

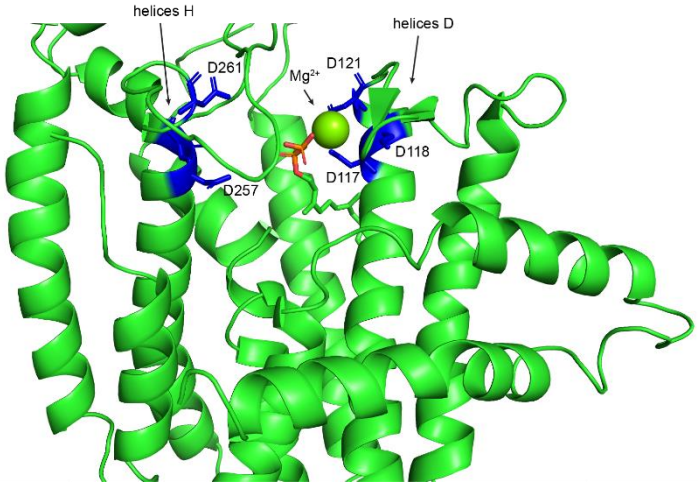

Figure 2. The X-ray structure of avian FPP synthase (PDB: 1UBX)[22]. Two DDXXD motifs are indicated located on the helices D and H (marked in blue). One Mg^{2+} ion is shown as green sphere. The figure was created using Pymol.

The catalytic mechanism of avian FPPS has been well investigated[23], in which both diphosphate groups of DMAPP and IPP are stabilized by two Asp-rich motifs respectively, and both require the participation of Mg^{2+}. After the ionization of DMAPP, the C3=C4 double bond of IPP attacks the allylic carbocation of DMAPP from the *Si*-face to yield a tertiary carbocation intermediate with inversion of configuration at C1, followed by elimination of the *pro-R* proton at C2 to result in the elongated product GPP which proceeds with an additional IPP molecule to form FPP (Scheme 3A). Poulter et al.[22] proposed the regulation of the product, in which the length of the product is controlled during the chain elongation process by two key residues F112 and F113 in avian FPP synthase, since their side chains form the base of the active pocket to serve as a template and to prevent the overextension of the product. Through mutagenesis experiments, two smaller amino acids (Ser and Ala) were introduced in these two positions. Poulter thereby obtained new FPPS variants that can produce GGPP and GFPP. A sequence alignment of 35 PTs revealed the conservation of these two residues, indicating that other PTs

possess the similar residues to work as a “stopper” in the active site. Despite the fact that CPTs share a similar catalytic mechanism in which only a *pro-S* proton at C2 is eliminated, opposite to TPTs, both classes of enzymes do not share any similarity in either primary or tertiary structure[24].

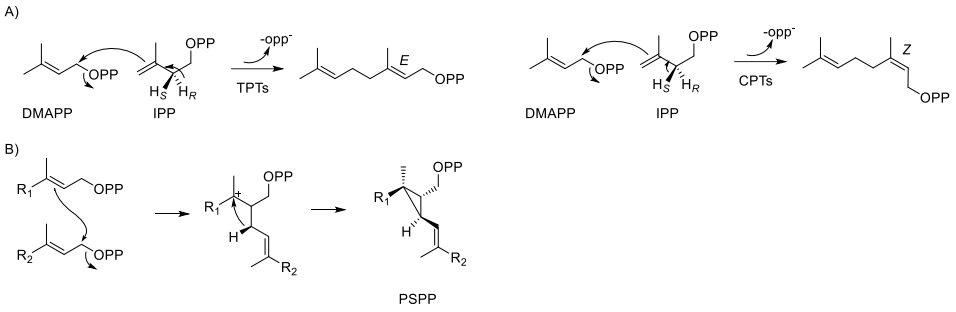

Scheme 3. Catalytic mechanism of the regular prenylation. The mechanism of A) head to tail and B) head to head coupling reaction.

Apart from the regular coupling reaction, there is also another condensation with two FPP molecules fused “head to head” to yield presqualene diphosphate (PSPP) (Scheme 3B), a compound involved in the biosynthesis of ergosterol, cholesterol, and hopanoids[25,26]. The archetype of these PTs is squalene synthase (SQS) which can be found in microbes, fungi, plants, and animals (including humans)[18]. In addition, two molecules of GGPP can also be coupled “head to head” by phytoene synthase found in *Brassica napus*, leading to the formation of phytoene, a C40 intermediate in the biosynthesis of carotenoids[27]. Last but not least, there are still more PTs such as aromatic prenyltransferase and UbiA-family prenyltransferases, that exist in nature, but they will not be discussed here.

1.4 Terpene synthases

After the formation of the acyclic precursors like GPP, FPP, GGPP, GFPP and FFPP by prenyltransferases, terpene synthases (TSs) further convert these substrates into structurally complex molecules with typically multiple fused rings and stereocenters. According to the different catalytic mechanisms, TSs are grouped into type I TSs, type II TSs, bifunctional TSs and non-canonical TSs (Scheme 4). An example of type I TSs is taxa-4,11-diene synthase from *Taxux brevifolia*[28] that converts GGPP to the key intermediate in the biosynthesis of paclitaxel taxa-4,11-diene (**18**), while another type of reaction is well exemplified by the formation of copalyl diphosphate (CPP, **19**), as a product of type II TSs. Geosmin synthase is a representative bifunctional enzyme that converts FPP to germacradienol (**20**) and germacrene D (**21**) followed by further cyclization to geosmin (**22**). More recently, non-canonical C17

terpenes like chlororaphen A[29] (**23**) and B (**24**) have been identified as the products of a novel mode of TS-catalyzed reactions.

Type I TSs usually adopt the same α-helical fold as that first observed in the structure of avian FPP synthase, and feature with α, $\alpha\beta$ and $\alpha\beta\gamma$ domain architectures. They promote the cyclic reaction by substrate ionization with the assistance of metal ions (Mg^{2+} is observed in most cases). It is worth mentioning that the active site of type I TSs exhibits several highly conserved motifs, including the aspartate-rich motif DDXXD located on helix D and the NSE triad (N,D)D(L, I, V)X(S,T)XXXE genetically originated from the second aspartate-rich motif of FPPs on helix H, a pyrophosphate sensor (a highly conserved Arg) and the C-terminal RY pair (Figure 3)[30-32]. The catalytic mechanism has been well studied: Firstly, three Mg^{2+} ions bind with the highly conserved Asp residues in the Asp-rich motif and the NSE triad to form a trinuclear cluster that in turn binds substrate's diphosphate group. Noel et al.[33] first observed this phenomenon in 5-*epi*-aristolochene synthase from tobacco that two Mg^{2+} coordinate to Asp^{301} and Asp^{305}, as the part of a DDXXD sequence, and constitute a diphosphate binding site. Subsequently, the RY motif forms hydrogen bonds to the diphosphate group and triggers a conformational change of the active pocket, leading to the departure of diphosphate and a cationic cascade reaction[34]. In addition, the active sites of type I TSs are precisely constructed by several non-polar and aromatic residues in a defined volumes[35], forcing the substrate in a fixed conformation and serving as a template of the product.

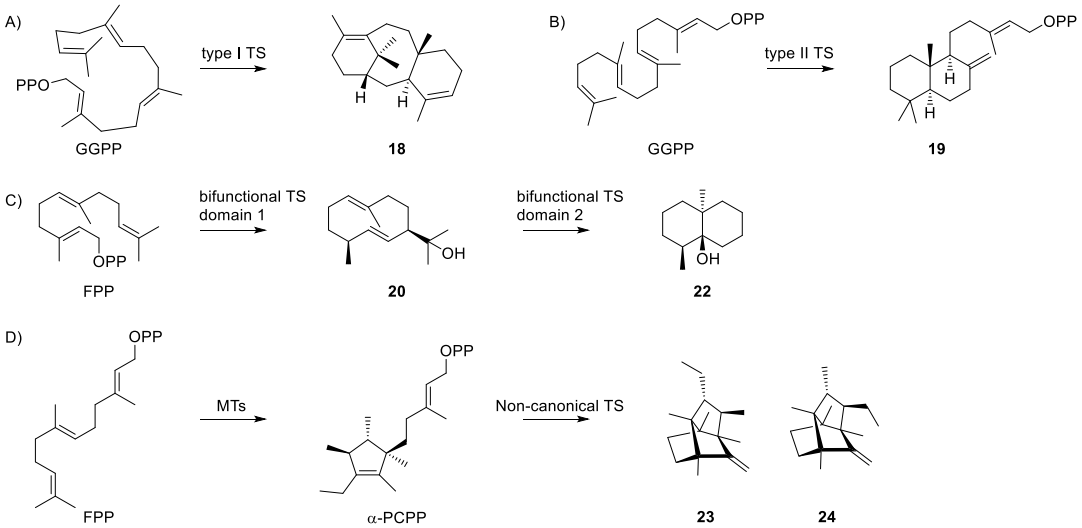

Scheme 4. Exemplary reactions of A) type I TS (taxa-4,11-diene synthase), B) type II (copalyl diphosphate synthase), C) bifunctional TS (geosmin synthase), and D) non-canonical TS (chlororaphen synthase) catalyzed reactions.

Different to type I TSs, type II TSs initialize the cationic cyclization by protonation or epoxidation of the double bond, which is conducted by a central aspartate in the highly conserved DXDD

motif (this motif is unrelated to the aspartate-rich DDXXD motif of type I terpene synthases)[1]. In addition to copalyl diphosphate synthase discussed above, several other type II TSs utilize GGPP in different conformations to yield enantiomeric series products like *ent*-CPP, *syn*-CPP, *syn*-*ent*-CPP, which can further proceed with the abstraction of diphosphate by a type I TS[36] or prenyltransferase[37] to contribute to diverse NPs.

Terpene biosynthesis occasionally provides examples of reaction sequences in which tandem terpene cyclization or coupling-cyclization reactions are catalyzed in two distinct active sites on the same protein, which is a so-called bifunctional enzyme. These two active sites can be functionalized as two type I TSs, type I plus type II TS, type I TS plus PT, or type II TS plus PT.

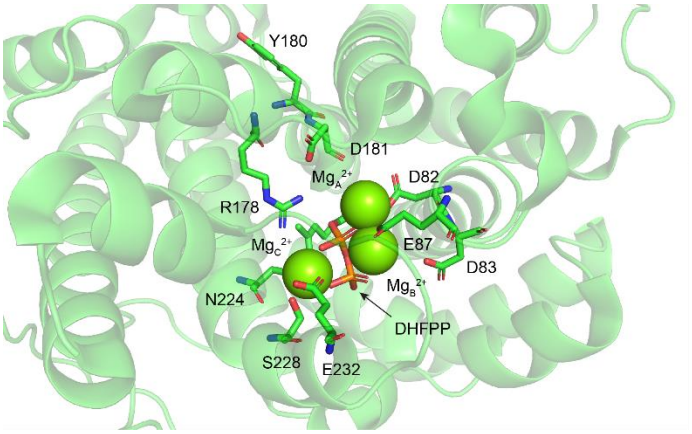

Figure 3. Stereoview of the active site in selina-4(15),7(11)-diene synthase (PDB: 4OKZ)[38]. D82, D83 and E87 are part of DDXXD motif, and N224, S228 and E232 are part of the NSE triad. R178 and Y180 belong to the RY pair. Three Mg^{2+} (A, B and C) coordinate with D82, D83 and E232 to form the trinuclear for the stabilization of diphosphate group. DHFPP: 2,3-dihydrofarnesyl diphosphate. This figure was generated by Pymol software.

In the case of bifunctional enzymes, two active sites are appropriately oriented with regard to each other to afford a proximity effect (proximity channeling), resulting in a higher probability that a product of one reaction can be taken over by the second active site. As mentioned above, geosmin synthase from *S. coelicolor*[39] represents one of the typical enzymes containing two domains, in which the first domain (residues 1-366) catalyzes the formation of **20** and **21** from FPP, while the second domain (residues 367-726) rebinds product **20** followed by a protonation to further generate **22** and acetone. Another example is abietadiene synthase which catalyzes the cyclization of GGPP through overall two consecutive steps to form (–)-abieta-7(8),13(14)-diene, a biosynthetic intermediate of (-)-abietic acid. Its formation includes the generation of (+)-**19** by type II active site, followed by the ionization and cyclization of (+)-**19** to yield abietadiene through type I active site[40]. The combination of PT activity and type I activity has frequently been observed in the case of biosynthesis of fusicoccadiene[41], ophiobolin F[42],

asperterpenol A[43], and sesterfisherol[44], where one domain is responsible for the formation of the acyclic precursor and the other one cyclizes it to yield a terpene compound. However, bifunctional enzymes containing type II and PT activities are indeed unusual. More recently, Abe[37] reported two diterpene synthases composed of three domains (α, β and γ) from *Penicillium* species with both type II TS and PT activities, in which the α domains at the C-terminus of both enzymes exhibit the PT activity for GGPP production, while the $\beta\gamma$ domains in the N-terminal region are responsible for the formation of **19**.

Non-canonical TSs are novel families of TSs that perform TS-like reactions but do not resemble canonical TSs in sequence or structure. Recently, more and more TSs belonging to this family have been discovered. In 2010, a C_{16} terpene sodorifen was detected from volatiles released by *S. odorifera*[45], and the corresponding TS and SAM-dependent C-methyltransferase also have been investigated[46,47]. More recently, Kampranis[48] reported a series of non-canonical TSs that are responsible for the formations of several C_{16} terpenes like heraclitene, anaximandrene, and aristotelene. All of these enzymes have been investigated in depth with isotopic labelling experiments in conjunction with DFT calculations by our group[49]. Subsequently, the chlororaphen synthase (ChloS) and two methyltransferases from *Pseudomonas chlororaphis*[29] were characterized through the identification of their products chlororaphen A (**23**) and B (**24**), for which a detailed mechanism towards their formations was addressed experimentally and theoretically[50].

1.5 Sesquiterpene biosynthesis

Type I sesquiterpene synthases (STSs) trigger the ionization of FPP to generate the reactive farnesyl cation (**A**), which can be attacked by the C10=C11 double bond to form the (*E,E*)-germacradienyl cation (**B**) or the (*E,E*)-humulyl cation (**C**) through 1,10 or 1,11-cyclization. Apart from that, FPP can also proceed with isomerization to yield nerolidyl diphosphate (NPP) harbouring a rotatable vinyl group around the C2-C3 single bond, which is essential for the installation of a (*Z*)-double bond between C2 and C3. Further *anti*-S_N2' reaction initialized from C3 triggers 1,10-cyclization to yield the (*E,Z*)-germacradienyl cation (**D**), 1,11-cyclization to the (*E,Z*)-humulyl cation (**E**), 1,6-cyclization to the bisabolyl cation (**F**), or 1,7-cyclization to the cycloheptenyl cation (**G**). These six cationic intermediates represent all the possibilities to initialize the biosynthesis of sesquiterpenes (Scheme 5).

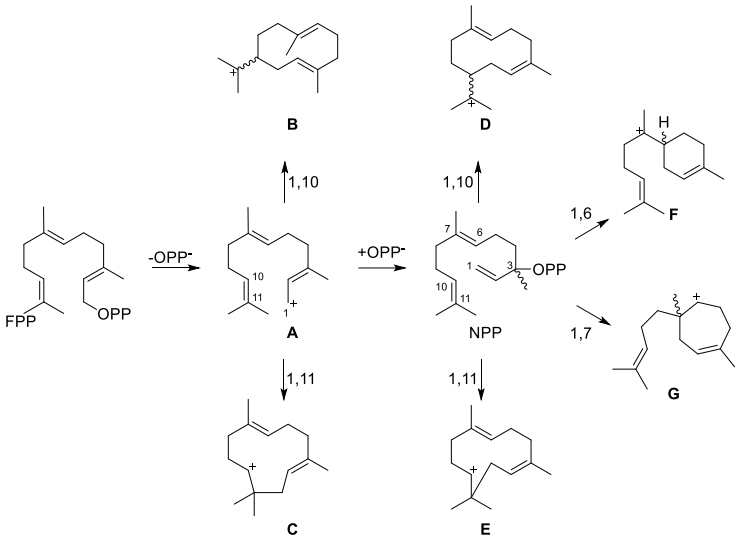

Scheme 5. Sesquiterpene cyclization modes starting from FPP.

Pentalenene (**26**), representing a typical tricyclic sesquiterpene with an initial 1.,11-cyclization mode, was first isolated from *Streptomyces* bacteria[51], then followed by extensive elementary biosynthetic proposals in understanding its formation[52-57]. As shown in Scheme 6, after the abstraction of diphosphate and 1,11-cyclization, the resulting humulyl cation (**C**) either proceeds through a consecutive deprotonation and reprotonation steps via humulene (**25**) to **H**, or directly undergoes a 1,2-hydride shift to **H**, followed by a cyclization to **I**, another 1,2-hydride shift to **J**, ring closure and deprotonation to **26** (Scheme 6, path A). This pathway is the earliest pathway suggested by Cane[58] raising the sequence of **C**-**25**-**H** and suggesting the only basic histidine residue (H309) in the active site may act as a base in the deprotonation-reprotonation sequence. Subsequently, the proposal was modified to a 1,2-hydride from **C** to **H** with skipping of **25**, since the replacement with another non-basic residues at the position of H309 (H309A) retained the production of pentalenene[59].

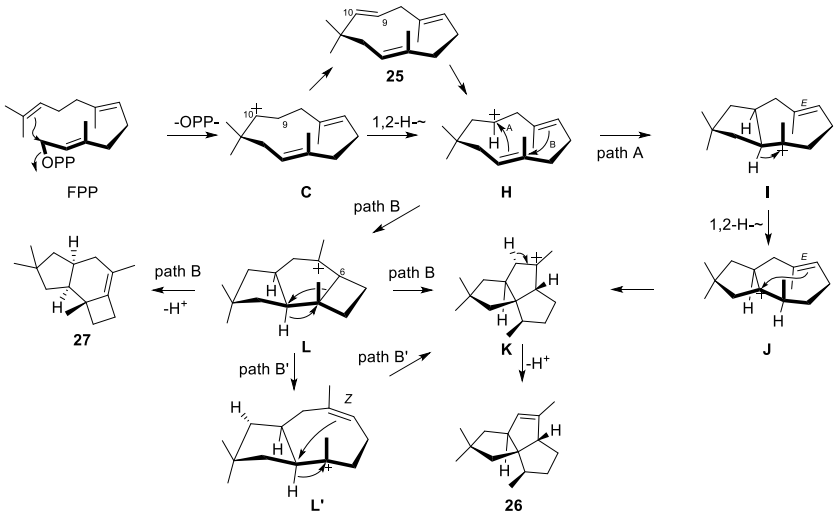

Scheme 6. Proposed biosynthetic mechanism towards **26** and **27**.

In 2006, Gutta and Tantillo[60] proposed an alternative pathway, in which the 7-protoilludyl cation (**L**) is formed directly after **H**, followed by a direct unusual dyotropic rearrangement to the direct deprotonated precursor of **26** (Scheme 6, path B). This mechanism is supported by quantum-chemical calculations, but revealing the computed barrier for the dyotropic rearrangement was ca. 30 kca/mol. In 2012, this result was further confirmed by the incubation of (6-^{2}H)FPP with purified enzyme variant H309A, which the productive distribution was shifted to more **26** and less Δ^{6}-protoilludene (**27**), as explained by a normal kinetic isotopic effect. Subsequently, a refinement of the DFT calculations suggested a pathway B' via ring opening of **L** to **L'**, followed by 1.2-hydride shift and cyclization to **K** with an overall barrier of only ~6 kcal/mol[56]. More recently, Xu et al.[61] characterized a sesquiterpene synthase from the liverwort *Radula lindenbergiana* with tiny production of **26**, pointing additional evidence towards the path B' in the biosynthesis of **26**. In addition, an isopentalene synthase from the fungus *Clitopilus passeckerianus* was also investigated in this dissertation, with two products **26** and isopentalene identified, which will be described in Chapter 6.

1.6 Diterpene biosynthesis

At present, more than 126 different diterpene carbon skeletons have been identified, contributing to more than 18,000 compounds[62]. As discussed above, two main classes of diterpene synthases (DTSs), type I and type II enzymes, dominate diterpene formation. Type I DTSs stand out as more outstanding catalysts in creating a vast diversity of terpene skeletons in comparison to type II DTSs. Different to FPP, the cyclization of GGPP by a DTS can proceed through a large variety of initial cyclization steps, resulting in a larger structural diversity of cyclized products. The resulting diterpenes can be divided into groups: compounds generated from 1,6 or 1,7-cyclization, from 1,10 or 1,11-cylization, and from 1,14 or 1,15-cyclization in terms of the different initial cyclization modes.

An example of terpen formed through initial 1,6-cyclization may be (-)-Vinigrol (**30**). This compound, featuring an unprecedented and highly congested 6-6-8 tricyclic ring system confirmed by the X-ray crystallographic analysis of its oxidized derivative (**30***), was first isolated from fungus *Virgaria nigra F-5408* by Hashimoto et al.[63] in Fujisawa Pharmaceutial company, Ltd in 1987. Due to its various potent pharmaceutical activities, this molecule attracted considerable attention on its total synthesis[64-68]. Its biosynthetic mode was unknown until its gene cluster was identified in 2024 by Xu and Zou[69]. The formation of **30** requires one cyclization step and two sequential steps of hydroxylation (Scheme 7), in which a corresponding DTS (VniA) catalyzes 1,6-cyclization of GGPP, a rarely observed mode in nature. In his

proposal, the formation of **28** requires an isomerization of GGPP and a 1,6-ring closure, followed by several unusual 1,4 or 1,5-hydride shifts and ring closures. Unfortunately, this mechanism was neither confirmed by experimental data nor theoretical calculations. While 1,6-cyclizations in diterpene biosynthesis appears to be rare, type I DTSs catalyzing the 1,7-cyclization mode so for is unknown.

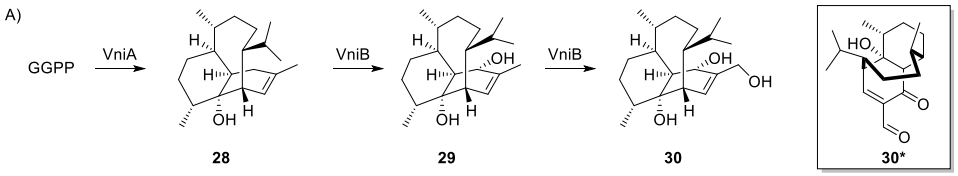

Scheme 7. Proposed biosynthetic pathway towards **30**. VniA and VniB represent a DTS and a cytochrome P450, respectively. The oxidized derivative **30*** is shown in the box.

The majority of diterpenes originates from a 1,10- or 1,11-cyclization mode, due to the fact that the resultant carbocation can easily be captured by other π electrons in GGPP. How this mode of cyclization can further proceed will be exemplified in more details here.

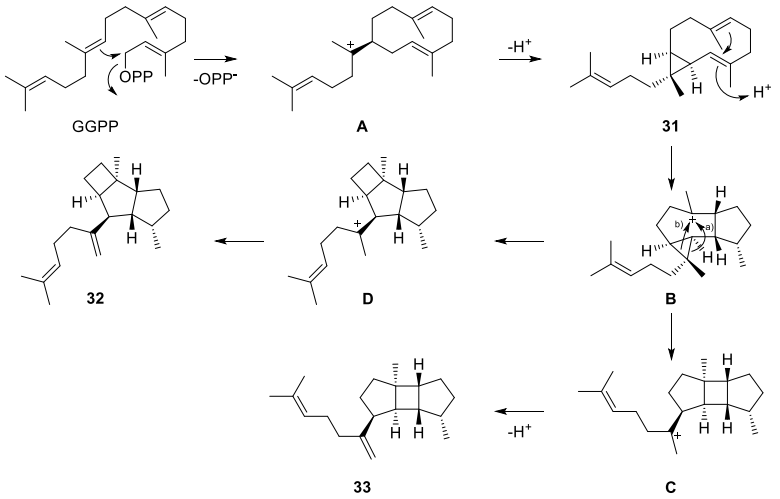

Scheme 8. Cyclization proposal towards the formation of **31**, **32** and **33**.

Spata-13,17-diene synthase (*Sx*SpS) from *Streptomyces xinghaiensis*[70] is a representative DTS that first catalyzes a 1,10-cyclization to yield the tertiary cation **A** followed by a deprotonation to cneorubin Y (**31**), a neutral molecule that can further proceeds through a protonation and cyclization to form intermediate **B.** Two alternative cyclizations proceeding with simultaneous sacrifice of cyclopropane ring towards **C** or **D** may result in the formation of prenylkelsoene (**32**) and spata-13,17-diene (**33**), respectively (Scheme 8). As a part of this study, *Sx*SpS is also deeply investigated to understand the unique mechanism of substrate promiscuity through enzyme crystallization and protein engineering.

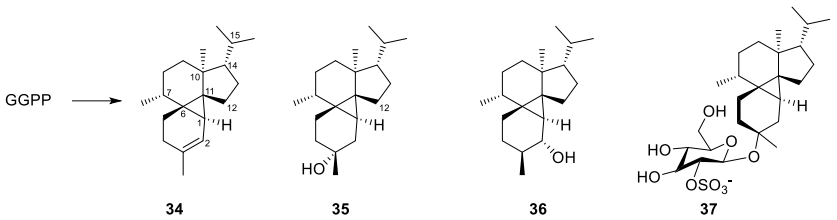

Scheme 9. Representative diterpenoids obtained with a 1,11-10,14 cyclization mode.

Due to the instability of secondary cations, a 1,11-cyclization mode usually is not favored during terpene formation, however, cyclization cascade followed by 10,14-cyclization can avoid this situation. An exemplary DTS catalyzing two sequential cyclizations is peysonnosene synthase (PeyS) from chloroflexota bacterium *Anaerolineaceae* sp[71] which is capable of converting GGPP into peysonnosene (**34**), a compound sharing the 5-6-3-6 fused tetracyclic skeleton observed in peyssonnosides from the marine red alga *Peyssonnelia* sp. The relative configuration of **34** was proposed to be the same as that of peyssonnoside A (**37**)[72] due to their structural similarity, while its absolute configuration was tentatively assigned as (1*S*,6*S*,7*R*,10*S*,11*S*,14*S*) through VCD measurement. Meanwhile, two derivatives of **34** named peyssonnosol A (**35**) and B (**36**), with absolute configuration assigned by X-ray structure, were identified as the enzymatic products of two DTSs (Scheme 9). Extensive isotopic labelling experiments disclosed their formations originating from a 1,11-10,14-cyclization mode[72]. In addition, many DTSs including cyclooctat-9-en-7-ol synthase (CotB2)[73], the first identified bacterial type I DTS, spiroviolene synthase (SvS) from *Streptomyces violens*[74], cattleyene synthase (CyS) from *Streptomyces cattleya*[75], and variediene synthase (AbVS) from the fungus *Emericella variecolor*[76] are capable of catalyzing initial 1,11-10,14-cyclizations. In Chapter 3-5, the usage of DTSs in the biotransformation of non-natural substrate analogs is described, showing how the structural modifications effect this cyclization mode and lead to different products. It is worth mentioning that the cyclization cascades of some DTSs proceed through secondary cations, exemplified by the cationic cascade of palmatol synthase (CpDTS1) recently cloned from *Chitinophaga pinensis*[77]. The mechanistic investigation of this enzyme demonstrated that a secondary cation formed through skeletal rearrangement, can be stabilized via cation-π interaction with the adjacent C14=C15 double bond, which was demonstrated by DFT calculations.

Another frequently observed mode is 1,14-cyclization which can generate the cembren-15-yl cation (**E**) followed by deprotonation to macrocyclic compounds such as casbene (**38**) and (+)-cembrene A (**39**) (described in Chapter 8). Apart from that, **E** can also undergo a 10,15-cyclization to yield compounds representing the verticillane skeleton such as verticilla-3,7,11-triene (**40**), or representing the taxane skeleton such as **18**. Compound **18** and related

diterpenes share unique long-range proton migrations in their biosynthesis, which will be described in Chapter 8. Interestingly, a similar mechanism was also observed in the formation of the 6-6-5-7 tetracyclic diterpene cephalotene (**41**), whose formation is catalyzed by cephalotene synthase (CsCTS) from *Cephalotaxus sinensis*[78]. As shown in Scheme 10, the formation of **41** requires a key intermediate **F**, which proceeds with a long range 1,7-proton shift to **G** and further yields cyclophomactene (**42**) by a variant of taxadiene synthase (TxS-G606A, Chapter 8).

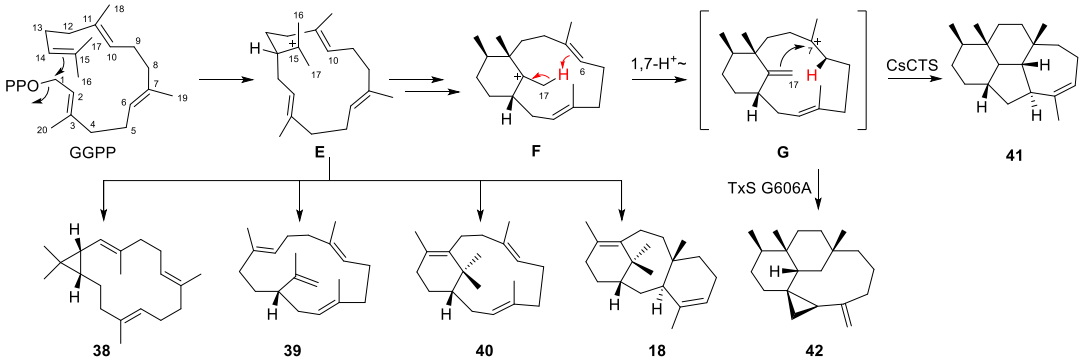

Scheme 10. Terpenes generated from the 1,14-cyclization mode.

Bonnadiene synthase (BdS) from *Allokutzneria albata*[79] represents a DTS with a 1,14-cyclization mode to yield bonnadiene (**43**). Its biosynthetic mechanism was experimentally confirmed by an isotopic labelling study, and proceeds with isomerization of GGPP to geranyllinalyl diphosphate (GLPP) and 1,14-cyclization through *anti*-S_N2' attack at C1 to **H** which undergoes a 1,3-hydride shift to **I** with the stereospecific migration of the 1-*pro*-R hydrogen, followed by 1,6-cyclization to **J**. The remaining steps include a 1,2-hydride transfer to **K**, 6,10-cyclization to **L** and deprotonation to **43** (Scheme 11). As observed, the active pocket of enzymes dedicates to the substrate's different folding conformation, leading to different initial cyclization mode. However, the non-natural terpene precursor *iso*-GGPP II can absolutely changes its folding conformation, resulting in a novel biosynthetic formation (Chapter 3).

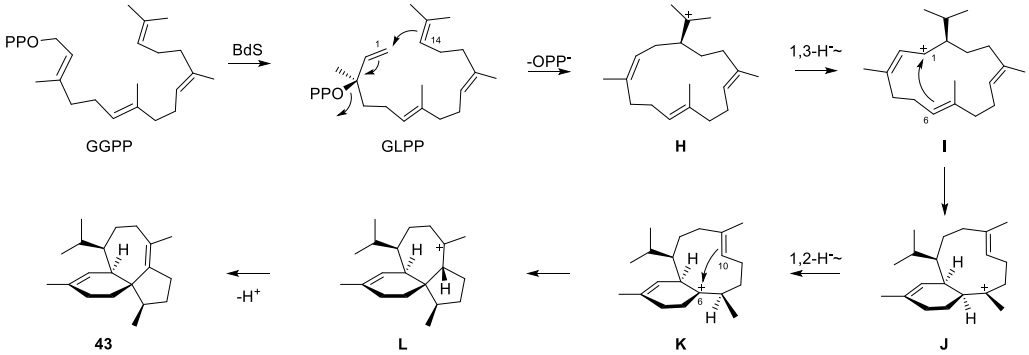

Scheme 11. Cyclization mechanism towards **43**.

In contrast to the frequently observed 1,14-cyclization mode, which results in 14-membered ring diterpenes, the 1,15-cyclization mode has rarely been reported in diterpene biosynthesis. Only six known examples, flexibilene (**44**) isolated from the soft coral *Sinularia flexibilis*[80,81], its corresponding alcohol (**45**) from *Streptomyces* sp. SANK 60404[82], micromonocyclol (**46**) and the related elimination products **47** and **48** from *Micromonospora marina*[83] were identified as the products of the 1,15-cyclization mode (Scheme 12).

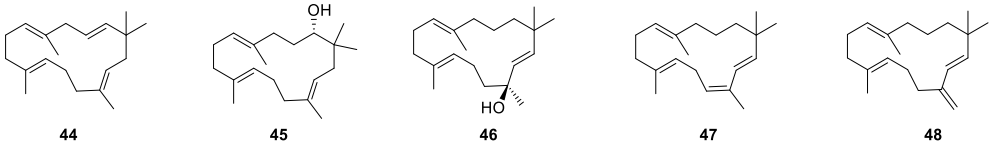

Scheme 12. Representative diterpenes generated from 1,15-cyclization.

1.7 Non-natural substrate analogs in terpene biosynthesis

Synthetic analogs have originally served as inhibitors of TSs to provide high-resolution of enzyme crystal structures with bound analogs, disclosing the relevant substrate conformations in the active pocket. Prominent examples include 5-*epi*-aristolochene synthase[33] bound to trifluorofarnesyl diphosphate and selina-4(15),7(11)-diene synthase coordinated with DHFPP[38]. In addition, non-natural substrate analogs that lack a specific reactivity can also be carefully designed to interrupt the enzyme's cyclization cascade, allowing the isolation of derailment product to provide additional insights into the proposed cyclization mechanism. In (+)-aristolochene (**50**) biosynthesis, (–)-germacrene A (**49**) had been proposed to be an intermediate arising by 1,10-cyclization and deprotonation[84] (Scheme 13A). Subsequently, **49** proceeds through reprotonation and cyclization to generate the bicyclic intermediate eudesmayl cation (**A**) which undergoes 1,2-hydride migration, Me migration and deprotonation to yield **50**. Despite **49** being regarded as an intermediate towards **50**, no trace of **49** was released from the active site of aristolochene synthase from *Aspergillus terreus*[85,86] (AT-AS). Incubation of the FPP analog (7*R*)-6,7-dihydro-FPP with AT-AS resulted in the formation of dihydrogermacrene (**51**, Scheme 13B), which was confirmed by GC/MS analysis in comparison to a synthetic standard[87], a compound that cannot be further cyclized due to the saturation of C6-C7 single bond. Moreover, Allemann[88] converted another FPP isomer 7-methylene FPP to 7-methylenene germacrene A (**52**) by the AT-AS homolog from *Penicillium roquefortii* (PR-AS), in which the formation of **52** follows the homologous reprotonation and cyclization steps like natural counterpart to yield **A**, finally to **50** (Scheme 13C).

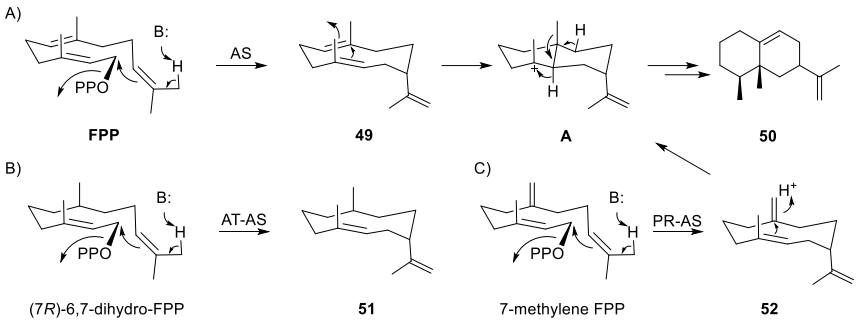

Scheme 13. Mechanistic investigation of aristolochene synthase (AS) by conversion of A) FPP, B) (7*R*)-6,7-dihydro-FPP and C) 7-methylene FPP.

As a remarkable biocatalyst in forming complex structures with high chemo-, regio-, diastereo- and enantioselectivity from merely limited natural acrylic precursors, TSs theoretically can tolerate various non-natural terpene precursors to create novel terpene backbones for further modifications.

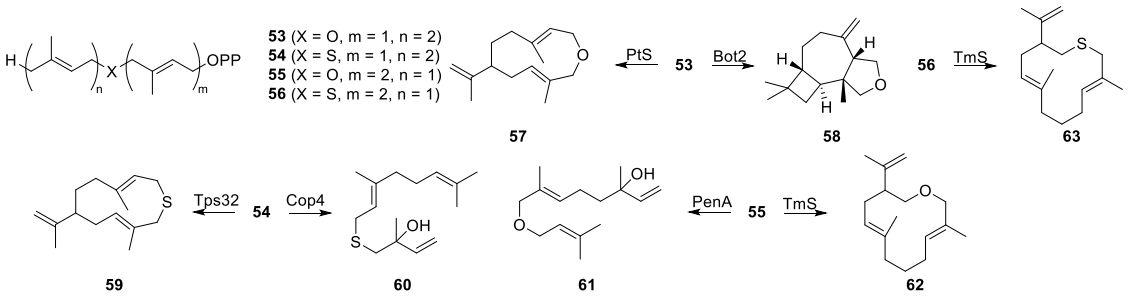

Scheme 14. Representative non-natural sesquiterpenes obtained from enzymatic conversion of FPP derivatives through various STSs.

Recently, In the collaboration with Kirschning[89], a series of synthetic heteroatom-modified FPP derivatives (Scheme 14) were synthesized and enzymatically transformed with several STSs like patchoulol synthase (PtS) from *Pogostemon cablin*[90], viridiflorene synthase (Tps32) from *Hyoscamus muticus*[89,91], (+)-T-muurolol synthase (TmS) from *Roseiflexus castenholzii*[92], pentalenene synthase (PenA) from *Streptomyces exfoliates*[52,89,93], presilphiperfolan-8b-ol synthase (Bot2) from *Botrytis cinerea*[89,94] and cubebol synthase (Cop4) from *Corinus cinereus*[89,95]. In comparison to enzymatic products obtained from FPP, several isolated non-natural sesquiterpenes featured novel skeletons such as tricyclic terpenoid **58** as shown in Scheme 14. However, the absolute configurations of all these non-natural terpenoids were not determined.

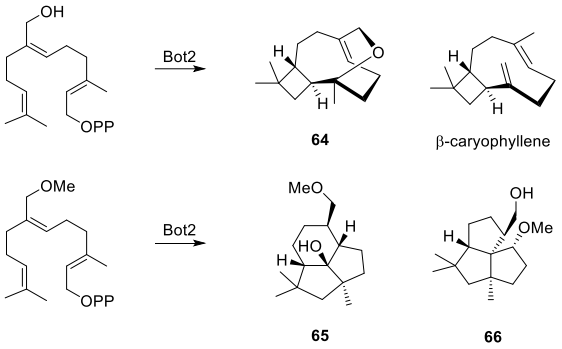

Scheme 15. Enzymatic conversion of FPP derivatives with Bot2 enzyme.

In the cases mentioned above, the initial purpose of oxygen insertion is to stabilize the cationic intermediate by formation of oxiran-1-ium cation and to further facilitate the cyclization cascade, oppositely, the cationic intermediates were interrupted at beginning, leading to the generation of macrocyclic compounds. More recently, Kirschning et al.[96] designed two more FPP analogs bearing a hydroxyl group or hydroxymethyl group at C14 with calculated van der Waals volumes of 350 and 370 Å^3, respectively. Further cavity calculations on the Alphafold model of Bot2 enzyme revealed a total of volume of its active site cavity of 570 Å^3, which theoretically can adopt both analogs. Upon product isolation and NMR-based characterization, compounds **64**-**66** were identified, with absolute configurations assigned through X-ray crystallographic analysis (Scheme 15).

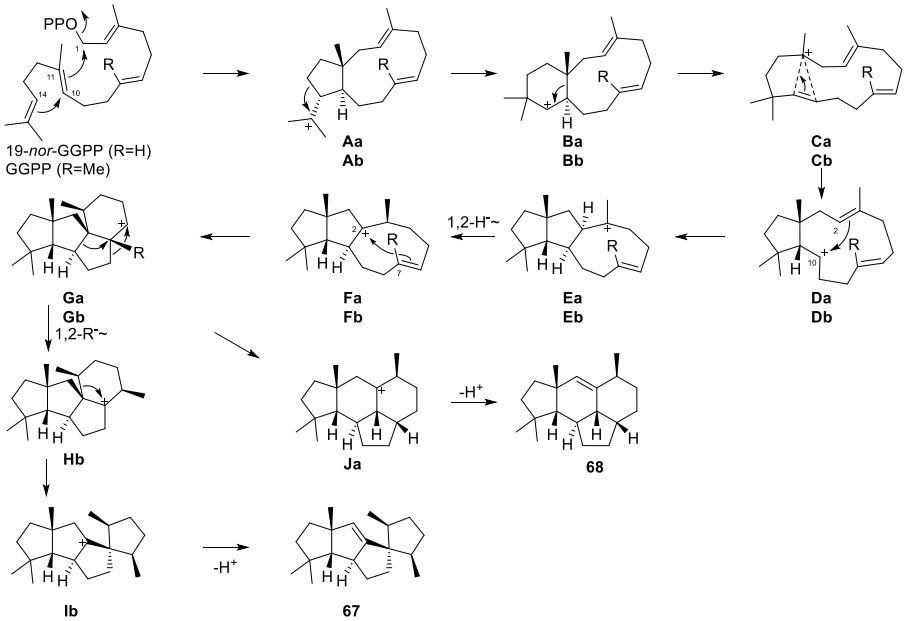

Scheme 16. Biosynthetic route to **67** and **68**. “a” series stands “R = H” and “b” series represents “R = Me”.

The majority of investigations on the substrate promiscuity of terpene synthases is focused on STSs, while conversions of non-natural substrates with DTSs are rare. One representative example is desmethylated GGPP analog 19-*nor*-GGPP[97], which was transformed by 20 DTSs resulting in the isolation of 23 non-natural diterpenoids. Xenoviolene (**68**), enzymatically obtained with SvS, exhibits a remarkable terpene skeleton as a result of a branched cyclization route. Mechanistically, 19-*nor*-GGPP follows an analogous cyclization like its natural counterpart GGPP until the intermediate **G**. At this stage with GGPP Me19 migrates into the neighboring position, but instead a ring contraction is observed for the non-natural case, leading to intermediates either **Hb** or **Ja** as the precursors of spiroviolene (**67**) or **68**, respectively (Scheme 16). This result demonstrates that small structural changes in GGPP can lead to novel cationic sequences and consequently to enzyme products with new skeletons. As part of this doctoral thesis, SvS was also confirmed to have moderate substrate tolerance towards *iso*-GGPP analogs, producing other novel terpenes. Moreover, diverse synthetic *iso*-GGPP analogs were studied systematically with DTSs previously investigated in our laboratory to gain a deeper understanding of how the activities of DTSs are triggered by structural modifications. The results of this work will be described in detail in Chapters 2-5.

1.8 Site-directed mutagenesis

With the development of X-ray crystallization and AI-based structure prediction, site-directed mutagenesis (SDM) is becoming a powerful and accessible tool to deepen our mechanistic understanding of TSs. As mentioned in Chapter 1.4, type I TSs harbour a typical α-helical fold with several highly conserved motifs that engage in substrate recognition, binding, and catalysis. In 2002, Cane et al.[98] first conducted a series of SDM experiments, creating the D84E, W308F, H309F, W308F/H309F, N219A, and N219L enzyme variants of bacterial type I TS pentalenene synthase. Among them, the W308F and W308F/H309F variants are not only capable of producing **26,** but also yield (+)-**49** and **27** as a consequence of a derailment of the cyclization reaction. They also addressed the significance of N219, a residue located in NSE triad by the observation of inactivity of N219A and N219L. In rare cases highly conserved motifs like the DDXXD motif and the NSE triad can be exchanged, as found for isoishwarane synthase (IWS) from *Streptomyces lincolnensis*[99,100]. IWS possesses an unusual ^{80}DDLHT motif instead of the classical DDXXD motif, where the reintroduction of the third Asp in the T84D variant gave a nearly unchanged activity towards isoishwarane formation. Apart from these highly conserved residues, several aromatic residues like Phe, Tyr, Trp also play an important role in stabilizing cationic intermediate via π-cation interactions, which is well explained in the fungal

sesterterpene synthase nigtetraene synthase from *Pestalotiopsis fici* (PfNS) through a quadruple mutagenesis. Based on the molecular dynamics simulations (MD) of PfNS/**A0** and the MD trajectories analysis, Liu et al.[101] enable finding the key aromatic residues located at the D-helix and G2-helix regions, where are reported to be associated to catalytic function[102,103]. Incubation of GFPP with the resulting quadruple variant PfNS-F89A/Y113F/W193L/T194W generated the tricyclic sesterterpene ophiobolin F (**69**) instead of the native bicyclic product nigtetraene (**70**, Scheme 17). Subsequent MD simulations with the triple variant Y113F/W193L/T194W revealed cation-π interactions between F89 and C15 of **A0**, and a C-H···π interaction with a distance of 3.9±0.3 Å between F89 and H14, promoting the 1,2-hydride shift from C14 to C15.

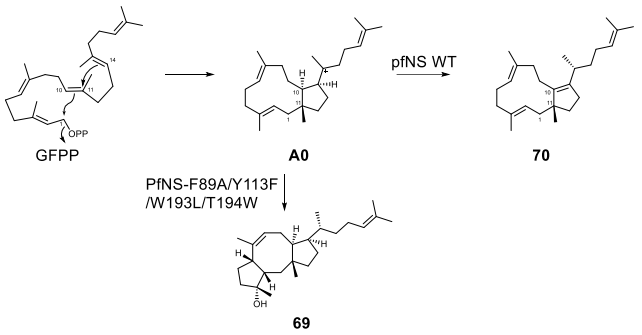

Scheme 17. The formation of **69** and **70** by PfNS and its variant.

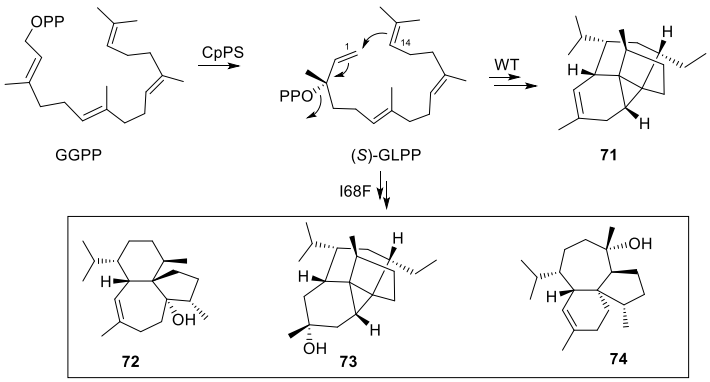

Scheme 18. Bioynthetic routes to **71**-**74** catalyzed by CpPS and its variant I68F.

As mentioned above, the active sites of type I TSs are precisely constructed by several non-polar and aromatic residues in a defined volumes[35]. Dickschat et al.[104] disclosed the conservation of thirteen residues, including I66 of polytrichastrene synthase from *Chryseobacterium polytrichastri* (CpPS), in analogous positions of many TSs through a sequence alignment with more than 100 characterised microbial type I TSs. This residue is occupied by an aromatic residue Phe in many other type I TSs. A variant I68F thereby was carefully designed with an enhanced diterpene production (195±43%) and a strongly changed

product profile. Consequently, besides polytrichastrene A (**71**), several new compounds wanju-2-en-6α-ol (**72**), polytrichastrene B (**73**) and bonn-2-en-11α-ol (**74**) were isolated. Their absolute configurations were determined by isotopic labelling experiments (Scheme 18).

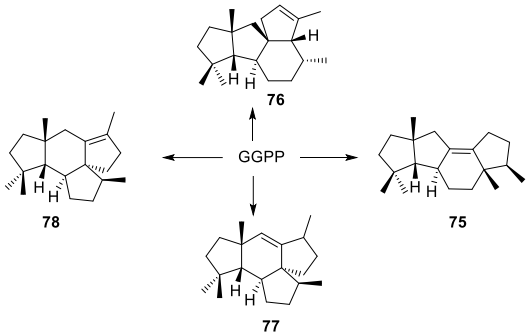

Scheme 19. Representative diterpens obtained from CyS WT and its variant.

With the assistance of crystallographic techniques, the co-crystal structure of cattleyene synthase bound to one GGPP and three Mg^{2+} (CyS-GGPP-Mg^{2+}) provided a deeper insight into the interactions between GGPP and five aromatic residues, four aliphatic and three polar residues, where GGPP is folded in a special conformation. The single variant C59A completely shifted the product profile from native cattleyene (**75**) to three novel diterpenes **76**, **77** and **78**, featuring unique 5-5-6-5, and 5-6-5-5 tetracyclic skeletons, respectively (Scheme 19)[105]. With the assistance of site-directed mutagenesis and MD simulation, a sesquiterpene synthase was also engineered to a diterpene synthase which will be described in Chapter 7.

Taking all these examples together, SDM is indeed a powerful tool in understanding the catalytic mechanisms of enzymes and in creating novel terpene products. Nowadays, the development of sequence-based, structure-based, machine learning-based computational tools will facilitate the identification of the beneficial mutations by creating smaller but smarter libraries[106].

Chapter 2

Isotopic Labelling Experiments and Enzymatic Preparation of *Iso*-Casbenes with Casbene Synthase from *Ricinus communis*

Heng Li[a] and Jeroen S. Dickschat[a]*

[a] Heng Li, Prof. Dr. Jeroen S. Dickschat, Kekulé-Institute for Organic Chemistry and Biochemistry, University of Bonn, Gerhard-Domagk-Straße 1, 53121 Bonn, Germany, E-mail: dickschat@uni-bonn.de

The publication “Isotopic Labelling Experiments and Enzymatic Preparation of *Iso*-Casbenes with Casbene Synthase from *Ricinus communis*” can be found in Appendix A.

Introduction

Although the casbene synthase (CS) has been characterized and investigated deeply[107,108], the stereochemical course for the cyclisation reaction catalyzed by CS remains open. This study investigated this issue by using isotopic labelling experiments, showing the same absolute configuration as reported for casbene[109]. Further labelling experiments gave insights into the EI-MS fragmentation mechanism of casbene. Casbene isomers were obtained by enzymatical conversion of two oligoprenyl diphosphate analogs with shifted double bonds, showing the analogous absolute configurations as for casbene.

Summary

The CS gene was cloned into the pYE-Express shuttle vector[110] and expressed in *E. coli* BL21 (DE3). The purified protein efficiently converted GGPP into (–)-**79**, while the cyclisation mechanism from GGPP to **79** proceeds through 1,14-cyclisation to the cembranyl cation (**A**), followed by deprotonation from C1 with cyclopropane ring closure (Scheme 20). Incubation of (*R*)- and (*S*)-(1-^{13}C,1-^{2}H)IPP with IDI, GGPPS and CS revealed the specific loss of the 1-*pro*-*S* hydrogen during product formation. Further incubation with DMAPP and (*E*)- or (*Z*)-(4-^{13}C,4-^{2}H)IPP allowed the identification of the absolute configuration of **79**.

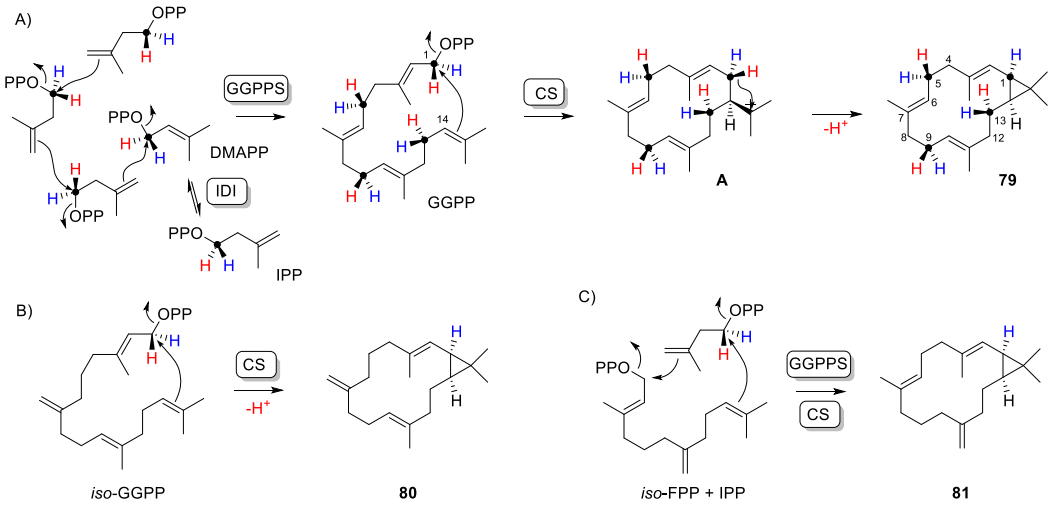

Scheme 20. A) Cyclisation of GGPP to **79**. Conversion of B) *iso*-GGPP to *iso*-casbene I (**80**), and C) *iso*-FPP to *iso*-casbene II (**81**).

Two substrate analogs *iso*-FPP and *iso*-GGPP with an olefinic methylene group at C7 instead of the C6=C7 double bond were synthesized and converted into *iso*-casbene I (**80**) and *iso*-casbene II (**81**), respectively (Scheme 20). The absolute configuration of **80** was determined

using GGPP analogs with an enantioselective deuteration at C1. For this purpose, (*R*)-(1-^{2}H)-*iso*-GGPP (blue H = ^{2}H) and (*S*)-(1-^{2}H)-*iso*-GGPP (red H = ^{2}H) were synthesized in high enantiomeric purity. Their conversions with CS into **80** resulted in the specific loss of 1-*pro*-*S* hydrogen, which is the same hydrogen as lost in the formation of **79**, pointing to the absolute configuration of (1*R*,14*S*)-**80**. The same conclusion is obtained for **81** in the incubation of *iso*-FPP and (*R*)-(1-^{2}H)IPP (blue H = ^{2}H) and (*S*)-(1-^{2}H)IPP (red H = ^{2}H) with GGPPS and CS, indicating the structure of (1*R*,14*S*)-**81**.

The EI-MS fragmentation mechanism of **79** was studied based on the GC/MS analysis of the twenty isotopomers of (^{13}C)-**79**. The results of these mass spectrometric analyses are summarized for prominent fragment ions *m*/*z* in a position specific mass shift analysis (PMA$_{m/z}$, Figure 4). In this method, EI-MS analysis of the crude products obtained from the enzymatic conversion of the twenty ^{13}C-labelled isotopomers of GGPP can identify the formation of a specific fragment ion from a specific portion of the analyte. The labelled product gives a mass shift of +1 in comparison to the unlabelled product. This PMA leads to a full picture of which carbon atoms of the product form a fragment ion (summarized as shown in Figure 4) with all 20 ($^{13}C_1$)GGPP isotopomers. The specific loss of the C15(-17)-16 portion (Figure 4) contributes to the formation of fragment ion *m*/*z* 229 (PMA$_{229}$) based on this analysis. This fragment is explained by α-fragmentation to **A**$^{+\bullet}$, hydrogen rearrangement (*r*H) to **B**$^{+\bullet}$ and another α-cleavage with loss of C_3H_7 to **C**$^{+}$ after electron ionization to **79**$^{+\bullet}$ (Scheme 21A).

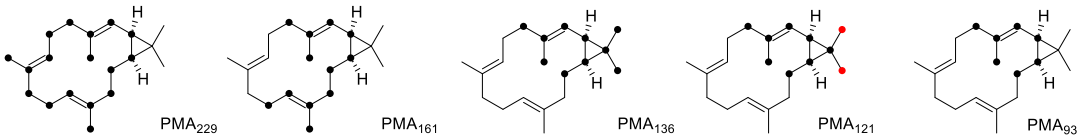

Figure 4. Position specific mass shift analysis for **79**.

Besides the cleavage of a fragment of 43 Da (C_3H_7), also a small peak for the cleavage of 44 Da ($C_3H_6{}^{2}H$) was observed with labelled **79** from (*R*)- and (*S*)-(1-^{13}C,1-^{2}H)IPP and (*E*)- and (*Z*)-(4-^{13}C,4-^{2}H)IPP. This indicates multiple mechanisms to the formation of **C**$^{+}$. Thus, plausible suggestions for the hydrogen rearrangements based on other fragment ions will be made. The PMA$_{161}$ analysis reveals loss of the C5-6-7(-19)-8 and C15(-17)-16 moieties (Figure 4). The ionization to **79**$^{+\bullet}$ and two α-cleavages lead to the neutral loss of isoprene via **D**$^{+\bullet}$ to **E**$^{+\bullet}$ (Scheme 21B). The terminal steps for the loss of C_3H_7 are then basically the same as in the formation of *m/z* 229. The analysis of PMA$_{136}$ shows the cleavage of C5-6-7(-19)-8-9-10-11(-18)-12 (Figure 4), resembling the loss of two neutral isoprene units. Starting from **E**$^{+\bullet}$ in which the first isoprene unit is already cleaved off, an α-fragmentation to **I**$^{+\bullet}$ and inductive cleavage to **J**$^{+\bullet}$ results in the neutral loss of a second isoprene unit (Scheme 21C). PMA$_{121}$ exhibits the additional loss of

either Me16 or Me17, which can directly be explained from **J**$^{+\bullet}$ through another α-cleavage. Finally, PMA$_{93}$ indicates the formation of this fragment ion from the C13-14-1-2-3(-20)-4 portion of **79** (Figure 4). A first α-cleavage of **79**$^{+\bullet}$ to **L**$^{+\bullet}$ followed by two inductive cleavages via **M**$^{+\bullet}$ to **N**$^{+\bullet}$ can be followed by α-fragmentation with cyclopropane ring opening to **O**$^{+\bullet}$ (Scheme 21D). Hydrogen rearrangement to **P**$^{+\bullet}$ and loss of the isopropyl group then lead to **Q**$^{+}$.

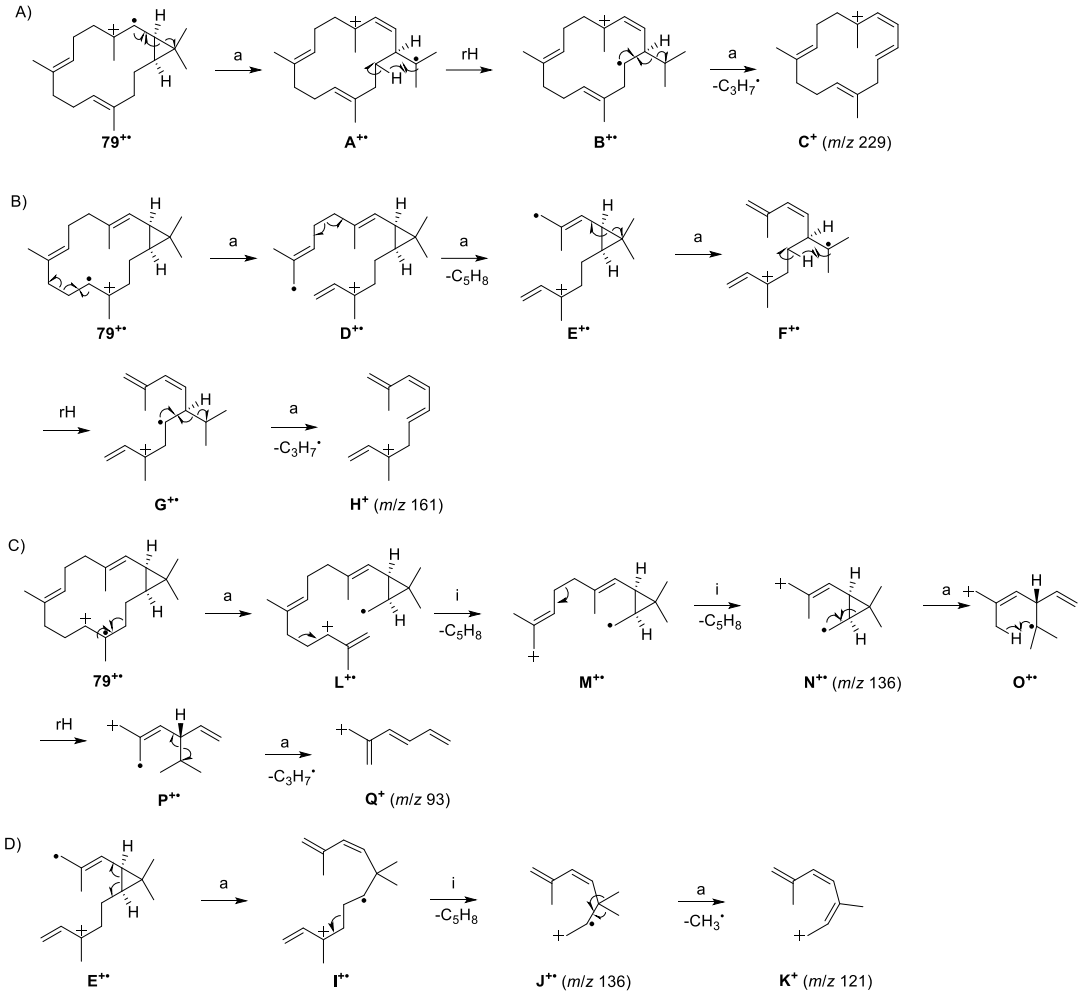

Scheme 21. Proposed mechanism for the formation of fragment ions.

In this work, I first expressed the CS gene into the *E. coli* BL21 (DE3) and isolated casbene from the incubation experiment with GGPP. Then, two synthetic GGPP analogs were converted by CS to yield the casbene isomers. Finally, I conducted all labelling experiments to study the stereochemical courses of casbene and its isomers, and to study the EI-MS fragmentation mechanism of casbene.

Chapter 3

Diterpene Biosynthesis from Geranylgeranyl Diphosphate Analogues with Changed Reactivities Expands Skeletal Diversity

Heng Li[a] and Jeroen S. Dickschat[a]*

[a] Heng Li, Prof. Dr. Jeroen S. Dickschat, Kekulé-Institute for Organic Chemistry and Biochemistry, University of Bonn, Gerhard-Domagk-Straße 1, 53121 Bonn, Germany, E-mail: dickschat@uni-bonn.de

The publication “Diterpene Biosynthesis from Geranylgeranyl Diphosphate Analogues with Changed Reactivities Expands Skeletal Diversity” can be found in Appendix B.

Introduction

After successful transformations of the two GGPP analogs *iso*-GGPP I and *iso*-GGPP II with casbene synthase, we continued our studies with twelve diterpene synthases from bacteria, fungi, and protists to investigate the activity change caused by the substrate modifications. In total 28 new diterpenes were isolated, and most of them exhibited novel skeletons.

Summary

The incubation of *iso*-FPP with GGPPS and bonnadiene synthase (BdS) from *Allokutzneria albata*[79] resulted in the compounds isonephthenol (**82**) and isocembrene A (**83**, Scheme 22A). Compounds **82** and **83** are the iso-compounds according to nephthenol (**84**) and cembrene A (**39**). The formation of **82** and **83** can be explained by the disturbance of the enzyme-substrate interaction caused by the structural modification in *iso*-GGPP II. The 1,14-cyclization occurring in the natural conversion with GGPP is still promoted but with retained 2*E* configuration in **A**, while the downstream steps of the cascade are interrupted. The spata-13,17-diene synthase (SpS) from *S. xinhaiensis*[70] catalyzes an initial 1,18-cyclization of *iso*-GGPP II to **B**, followed by a subsequent 1,3-hydride shift and attack of water to pseudoobscuronatin (**85**, Scheme 22B). This compound was named a pseudo-derivative based on the similar natural cyclization mechanism towards obscuronatin (**86**).

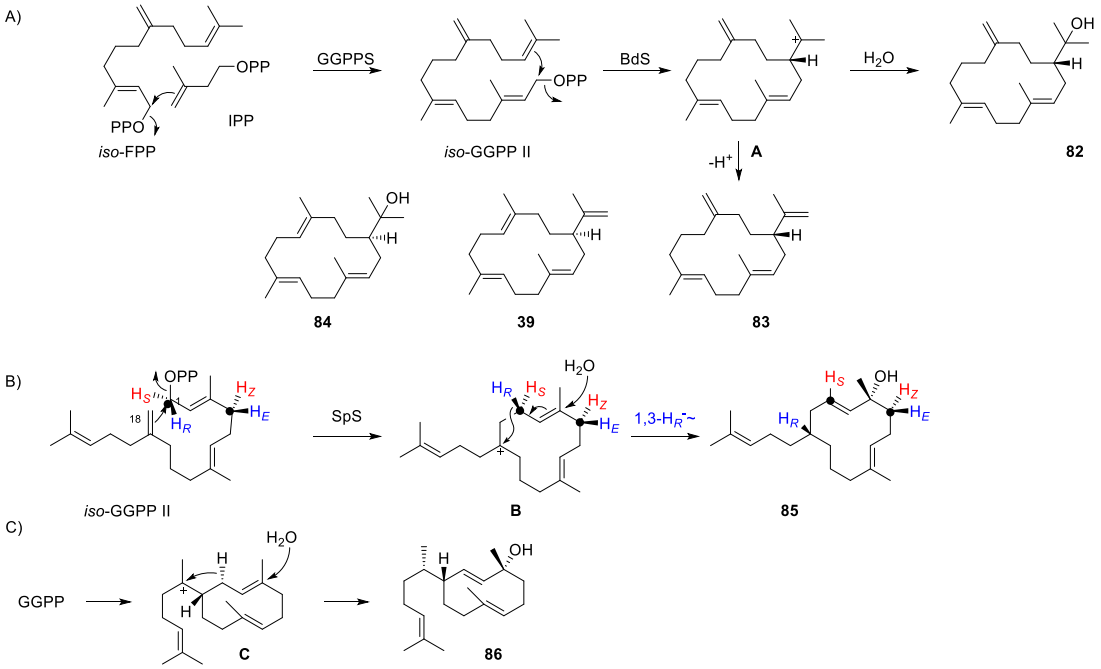

Scheme 22. Diterpenes from *iso*-GGPP II.

All compounds prenylpseudogermacrene A (**87**), prenylpseudogermacrene B (**88**), prenylpseudogermacrene C (**89**) and prenylpseudogermacrene D (**90**) are from the same cationic intermediate **B** which is a result of the 1,18-cyclization from various diterpene synthases.

Meanwhile, with phomopsene synthase from *Nocardiopsis rhamnosiphilia* (NrPS)[75] and *iso*-GGPP II, a new diterpene alcohol prenylpseudohedycaryol (**91**) and a new diterpene hydrocarbon pseudodolabella-3,7,18-triene (**92**) were isolated. The formation of **91** is explained with 1,18-cyclization and quenching with water, while formation of **92** requires a 1,2-hydride shift, cyclization and deprotonation (Scheme 23).

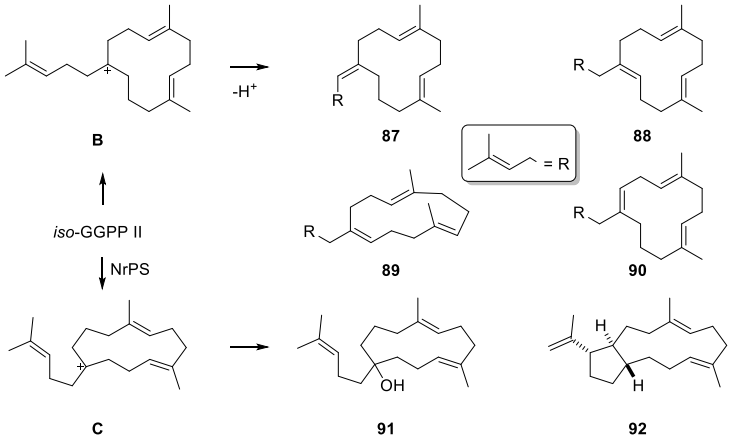

Scheme 23. Diterpenes from *iso*-GGPP II.

Because the conformational flexibility of macrocyclic ring compounds sometimes does not allow for an unambiguous interpretation of NOESY spectra, our stereoselective deuteration strategy is not always suitable. However, the optical rotations of **82** and **83** (**82**: $[\alpha]_D^{25}$ = +11.4, *c* 0.07, Me_2CO, **83**: $[\alpha]_D^{25}$ = +84.6, *c* 0.13, Me_2CO) are of opposite sign to the reported optical rotations of (*R*)-**84** ($[\alpha]_D^{25}$ = –46.3, *c* 1.20, $CHCl_3$) and (*R*)-**39** ($[\alpha]_D^{25}$ = –14.2, *c* 0.48, $CHCl_3$) from plants[111,112], indicating opposite absolute configurations. Isotopic labelling experiments with (*E*)- and (*Z*)-(4-^{13}C,4-^{2}H)IPP pointed to the absolute configuration of **85** as shown in Scheme 22. For compound **91** the results showed a high enantiomeric purity of **91** obtained with HdS (90% *ee*), but only 70% *ee* for **91** from NrPS. For **92** the production was not sufficient to gain conclusive insights into its absolute configuration.

The conversion of *iso*-GGPP I harbouring C7=C14 double bond resulted in the *iso*-compounds showing the corresponding double bond shift compared to the native products from GGPP. For example, β-pinacene synthase (PcS) from *Dyctostelium discoideum*[113] produced *iso*-β-pinacene (**93**) as main product, and 18-hydroxydolabella-3,8(17)-diene (**94**) was produced by conversion of *iso*-GGPP I with 18-hydroxydolabella-3,7-diene synthase (HdS) from *Chitinophaga pinensis*[114]. Similarly, dolabella-3,8(17),18-triene (**95**) and its isomer dolabella-

3,8(17),11-triene (**96**), sharing the same skeleton as **94**, were obtained from the incubation of *iso*-GGPP I with NrPS and dolasta-1(15),8-diene synthase (CgDS)[115], respectively (Scheme 24).

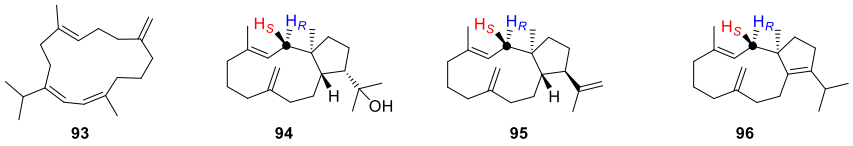

Scheme 24. Diterpenes from *iso*-GGPP I with PcS, HdS, NrpS and CgDS.

The incubation of AbVS[76] with *iso*-GGPP I yielded the two diterpene alcohols variexenol A (**97**) and B (**98**). The initial cyclization steps towards **D** to those observed with GGPP are similar, but later the *exo*-methylene C19 is involved in a 3,19-cyclization with attack of water, leading to the formation of compounds with new skeletons (Scheme 25A). For **98** the initial 1,11-10,14-cyclization is modified to a 1,11-2,10-cyclization to **E**, followed by 3,19-cyclization and attack of water. Similar findings have been made for cyclooctat-9-en-7-ol synthase (*Si*CotB2) from *Streptomyces iakyrus*[73] that converted *iso*-GGPP I into 2,3,7-*triepi*-variexenol B (**99**), isoxeniaphyllene (**100**) and prenylisodauca-3,7(14)-diene (**101**).

Isothunbergene A (**102**) and B (**103**), besides the alcohol albataxenol (**104**) were isolated from the incubation of *iso*-GGPP I with SaS[116]. Notably, the 1,14-cyclization of *iso*-GGPP I and two sequential 1,2-hydride shifts to **F**, similarly to the reactions with the native substrate GGPP, are required for the formation of **99** and **100**. If the cyclization is continued as for GGPP until to **H**, the last remaining double bond becomes involved, resulting in a new cyclisation mode with attack of water leading to **104** (Scheme 25B).

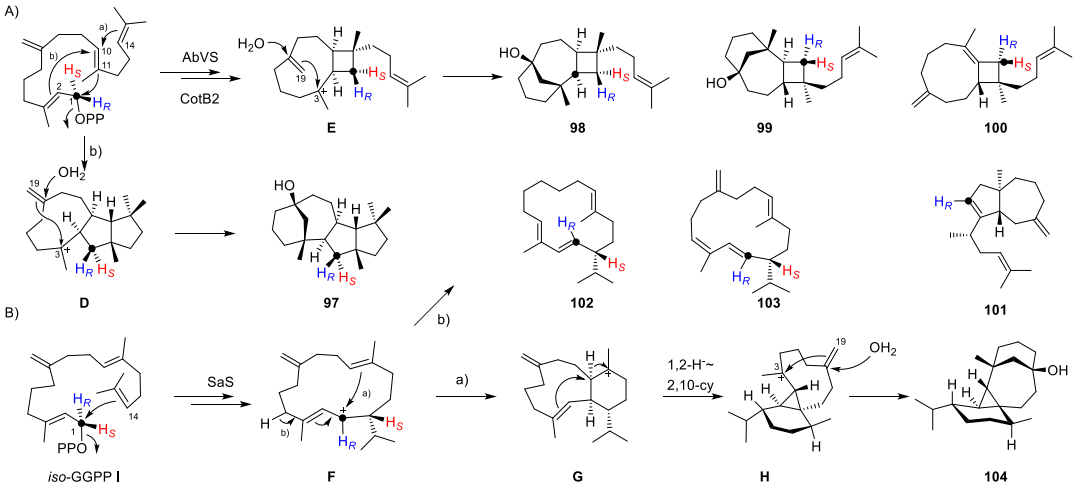

Scheme 25. Diterpenes from *iso*-GGPP I with AbVS and SaS. Cyclization of *iso*-GGPP I with A) AbVS to form **97**, **98**, and with *Si*CotB2 to form **99**, **100**, **101**, and with B) SaS to form **102**, **103**, and **104**.

With wanjudiene synthase (CwWS)[117] *iso*-GGPP I was converted into prewanjuxenene (**105**) and wanjuxenene (**106**). The cyclization cascade proceeds with its initial steps analogically as natural wanjudiene in this case. However, starting from intermediate **M**, the different double bond location in *iso*-GGPP I leads to a distinct cyclisation mode. A 1,2-hydride shift to **N** and 2,19-cyclization result in a secondary cation **O**. This cation may be a transient species that is stabilized by a 1,2-hydride shift to **P**, followed by a final deprotonation step to **106** (Scheme 26). The 1,3-hydride shift from **I** to **J** and 1,2-hydride shift from **O** to **P** both were demonstrated by conversion of (*R*)- and (*S*)-(1-^{13}C,1-^{2}H)-*iso*-GGPP I followed by GC/MS analysis.

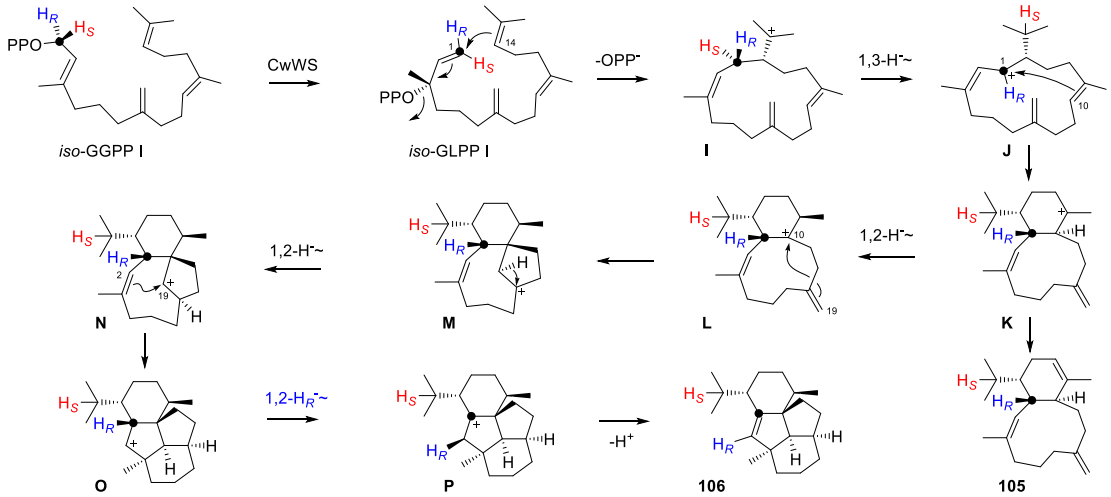

Scheme 26. Cyclization of *iso*-GGPP I with CsWS

In addition, two diterpene alcohols precatenulixenol (**107**) and catenulixenol (**108**) were isolated with catenul-14-en-6-ol synthase (CaCS) from *Catenulispora acidiphila*[118], and one diterpene hydrocarbon isocneorubin Y (**109**) was obtained with SpS, respectively (Scheme 27). Their formations follow the natural cyclization casades with GGPP very closely.

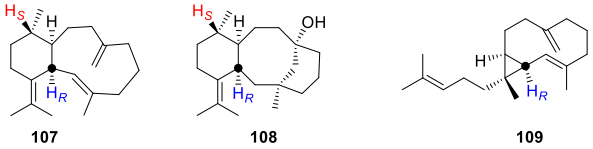

Scheme 27. Diterpenes from *iso*-GGPP I with CaCS and SpS

The enantioselective labelling strategy was used to determine absolute configurations of the products derived from *iso*-GGPP I. For this purpose, (*R*)- and (*S*)-(1-^{13}C,1-^{2}H)-*iso*-GGPP I were synthesized with 94% *ee* and 96% *ee*, respectively. Their conversions with several DTSs and HSQC analysis of the products showed the absolution configurations of **94**, **95**, **97**, **98**, **99**, and **100**. While this strategy is not always suitable, since one of the hydrogens at C1 for some compounds migrates during the cyclization process. We hereby suggest their absolute configurations should be analogous to their natural counterparts.

In this work, I was responsible for performing all the enzymatic transformations, product isolations and structure elucidations, and also conducted all the labelling experiments to determine the absolute configurations of different compounds.

Chapter 4

Enzymatic Synthesis of Diterpenoids from *iso*-GGPP III, a Geranylgeranyl Diphosphate Analog with Shifted Double Bond

Heng Li[a] and Jeroen S. Dickschat[a]*

[a] Heng Li, Prof. Dr. Jeroen S. Dickschat, Kekulé-Institute for Organic Chemistry and Biochemistry, University of Bonn, Gerhard-Domagk-Straße 1, 53121 Bonn, Germany, E-mail: dickschat@uni-bonn.de

The publication “Enzymatic Synthesis of Diterpenoids from *iso*-GGPP III, a Geranylgeranyl Diphosphate Analog with Shifted Double Bond” can be found in Appendix C.

Introduction

The successful biotransformations of *iso*-GGPP I and *iso*-GGPP II demonstrated high substrate tolerance of many diterpene synthases, which inspired us to investigate the relationship between substrate structure and diterpene activity. Here, a new GGPP analog with a shifted double bond from C14=C15 to C15=C16 (named *iso*-GGPP III) was synthesized and enzymatically converted by six DTSs, allowing for the isolation of nine non-natural diterpenes (Scheme 29). Their absolute configurations were addressed by the stereoselective labelling strategy.

Summary

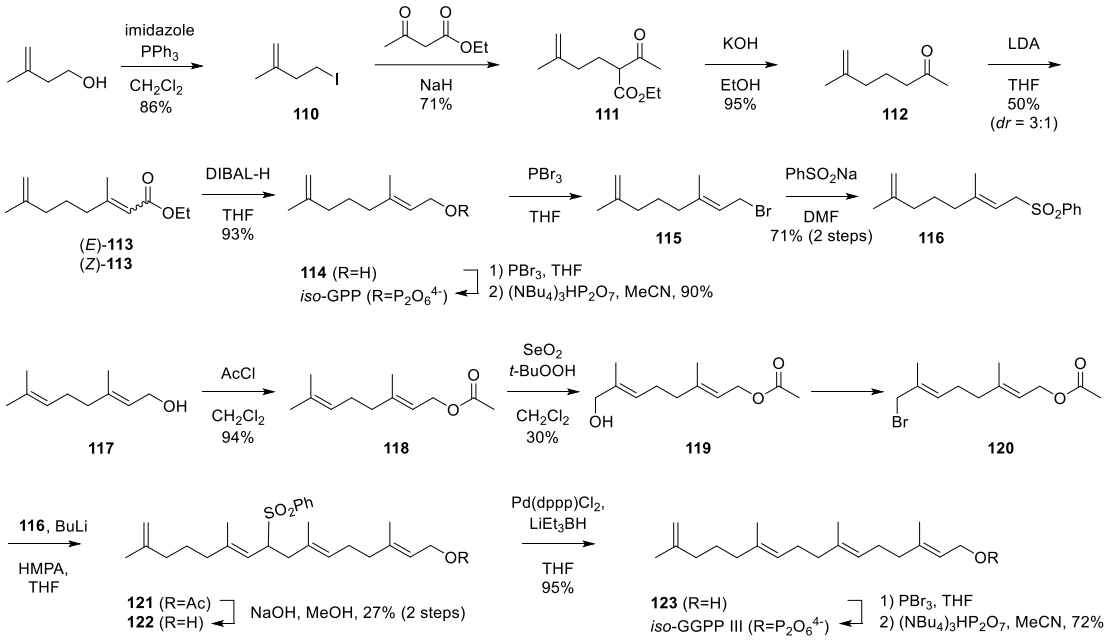

Scheme 28. Synthesis of *iso*-GPP and *iso*-GGPP III.

The synthesis of *iso*-GGPP III started with iodination of isopentenol to **110**, followed by alkylation to **111**. Saponification and decarboxylation gave 6-methylhept-6-en-5-one (**112**) that was elongated to (*E*)- and (*Z*)-**113** through Horner-Wadsworth-Emmons reaction. After separation by column chromatography, (*E*)-**113** was reduced and phosphorylated to yield *iso*-GPP with the C6=C7 double bond shifted. Deprotonated **116** was coupled with **120** which derives from actetylation of farnesol (**117**), SeO_2 oxidation of **118** and bromination of **119** to obtain **121**. Sponification and reductive cleavage of the sulfinate group resulted in the geranylgeraniol isomer **123** that was further converted into *iso*-GGPP III (Scheme 28). *Iso*-GPP and *iso*-GGPP III can be accepted by six diterpene synthases, but *iso*-GGPP III showed a better

diterpene production in comparison to *iso*-GPP, because no GGPPS is required for the elongation of two isoprene units.

The previous chapter showed that HdS[114] has a good tolerance towards *iso*-GGPP I and II, while it also accepted *iso*-GGPP III to form four major compounds. Two of them have been isolated, but the main product showed strong line broadening in the NMR spectra even at an elevated temperature (343K), preventing its structure elucidation. Another one was characterized as (11*E*)-12-isopentenyl-α-selinene (**124**), its formation can be easily explained from the cyclization of a germacrene A derivative[119]. Surprisingly, the isomer (11*Z*)-12-isopentenyl-α-selinene (**126**) was obtained from the incubation of *iso*-GGPP III with HpS from *Streptomyces clavuligerus*[113]. Hydropyrene (**127**) and hydropyrenol (**128**) derives from the intermediate prehydropyrene (**125**) which is catalyzed by HpS through 1,10-cyclization of GGPP to **A**, followed by 1,3-hydride migration to **B**, 1,14-cyclization and deprotonation. The reprotonation of **125** at C6 can further open two more cyclizations, resulting in **127** and **128**, respectively. The formation of **126** can be explained from a similar conformational fold as for GGPP towards **127** and **128**, but at the stage **C** the cascade is interrupted with the deprotonation to **125'** to introduce the *Z*-configured double bond. Further reprotonation and cyclization leads to **126**. Besides **126**, isoelisabethatriene C (**129**) was also isolated from the same enzymatic conversion with HpS.

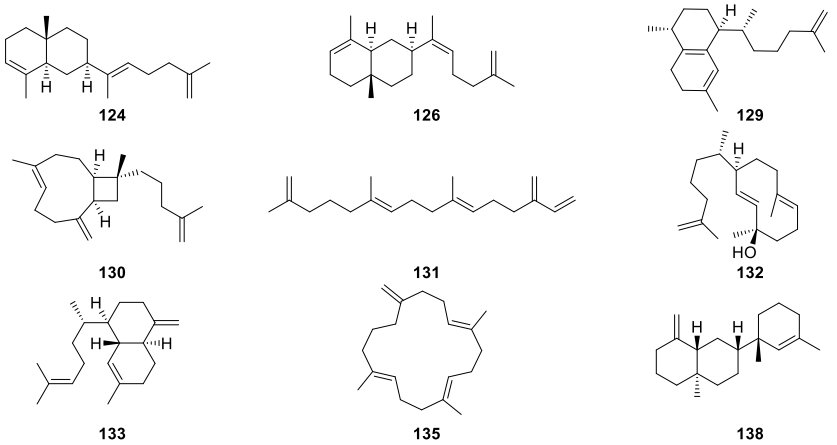

Scheme 29. Diterpenes obtained with *iso*-GGPP III and different diterpene synthases.

Two diterpene hydrocarbons isoxeniaphyllene II (**130**) and *iso*-β-springene (**131**), and one diterpene alcohol xeniaphyllenol (**132**) were isolated from the conversion of *iso*-GGPP III with phomopsene synthase from *Nocardia testacea* (NtPS, Scheme 30)[75]. Instead of a 1,11-10,14-cyclization mode of GGPP to phompsene, the initial cyclization of *iso*-GGPP III is altered to 1,11-2,10-cyclization to **130**, while the secondary cation **E** may be stabilized by π-coordination with the C2=C3 alkene unit. The formation of isoobscuronatin (**132**) can be explained from the 1,10-cyclization of *iso*-GGPP III, 1,3-hydride shift to **G** and attack of water to **132**, a double bond

isomer of obscuronatin (**134**)[120], while biflora-4,10(19),16-triene (**133**) generated from the decomposition of **132** during chromatographic purification on silica gel. The compound bucket-wheelene (**135**) that isolated with *Si*CotB2 was given its name, because its shape reminds of a bucket wheel (Scheme 31C).

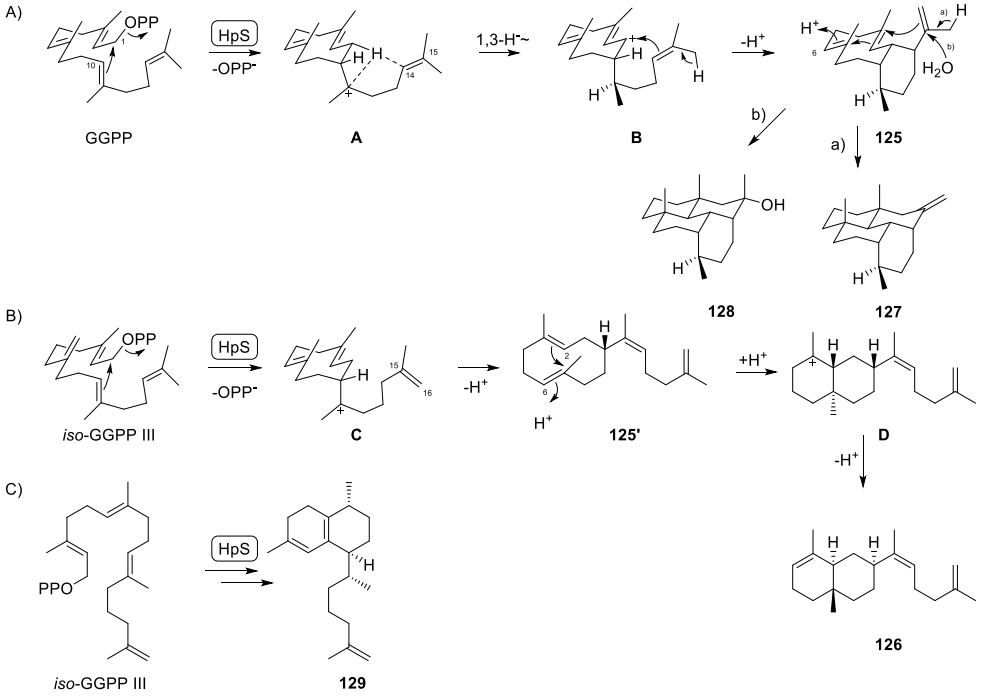

Scheme 30. Cyclization of A) GGPP to form **127** and **128**, B) *iso*-GGPP III to form **126** and C) *iso*-GGPP III to form **129**.

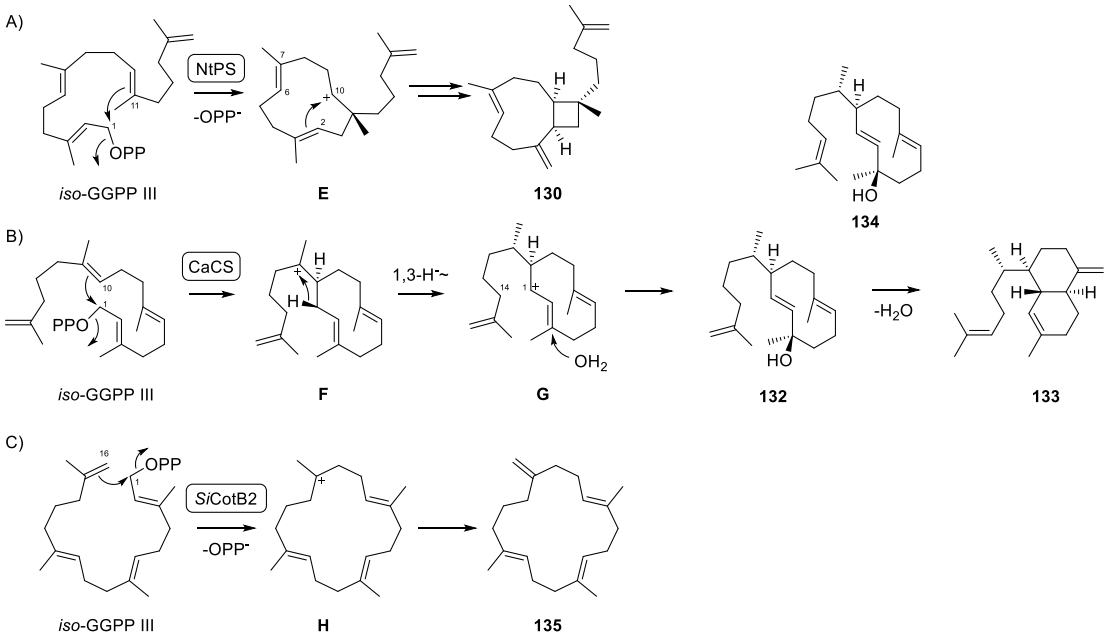

Scheme 31. Diterpenes obtained from NtPS, CaCS and *Si*CotB2. Cyclization of *iso*-GGPP III with A) NtPS to form **130**, with B) CaCS to form **132** and **133**, and with C) *Si*CotB2 to form **135**.

With CgDS, the natural substrate GGPP was converted to δ-araneosene (**136**) and dolasta-1(15),8-diene (**137**), while unnatural *iso*-GGPP III was converted to dolastaxenene (**138**). The formation of **137** starts from 1,11-10,14-cyclization while the formation of **138** is altered to 1,10-11,16-cyclization, in which the shifted double bond at C16=C17 was involved, leading to the cation **L**. Then cyclization cascade continues with a deprotonation to **136'**, followed by a reprotonation and 2,7-cyclization to **138**. The whole process is as observed with the natural intermediate **136** towards **137**. (Scheme 32)

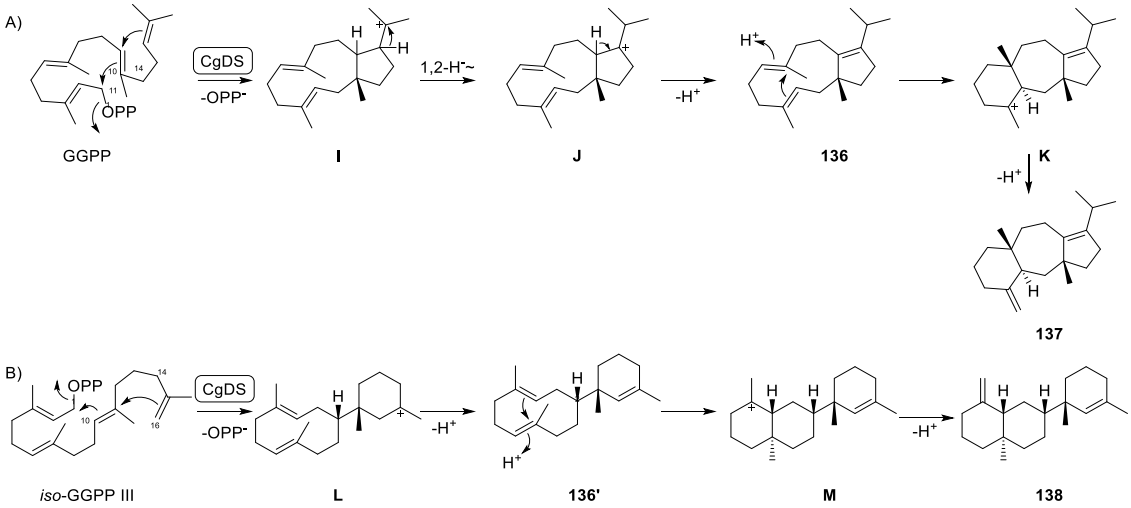

Scheme 32. Diterpenes obtained from CgDS. Cyclization of A) GGPP to form **136** and **137**, and of B) to form **138**.

Like the cases mentioned in other chapters, the absolute configurations of the terpene analogs were investigated by a stereoselective isotopic labelling strategy. In this chapter, the absolute configurations of **129**, **130**, **132**, **133** and **138** were assigned as shown in the schemes above. In this study, I conducted all enzymatic transformations, product isolations and structure elucidations, and also performed all the labelling experiments to determine the absolute configurations of different compounds.

Chapter 5

Enzyme-Catalysed Formation of Hydrocarbon Scaffolds from Geranylgeranyl Diphosphate Analogs with Shifted Double Bonds

Heng Li[a], Bernd Goldfuss[b] and Jeroen S. Dickschat[a]*

[a] Heng Li, Prof. Dr. Jeroen S. Dickschat, Kekulé-Institute for Organic Chemistry and Biochemistry, University of Bonn, Gerhard-Domagk-Straße 1, 53121 Bonn, Germany, E-mail: dickschat@uni-bonn.de

[b] Prof. Dr. Bernd Goldfuss, Department for Chemistry, University of Cologne, Greinstraße 4, 50939 Cologne, Germany

The publication “Enzyme-Catalysed Formation of Hydrocarbon Scaffolds from Geranylgeranyl Diphosphate Analogs with Shifted Double Bonds” can be found in Appendix D.

Introduction

The investigation of *iso*-GGPPs was continued with the synthesis of four new *iso*-GGPP analogs featuring different double bond shifts and the activity tests on 14 known DTSs. The corresponding unnatural diterpenes were isolated and characterised. This work showed that unnatural biotransformations can not only lead to the formation of terpenes with new skeletons, but also can be useful for detailed mechanistic investigation of natural terpene synthases. Here, two new diterpene synthase homologs benditerpe-2,6,15-triene synthase (Bnd4) and venezuelaene synthase (VenA), were characterised. The hydride migrations in the biosynthesis of benditerpe-2,6,15-triene and venezuelaene including their unnatural diterpene counterparts from *iso*-GGPP I were investigated.

Summary

The benditerpe-2,6-15-triene synthase Bnd4 (accession number: WP_033312626) from *Streptomyces iakyrus* NRRL ISP-5482 exhibits 92% sequence identity towards its previously reported homolog Bnd4 from *Streptomyces* sp. CL12-4[121]. After an activity test with GGPP, its product was confirmed by GC/MS, which is the thermally unstable compound benditerpe-2,6,15-triene (**139**).

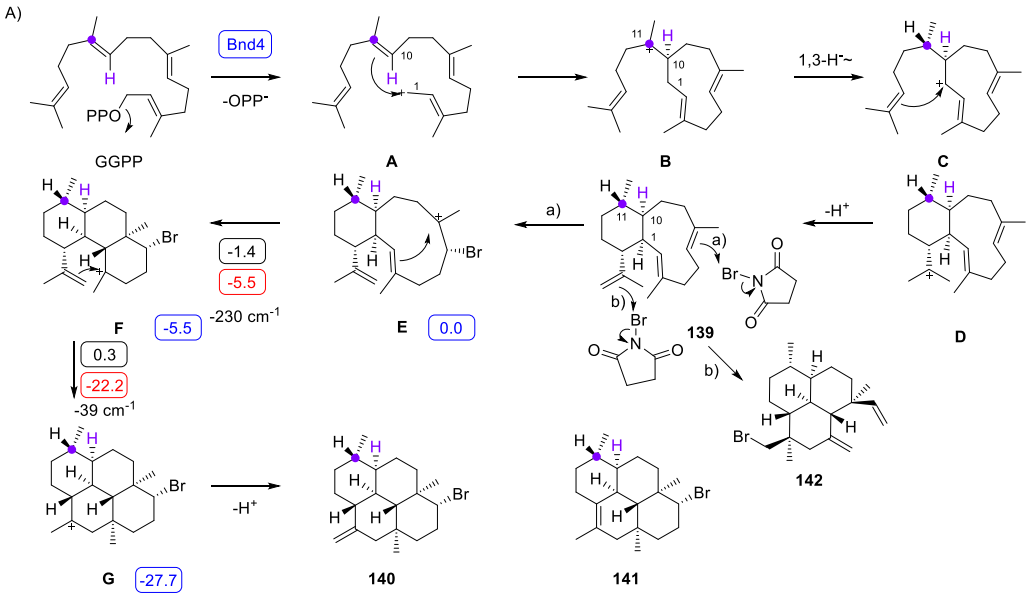

Scheme 33. Biosynthetic proposal for the compounds **139**-**142**.

The biosynthesis of **139** had been investigated and the 1,3-hydride migration from **B** to **C** (Scheme 33) was proposed based on the incubation of (1,1-$^2H_2$)GGPP, product isolation and

NMR spectroscopy in conjunction with DFT calculations[122]. Here, we proposed an easier method with the incubation of a substrate with deuterium at C1 and ^{13}C at C11. If the 1,3-hydride migration happens, the ^{13}C-^{2}H coupling will give the obvious triplet signal in the ^{13}C-NMR spectrum. However, the line broadening caused by the flexible ring system of **139** prevented triplet observation, and this issue was further solved by conversion of **139** with NBS to rigidify its skeleton. Consequently, three brominated compounds **140**-**142** were isolated and structurally characterized, and their mechanisms of formation were investigated by quantum chemical calculations. The results showed that the bromonium intermediate **E** can undergo a barrierless cyclization to **F**. Further conversion of (7-^{13}C,6-^{2}H)FPP plus IPP with GGPPS and Bnd4, followed by NBS treatment yielded labelled **140** with an upfiled shifted singlet for C11 ($\Delta\delta$ = –0.06 ppm), indicating a deuterium effect from the neighboring position. This result further supports the 1,3-hydride migration from **B** to **C**, while a similar 1,3-hydride shift was observed in the biosynthesis of benditerpe-2,7(19),15-triene (**143**) that was isolated from the incubation of *iso*-GGPP I with Bnd4 (Scheme 34).

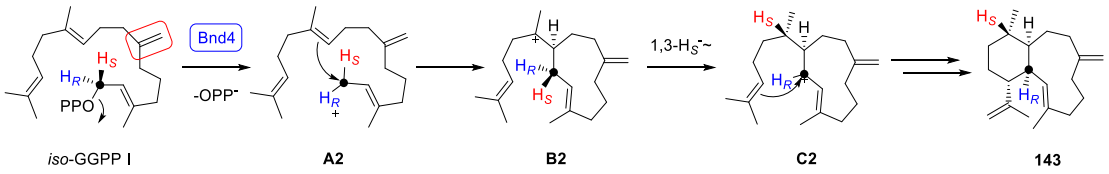

Scheme 34. Biosynthetic proposal for the compounds **143**.

The second investigated enzyme is a VenA homolog from *Streptomyces exfoliatus* DSM 41693, which shares 97% sequence identity towards the previously reported VenA from *Streptomyces venezuelae* ATCC 15439[123]. After the isolation of venezuelaene A (**144**), its biosynthesis was proposed as shown in Scheme 3, but the biosynthetic mechanism regarding a single 1,3-hydride shift or two sequential 1,2-hydride shifts from **I** to **K** was not clear. In order to distinguish these two possible pathways, an incubation experiment with (7-^{13}C,6-^{2}H)FPP plus IPP, GGPPS and VenA was conducted, and the corresponding triplet signal for C11 of **144** ($\Delta\delta$ = – 0.52 ppm, $^{1}J_{C,D}$ = 19.4 Hz) was observed. Another conversion of (3-^{13}C)GPP plus (1,1-$^{2}H_2$)IPP with GGPPS and VenA gave a singlet peak for C11 of **144** ($\Delta\delta$ = –0.12 ppm), which indicates the deuterium being located in a neighboring position of C11. Both experiments uncovered the two sequential 1,2-hydride migrations in the biosynthesis of **144**. Analogously, similar hydride shifts in the biosynthesis of the unnatural counterpart **145** was also confirmed by the incubation of (*R*)- and (*S*)-(1-^{13}C,1-^{2}H)-*iso*-GGPP I with VenA (Scheme 35).

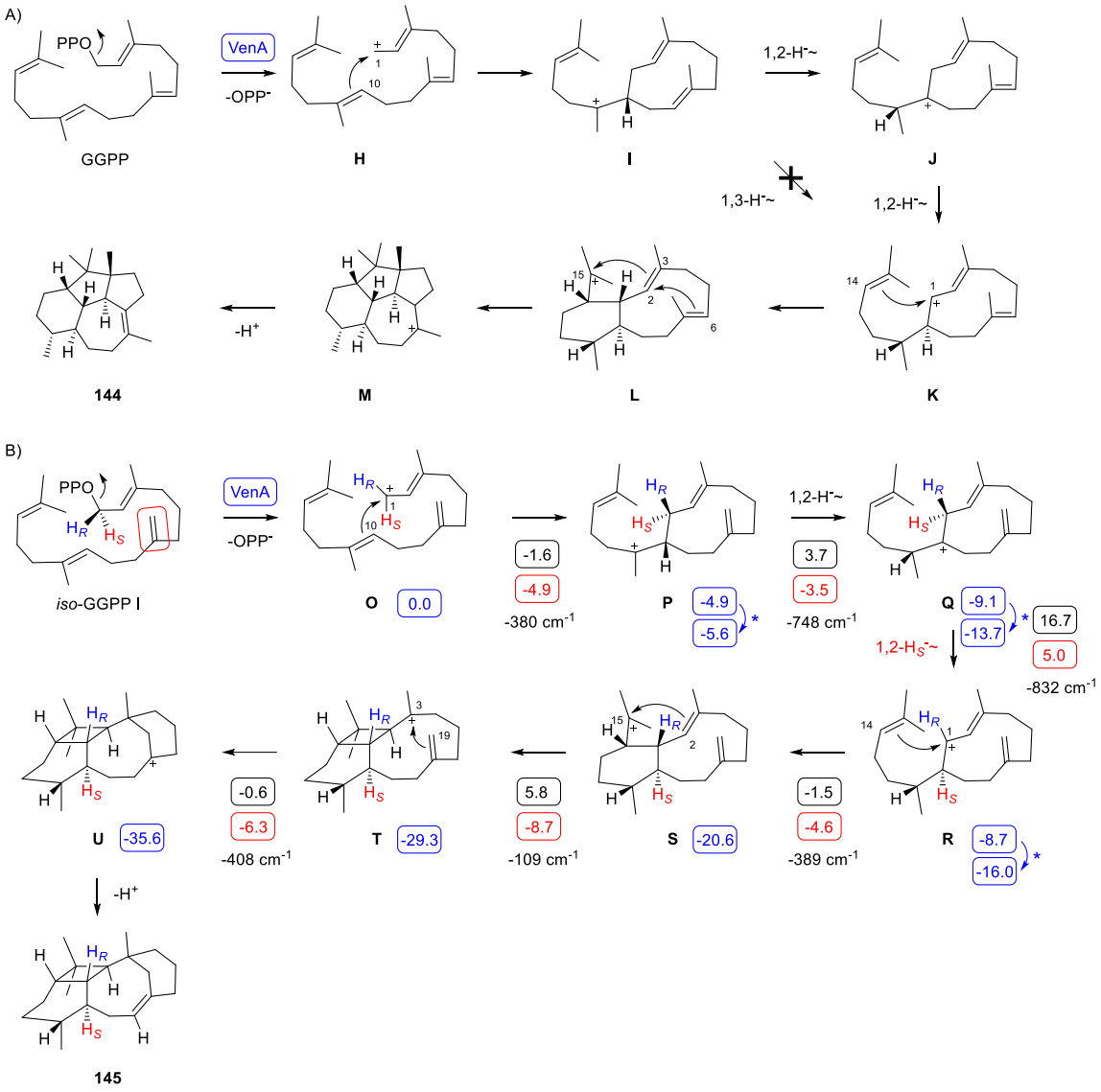

Scheme 35. The diterpene synthase VenA. A) The formation of **144** from GGPP, and B) the formation of **145** from iso-GGPP I.

The FPP homolog *iso*-FPP III was synthesized and was enzymatically elongated to *iso*-GGPP VI by GGPPS (Scheme 36), while other substrate analogs were chemically synthesized based on similar methods as mentioned in the last three chapters.

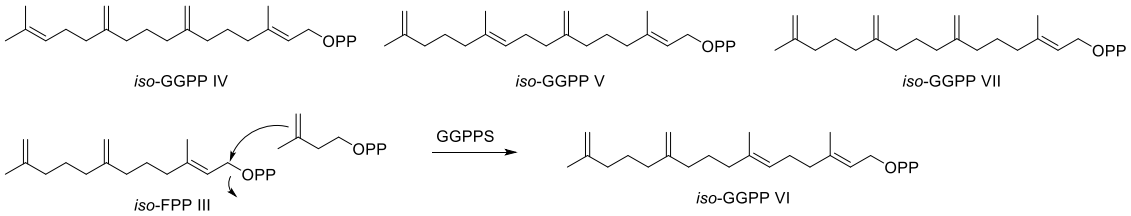

Scheme 36. The structures of *iso*-GGPP analogs.

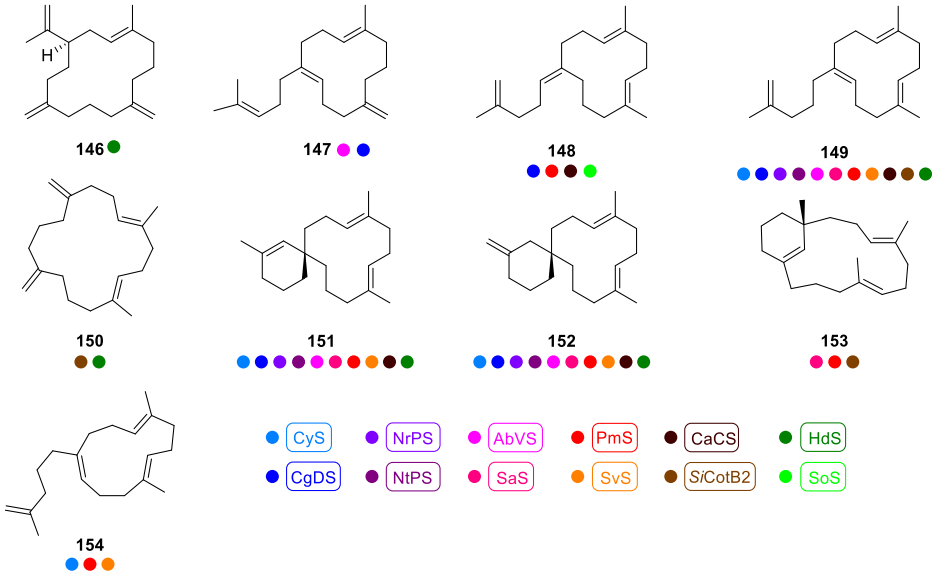

Scheme 37. Isolated compounds from the incubation of *iso*-GGPPs with various DTSs. Coulored dots indicate compound production by enzymes according to the colour code at the bottom of the scheme.

Large scale enzymatic incubations were performed to give new unnatural terpenes (Scheme 37). For example, diisocembrene A (**146**) and prenylpseudogermacrene B (**147**) were both isolated from the incubation of *iso*-GGPP IV, but with different enzymes HdS and AbVS, respectively. Their formations can be explained with a one-step cyclization and deprotonation. In addition, the compounds from **148**-**154** all were obtained from the enzymatic conversion of *iso*-GGPP VI which derived from its precursor *iso*-FPP III with different diterpene synthases. Interestingly, α-spirocattleyaxenene (**151**) and β-spirocattleyaxenene (**152**) occurred in many crude products of enzymatic reactions, but these compounds coeluted in the GC/MS analysis and shared very similar mass spectra. In order to distinguish the product profile between different enzymes, the incubations of *iso*-FPP III plus (1-^{13}C)IPP with GGPPS and diterpene synthases were performed. Based on the enhanced ^{13}C-NMR signal and the different chemical shifts of C1 in **151** and **152**, NtPS, HdS, SVS and CotB2 were confirmed as the producers of both compounds, while CyS, NrPS, SaS, CaCS, and AbVS are producers of only **151**, and CgDS and PmS only produces **152**.

In this study, I was responsible for performing the gene cloning, protein expressions, enzymatic transformations, product isolations and structure elucidations, and also conducted all the labelling experiments to determine the different hydrides migrations.

Chapter 6

Mechanistic Characterisation of the Diterpene Synthase for Clitopilene and Identification of Isopentalenene Synthase from the fungus *Clitopilus passeckerianus*

Heng Li,[a] Bernd Goldfuss[b] and Jeroen S. Dickschat[a]*

[a] Heng Li, Prof. Dr. Jeroen S. Dickschat, Kekulé-Institute for Organic Chemistry and Biochemistry, University of Bonn, Gerhard-Domagk-Straße 1, 53121 Bonn, Germany, E-mail: dickschat@uni-bonn.de

[b] Prof. Dr. Bernd Goldfuss, Department for Chemistry, University of Cologne, Greinstraße 4, 50939 Cologne, Germany

The publication “Mechanistic Characterisation of the Diterpene Synthase for Clitopilene and Identification of Isopentalenene Synthase from the fungus *Clitopilus passeckerianus*” can be found in Appendix E.

Introduction

Besides the discovery of artificial terpenoids, genome mining for novel natural terpenoids has also been studied in this thesis. Here, the producer of the antibacterial drug pleuromutilin *Clitopilus passeckerianus*, was chosen as a target for bioinformatics analysis, and the antiSMASH analysis showed several unknown terpene synthases encoded in the genome of *C. passeckerianus* DSM 1602. One diterpene named clitopilene exhibiting a novel 6-6-5-5 terpene skeleton and one sesquiterpene identified as isopentalenene were confirmed as the products of the enzyme CpTS1 and CpTS2, respectively.

Summary

The total mRNA of *C. passeckerianus* DSM 1602 was isolated and used as a template in a reverse transcriptase polymerase chain reaction (RT-PCR) to obtain a cDNA library containing the coding sequences of two new terpene synthase candidates. After gene cloning and protein expression in *E. coli* BL21 (DE3), both enzymes were tested for their functions through the incubation of GPP, FPP, GGPP and GFPP. The first enzyme (CpTS1, accession number: PP777465) was identified as a diterpene synthase based on the GCMS analysis of the crude extract from the enzymatic reaction with GGPP. A large scale enzymatic incubation was performed for the isolation of the major product, and its structure was elucidated through NMR spectroscopy as a new diterpene clitopilene (**155**) with a 6-6-5-5 tetracyclic skeleton.

The NOESY based assignments were used to determine the relative configuration of **155**, and as mentioned in Chapter 2, artificial stereogenic centers of known configurations at C1, C5, C9 and C13 can be introduced by the incubation of (*R*)- or (*S*)-(1-^{13}C, 1-^{2}H)IPP with IDI, GGPPS and CpTS1. These data were combined with the relative orientation of hydrogens at these position in **155**, pointing to the absolute configuration of **155** as shown in Scheme 38. Additional experiments using DMAPP and (*E*)- or (*Z*)-(4-^{13}C,4-^{2}H) gave further support for the assigned absolute configuration.

The biosynthesis of **155** shared a similar pathway as other diterpenes including phomopsene[75], spiroviolene[74], and allokutznerene[79], proceeding through the same intermediate **A** to **E** with 1,11-10,14-cyclization of GGPP, ring closure and reopening. Our DFT calculations showed all steps are energetically feasible, which is agreement with the previous computations by Hong and Tantillo[124]. Subsequently, a specific 1,2-hydride shift from **E** to **F** was proposed, that was also evident from the detection of a triplet for C3 of **155** ($\Delta\delta$ = –0.50 ppm, $^{1}J_{C,D}$ = 19.2 Hz) obtained from the conversion of (3-^{13}C,2-^{2}H)GGPP with CpTS1. After a 2,6-cyclization, another

1,2-hydride shift from **G** to **H** was also confirmed through the incubation of (3-^{13}C,2-^{2}H)FPP with GGPPS and CpTS1. As the result, the ^{13}C-^{2}H spin coupling gave a triplet signal for C7 ($\Delta\delta$ = –0.54 ppm, $^{1}J_{C,D}$ = 19.5 Hz) in the ^{13}C-NMR spectrum. The remaining steps from **H** to **155** contain a 1,3-hydride shift, a skeleton rearrangement and deprotonation. Similarly, (2-^{13}C)FPP plus (1,1-^{2}H$_2$)IPP were converted by GGPPS to yield (6-^{13}C,1,1-^{2}H$_2$)GGPP which was subsequently converted by CpTS1 to yield labelled **155** with a deuterium residing at C6 ($\Delta\delta$ = –0.52 ppm, $^{1}J_{C,D}$ = 19.0 Hz). Additional experiments with (*R*)- and (*S*)-(1-^{13}C,1-^{2}H)IPP showed that only the specific 1-*pro-R* hydrogen of GGPP migrates to C6, which answers the question about the precise stereochemical course of the migration of two enantiotropic hydrogens. The last surprising skeletal rearrangement was particularly confirmed by the enzymatic conversion of 20 isotopomers of (^{13}C)GGPP (Scheme 38).

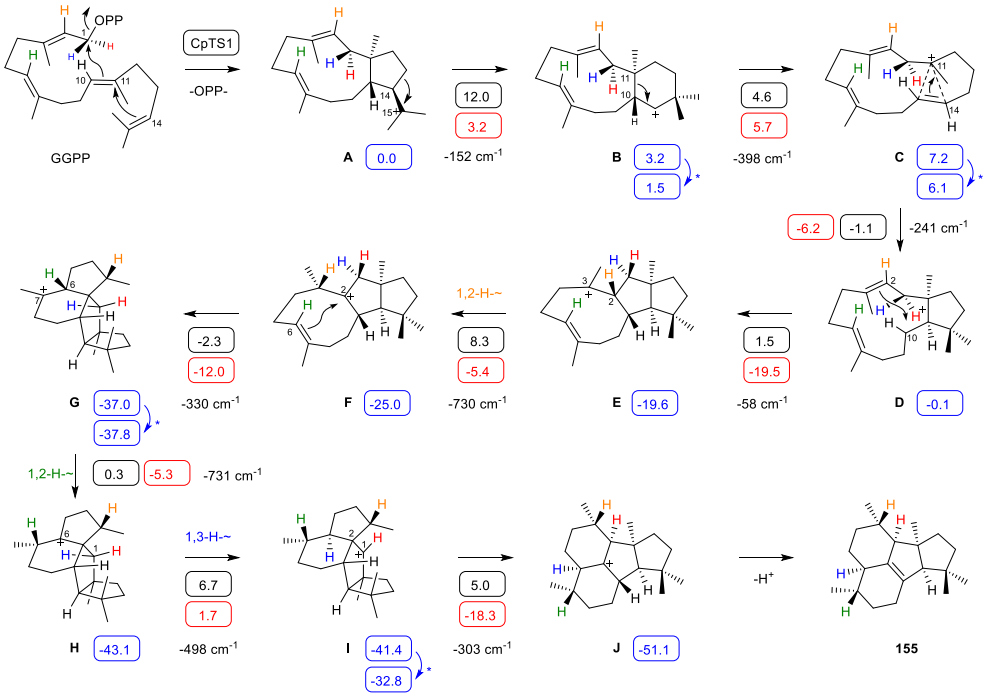

Scheme 38. Proposed cyclization mechanism from GGPP to clitopilene (**155**). The numbers in blue boxes are computed energies relative to A (set as 0.0 kcal/mol), numbers in black boxes are reaction barriers, and numbers in red boxes are Gibbs free energies (all in kcal/mol, mPW1PW91/6-311+G(d,p)//B97D3/6-31 g(d,p), 298 K).

The second enzyme (CpTS2, accession number: PP777466) was identified as isopentalenene synthase. The incubation of FPP with this enzyme yielded a large quantity of isopentalenene (**156**) besides minor amounts of pentalenene (**26**) and other trace compounds (Scheme 39). After labelling experiments with (*E*)- and (*Z*)-(4-^{13}C,4-^{2}H)IPP, its absolute configuration was determined as shown in Scheme 39. The biosynthetic proposal of **156** is similar to **26**, a

sesquiterpene that has been studied intensively[52-55,57,58,61], while the final deprotonation happened from C6 not C8.

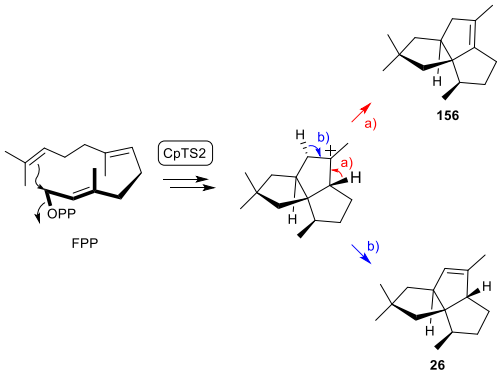

Scheme 39. Conversion of FPP into isopentalenene (**156**, main product) and pentalenene (**26**, minor product) by CpTS2.

In this study, I performed gene cloning, protein expression, enzymatic transformations, product isolations and structure elucidations, and also conducted all the labelling experiments.

Chapter 7

A Hydrophobic Tunnel and a Gatekeeper at the Active Site Entrance in Two Type I Terpene Synthases

Heng Li,[1,‡] Zhaoye Bai,[2,‡] Georges B. Tabekoueng,[1] Baiying Xing,[2] Bernd Goldfuss,[3] Ming Ma,[3] Donghui Yang*,[3] and Jeroen S. Dickschat*,[1]

[1]Kekulé-Institute for Organic Chemistry and Biochemistry, University of Bonn, Gerhard-Domagk-Straße 1, 53121 Bonn, Germany

[2]State Key Laboratory of Natural and Biomimetic Drugs, School of Pharmaceutical Sciences, Beijing University, 38 Xueyuan Road, Haidian District, Beijing 100191, China

[3]Department for Chemistry, University of Cologne, Greinstraße 4, 50939 Cologne, Germany

The publication “A Hydrophobic Tunnel and a Gatekeeper at the Active Site Entrance in Two Type I Terpene Synthases” can be found in Appendix F.

Introduction

The substrate scope of terpene synthases is often highly strict, limiting their applications in the terpene field. The diterpene synthase, spatadiene synthase (*Sx*SpS) is a well-known enzyme that can accept FPP, GGPP and GFPP as substrates. Here, we demonstrated that *Sx*SpS is even able to accept FFPP as a substrate to produce two triterpenes. With the help of enzyme crystallography, docking studies and site-directed mutagenesis, we demonstrated the existence of a hydrophobic tunnel that is connected to the active site and can adopt non-reacting spectator isoprenoid units in *Sx*SpS. The application of this finding on selina-4(15),7(11)-diene synthase (SdS) allowed us to expand its substrate scope from FPP to GGPP.

Summary

The enzyme *Sx*SpS from *Streptomyces xinghaiensis*[70] can produce spata-13,17-diene (**157b**) as the main product, and prenylkelsoene (**158b**) and cneorubin Y (**159b**) as the side products. Their biosynthesis can be explained from the 1,10-cyclization (accounting based on GGPP) and subsequent cyclization reaction with participation of the first three terpene units[70]. Further incubation experiments with FPP and GFPP yielded the products sharing the same core skeletons as shown in Scheme 40, indicating that they follow similar cyclization steps. In this study, a TS homolog from *Streptomyces platensis* DSM 40041 (*Sp*SpS, accession number: WP_085926110) was investigated with the same function as *Sx*SpS, but only 28% sequence identity to the latter. Differently, the activity of *Sp*SpS towards GFPP is higher than that of the *Sx*SpS, which allowed for the isolation and characterization of geranylkelsoene (**158c**), one compound that was previously identified as the product of *Sx*SpS by GC/MS, but has never been isolated before.

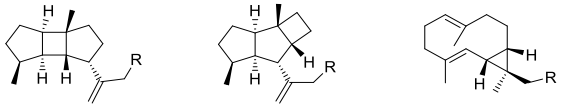

157a (R=H)
157b (R=prenyl)
157c (R=geranyl)
157d (R=farnesyl)

158a (R=H)
158b (R=prenyl)
158c (R=geranyl)
158d (R=farnesyl)

159a (R=H)
159b (R=prenyl)
159c (R=geranyl)
159d (R=farnesyl)

Scheme 40. The products of *Sx*SpS.

All known triterpenes are generated by triterpene synthases from squalene[125] or oxidosqualene[126,127] before the first type I triterpene synthases discovered[128]. Here, we surprisingly found *Sx*SpS and *Sp*SpS both can convert FFPP to triterpenes, but the *Sx*SpS exhibits higher activity. Product isolation and NMR based characterization identified the main

product as geranylspata-13,17-diene (**157d**). In addition, farnesylkelsoene (**158d**) was tentatively identified as a side product of the *Sx*SpS by GC/MS.

In order to deeply investigate the molecular basis behind the special cyclization mode that only first three isoprene units are involved in the cyclization, an X-ray crystal structure of *Sx*SpS was obtained in the open conformation in complex with one Mg^{2+} bound to the NSE triad, named *Sx*SpS-Mg^{2+} (Figure 5). The structure features the typical α-helical fold as reported for many type I terpene synthases[30,33,105], and possesses the unique helix G break motif with the effector triad for the substrate ionization. Interestingly, we also observed a hydrophobic tunnel between helices C and F which is directly connected to the active site and closed at the back by the three residues F170, L174 and V211 (Figure 5B). Another three aligned small residues (C177, A181, and A185) shape a space of ~250 $Å^3$ (ca. 12 Å long and 5 Å in diameter), which is sufficient to adopt up to three isoprene units (the calculated van der Waals volume of one unit is 74 $Å^3$). We assumed that the function of this tunnel is related to the accommodation of the spectator units of the substrates, which can explain their non-participations in the cyclization process. Further docking studies with FFPP showed that its tail stretches out into the tunnel, which supports our hypothesis (Figure 5C).

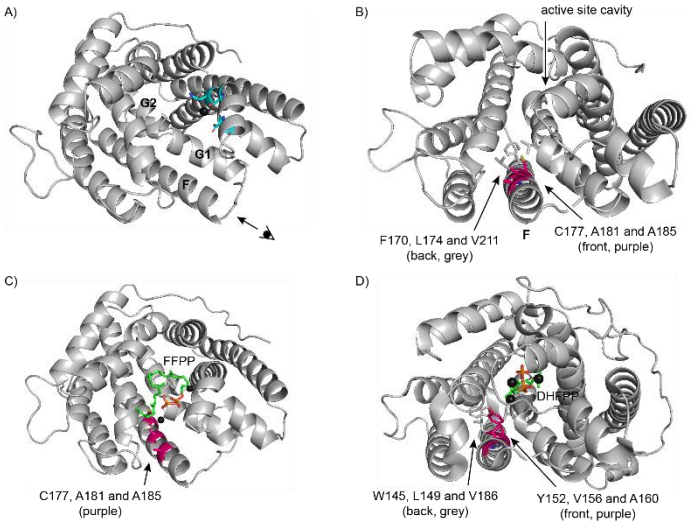

Figure 5. The X-ray structure of *Sx*SpS-Mg^{2+}. A) Open conformation in complex with one Mg^{2+}. The stylized eye and arrow indicate the view into the tunnel. B). View into the substrate tunnel which is closed by F170, L174 and V211. C) Docking of FFPP to *Sx*SpS. D) Crystal structure of SdS (PDB: 4OKZ), DHFPP = 1,2-dihydro-FPP.

We also found a similar tunnel in the structure of selina-4(15),7(11)-diene synthase (SdS, PDB: 4OKZ) in complex with the substrate analog 1,2-dihydro-FPP (Figure 5D). The structural comparison of SdS and *Sx*SpS disclosed that the larger residues (Y152 and V156) occupied the positions of the spacious substrate tunnel, while the smaller residue Ala in both cases is far

away from the active site (Figure 5B and 5D). We thereby assumed the function of the key residue Y152 in SdS working as a gatekeeper to block the substrate tunnel, resulting in the acceptance of only FPP. Furthermore, C177 is highly conserved in *Sx*SpS and other 36 SpS homologs, while this position is occupied by a Tyr in 212 *epi*-cubenol synthase homologs, indicating the importance of this position to differentiate the function as a synthase for sesquiterpenes, diterpenes or even higher terpenes.

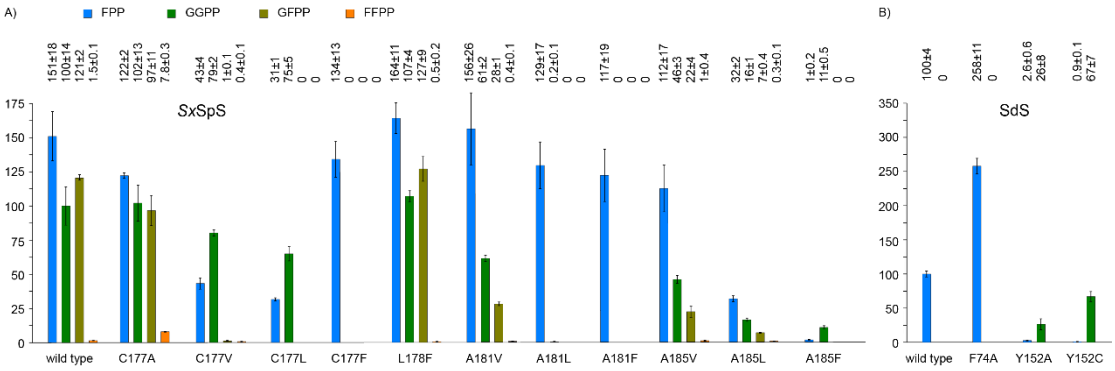

Figure 6. Relative terpene production of A) *Sx*SpS and B) SdS (wild type and enzyme variants).

Site-directed mutagenesis experiments with both *Sx*SpS and SdS were performed (Figure 6) to investigate the function of some key residues in the tunnel. As a consequence, the C177F variant of *Sx*SpS indeed completely abolished the activity towards GGPP and the larger substrates, while the C177L and C177V variants lost the ability of converting GFPP and FFPP. On the contrary, exchange with a smaller residue Ala in this position significantly increased (almost four times higher than the wild type) the production of triterpenes. Further mutations were conducted with the exchange of Phe, Leu and Val in the positions of A181 and A185 which are more going out from the active site. Two clear trends were observed: 1. the larger the residues in these two positions are, the smaller the substrate that can be accepted; 2. the more exterior from the active site the positions are, the less pronounced the observed effect on the substrate tolerance was.

In addition, the smaller residues Ala and Cys against the gatekeeper Y152 (Y152A and Y152C) in SdS resulted in the acceptance of GGPP and the formation of one diterpene hydrocarbon. The more productive variant Y152C was used for the large scale enzymatic transformation with the identification of prenylgermacrene A (**160**), after product isolation and NMR-based charactization. Lobophytumin C (**161**) and prenyl-α-selinene (**162**) were also isolated during the chromatographic purification due to the cyclic reaction of **160** catalyzed by slightly acidic silica gel, which is similar to the reported behavior of germacrene A[129-131] The thermal instability of **160** allowed us to obtain the Cope rearrangement product **160***, by heating the solution of **160** in Ph_2O to 180 °C in a pressurized tube (Scheme 41).

The optical rotations of compounds **160**-**162** and **160*** were compared to the previously reported data for the same or structurally related compounds, leading to the conclusion of the absolute configurations of these compounds. Further evidence was obtained from our labelling experiments with (*R*)- or (*S*)- and (*E*)- or (*Z*)-substrates as mentioned in the previous chapters. Subsequently, all four labelling samples were heated to obtain the rearranged compound **160***, and the analysis through HSQC spectroscopy gave insights into its absolute configuration.

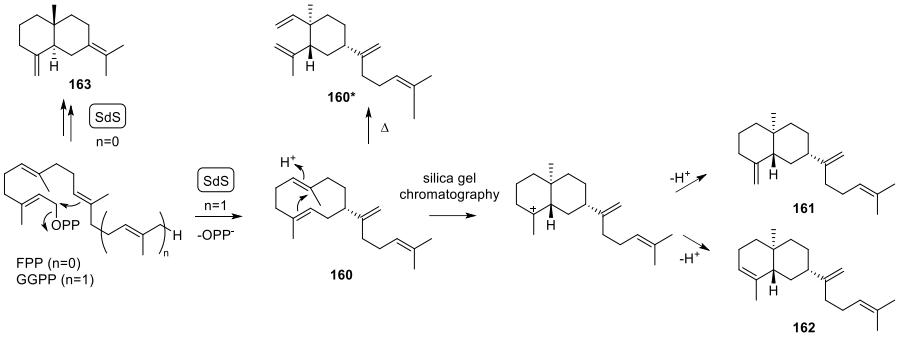

Scheme 41. Conversion of FPP into selina-4(15),7(11)-diene (**163**) and of GGPP into **160** by SdS, thermal rearrangement to **160*** and silica gel induced formation of **161** and **162**.

In this study, I performed the site-directed mutagenesis, enzymatic transformations, product isolations and structure elucidations, and also conducted all the labelling experiments to determine the absolute configurations of compounds.

Chapter 8

On the Role of Hydrogen Migrations in the Taxadiene System

Heng Li,[a] Bernd Goldfuss[b] and Jeroen S. Dickschat[a]*

[a] Heng Li, Prof. Dr. Jeroen S. Dickschat, Kekulé-Institute for Organic Chemistry and Biochemistry, University of Bonn, Gerhard-Domagk-Straße 1, 53121 Bonn, Germany, E-mail: dickschat@uni-bonn.de

[b] Prof. Dr. Bernd Goldfuss, Department for Chemistry, University of Cologne, Greinstraße 4, 50939 Cologne, Germany

The publication “On the Role of Hydrogen Migrations in the Taxadiene System” can be found in Appendix G.

Introduction

The biosynthesis of taxa-4,11-diene has extensively been investigated through isotopic labelling experiments and computational study[132-140], and selective long range hydrogen migrations in the biosynthesis have been confirmed[133]. In our study, we revealed that this unique migration also plays a role in the high energy process of the EI-MS fragmentation of taxa-4,11-diene. Site-directed mutagenesis and biotransformation of a substrate analog were involved in this study to obtain cyclophomactene and taxaxenene, two compounds with taxane system that both showed similar long range proton shifts in their biosynthesis.

Summary

Taxa-4,11-diene synthase (TxS) from *Taxus brevifolia* exhibits a low protein expression which is the limited step for the conversion of GGPP to taxa-4,11-diene. Thus, 78 amino acids were removed from the N-terminal of TxS, which is known for the improvement of the soluble protein in the expression in *Escherichia coli*[141]. In this study, the N-truncated enzyme was referred to as “TxS”, which can convert GGPP to taxa-4,11-diene (**18**) and its isomer taxa-4(20),11-diene (**164**). Both compounds were isolated from a preparative incubation of GGPP followed by an NMR-based assignment. The labelling experiments with stereoselective deuterated substrates allowed us to assign the absolute configuration of **18** as that of taxol that has been established through enantioselective synthesis[142].

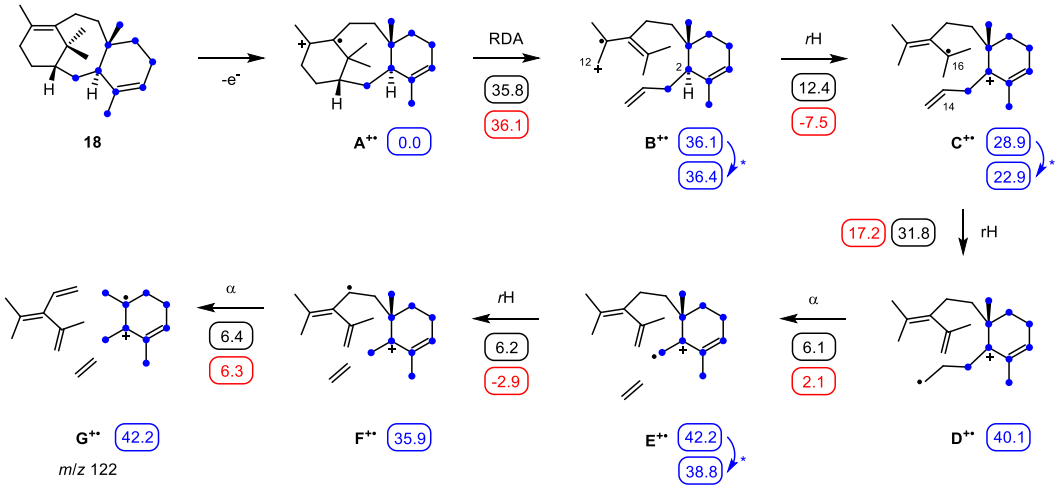

Scheme 42. EI mass fragmentation mechanism for the base peak ion *m/z* 122 of **18**.

The twenty isotopomers of (^{13}C)GGPP, obtained through chemical synthesis or by enzymatic transformations from their corresponding labelled diphosphate precursors, were converted by TxS to obtain ^{13}C-labelled **18**, showing the general carbon skeleton assembly. The base peak

at *m*/*z* 122 in the EI mass spectrum of **18** will increase to *m*/*z* 123 for its singly ^{13}C-labelled isotopomers. As shown in Scheme 42, the nine carbons in the eastern portion of **18** are marked by the blue dots, indicating their contributions to the base peak at *m*/*z* 122. Mechanistically, it can be explained by the ionization of **18** to $\mathbf{A}^{+\bullet}$ followed by a Retro-Diels-Alder (RDA) fragmentation to $\mathbf{B}^{+\bullet}$ and hydrogen migration to $\mathbf{C}^{+\bullet}$. Subsequently, the steps from $\mathbf{C}^{+\bullet}$ to $\mathbf{G}^{+\bullet}$ contain a hydrogen migration, α-fragmentation to lose ethylene, another hydrogen rearrangement and final α-cleavage (Scheme 42). DFT calculations showed that the highest activation barrier is +35.8 kcal/mol and the strongly positive Gibbs free energy for RDA is +36.1 kcal/mol, which can be overcome by the high ionization energy used (70 eV ≈ 1614 kcal/mol). The second high barrier (31.8 kcal/mol) is from $\mathbf{C}^{+\bullet}$ to $\mathbf{D}^{+\bullet}$, because this reaction leads to a primary radical cation, while the reaction barriers for the steps from $\mathbf{D}^{+\bullet}$ to $\mathbf{F}^{+\bullet}$ are only ca. 6 kcal/mol low. The incubation of (2-^{2}H)GGPP with TxS and the subsequent GC/MS analysis of the product showed no increase for the base peak at *m*/*z* 122, indicating the loss of a deuterium from the corresponding fragment ion. This experiment supported the key step from $\mathbf{B}^{+\bullet}$ to $\mathbf{C}^{+\bullet}$, a long distance hydrogen migration during the fragmentation reaction.

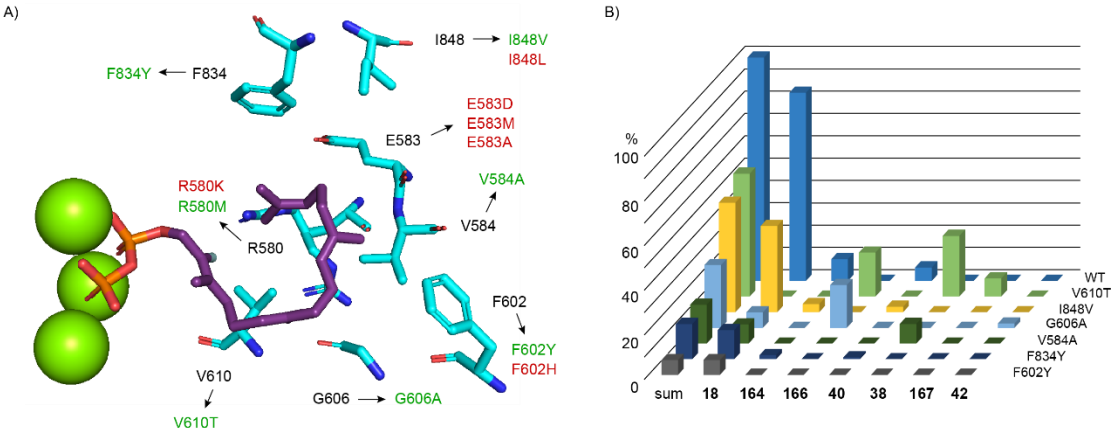

Figure 7. Site-directed mutagenesis of TxS. A) Active site residues selected for the site-directed mutagenesis study. B) Relative production of enzyme variants.

Several residues were selected as targets for site-directed mutagenesis experiments based on the crystal structure of the TxS. Many of the tested enzyme variants were inactive or exhibited a strongly reduced production. The residue I848 is close to F843, a residue that may be involved in a cation-π stabilization of the cationic intermediate. A comparison of the X-ray structure of TxS with the Alphafold model of the I848L variant demonstrated a strong disturbance of F834 caused by this variant, explaining the complete abolishment of the activity. Further variants E583D, E583M, E583A, R580K, R580M and F602H are inactive, while V584A, F602Y, F834Y and I848V all showed a reduced activity (Figure 7). Besides **18** and **164**, compounds verticilla-4(20),7,11-triene (**165**), verticilla-3,7,12-triene (**166**), verticilla-3,7,11-triene (**40**) and cembrene

A (**38**) are frequently observed. However, the structure of compound **40** was just assigned based on a comparison of the mass spectrum of **40** with the reported data by Brück and coworkers[143], leading to a tentative structural assignment. Among the variants, G606A showed a good selectivity towards compound **166**, and also formed a side product that was isolated and structurally characterised as a new compound cyclophomactene (**42**). Another variant V610T completely lost the activity towards **18**, but compounds **166**, **38** and cembrene D (**167**) were still formed.

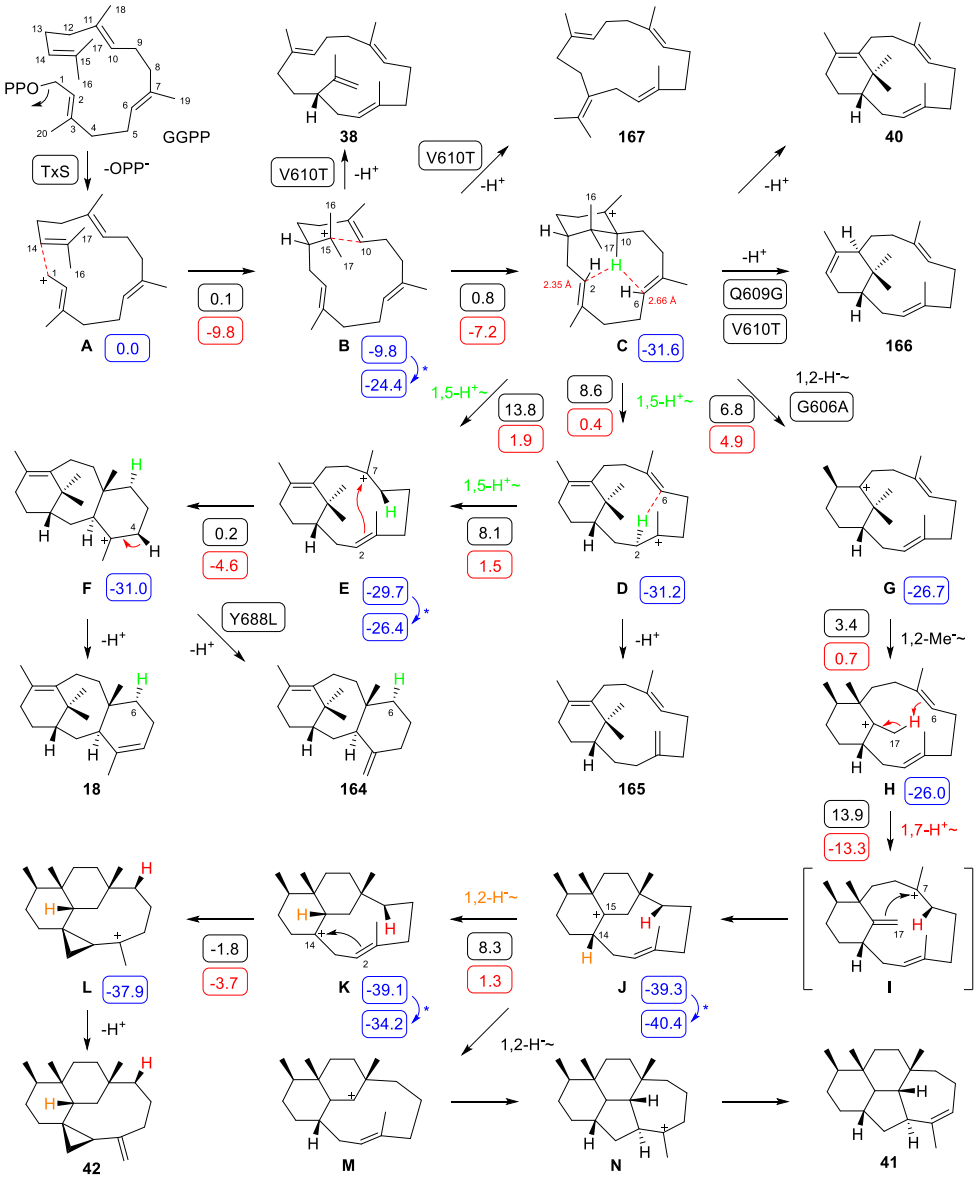

Scheme 43. Taxa-4,11-diene biosynthesis. Mechanism for the cyclisation of GGPP to **18** and biosynthetically related products by TxS and its enzyme variants.

Further DFT calculations were performed to help us understand the formation of **42**. The calculated results for the reactions from **A** to **F** are similar to the previous reports[135,136]. Our

calculations showed the sequence of two 1,5-proton shifts (**C**-**D**-**E**) was favored over the direct proton shift (**C**-**E**) with the lower reaction barriers. A 1,2-hydride shift from **C** to **G** branches out to the formation of **42**, with a 1,2-methyl group migration to **H**, an intramolecular 1,7-proton shift to **I**, an unusual 7,17-cyclization to **J**, 1,2-hydride shift to **K**, a 2,14-cyclization to **L** and deprotonation to **42**. The direct transformation from **H** to **J** with skipping of the intermediate **I** showed the highest activation barrier of 13.9 kcal/mol, indicating this is the rate-limiting step towards **42**. This step from **H** to **J** was also experimentally investigated with the conversion of the (4,4,4,5,5,5-$^{2}H_6$)DMAPP plus (2-^{13}C)IPP by GGPPS and TxS-G606A variant. Because of the kinetic isotope effect which was calculated as K_H/K_D = 7.2, this conversion was strongly reduced in comparison to that from unlabelled GGPP. Thus, the expected triplet signal in the ^{13}C-spectrum (as the result of ^{13}C-^{2}H coupling) for C6 of **42** was not observed. However, the GC/MS analysis showed that all six deuterium atoms of the substrate remained in the product **42**, supporting the proton shift from C17 to C6. A similar 1,7-proton shift has also been proposed for the biosynthesis of cephalotene (**41**). Differently, the biosynthesis of cephalotene proceeds to the intermediate **J** and branches out to **M** and **N** (Scheme 43)[78].

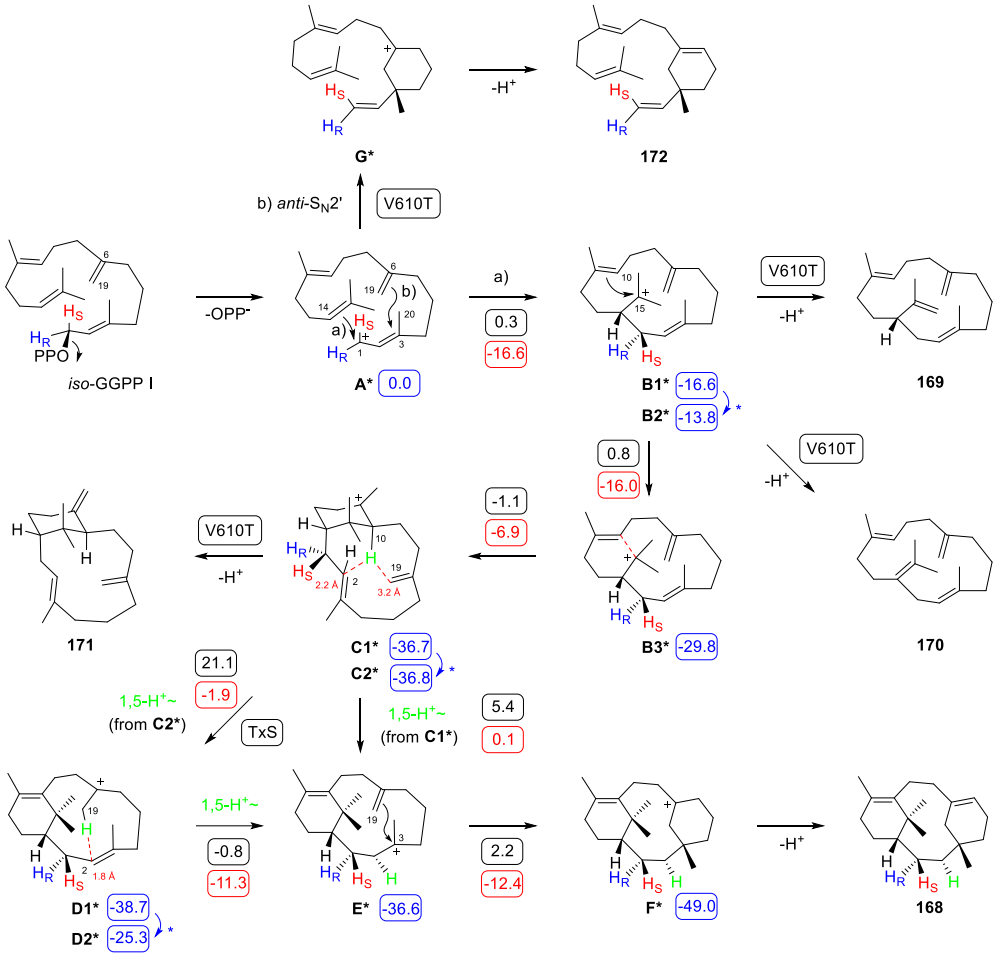

Scheme 44. Mechanism for the cyclization of *iso*-GGPP I to **168** by TxS.

We also isolated and structurally characterized a new compound taxaxenene (**168**) from the incubation of *iso*-GGPP I with TxS wild type, and its biosynthetic proposal has been shown in Scheme 44. Similar to the biosynthesis of **18**, a direct 1,5-proton shift from the intermediate **C*** to **E*** can be substituted by two sequential 1,5-proton shifts (**C***-**D***-**E***). In order to investigate the intramolecular proton shift, the substrate (10-^{2}H)-*iso*-GGPP I was synthesized and used for a large scale biotransformation with TxS to obtain labelled **168**. If deuterium directly migrates to C2, one of the signals for the hydrogens at C2 in the HSQC spectrum should be vanished. On the contrary, if deuterium first migrates to C19, a distribution of the three homotopic hydrogens in the methyl group will happen, and because of the kinetic isotope effect, a proton rather than a deuterium migration from C19 to C2 should be observed. Thus, the signals for both hydrogens at C2 in the HSQC spectrum will be expected. The isolated labelled-**168** with the vanished signal in the HSQC spectrum for C2 (H2α) gave experimental evidence for the direct proton migration, and the computational data also favoured the direct conversion from **C1*** to **E***. Further conversion of *iso*-GGPP I was performed with the variant V610T, a variant that showed the best diterpene production among all the created variants. Four compounds were isolated and characterized as isocembrene A (**169**), isocembrene C (**170**), verticilla-3,8(19),12(18)-triene (**171**) and taxasimplene (**172**). Their formation can be explained as the deprotonation products of the intermediates as shown in Scheme 44.

The absolute configurations of compounds **168** and **171** were assigned based on stereoselective isotopic labelling experiments with (*R*)- or (*S*)-(1-^{13}C,1-^{2}H)-*iso*-GGPP I as the substrates. For compound **172**, it biosynthetically starts from the ionization of *iso*-GGPP I with the analogous conformation as for GGPP to yield intermediate **A***. In this process, diphosphate will leave from the front side, and then 3,19-cyclization yielded **G*** with C3 attack from the *Re* face (back side, *anti*-S_N2' reaction). Thus, the 1-*pro*-*R* hydrogen at C1 turns into the (*E*)-position of the vinyl group of **172** while the 1-*pro*-*S* hydrogen turns into the (*Z*)-position as shown in Scheme 44.

In this study, I first cloned the enzyme and performed the site-directed mutagenesis experiments. Then I isolated all the related natural products and synthesized the labelled compounds. At last, I did the isotopic labelling experiments to investigate their biosynthesis and absolute configurations.

Chapter 9

Summary and outlook

The studies for this dissertation concentrate on the biosynthesis of terpenes with 7 articles included, providing novel insights into recent advances in the terpene field. To gain this knowledge a combination of chemical synthesis, genome mining, biotransformation, chromatography, isotopic labelling and site-directed mutagenesis was employed and enabled the discovery of novel terpenes and the investigation of catalytic mechanism of utilized terpene synthases.

The study started from the cloning of a casbene synthase, an enzyme that has already been reported but with lacking the investigations of the relevant stereochemical course in depth. This enzyme also well exemplified the potential of diterpene synthase (DTS) on conversions of non-natural substrate analogs which is rarely reported for DTSs, through the isolation of two casbene isomers. Apart from that, the formation of casbene isomers illustrated an unaffected 1,14-cyclization mode by a small structural modification, which promoted me to broaden my studies with more DTSs, as described in Chapters 3-5. Additionally, the combination of isotopic labelling study and non-natural *iso*-product isolations disclosed the stereochemical course of the cyclopropane ring formation, pointing to the same absolute configuration of casbene as reported.

The second article demonstrates how the substrate scopes of well-investigated DTSs can be widened through the isolation of 28 new diterpenes with some of them featuring amazing skeletons. According to the experimentally confirmed biosynthetic pathways of their natural counterparts, the formation of non-natural terpenes can be well explained as intermediates of the interrupted cyclization cascade at a certain stage, which is presumably a result of substrate modifications. Specifically, the enzymatic conversion of *iso*-GGPP II, a GGPP derivative harbouring a C11 methylene group instead of the classical C10=C11 double bond, resulted in the formation of several macrocyclic ring compounds via a modified cyclization mode. One explanation is that the structural modification dedicates the conformational change of *iso*-GGPP II, blocking the interactions between the substrate and key residues in the enzyme's active site, while another one is that the inheritance of *iso*-GGPP II does not allow the 1,11-cyclization mode to yield the instable primary cation. On the contrary, certain diterpenes with astonishing core skeletons like wanjuxenene (**106**) and albataxenol (**104**) were obtained with the transformations of another isomer *iso*-GGPP I, in which the cyclization mode is facilitated in a higher degree than that of the natural case. The determination of absolute configurations of the natural products requires either a direct method like X-ray crystallographic analysis of the

molecules, or indirect methods like ECD calculations and Mosher derivative analysis. The enantioselective isotopic labelling strategy gives the third possibility that enables the combination of the relative configuration, typically assigned based on the NOESY correlation, and the artificially introduced stereogenic centers in terpene precursors like synthetic (*R*)- and (*S*)-(1-^{13}C,1-^{2}H)-*iso*-GGPP I, to accurately point out the absolute configurations.

Subsequently as presented in Chapter 4, *iso*-GGPP III was synthesized in over 14 steps, after insufficient biotransformations of *iso*-GPP and IPP with GGPPS, followed by enzymatic conversions with only six DTSs in success and many frustrated cases, exhibiting the moderate tolerance of enzymes towards *iso*-GGPP III. Nine non-natural diterpenes were isolated with six enzymes that is capable of catalyzing the 1,11-10,14-cyclization reaction, which provides additional insights towards the relationship between substrate analogs and terpene synthases. The three analogs *iso*-GGPP I to III explored the substrate scopes of diverse DTSs, providing extensive examples for the investigations of non-natural terpene products and their corresponding enzymes. In order to compensate for this large topic, four more analogs featuring the combinations of different methylene groups were synthesized, whose all C2=C3 double bonds remained due to the importance of the allylic system to facilitate abstraction of the disphosphate group. In comparison to that towards analogs sharing one methylene group, the enzymatic efficiency towards substrates sharing two more ethylene groups indeed decreased, presumably due to the more relaxing conformational change caused by structural engineering. The substrate *iso*-GGPP VII with three methylene groups was not accepted by any DTSs in my hands. All taken together, the combination of systematical substrate engineering and many enzymatic conversions provides a novel aspect in the terpene field. Two trends between substrate structures and activities of DTSs are observed in this topic: 1. the efficiency of converting substrate analogs featuring two or more modified methylene groups is lower in comparison of converting the substrate habouring one modified methylene group. 2. the activities of DTSs catalyzing different initial cyclization modes is strongly influenced by the analogously modified precursors.

Nowadays, numerous terpenes are identified with tentative biosynthetic pathways, but much fewer suggestions have been experimentally validated, as exemplified by benditerpe-2,6,15-triene (**139**) and venezuelaene A (**144**). As a part of my studies, the hydride shifts in their biosynthesis are investigated through isotopic labelling studies, non-natural biotransformations, product derivations and DFT calculations.

The biosynthetic studies on terpenes also require investigation of TSs from diverse species. As a consequence, the discovery of two novel TSs from the fungus *Clitopilus passeckerianus* DSM1602 was also performed by genome mining, followed by raising a biosynthetic proposal

for one of the enzymatic products clitopilene (**155**). At the end, its cyclization mechanism has been investigated theoretically and experimentally by DFT calculations and isotopic labelling experiments, respectively.

Additionally, site-directed mutagenesis is useful in other aspects such as understanding of the product formation and differentiation of substrate scopes, which is well represented by spata-13,17-diene synthase from *Streptomyces xinghaiensis* (SxSpS), a multifunctional enzyme that can catalyze the formations of diverse sesquiterpenes, diterpenes, sesterterpenes, and triterpenes. Surprisingly, its products share the same 5-4-5 core skeleton and a hydrocarbon chain with different length, fitting to the observation of a hydrophobic tunnel between helices C and F in the crystal structure of *Sx*SpS. The subsequent mutagenesis studies on C177 resulted in a highly increased production of triterpenes with the C177A variant and absolutely abolished activities towards GGPP and GFPP with the C177F variant, disclosing the role of this residue on substrate tolerance. Furthermore, by altering the residue Y152 in the analogous position of selina-4(15),7(11)-diene synthase (SdS) to Ala, the function of SdS was switched from a STS to a DTS, which illustrates the key function of this residue as indicated by the conservation of this residue in 36 SpS homologs.

Another method to study the biosynthesis of terpenes is rooted in DFT calculations, that can show activation barriers for each single transient step, providing additional insights towards the proposed biosynthetic pathway. However, the mere usage of itself has a disadvantage that two similar pathways cannot be differentiated, as presented by the case of taxa-4,11-diene. During the history of study on this molecule, a long-range intramolecular proton shift in its biosynthesis has been suggested. However, the knowledge about the direct proton shift (from **C** to **E**, in Scheme 43 of Chapter 8) or indirect proton shift (**C**-**D**-**E**, Scheme 43 of Chapter 8) is not fully clear since both pathways have been calculated with a minor difference. Interestingly, this proton shift is also observed in the formations of taxaxenene (**168**) obtained from enzymatic conversion of *iso*-GGPP I, cyclophomactene (**42**) and cephalotene (**41**) produced by variants V610T and G606A respectively. Accounting on these phenomena, the indirect proton transfer via two steps seems more reasonable than the direct migration in the formation of the taxane skeleton. Apart from that, the study on the EI-MS fragmentation mechanism of taxa-4,11-diene also disclosed the long distance hydrogen migration during the fragmentation, which is validated by our isotopic labelling experiment.

All in all, some conclusions and outlooks are summarized here. First of all, comprehensive methods like non-natural enzymatic transformation, genome mining, isotopic labelling study, and site-directed mutagenesis are conducted in this dissertation to understand the fascinating terpene formations from different aspects. As discussed above, many TSs can tolerate various

substrate modifications, which allowed us to design specific terpene precursors for purposeful transformation of valuable targets like taxadiene-5α-ol, an early key intermediate in the biosynthesis of paclitaxel. By using chemical synthesis, the hydroxyl group can be introduced at C4 of GGPP, followed by the potential transformation by taxadiene synthase or its engineered variants to yield this intermediate.

In addition, the formation of terpenes discussed above are from a single enzyme, while terpenes are occasionally incorporated in the biosynthesis of more complex natural products. During the investigation of SpS from *Streptomyces platensis* (*Sp*SpS, in Chapter 7), two more cytochromes P450 and one glycosyltransferase were found encoded in the genome around the *Sp*SpS gene, indicating this terpene product may only serve as the intermediate of another post-modified product. It would be ideal to also study these enzymes and investigate the post-modification process to discover the final product. However, many cytochromes P450 are membrane-bound proteins, which of course requires more complicated gene expression systems or *in vivo* expression hosts.

Apart from the investigated clitopilene synthase, *Clitopilus passeckerianus* DSM1602 is on the one hand also reported as a host that can produce the well-investigated antibacterial drug pleuromutilin. Its biosynthesis has been investigated deeply, while the corresponding bifunctional diterpene synthase containing class I and class II domains are responsible for the formation of its precursor premutilin. The cyclization mechanism of premutilin has been proposed with a special ring arrangement which has also been studied with quantum chemical calculations. However, there is so far no experimental validation for the proposal, hereby it would be an ideal target for the isotopic labelling toolbox. On the other hand, numerous terpene synthase homologs are also found in its genome based on the *anti*SMASH analysis. In order to characterize these enzymes *in vitro*, a suitable cultivation condition of this strain with a high gene expression level is required for the reverse transcriptase PCR amplification.

Nowadays, with the development of artificial intelligence (AI), Alpha Fold can predict a highly reliable structural model as described in Chapter 7, however the crystal structures especially for structures co-crystalized with a ligand, are still of vital importance, because the co-crystalized structures can show a clear interaction between the substrate and the active pocket, which will benefit the site-directed mutagenesis study. Furthermore, the reliability of QM/MM molecular dynamics simulation (QM/MM MD simulation) that can simulate the reaction considering the role of the protein is ideally based on ligand bounded structures of enzymes. The combination of co-crystallization and QM/MM MD simulations can provide an additional view of how the cationic intermediates proceeded during the cyclization and what is the function of key residues in this process.

Chapter 10

Literatures

1 J. S. Dickschat, *Angew. Chem. Int. Ed.*, **2019**, *58*, 15964-15976.

2 J. K. Laylin, Nobel Laureates in Chemistry, 1901-1902, Wiley, **1993**.

3 A. Eschenmoser, *Chimia.*, **1990**, *44*, 1-21.

4 L. Ružička, *Pure Appl. Chem.*, **1963**, *6*, 493-524.

5 J. Gershenzon, N. Dudareva, *Nat. Chem. Biol.*, **2007**, *3*, 408-414.

6 M. Hilker, C. Kobs, M. Varama, K. Schrank, *J Exp Biol.*, **2002**, *205*, 455-461.

7 J. Gallego-Jara; G. Lozano-Terol, R.A. Sola-Martínez, M. Cánovas-Díaz, T. de Diego Puente, Molecules., **2020**, *25*, 5986.

8 P. M. O'Neill, V.E. Barton, S. A. Ward, Molecules., **2010**, *15*, 1705-1721.

9 J. Lombard, D. Moreira, *Mol. Biol. Evol.*, **2011**, *28*, 87–99.

10 J. M. Vinokur, T. P. Korman, Z. Cao, J. U. Bowie, *Biochem*, 2014, *53*, 4161-4168.

11 N. Dellas, S. T. Thomas, G. Manning, J. P. Noel, *eLife.*, **2013**, 2:e00672.

12 K. Clifford, J. W. Cornforth, R. Mallaby, G. T. Phillips, *J. Chem. Soc. D.*, **1971**, *24*, 1599-1600.

13 W. Eisenreich, A. Bacher, D. Arigoni, *Cell. Mol. Life Sci.,* **2004**, *61*, 1401–1426.

14 H. K. Lichtenthaler, *Annu. Rev. Plant Biol.*, **1999**, *50*, 47-65.

15 A. J. Wiemer, C. H. Hsiao, D. F. Wiemer, *Curr. Top. Med. Chem.*, **2010**, *10*, 1858–1871.

16 A. M. Guggisberg, R. E. Amthor, A. R. Odom, *Eukaryot Cell.*, **2014**, *13*.

17 D. W. Christianson, *Chem. Rev.*, **2017**, *117*, 11570-11648.

18 H. Y. Chang, T. H. Cheng, A. J. Wang, *IUBMB Life.*, **2021**, *73*, 40–63.

19 P. H. Liang, T. P. Ko, A. H. Wang, *Eur. J. Biochem.*, **2002**, *269*, 3339-3354.

20 M. Ito, M. Kobayashi, T. Koyama, K. Ogura, *Biochem.*, **1987**, *26*, 4745-4750.

21 L. C. Tarshis, M. Yan, C. D. Poulter, J. C. Sacchettini, *Biochem.*, **1994**, *33*, 10871-10877.

22 L. Tarshis, P. Proteau, B. Kellogg, J. Sacchettini, C. Poulter, Proc. *Natl. Acad. Sci. U.S.A.*, **1996**, *93*, 15018-15023.

23 H. V. Thulasiram, C. D. Poulter, *J. Am. Chem. Soc.*, **2006**, *128*, 15819–15823.

24 S. Takahashi, T. Koyama, *Chem Record.*, **2006**, *6*, 194-205.

25 M. Kobayashi, T. Kuzuyama, *ChemBioChem.*, **2019**, *20*, 29.

26 B. M. Jarstfer, B. S. J. Blagg, D. H. Rogers, C. D. Poulter, *J. Am. Chem. Soc.*, **1996**, *118*, 13089–13090.

27 C. K. Shewmaker, J. A. Sheehy, M. Daley, S. Colburn, D. Y. Ke, *The Plant Journal.*, **1999**, *20*, 401-412.

28 M. C. Wani, H. L. Taylor, M. E. Wall, P. Coggon, A. T. McPhail, *J. Am. Chem. Soc.*, **1971**, *93*, 2325-2327.

29 N. Magnus, S. H. von Reuss, F. Braack, C. Zhang, K. Baer, A. Koch, P. L. Hampe, S. Sutour, F. Chen, B. Piechulla, *Angew. Chem. Int. Ed.*, **2023**, *62*, e202303692.

30 D. E. Cane, Q. Xue, B. C. Fitzsimons, *Biochem.*, **1996**, *35*, 12369–12376.

31 D. E. Cane, I. Kang, *Arch. Biochem. Biophys.*, **2000**, *376*, 354–364.

32 D. E. Cane, J. H. Shim, Q. Xue, B. C. Fitzsimons, *Biochem.*, **1995**, *34*, 2480–2488.

33 C. M. Starks, K. Back, J. Chappell, J. P. Noel, *Science*, **1997**, *277*, 1815-1820.

34 M. J. Rynkiewicz, D. E. Cane, D. W. Christianson, Proc. *Natl. Acad. Sci. U.S.A.*, **2001**, *98*, 13543-13548.

35 H. Xu, J. S. Dickschat, *synthesis*, **2022**, *54*, 1551-1565.

36 J. Yu, T. Shiraishi, K. A. Taizoumbe, Y. Karasuno, A. Yoshida, M. Nishiyama, J. S. Dickschat, T. Kuzuyama, *J. Am. Chem. Soc.*, **2025**, *147*, 11896-11905.

37 T. Mitsuhashi, M. Okada, I. Abe, *ChemBioChem.*, **2017**, *18*, 2104-2109.

38 P. Baer, P. Rabe, K. Fischer, C. A. Citron, T. A. Klapschinski, M. Groll, J. S. Dickschat, *Angew. Chem. Int. Ed.*, **2014**, *53*: 7652-7656.

39 J. Jiang, D. E. Cane, *J. Am. Chem. Soc.*, **2008**, *130*, 428-429.

40 R. E. Lafever, B. S. Vogel, R. Croteau, *Arch. Biochem. Biophys.*, **1994**, *313*, 139-149.

41 M. Chen, W. K. W. Chou, T. Toyomasu, D. E. Cane, D. W. Christianson, *ACS Chem. Biol.*, **2016**, *11*, 889-899.

42 Z. Quan, J. S. Dickschat, *Org. Biomol. Chem.*, **2020**, *18*, 6072-6076.

43 Z. Quan, J. S. Dickschat, *Org. Lett.*, **2020**, *22*, 7552-7555.

44 Y. Ye, A. Minami, A. Mandi, C. Liu, T. Taniguchi, T. Kuzuyama, K. Monde, K. Gomi, H. Oikawa, *J. Am. Chem. Soc.*, **2015**, *137*, 36, 11846–11853.

45 S. Von Reuss, M. Kai, B. Piechulla, W. Francke, *Angew. Chem.*, **2010**, *22*, 2053-2054.

46 S. von Reuss, D. Domik, M. C. Lemfack, N. Magnus, M. Kai, T. Weise, B. Piechulla, *J. Am. Chem. Soc.*, **2018**, *140*, 11855-11862.

47 H. Xu, L. Lauterbach, B. Goldfuss, G. Schnakenburg, J. S. Dickschat, *Nat. Chem.*, **2023**, *15*, 1164-1171.

48 Y. T. Duan, A. Koutsaviti, M. Harizani, C. Ignea, V. Roussis, Y. Zhao, E. Ioannou, S. C. Kampranis, *Nat. Chem. Biol.*, **2023**, *19*, 1532-1539.

49 H. Xu, B. Goldfuss, J. S. Dickschat, *Angew. Chem. Int. Ed.*, **2024**, *63*, e202408809.

50 H. Xu, H. Li, B. Goldfuss, G. Schnakenburg, J. S. Dickschat, *Angew. Chem. Int. Ed.*, **2024**, *63*, e202412040.

51 H. Seto, H.Yonehara, *J. Antibiot.*, **1980**, *33*, 92.

52 D. E. Cane, J. S. Oliver, P. H. Harrison, C. Abell, B. R. Hubbard, C. T. Kane,R. Lattman, *J. Am. Chem. Soc.*, **1990**, *112*, 4513-4524.

53 D. E. Cane, A. Tillman, *J. Am. Chem. Soc.*, **1983**, *105*, 122-124.

54 D. E. Cane, C. Abell, A. Tillman, *Bioorg. Chem.*, **1984**, *12*, 312.

55 D. E. Cane, C. Abell, R. Lattman, C. T. Kane, B. R. Hubbard, P. H. M. Harrison, *J. Am. Chem.Soc.*, **1988**, *110*, 4081.

56 L. Zu, M. Xu, M. W. Lodewyk, D. E. Cane, R. Peters, D. J. Tantillo, *J. Am. Chem. Soc.*, **2012**, *134*, 11369-11371.

57 P. H. M. Harrison, J. S. Oliver, D. E. Cane, *J. Am. Chem.Soc.*, **1988**, *110*, 5922−5923.

58 D. E. Cane, J. K. Sohng, C. R. Lamberson, S. M. Rudnicki, Z. Wu, M. D. Lloyd, J. S. Oliver, B. R. Hubbard, *Biochemistry*, **1994**, *33*, 5846-5857.

59 M. Seemann, G. Zhai, K. Umezawa and D. E. Cane, *J. Am. Chem. Soc.*, **1999**, *121*, 591-592.

60 P. Gutta, D. J. Tantillo, *J. Am. Chem. Soc.*, **2006**, *128*, 6172-6179.

61 H. Xu, T. G. Köllner, F. Chen, J. S. Dickschat, *Org. Biomol. Chem.*, **2024**, *22*, 1360-1364.

62 Z. Hu, X. Liu, M. Tian, Y. Ma, B. Jin, W. Gao, G. Cui, J. Guo,L. Huang, *Med. Res. Rev.*, **2021**, *41*, 2971–2997.

63 I. Uchida, T. Ando, N. Fukami, K. Yoshida, M. Hashimoto, T. Tada, S. Koda, Y. J. Morimoto, *Org. Chem.*, **1987**, *52*, 5292−5293.

64 L. Gentric, I. Hanna, L. Ricard, *Org. Lett.*, **2003**, *5*, 1139–1142.

65 T. J. Maimone, J. Shi, S. Ashida, P. S. Baran, *J. Am. Chem.Soc.*, **2009**, *131*, 17066-17067.

66 J. Poulin, C. M. Grisé-Bard, L. Barriault, *Angew. Chem. Int. Ed.*, **2012**, *51*, 2111-2114.

67 Q. Yang, J. T. Njardarson, C. Draghici, F. Li, *Angew. Chem. Int. Ed.*, **2013**, *52*, 8648-8651.

68 L. Min, X. Lin, C. Li, *J. Am. Chem.Soc.*, **2019**, *141*, 15773-15778.

69 R. Xu, Y. Zou, *Angew. Chem. Int. Ed.*, **2024**, e202416795.

70 J. Rinkel, L. Lauterbach, J. S. Dickschat, *Angew. Chem. Int. Ed.*, **2017**, *56*, 16385-16389.

71 X. Wei, W. Ning, C. A. McCadden, T. A. Alsup, Z. Li, D. P. Łomowska-Keehner, J. Nafie, T. Qu, M. O. Opoku, G. R. Gillia, B. Xu, D. G. Icenhour, J. D. Rudolf, *Nat. Comm.*, **2025**, *16*, 3721.

72 Z. Yin, Z. Hu, K. Yang, G. Lu, G. B. Tabekoueng, P. Wu, Q. Luo, J. Xu, B. Goldfuss, J. S. Dickschat, G. Bian, *Angew. Chem. Int. Ed.*, **2025**, *64*, e202507752.

73 S. Y. Kim, P. Zhao, M. Igarashi, R. Sawa, T. Tomita, M. Nishiyama, T. Kuzuyama, *Chem. Biol.*, **2009**, *16*, 736-743.

74 P. Rabe, J. Rinkel, E. Dolja, T. Schmitz, B. Nubbemeyer, T. H. Luu, J. S. Dickschat,

Angew. Chem. Int. Ed., **2017**, *56*, 2776.

75 J. Rinkel, S. T. Steiner, J. S. Dickschat, *Angew. Chem. Int. Ed.*, **2019**, *58*, 9230-9233.

76 B. Qin, Y. Matsuda, T. Mori, M. Okada, Z. Quan, T. Mitsuhashi, T. Wakimoto, I. Abe, *Angew. Chem. Int. Ed.*, **2016**, *55*, 1658-1661.

77 G. B. Tabekoueng, H. Li, B. Goldfuss, G. Schnakenburg, J. S. Dickschat, *Angew. Chem. Int. Ed.*, **2024**, *63*, e202413860.

78 C. Li, S. Wang, X. Yin, A. Guo, K. Xie, D. Chen, S. Sui, Y. Han, J. Liu, R. Chen, J. Dai, *Angew. Chem. Int. Ed.*, **2023**, *62*, e202306020.

79 L. Lauterbach, J. Rinkel, J. S. Dickschat, *Angew. Chem. Int. Ed.*, **2018**, *57*, 8280.

80 M. Hérin, M. Colin, B. Tursch, Bull. *Soc. Chim. Belg.*, **1976**, *85*, 801-803.

81 R. Kazlauskas, P. T. Murphy, R. J. Wells, P. Schonholzer, J.C. Coll, *J. Aust. J. Chem.*, **1978**, *31*, 1817-1824.

82 A. Meguro, T. Tomita, M. Nishiyama, T. Kuzuyama, *ChemBioChem.*, **2013**, *14*, 316-321.

83 J. Rinkel, J. S. Dickschat, *Org.lett.*, **2019**, *21*, 9442-9445.

84 M. J. Calvert, P. R. Ashton, R. K. Allemann, *J. Am. Chem.Soc.*, **2002**, *124*, 11636-11641.

85 B. Felicetti, D. E. Cane, *J. Am. Chem. Soc.*, **2004**, *126*, 7212-7221.

86 D. E. Cane, P. C. Prabhakaran, J. S. Oliver, D. B. McIlwaine, *J. Am. Chem. Soc.*, **1990**, *112*, 3209.

87 D. E. Cane, Y. S. Tsantrizos, *J. Am. Chem.Soc.*, **1996**, *118*, 10037-10040.

88 J. A. Faraldos, D. J. Grundy, O. Cascon, S. Leoni, M. W. van der Kamp, R. K. Allemann, *Chem. Commun.*, **2016**, *52*, 14027-14030.

89 C. Oberhauser, V. Harms, K. Seidel, B. Schröder, K. Ekramzadeh, S. Beutel, S. Winkler, L. Lauterbach, J. S. Dickschat, A. Kirschning, *Angew. Chem. Int. Ed.*, **2018**, *57*, 11802-11806.

90 R. Croteau, S. L. Munck, C. C. Akoh, H. J. Fisk, D. M. Satterwhite, *Arch. Biochem. Biophys.*, **1987**, *256*, 56-68.

91 V. Falara, T. A. Akhtar, T. T. H. Nguyen, E. A. Spyropoulou, P. M. Bleeker, I. Schauvinhold, Y. Matsuba, M. E. Bonini, A. L. Schilmiller and R. L. Last, *Plant Physiol.*, **2011**, *157*, 770-789.

92 P. Rabe, J. S. Dickschat, *Angew. Chem. Int. Ed.*, **2013**, *52*, 1810-1812.

93 C. A. Lesburg, G. Zhai, D. E. Cane, D. W. Christianson, *Science*, **1997**, *277*, 1820-1824.

94 C. Wang, R. Hopson, X. Lin, D. E. Cane, *J. Am.Chem. Soc.*, **2009**, *131*, 8360-8361.

95 S. A. Agger, F. Lopez-Gallego, C. Schmidt-Dannert, *Mol. Microbiol.*, **2009**, *72*, 1181-1195.

96 M. Moeller, D. Dhar, G. Dräger, M.l Özbasi, H. Struwe, M. Wildhagen, M. D. Davari, S. Beutel, A. Kirschning, *J. Am. Chem.Soc.*, **2024**, *146*, 17838-17846.

97 K. A. Taizoumbe, B. Goldfuss, J. S. Dickschat, *Angew. Chem. Int. Ed.*, **2024**, *63*, e202318375.

98 M. Seemann, G Zhai, J. W. de Kraker, C. M. Paschall, D. W. Christianson, D. E. Cane, *J. Am. Chem.Soc.*, **2002**, *124*, 7681-7689.

99 N. G. H. Leferink, N. S. Scrutton, *ChemBioChem*, **2022**, *23*, e202100484.

100 Xu, H.; Rinkel, J.; Dickschat, J. S. *Org. Chem. Front.*, **2021**, *8*, 1177-1184.

101 W. Zhang, X. Wang, G. Zhu, B. Zhu, K. Peng, T. Hsiang, L. Zhang, X. Liu, *Angew. Chem. Int. Ed.*, **2024**, *63*, e202406246.

102 Q. Chen, J. Li, Z. Liu, T. Mitsuhashi, Y. Zhang, H. Liu, Y. Ma,J. He, T. Shinada, T. Sato, Y. Wang, H. Liu, I. Abe, P. Zhang,G. Wang, *Plant Commun.*, **2020**, *1*, 100051.

103 Y. Wang, H. Xu, J. Zou, X. Chen, Y. Zhuang, W. Liu, E. Celik, G. Chen, D. Hu, H. Gao, R. Wu, P. Sun, J. S. Dickschat, *Nat. Catal.*, **2022**, *5*, 128–135.

104 A. Hou, B. Goldfuss, J. S. Dickschat, *Angew. Chem. Int. Ed.*, **2021**, *60*, 20781-20785.

105 B. Xing, H. Xu, A. Li, T. Lou, M. Xu, K. Wang, Z. Xu, J. S. Dickschat, D. Yang, M. Ma, *Angew. Chem. Int. Ed.*, **2022**, *61*, e202209785.

106 Y. Wang, P. Xue, M. Cao, T. Yu, S. T. Lane, H. Zhao, *Chemical Reviews*, **2021**, *121*, 12384-12444.

107 A. M. Hill, D. E. Cane, C. J. Mau, C. A. J. A. o. b. West, biophysics, *Arch. Biochem. Biophys.*, **1996**, *336*, 283-289.

108 K. K. Reiling, Y. Yoshikuni, V. J. Martin, J. Newman, J. Bohlmann, J. D. J. B. Keasling, bioengineering, *Biotechnol. Bioeng.*, **2004**, *87*, 200-212.

109 L. Crombie, G. Kneen, G. Pattenden and D. Whybrow, *J. Chem. Soc. Perkin Trans.*, **1980**, *1*, 1711.

110 R. D. Gietz, R. H. Schiestl, *Nat. Protoc.*, **2007**, *2*, 31-34.

111 Y. Jin, R. M. Coates, *Chem. Comm.*, **2006**, *27*, 2902-2904.

112 I. Farkas, H. Pfander, *Helv. Chim. Acta.*, **1990**, *73*, 1980-1985.

113 J. Rinkel, P. Rabe, X. Chen, T. G. Köllner, F. Chen, J. S. Dickschat, *Chem. Eur. J.*, **2017**, *23*, 10501-10505.

114 J. S. Dickschat, J. Rinkel, P. Rabe, A. B. Kashkooli, H. Bouwmeester, *Beilstein J. Org. Chem.*, **2017**, *13*, 1770–1780.

115 G. Bian, J. Rinkel, Z. Wang, L. Lauterbach, A. Hou, Y. Yuan, Z. Deng, T. Liu, J. S. Dickschat, *Angew. Chem. Int. Ed.*, **2018**, *57*, 15887-15890.

116 J. Rinkel, L. Lauterbach, P. Rabe, J. S. Dickschat, *Angew. Chem. Int. Ed.*, **2018**, *57*, 3238-3241.

117 L. Lauterbach, B. Goldfuss, J. S. Dickschat, *Angew. Chem. Int. Ed.*, **2020**, *59*, 11943-

11947.

118 G. Li, Y.-W. Guo, J. S. Dickschat, *Angew. Chem. Int. Ed.*, **2021**, *60*, 1488-1492.

119 A. J. Weinheimer, W. W. Youngblood, P. H. Washecheck, T. K. B. Karns, L. S. Ciereszko, *Tetrahedron Lett.*, **1970**, *26*, 497-500.

120 Y. Kashman, A. Groweiss, *J. Org. Chem.*, **1980**, *45*, 3814-3824.

121 C. Zhu, B. Xu, D. A. Adpressa, J. D. Rudolf, S. Loesgen, *Angew. Chem. Int. Ed.*, **2021**, *60*, 14163-14170.

122 B. Xu, D. J. Tantillo, J. D. Rudolf, *Angew. Chem. Int. Ed.*, **2021**, *60*, 23156-23163.

123 Z. Li, Y. Jiang, X. Zhang, Y. Chang, S. Li, X. Zhang, S. Zheng, C. Geng, P. Men, L. Ma, Y. Yang, Z. Gao, Y.-J. Tang, S. Li, *ACS Catal.*, **2020**, *10*, 5846-5851.

124 Y. J. Hong, D. J. Tantillo, *Aust. J. Chem.*, **2017**, *70*, 362-366.

125 I. Abe, *Nat. Prod. Rep.*, **2007**, *24*, 1311–1331.

126 M. Basyuni, H. Oku, E. Tsujimoto, K. Kinjo, S. Baba, K. Takara, *FEBS J.*, **2007**, 274, 5028-5042.

127 D. R. Phillips, J. M. Rasbery, B. Bartel, S. P. T. Matsuda, Curr. *Opin. Plant Biol.*, **2006**, *9*, 305-314.

128 H. Tao, L. Lauterbach, G. Bian, R. Chen, A. Hou, T. Mori, S. Cheng, B. Hu, L. Lu, X. Mu, M. Li, N. Adachi, M. Kawasaki, T. Moriya, T. Senda, X. Wang, Z. Deng, I. Abe, J. S. Dickschat, T. Liu, *Nature*, **2022**, *606*, 414-419.

129 J. A. Faraldos, S. Wu, J. Chappell, R. M. Coates, *Tetrahedron*, **2007**, *63*, 7733-7742.

130 J. Rinkel, J. S. Dickschat, *Org. Lett.*, **2019**, *21*, 2426-2429.

131 L. Li, L. Sheng, C. Wang, Y. Zhou, H. Huang, X. Li, J. Li, E. Mollo, M. Gavagnin, Y. Guo, *J. Nat. Prod.*, **2011**, *74*, 2089-2094.

132 A. E. Koepp, M. Hezari, J. Zajicek, B. Stofer Vogel, R. E. LaFever, N. G. Lewis, R. Croteau, *J. Biol. Chem.*, **1995**, *270*, 8686-8690.

133 D. C. Williams, B. J. Carroll, Q. Jin, C. D. Rithner, S. R. Lenger, H. G. Floss, R. M. Coates, R. M. Williams, R. Croteau, *Chem. Biol.*, **2000**, *7*, 969-977.

134 Q. Jin, D. C. Williams, M. Hezari, R. Croteau, R. B. Coates, *J. Org. Chem.*, **2005**, *70*, 4667-4675.

135 P. Gutta, D. J. Tantillo, *Org. Lett.*, **2007**, *9*, 1069-1071.

136 Y. J. Hong, D. J. Tantillo, *J. Am. Chem. Soc.*, **2011**, *133*, 18249-18256.

137 Y. Freud, T. Ansbacher, D. T. Major, *ACS Catal.*, **2017**, *7*, 7653-7657.

138 T. Ansbacher, Y. Freud, D. T. Major, *Biochem.*, **2018**, *57*, 3773-3779.

139 A. M. Escorcia, J. P. M. van Rijn, G.-J. Cheng, P. Schrepfer, T. B. Brück, W. Thiel, *J. Comput. Chem.*, **2018**, *39*, 1215-1225.

140 J. P. M. van Rijn, A. M. Escorcia, W. Thiel, *J. Comput. Chem.*, **2019**, *40*, 1902-1910.

141 Q. Huang, H. J. Williams, C. A. Roessner, A. I. Scott, *Tetrahedron Lett.*, **2000**, *41*, 9701-9704.

142 A. Mendoza, Y. Ishihara, Phil S. Baran, *Nat. Chem.*, **2012**, *4*, 21-25.

143 P. Schrepfer, A. Buettner, C. Goerner, M. Hertel, J. van Rijn, F. Wallrapp, W. Eisenreich, V. Sieber, R. Kourist, T. Brück, *Proc. Natl. Acad. Sci. USA.*, **2016**, *113*, E958-E967.

Chapter 11

Appendices A-G

Appendices A

Isotopic Labelling Experiments and Enzymatic Preparation of *Iso*-Casbenes with Casbene Synthase from *Ricinus communis*

Org. Chem. Front. **2022**, *9*, 795-801.

Doi: 10.1039/D1QO01707A

ORGANIC CHEMISTRY FRONTIERS

RESEARCH ARTICLE

View Article Online
View Journal | View Issue

Cite this: *Org. Chem. Front.*, 2022, **9**, 795

Isotopic labelling experiments and enzymatic preparation of iso-casbenes with casbene synthase from *Ricinus communis*†

Heng Li and Jeroen S. Dickschat *

Received 12th November 2021,
Accepted 21st December 2021

DOI: 10.1039/d1qo01707a

rsc.li/frontiers-organic

Isotopic labelling experiments gave insights into the enzyme mechanism of casbene synthase from *Ricinus communis*, showing a clear stereochemical course for the cyclisation reaction, in agreement with the reported absolute configuration of casbene. Two oligoprenyl diphosphate analogs with shifted double bonds were synthesised and enzymatically converted with casbene synthase to yield casbene isomers. Their absolute configurations were evident from a terpene cyclisation through the same stereochemical course as for casbene. Additional labelling experiments gave insights into the EI-MS fragmentation mechanism of casbene.

Introduction

Casbene (**1**, Fig. 1) is a 14-membered diterpene hydrocarbon that was first isolated from an incubation of mevalonic acid with an enzyme preparation from seedlings of castor bean (*Ricinus communis*).[1] In this plant **1** serves as the parent hydrocarbon of many diterpenoids with related skeletons such as lathyranes, tiglianes and ingenanes. The most important representative of these diterpenoids is ingenol mebutate (ingen-3-yl angelate, **2**) from the sap of *Euphorbia paralias*[2] and *Euphorbia peplus*[3] that has entered the market for the treatment of actinic keratosis. Full structure elucidation of **1** required a synthesis of the racemate, revealing a *cis*-cyclopropane moiety,[4] followed by an enantioselective synthesis from (+)-chrysanthemic acid to establish the structure of (1*R*,14*S*)-(−)-**1**.[5]

After partial purification of casbene synthase (CS) from *R. communis*[6] and cloning of the cDNA,[7] a biochemical characterisation of purified recombinant CS showed formation of **1** as the main product *in vitro*.[8] Also expression of the CS gene together with geranylgeranyl pyrophosphate (GGPP) precursor providing genes in *Escherichia coli*,[9] in a metabolically engineered *Saccharomyces cerevisiae*[10] or in *Nicotiana benthamiana*[11] resulted in the same product **1**.[11] Downstream oxidations of **1** by two cytochrome P450 monooxygenases and an alcohol dehydrogenase establish the lathyrane skeleton of jolkinol C (**3**).[12–14] Reconstitution of the pathway in an engineered *S. cerevisiae* resulted in a high yielding production strain for **3** (800 mg L^{-1}),[15] which is a promising result for the future supply with the difficult to obtain drug **2**[16] that has been made available by semi-synthesis from ingenol[17] and total synthesis.[18]

Enzymatic conversions of isotopically labelled oligoprenyl diphosphates are not only useful to study the enzyme reaction mechanisms of terpene synthases, but also the EI-MS fragmentation mechanisms and, if stereoselectively deuterated compounds are used, the absolute configurations of their products.[19] Along further lines of recent research it was shown that many terpene synthases can accept non-natural substrate analogs,[20] including modified oligoprenyl diphosphates with halogen atoms,[21,22] hydroxy groups,[23] ketones,[24] heteroatoms

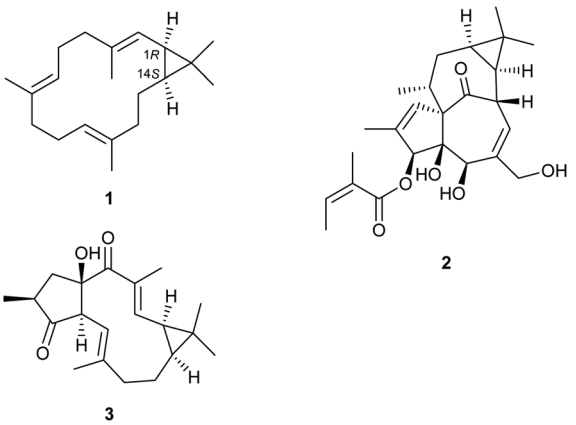

Fig. 1 Structures of compounds **1**–**3**.

Kekulé-Institut für Organische Chemie und Biochemie, Rheinische Friedrich-Wilhelms-Universität Bonn, Gerhard-Domagk-Straße 1, 53121 Bonn, Germany. E-mail: dickschat@uni-bonn.de

†Electronic supplementary information (ESI) available: Synthetic procedures and compound characterisation data, enzyme incubations and labelling experiments, NMR spectra of casbene and iso-casbenes. See DOI: 10.1039/d1qo01707a

inserted into the carbon chain,[25,26] epoxidised[27] or hydrogenated double bonds,[24,28,29] and altered methylation patterns.[30–32] Here we report on isotopic labelling experiments to study the cyclisation mechanism of CS and the EI-MS fragmentation mechanisms of its product **1**. A synthesis of two new oligoprenyl diphosphate analogs and their enzymatic conversion with CS into iso-casbenes was performed. In a combined approach using substrate analogs with isotopic labellings their absolute configurations were solved.

Results and discussion

The enzyme mechanism of casbene synthase

A synthetic gene codon optimised for *Escherichia coli* and cloned into the vector pYE-Express[33] was used for gene expression. The purified protein (Fig. S1†) efficiently converted geranylgeranyl diphosphate (GGPP) into a diterpene hydrocarbon (Fig. S2†) that was identified as (−)-**1** through NMR spectroscopy (Table S1 and Fig. S3–S10†). The cyclisation mechanism from GGPP to **1** proceeds through 1,14-cyclisation of GGPP to the cembranyl cation (**A**), followed by deprotonation from C1 with cyclopropane ring closure (Scheme 1). The stereochemical course for this process was investigated by incubation of (*R*)- and (*S*)-(1-^{13}C,1-^{2}H)IPP[34] with isopentenyl diphosphate isomerase (IDI) from *E. coli*[34,35] and GGPP synthase (GGPPS) from *Streptomyces cyaneofuscatus*[36] and CS, revealing the specific loss of the 1-*pro-S* hydrogen during product formation (Fig. S11,† a summary of all labelling experiments is given in Table S2†). Assuming inversion of configuration at C1 of GGPP in the cyclisation to **A**, this observation is in agreement with the absolute configuration of (1*R*,14*S*)-**1**, because the abstracted 1-*pro-S* hydrogen is closest to the cationic centre in **A**. This labelling experiment also allowed to unambiguously assign the chemical shifts for the diastereotopic hydrogen atoms at C5, C9 and C13 through HSQC spectroscopy in which the signals were strongly enhanced by the ^{13}C-labels at these carbons (Fig. S12†). Similar experiments with DMAPP and (*E*)- or (*Z*)-(4-^{13}C,4-^{2}H)IPP[37] that were enzymatically converted with GGPP and CS allowed to assign the hydrogen signals at C4, C8 and C12 (Fig. S13†).

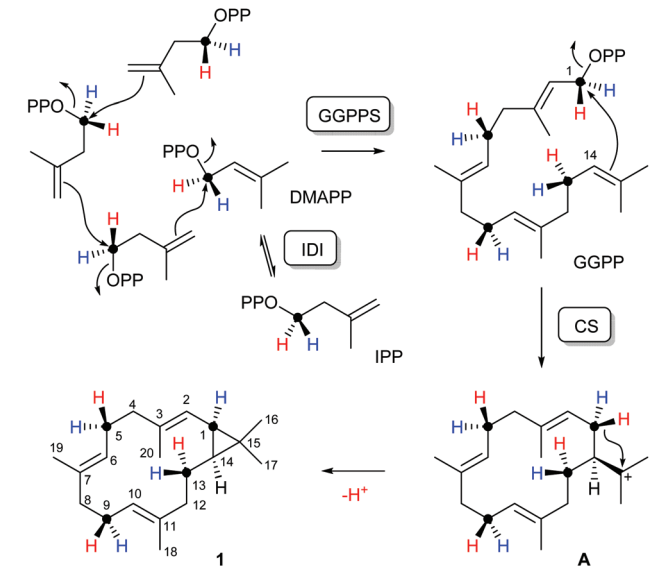

Scheme 1 Cyclisation of GGPP to **1** through 1,14-cyclisation to **A** and deprotonation with cyclopropane ring formation. The stereochemical course for the deprotonation was investigated by enzymatic conversion of (*R*)-(1-^{13}C,1-^{2}H)IPP (blue H = ^{2}H) and (*S*)-(1-^{13}C,1-^{2}H)IPP (red H = ^{2}H) with IDI, GGPPS and CS. Black dots represent ^{13}C-labelled carbons.

Synthesis of iso-FPP and iso-GGPP

For the enzymatic synthesis of new casbene isomers, the substrate analog iso-FPP with an olefinic methylene group at C7 instead of the natural C6=C7 double bond was synthesised as shown in Scheme 2. Treatment of isopentenol (**4**) with two

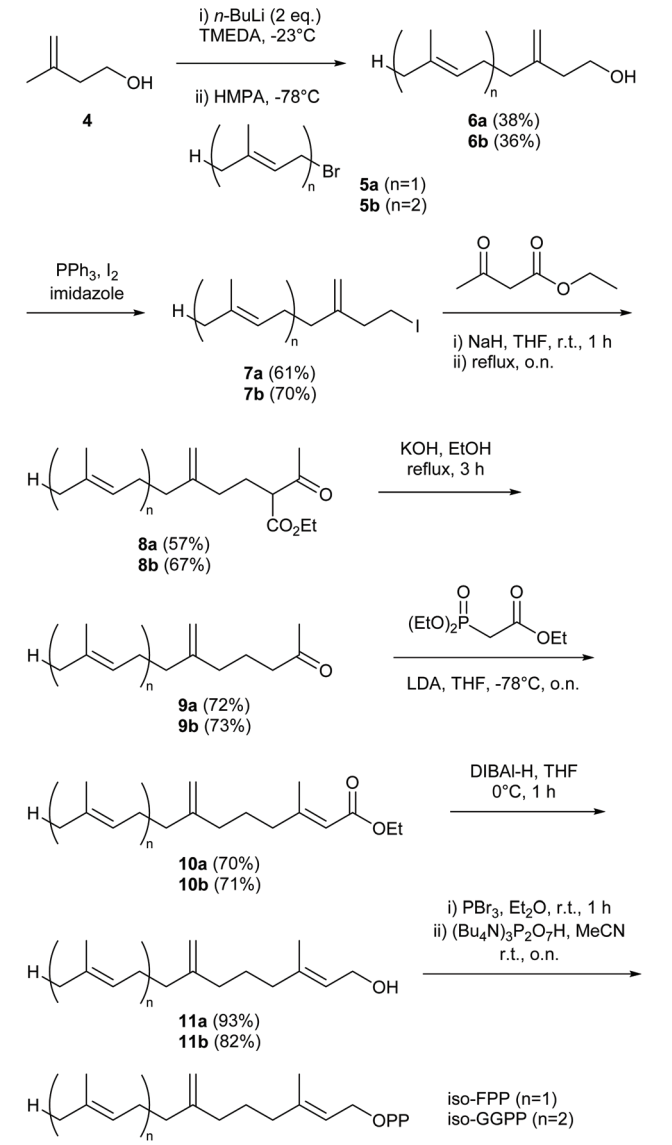

Scheme 2 Synthesis of iso-FPP and iso-GGPP.

equivalents of *n*-BuLi in the presence of TMEDA resulted in the dianion of **4** that was alkylated with prenyl bromide (**5a**) to give alcohol **6a**.[38] The iodide **7a** obtained by conversion with PPh_3, I_2 and imidazole was then used in an alkylation of ethyl acetoacetate to yield **8a**. Saponification with spontaneous decarboxylation resulted in the ketone **9a** that was elongated in a Horner–Wadsworth–Emmons reaction to ester **10a**. Reduction with DIBAl-H to the alcohol **11a**, conversion into the bromide and nucleophilic substitution with $(Bu_4N)_3P_2O_7H$ yielded the target compound iso-FPP. Starting from geranyl bromide (**5b**), the same sequence of steps gave access to iso-GGPP.

Enzymatic conversion into iso-casbenes

Both synthetic oligoprenyl diphosphate analogs were successfully converted into casbene isomers (Scheme 3). While iso-GGPP was directly converted with CS to give iso-casbene I (**13**), iso-FPP was first elongated with IPP and GGPPS to yield iso-GGPP II, followed by cyclisation to iso-casbene II (**14**). The obtained diterpene analogs were isolated and their structures were characterised by NMR spectroscopy (Tables S3, S4 and Fig. S14–S29†). The absolute configurations of **13** and **14** were determined using GGPP analogs with an enantioselective deuteration at C1. For this purpose, (*R*)-(1-^{2}H)iso-GGPP (blue H = ^{2}H) and (*S*)-(1-^{2}H)iso-GGPP (red H = ^{2}H) were synthesised in high enantiomeric purity (Scheme S1 and Fig. S30†). Their conversion with CS into **13** resulted in the specific loss of the 1-*pro-S* hydrogen (Fig. S31†), which is the same hydrogen as lost in the formation of **1** from GGPP, pointing to the absolute configuration of (1*R*,14*S*)-**13**. Analogous results were obtained for **14** in the incubation of iso-FPP and (*R*)-(1-^{2}H)IPP (blue H = ^{2}H) and (*S*)-(1-^{2}H)IPP[39] (red H = ^{2}H) with GGPPS and CS, revealing specific loss of the 1-*pro-S* hydrogen (Fig. S32†) and thus the structure of (1*R*,14*S*)-**14**.

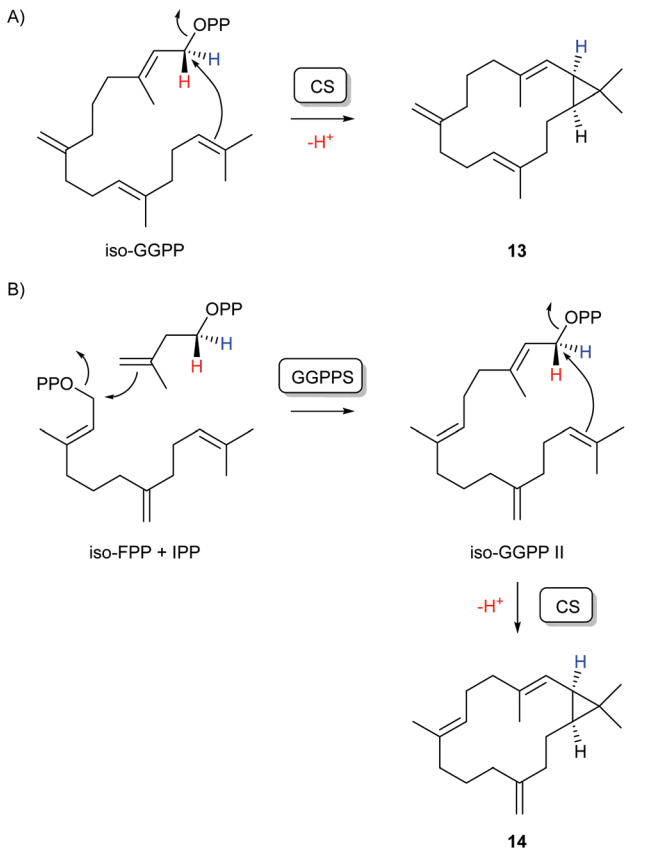

Scheme 3 Enzymatic conversion of (A) iso-GGPP (**12b**) and (B) iso-FPP (**12a**).

^{13}C-Labelling experiments with CS

The stereochemical course of the GGPP cyclisation by CS regarding the face selectivity for the attack at C15 was further investigated with (16-^{13}C)GGPP and (17-^{13}C)GGPP, enzymatically prepared with GGPPS from (12-^{13}C)FPP and (13-^{13}C)FPP[40] (Scheme 4). Product analysis through ^{13}C NMR (Fig. S33†) showed specific incorporations into the geminal Me groups of **1**, without any distribution of labelling and with *Si* face attack at C15. Further incubation experiments were performed with all other eighteen isotopomers of (^{13}C)GGPP that were synthesised as reported previously[36,41] or obtained enzymatically from correspondingly labelled FPP or GPP isotopomers[40,42] with IPP and GGPPS (Table S2;† (1-^{13}C)GPP was synthesised in this study according to Scheme S2†). Their conversion by CS resulted in the incorporation of labellings into the expected positions in all cases (Fig. S33†).

EI-MS fragmentation mechanism of casbene

The twenty isotopomers of (^{13}C)-**1** were also investigated by GC/MS (Fig. S34†), allowing to study the EI-MS fragmentation mechanisms of **1**. The results of these mass spectrometric analyses are summarised for prominent fragment ions *m*/*z* in a position specific mass shift analysis ($PMA_{m/z}$, Fig. 2).[43] While isotopic labellings have long been used to study EI-MS fragmentation mechanisms of organic compounds,[44–49] the systematic method combining singly ^{13}C-labelled substrates with their conversion through terpene synthases has recently been introduced by us and applied to study EI-MS fragmentation mechanisms of several terpenes.[34,50–54] The systematic labelling approach makes use of the following: If a fragment ion *m*/*z* for (*n*-^{13}C)-**1** is increased by 1 Da in comparison to unlabelled **1**, the carbon of the n-position must contribute to its formation (black dots), and if such an increase is not

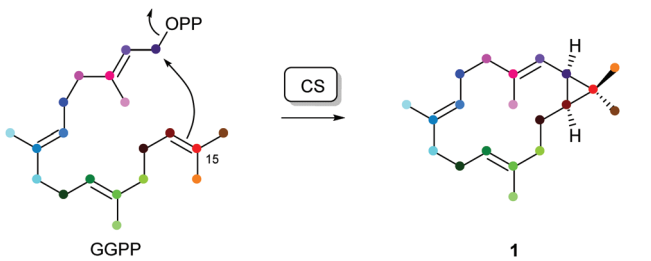

Scheme 4 Enzymatic conversion of all twenty isotopomers of (^{13}C)GGPP with CS. Each coloured dot indicates a single ^{13}C-labelling experiment.

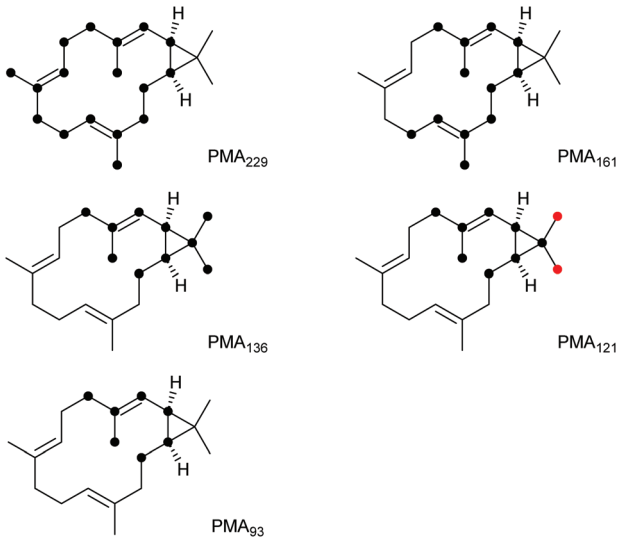

Fig. 2 Position specific mass shift analysis for **1**.

observed, the carbon must be lost in the fragmentation reaction. Labelled carbons showing partial increase of a fragment ion (red dots) indicate that more than one mechanism lead to formation of different fragment ions of the same nominal mass, but representing different parts of the molecule.

The position specific mass shift analysis for fragment ion *m*/*z* 229 (PMA_{229}) reveals its formation with specific loss of the C15(-17)-16 portion (Fig. 2). After electron ionisation (EI) to $\mathbf{1}^{\bullet+}$, this is explainable by α-fragmentation to $\mathbf{A}^{\bullet+}$, hydrogen rearrangement (*r*H) to $\mathbf{B}^{\bullet+}$ and another α-cleavage with loss of C_3H_7 to $\mathbf{C}^+$ (Scheme 5A). The ^{13}C-labelling experiments cannot indicate which hydrogen of **1** is shifted into the iPr group and is lost from the core structure, but the mass spectra of labelled **1** prepared from (*R*)- and (*S*)-(1-^{13}C,1-^{2}H)IPP and (*E*)- and (*Z*)-(4-^{13}C,4-^{2}H)IPP all show besides the cleavage of a fragment of 43 Da (C_3H_7) also a small peak for the cleavage of 44 Da ($C_3H_6{}^2H$) (Fig. S35†). This demonstrates that multiple mechanisms involving hydrogen scrambling may contribute to the formation of $\mathbf{C}^+$. Therefore, also for the other fragment ions discussed next only the relevant carbon portions will be taken into account, while for hydrogen rearrangements sterically and electronically plausible suggestions will be made.

The PMA_{161} reveals loss of the C5-6-7(-19)-8 and C15(-17)-16 moieties (Fig. 2). This can be explained by ionisation to $\mathbf{1}^{\bullet+}$ and two α-cleavages with neutral loss of isoprene *via* $\mathbf{D}^{\bullet+}$ to $\mathbf{E}^{\bullet+}$ (Scheme 5B). The terminal steps for the loss of C_3H_7 are then basically the same as for the cleavage of C15(-17)-16 in the formation of *m*/*z* 229.

The analysis of PMA_{136} shows the cleavage of C5-6-7(-19)-8-9-10-11(-18)-12 (Fig. 2), resembling the loss of two neutral isoprene units. Starting from $\mathbf{E}^{\bullet+}$ in which the first isoprene unit is already cleaved off, an α-fragmentation to $\mathbf{I}^{\bullet+}$ and inductive cleavage to $\mathbf{J}^{\bullet+}$ results in the neutral loss of a second isoprene unit (Scheme 6A). PMA_{121} exhibits the additional loss of either Me16 or Me17, which can directly be explained from $\mathbf{J}^{\bullet+}$ through another α-cleavage. Finally, PMA_{93} indicates formation

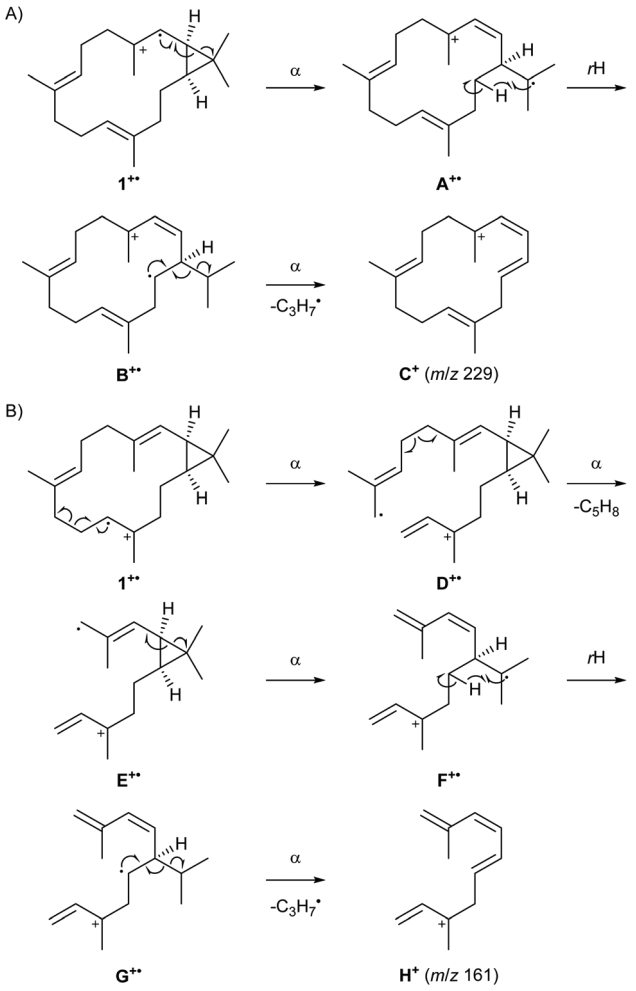

Scheme 5 Proposed mechanisms for the formation of the fragment ions (A) *m*/*z* 229 and (B) *m*/*z* 161 of **1**.

of this fragment ion from the C13-14-1-2-3(-20)-4 portion of **1** (Fig. 2). A first α-cleavage of $\mathbf{1}^{\bullet+}$ to $\mathbf{L}^{\bullet+}$ followed by two inductive cleavages *via* $\mathbf{M}^{\bullet+}$ to $\mathbf{N}^{\bullet+}$ (giving an alternative explanation for *m*/*z* 136) can be followed by α-fragmentation with cyclopropane ring opening to $\mathbf{O}^{\bullet+}$ (Scheme 6B). Hydrogen rearrangement to $\mathbf{P}^{\bullet+}$ and loss of the isopropyl group then lead to $\mathbf{Q}^+$.

Conclusions

The cyclisation mechanism of casbene synthase (CS) has been investigated in isotopic labelling experiments, revealing a stereochemical course that is in agreement with the reported absolute configuration of casbene. Besides GGPP, CS is able to convert GGPP analogs with shifted double bond positions into casbene analogs (iso-casbenes), and similar isotopic labelling experiments as performed for the native substrate revealed an identical stereochemical course, from which the absolute configurations of the iso-casbenes could be established. A similar approach has previously been used to determine the absolute configurations of sesquiterpenes.[55] Since the assignment of

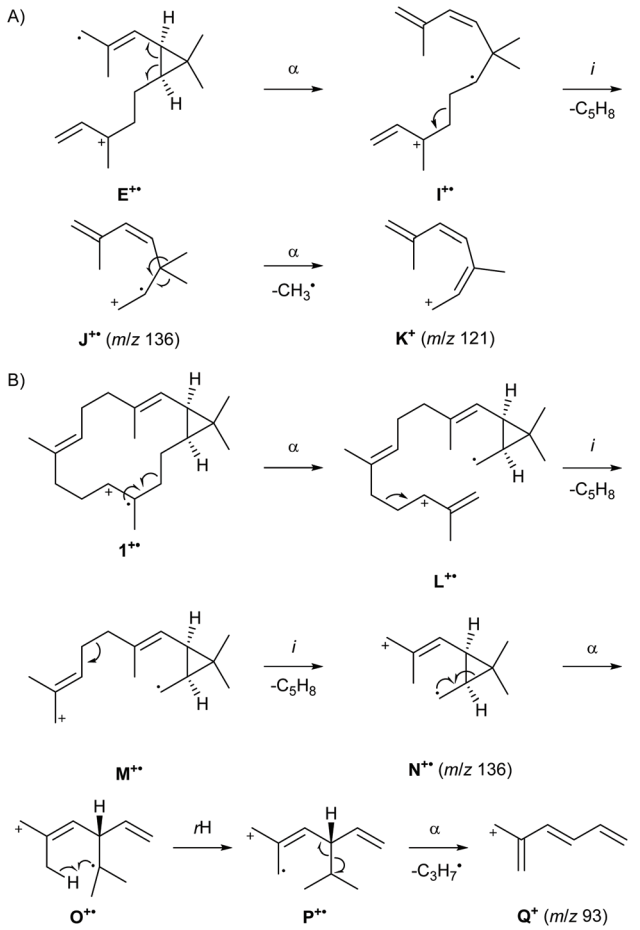

Scheme 6 Proposed mechanisms for the formation of the fragment ions (A) *m/z* 136 and *m/z* 121, and (B) *m/z* 93 of **1**.

absolute configurations for terpene hydrocarbons is a generally difficult task, this strategy may be useful also for the assignment of absolute configurations for other terpenes. Furthermore, ^{13}C-labelling experiments were performed to address the EI-MS fragmentation mechanism of casbene, showing the preferred cleavage of isoprene units from the macrocyclic core structure and of an isopropyl group originating from the dimethylcyclopropane moiety. Similar fragmentation mechanisms may be relevant for other macrocyclic diterpenes such as cembrenes. We will continue to study these and other aspects of terpene biosynthesis and chemistry through isotopic labellings in our future work.

Conflicts of interest

There are no conflicts to declare.

Acknowledgements

This work was funded by the Deutsche Forschungsgemeinschaft (DI1536/7-2).

References

1 D. R. Robinson and C. A. West, Biosynthesis of cyclic diterpenes in extracts from seedlings of *Ricinus communis*. I. Identification of diterpene hydrocarbons formed from mevalonate, *Biochemistry*, 1970, **9**, 70.
2 M. D. Sayed, A. Riszk, F. M. Hammouda, M. M. El-Missiry, E. M. Williamson and F. J. Evans, Constituents of Egyptian Euphorbiaceae. IX. Irritant and cytotoxic ingenane esters from *Euphorbia paralias* L, *Experientia*, 1980, **36**, 1206.
3 H. Gotta, W. Adolf, H. J. Opferkuch and E. Hecker, On the active principles of the Euphorbiaceae, IXa ingenane type diterpene esters from five *Euphorbia* species, *Z. Naturforsch., B: Anorg. Chem., Org. Chem.*, 1984, **39**, 683.
4 L. Crombie, G. Kneen and G. Pattenden, Synthesis of Casbene, *J. Chem. Soc., Chem. Commun.*, 1976, 66.
5 L. Crombie, G. Kneen, G. Pattenden and D. Whybrow, Total synthesis of the macrocyclic diterpene (–)-casbene, the putative biogenetic precursor of lathyrane, tigliane, ingenane, and related terpenoid structures, *J. Chem. Soc., Perkin Trans. 1*, 1980, 1711.
6 M. T. Duebner, W. Adolf and C. A. West, Biosynthesis of the Diterpene Phytoalexin Casbene: Partial Purification and Characterization of Casbene Synthetase from *Ricinis communis*, *Plant Physiol.*, 1978, **62**, 598.
7 C. J. D. Mau and C. A. West, Cloning of casbene synthase cDNA: evidence for conserved structural features among terpenoid cyclases in plants, *Proc. Natl. Acad. Sci. U. S. A.*, 1994, **91**, 8497.
8 A. M. Hill, D. E. Cane, C. J. D. Mau and C. A. West, High Level Expression of *Ricinus communis* Casbene Synthase in *Escherichia coli* and Characterization of the Recombinant Enzyme, *Arch. Biochem. Biophys.*, 1996, **336**, 283.
9 K. K. Reiling, Y. Yoshikuni, V. J. J. Martin, J. Newman, J. Bohlmann and J. D. Keasling, Mono and diterpene production in *Escherichia coli*, *Biotechnol. Bioeng.*, 2004, **87**, 200.
10 J. Kirby, M. Nishimoto, J. G. Park, S. T. Withers, F. Nowroozi, D. Behrendt, E. J. Garcia Rutledge, J. L. Fortman, H. E. Johnson, J. V. Anderson and J. D. Keasling, Cloning of casbene and neocembrene synthases from *Euphorbiaceae* plants and expression in *Saccharomyces cerevisiae*, *Phytochemistry*, 2010, **71**, 1466.
11 K. Brückner and A. Thissier, High-level diterpene production by transient expression in *Nicotiana benthamiana*, *Plant Methods*, 2013, **9**, 46.
12 A. J. King, G. D. Brown, A. D. Gilday, E. Forestier, T. R. Larson and I. A. Graham, A Cytochrome P450-Mediated Intramolecular Carbon–Carbon Ring Closure in the Biosynthesis of Multidrug-Resistance-Reversing Lathyrane Diterpenoids, *ChemBioChem*, 2016, **17**, 1593.
13 D. Luo, R. Callari, B. Hamberger, S. Gizachew Wubshet, M. T. Nielsen, J. Andersen-Ranberg, B. M. Hallström, F. Cozzi, H. Heider, B. L. Möller, D. Staerk and B. Hamberger, Oxidation and cyclization of casbene in the biosynthesis of *Euphorbia* factors from mature seeds of

Euphorbia lathyris L., *Proc. Natl. Acad. Sci. U. S. A.*, 2016, **113**, E5082.
14 A. J. King, G. D. Brown, A. D. Gilday, T. R. Larson and I. A. Graham, Production of Bioactive Diterpenoids in the Euphorbiaceae Depends on Evolutionarily Conserved Gene Clusters, *Plant Cell*, 2014, **26**, 3286.
15 J. Wong, T. de Rond, L. d'Espaux, C. van der Horst, I. Dev, L. Rios-Solis, J. Kirby, H. Scheller and J. Keasling, High-titer production of lathyrane diterpenoids from sugar by engineered *Saccharomyces cerevisiae*, *Metab. Eng.*, 2018, **45**, 142.
16 G. Appendino, *Omnia praeclara rara*. The Quest for Ingenol Heats Up, *Angew. Chem., Int. Ed.*, 2014, **53**, 927.
17 X. Liang, G. Grue-Sörensen, A. K. Petersen and T. Högberg, Semisynthesis of ingenol 3-angelate (PEP005): efficient stereoconservative angeloylation of alcohols, *Synlett*, 2012, **23**, 2647.
18 L. Jörgensen, S. J. McKerrall, C. A. Kuttruff, F. Ungeheuer, J. Felding and P. S. Baran, 14-Step Synthesis of (+)-Ingenol from (+)-3-Carene, *Science*, 2013, **341**, 878.
19 J. S. Dickschat, Bacterial Diterpene Biosynthesis, *Angew. Chem., Int. Ed.*, 2019, **58**, 15964.
20 V. Harms, A. Kirschning and J. S. Dickschat, Nature-driven approaches to non-natural terpene analogs, *Nat. Prod. Rep.*, 2020, **37**, 1080.
21 Y. Jin, D. C. Williams, R. Croteau and R. M. Coates, Taxadiene Synthase-Catalyzed Cyclization of 6-Fluorogeranylgeranyl Diphosphate to 7-Fluoroverticillenes, *J. Am. Chem. Soc.*, 2005, **127**, 7834.
22 O. Cascón, S. Touchet, D. J. Miller, V. Gonzalez, J. A. Faraldos and R. K. Allemann, Chemoenzymatic preparation of germacrene analogues, *Chem. Commun.*, 2012, **48**, 9702.
23 M. Demiray, X. Tang, T. Wirth, J. A. Faraldos and R. K. Allemann, An Efficient Chemoenzymatic Synthesis of Dihydroartemisinic Aldehyde, *Angew. Chem., Int. Ed.*, 2017, **56**, 4347.
24 A. Hou and J. S. Dickschat, Using Terpene Synthase Plasticity in Catalysis: On the Enzymatic Conversion of Synthetic Farnesyl Diphosphate Analogues, *Chem. – Eur. J.*, 2021, **27**, 15644.
25 C. Oberhauser, V. Harms, K. Seidel, B. Schröder, K. Ekramzadeh, S. Beutel, S. Winkler, L. Lauterbach, J. S. Dickschat and A. Kirschning, Exploiting the synthetic potential of sesquiterpene cyclases for generating unnatural terpenoids, *Angew. Chem., Int. Ed.*, 2018, **57**, 11802.
26 V. Harms, V. Ravkina and A. Kirschning, Mechanistic Similarities of Sesquiterpene Cyclases PenA, Omp6/7, and BcBOT2 Are Unraveled by an Unnatural "FPP-Ether" Derivative, *Org. Lett.*, 2021, **23**, 3162.
27 F. Huynh, D. J. Grundy, R. L. Jenkins, D. J. Miller and R. K. Allemann, Sesquiterpene Synthase-Catalysed Formation of a New Medium-Sized Cyclic Terpenoid Ether from Farnesyl Diphosphate Analogues, *ChemBioChem*, 2018, **19**, 1834.
28 S. Y. Chow, H. J. Williams, Q. Huang, S. Nanda and A. I. Scott, Studies on Taxadiene Synthase: Interception of the Cyclization Cascade at the Isocembrene Stage with GGPP Analogues, *J. Org. Chem.*, 2005, **70**, 9997.
29 G. Li, Y.-W. Guo and J. S. Dickschat, Diterpene Biosynthesis in *Catenulispora acidiphila*: On the Mechanism of Catenul-14-en-6-ol Synthase, *Angew. Chem., Int. Ed.*, 2021, **60**, 1488.
30 A. Hou, L. Lauterbach and J. S. Dickschat, Enzymatic Synthesis of Methylated Terpene Analogs Using the Plasticity of Bacterial Terpene Synthases, *Chem. – Eur. J.*, 2020, **26**, 2178.
31 V. Harms, B. Schröder, C. Oberhauser, C. D. Tran, S. Winkler, G. Dräger and A. Kirschning, Methyl-Shifted Farnesyldiphosphate Derivatives Are Substrates for Sesquiterpene Cyclases, *Org. Lett.*, 2020, **22**, 4360.
32 L. Lauterbach, A. Hou and J. S. Dickschat, Rerouting and Improving Dauc-8-en-11-ol Synthase from *Streptomyces venezuelae* to a High Yielding Biocatalyst, *Chem. – Eur. J.*, 2021, **27**, 7923.
33 J. S. Dickschat, K. A. K. Pahirulzaman, P. Rabe and T. A. Klapschinski, An Improved Technique for the Rapid Chemical Characterisation of Bacterial Terpene Cyclases, *ChemBioChem*, 2014, **15**, 810.
34 J. Rinkel and J. S. Dickschat, Addressing the Chemistry of Germacrene A by Isotope Labeling Experiments, *Org. Lett.*, 2019, **21**, 2426.
35 F. M. Hahn, A. P. Hurlburt and C. D. Poulter, *Escherichia coli* Open Reading Frame 696 Is *idi*, a Nonessential Gene Encoding Isopentenyl Diphosphate Isomerase, *J. Bacteriol.*, 1999, **181**, 4499.
36 P. Rabe, J. Rinkel, E. Dolja, T. Schmitz, B. Nubbemeyer, T. H. Luu and J. S. Dickschat, Mechanistic investigantions on two bacterial diterpene cyclases: Spiroviolene Synthase and Tsukubadiene Synthase, *Angew. Chem., Int. Ed.*, 2017, **56**, 2776.
37 L. Lauterbach, J. Rinkel and J. S. Dickschat, Two Bacterial Diterpene Synthases from *Allokutzneria albata* for Bonnadiene and for Phomopsene and Allokutznerene, *Angew. Chem., Int. Ed.*, 2018, **57**, 8280.
38 L. Poppe, L. Novák and C. Szántay, A Convenient Synthesis of (*E*)-β-Farnesene, *Synth. Commun.*, 1987, **17**, 173.
39 J. Rinkel, L. Lauterbach and J. S. Dickschat, A Branched Diterpene Cascade: The Mechanism of Spinodiene Synthase from *Saccharopolyspora spinosa*, *Angew. Chem., Int. Ed.*, 2019, **58**, 452.
40 P. Rabe, L. Barra, J. Rinkel, R. Riclea, C. A. Citron, T. A. Klapschinski, A. Janusko and J. S. Dickschat, Conformational Analysis, Thermal Rearrangement and EI-MS-Fragmentation Mechanism of (1(10)*E*,4*E*,6*S*,7*R*)-Germacradien-6-ol by 13C-Labeling Experiments, *Angew. Chem., Int. Ed.*, 2015, **54**, 13448.
41 Z. Quan and J. S. Dickschat, On the mechanism of ophiobolin F synthase and the absolute configuration of its product by isotopic labelling experiments, *Org. Biomol. Chem.*, 2020, **18**, 6072.

42 G. Bian, J. Rinkel, Z. Wang, L. Lauterbach, A. Hou, Y. Yuan, Z. Deng, T. Liu and J. S. Dickschat, A Clade II-D Fungal Chimeric Diterpene Synthase from *Colletotrichum gloeosporioides* Making Dolasta-1(15),8-diene, *Angew. Chem., Int. Ed.*, 2018, **57**, 15887.

43 P. Rabe, T. A. Klapschinski and J. S. Dickschat, Position-specific mass shift analysis: a systematic method to investigate the EI-MS fragmentation mechanism of *epi*-isozizaene, *ChemBioChem*, 2016, **17**, 1333.

44 D. S. Weinberg and C. Djerassi, Mass Spectrometry in Structural and Stereochemical Problems. LXXXVIII. Rearrangements of Simple Terpenes on Electron Impact, *J. Org. Chem.*, 1966, **31**, 115.

45 J. Karliner and C. Djerassi, Terpenoids. LVII. Mass Spectral and Nuclear Magnetic Resonance Studies of Pentacyclic Triterpene Hydrocarbons, *J. Org. Chem.*, 1966, **31**, 1945.

46 R. R. Muccino and C. Djerassi, Mass Spectrometry in Structural and Stereochemical Problems. CCXL. The Effect of a 1401-Angular Methyl Group upon the Mass Spectral Fragmentation of 11- and 7-Keto Steroids, *J. Am. Chem. Soc.*, 1973, **95**, 8726.

47 R. Ryhage and E. Stenhagen, Mass spectrometric examinations. Part 5. Methyl esters of mono alkyl substituted acids with ethyl or longer side chain and methyl esters of di and polyalkyl substituted acids, *Ark. Kemi*, 1960, **15**, 291.

48 D. Kuck and H.-F. Grützmacher, Hydrogen Rearrangement in Molecular Ions of Alkyl Benzenes: Appearance Potentials and Substituent Effects on the Formation of $[C_7H_8]^+$ Ions, *Org. Mass Spectrom.*, 1978, **13**, 81.

49 D. Kuck and H.-F. Grützmacher, Hydrogen Rearrangement in Molecular Ions of Alkyl Benzenes: Mechanism and Time Dependence of Hydrogen Migrations in Molecular Ions of 1,3-Diphenylpropane and Deuterated Analogues, *Org. Mass Spectrom.*, 1978, **13**, 90.

50 P. Rabe and J. S. Dickschat, The EIMS fragmentation mechanisms of the sesquiterpenes corvol ethers A and B, epi-cubebol and isodauc-8-en-11-ol, *Beilstein J. Org. Chem.*, 2016, **12**, 1380.

51 J. Rinkel, P. Rabe and J. S. Dickschat, The EI-MS fragmentation mechanisms of bacterial sesquiterpenes and diterpenes, *Eur. J. Org. Chem.*, 2019, 351.

52 A. Hou and J. S. Dickschat, On the mass spectrometric fragmentations of the bacterial sesterterpenes sestermobaraenes A – C, *Beilstein J. Org. Chem.*, 2020, **16**, 2807.

53 H. Xu, J. Rinkel and J. S. Dickschat, Isoishwarane Synthase from *Streptomyces lincolnensis*, *Org. Chem. Front.*, 2021, **8**, 1177.

54 G. Li, Y.-W. Guo and J. S. Dickschat, The mass spectrometric fragmentation mechanisms of catenulane and isocatenulane diterpenes, *Org. Biomol. Chem.*, 2021, **19**, 2224.

55 J. Rinkel, P. Rabe, P. Garbeva and J. S. Dickschat, Lessons from 1,3-Hydride Shifts in Sesquiterpene Cyclisations, *Angew. Chem., Int. Ed.*, 2016, **55**, 13593.

Appendices B

Diterpene Biosynthesis from Geranylgeranyl Diphosphate Analogues with Changed Reactivities Expands Skeletal Diversity

Angew. Chem. **2022***, 134,* e202211054.

DOI: 10.1002/ange.202211054

Angew. Chem. Int. Ed., **2022**, *61*, e202211054

DOI: 10.1002/anie.202211054

How to cite: *Angew. Chem. Int. Ed.* **2022,** *61,* e202211054
International Edition: doi.org/10.1002/anie.202211054
German Edition: doi.org/10.1002/ange.202211054

Biosynthesis

Diterpene Biosynthesis from Geranylgeranyl Diphosphate Analogues with Changed Reactivities Expands Skeletal Diversity

*Heng Li and Jeroen S. Dickschat**

Abstract: Two analogues of the diterpene precursor geranylgeranyl diphosphate with shifted double bonds, named iso-GGPP I and iso-GGPP II, were enzymatically converted with twelve diterpene synthases from bacteria, fungi and protists. The changed reactivity in the substrate analogues resulted in the formation of 28 new diterpenes, many of which exhibit novel skeletons.

Introduction

The astonishing structural complexity observed in terpenes is generated from very few acyclic and achiral precursors. Only two C_5 building blocks, dimethylallyl diphosphate (DMAPP) and isopentenyl diphosphate (IPP), are required that are made via the mevalonate or the deoxyxylulose phosphate pathway.[1] While DMAPP is an electrophile, IPP can react as a nucleophile, allowing their fusion to oligoprenyl diphosphates by prenyltransferases. Starting from DMAPP, successive elongation reactions with IPP first lead to the monoterpene precursor geranyl diphosphate (GPP, C_{10}),[2] and then to farnesyl diphosphate (FPP, C_{15})[3] as the precursor to sesquiterpenes, the diterpene precursor geranylgeranyl diphosphate (GGPP, C_{20}),[4] geranylfarnesyl diphosphate (GFPP, C_{25})[5] for sesterterpene biosynthesis, and—as recently discovered—even farnesylfarnesyl diphosphate for non-squalene derived triterpene biosynthesis.[6] Class I terpene synthases (TSs)[7] exhibit several highly conserved residues and motifs, including the aspartate-rich region (DDXX(X)D)[7] and the NSE triad (ND-(L,I,V)XSXX(K,R)E)[8] for binding of a trinuclear $(Mg^{2+})_3$ cluster that in turn binds to the substrate's diphosphate. The pyrophosphate sensor,[9] a highly conserved Arg, and the RY pair form hydrogen bridges to the diphosphate.[10] With assistance of an effector triad substrate ionisation by the abstraction of diphosphate is achieved,[9] which initiates a cationic cascade reaction with cyclisations, hydride or proton migrations, and Wagner–Meerwein rearrangements. Termination of the cascade by deprotonation or water quenching ultimately leads to terpene hydrocarbons or alcohols. Further roles of the enzyme include to provide a hydrophobic pocket that defines the reactive substrate conformation,[11] to stabilise cationic intermediates, and to participate in acid base catalysis for which a carbonyl oxygen at the helix G break is responsible in selinadiene biosynthesis.[12]

Interference with terpene biosynthesis aiming at novel TS products is possible in two ways: Either the enzyme can be modified through site-directed mutagenesis,[13] or structurally modified substrate analogues can be used in enzymatic conversions.[14] Recent studies have shown that many TSs accept and convert non-natural substrate analogues such as halogenated oligoprenyl diphosphates,[15] allyl alcohols and epoxides,[16] ketones,[17] derivatives with heteroatom insertions into the chain,[18] with changed Me group substitutions,[15d,17b,19] double bond shifts,[17,20] *Z*-configured or hydrogenated double bonds.[17a,21] Most of these studies have used FPP analogues in conjunction with sesquiterpene synthases (STSs), but only in a few cases GGPP analogues were converted with diterpene synthases (DTSs), exemplified by previous work using taxadiene synthase[15a,21a] and casbene synthase[20] from plants, and the bacterial catenul-14-en-6-ol synthase from *Catenulispora acidiphila*.[21b] The often intriguing cyclisation mechanisms of DTSs[22] prompted us to broadly investigate the DTSs recently characterised in our group for their potential to convert GGPP analogues into non-natural diterpenes. The natural products of the terpene synthases used in this study and their cyclisation mechanisms are summarised in Schemes S1–S12.

Results and Discussion

The incubation of iso-FPP[20] in which the C6=C7 double bond is shifted to a C7=C14 double bond with IPP, GGPP synthase (GGPPS) from *Streptomyces cyaneofuscatus*[23] and bonnadiene synthase (BdS) from *Allokutzneria albata*[24] resulted in the formation of a diterpene alcohol and minor amounts of a diterpene hydrocarbon (Figure S1). Both compounds were isolated and structurally characterised by NMR spectroscopy (Tables S2 and S3, Figures S2–S17), revealing macrocyclic structures for which we suggest the names isonephthenol (**1**) and isocembrene A (**2**, Scheme 1A). Generally, compounds obtained in this study in which the shifted double bond of the substrate analogue is

[*] H. Li, Prof. Dr. J. S. Dickschat
Kekulé-Institute for Organic Chemistry and Biochemistry, University of Bonn
Gerhard-Domagk-Straße 1, 53121 Bonn (Germany)
E-mail: dickschat@uni-bonn.de

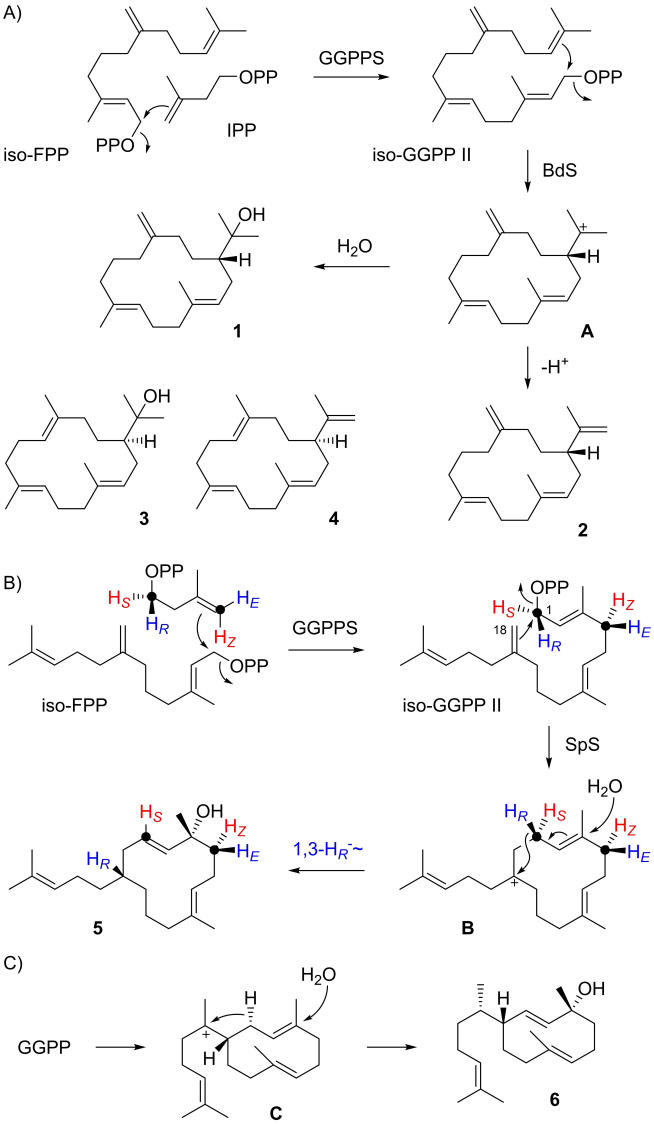

Scheme 1. Diterpenes from iso-FPP. A) Formation of iso-GGPP II from iso-FPP and IPP by GGPPS and conversion into **1** and **2** by BdS, B) biosynthesis of **5** using SpS, and C) cyclisation of GGPP to the related natural product **6**. Red and blue hydrogens are substituted with deuterium in the stereoselectively deuterated probes (*R*)- and (*S*)-(1-^{13}C,1-^{2}H)IPP, and (*E*)- and (*Z*)-(4-^{13}C,4-^{2}H)IPP for determination of absolute configurations. Black dots represent ^{13}C-labelled carbons in these probes.

reflected, will be named iso-compounds of the corresponding natural product. Specifically, **1** and **2** are the iso-compounds corresponding to nephthenol (**3**) and cembrene A (**4**). With GGPP the BdS-catalysed reaction to bonnadiene starts with an isomerisation to geranyllinalyl diphosphate (GLPP) and subsequent 1,14-cyclisation to a 2*Z* configured macrocycle, followed by further cyclisation steps (Scheme S1). The structural modification in iso-GGPP II, formed from iso-FPP and IPP by GGPPS, leads to a disturbed enzyme-substrate interaction in which the 1,14-cyclisation is still promoted, but with retained 2*E* configuration in **A**, while the downstream steps of the cascade are interrupted and direct formation of **1** and **2** is observed.

The enzymatic conversion of iso-FPP and IPP with GGPPS and spata-13,17-diene synthase (SpS) from *S. xinhaiensis*[25] gave a complex product mixture (Figure S18) from which a diterpene alcohol **5** was isolated (Table S4, Figures S19–S26). With GGPP as substrate SpS catalyses an initial 1,10-cyclisation (Scheme S2), which is not possible with iso-GGPP II. Remarkably, a very similar 1,18-cyclisation to **B** substitutes for the natural cyclisation mode. A subsequent 1,3-hydride shift and attack of water result in **5** (Scheme 1B). Compound **5** was named pseudoobscuronatin, because its formation follows a very similar mechanism as for obscuronatin (**6**)[26] that proceeds by 1,10-cyclisation of GGPP to **C**, followed by 1,3-hydride shift and attack of water (Scheme 1C).[21b] Compounds isolated in this study will be named pseudo-derivatives of known natural products with a similar cyclisation cascade, if this cascade is logically modified because of the double bond shift in the substrate analogue.

With GGPPS and spinodiene synthase (SoS) from *Saccharopolyspora spinosa*[27] the substrates iso-FPP and IPP were efficiently converted into one main diterpene, besides traces of a few side products (Figure S27). The purified main compound showed no optical rotation, suggesting an achiral product, which was confirmed by NMR spectroscopy (Table S5, Figures S28–S35), resulting in the structure of **7** (Scheme 2A). The natural spinodiene cyclisation cascade is initiated with a 1,11–10,14 cyclisation (Scheme S3), which is altered with iso-GGPP II to the similar 1,18-cyclisation to **B**. Herein, the second ring closure is not realised, because a tertiary cationic intermediate could only be reached through formation of a strained cyclobutane ring. Consequently, **B** simply reacts by deprotonation to **7**. Because of the similarities between the cyclisation reactions to **7** and to germacrene A (**13**, Scheme 2C), compound **7** was named prenylpseudogermacrene A.

With FPP as substrate alternative reactions from intermediate **E** include the deprotonation to germacrene B (**14**) or quenching with water to hedycaryol (**15**, Scheme 2C). Analogous reactions were observed for the conversion of iso-GGPP II with other diterpene synthases. *A. albata* spiroalbatene synthase (SaS)[28] resulted in the highly selective formation (Figure S36) of the new compound prenylpseudogermacrene B (**8**, Table S6, Figures S37–S44). The pseudo-C_3 symmetry of the macrocycle in **8** resulted in almost identical chemical shifts for carbons in corresponding positions of the two isoprene units marked in bold. An unambiguous assignment was possible using iso-FPP in conjunction with the five isotopomers of singly labelled (^{13}C)IPP and product analysis through ^{13}C NMR (Figure S45). With GGPP SaS shows an initial 1,14-cyclisation (Scheme S4) that is surprisingly turned into a 1,18-cyclisation with iso-GGPP II, although the C14=C15 double bond remains unchanged in this substrate analogue. A possible explanation lies in the second ring closure in spiroalbatene biosynthesis that happens between C1 and C10, suggesting that the C10=C11 double bond of GGPP is also close to C1 in the active site of SaS. Therefore, only a small conforma-

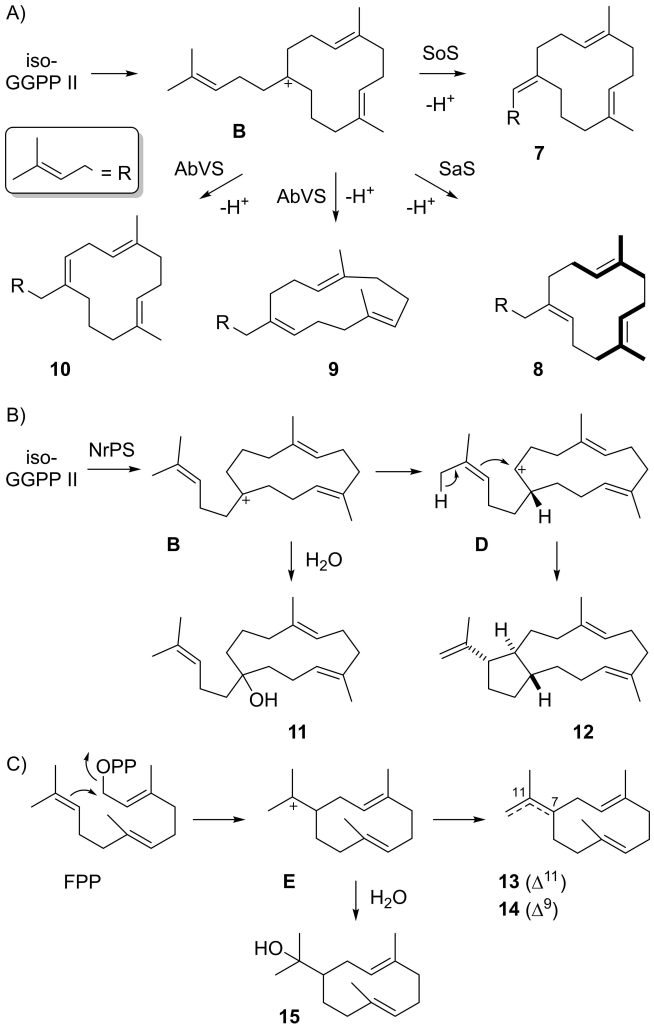

Scheme 2. Diterpenes from iso-FPP. A) Formation of **7** by SoS, **8** by SaS, and **9** and **10** by AbVS, B) formation of **11** and **12** by NrPS, and C) biosynthesis of related sesquiterpenes **13**–**15**.

tional change for iso-GGPP II may lead to the observed altered cyclisation mode.

Further alternative deprotonation products from cation **B** were obtained by conversion of iso-GGPP II with variediene synthase from *Aspergillus brasiliensis* (AbVS, Scheme 2A, Figure S46).[29] This bifunctional fungal enzyme contains a prenyltransferase (PT) domain for the biosynthesis of GGPP and a TS domain for its cyclisation. Therefore, the substrate iso-GGPP II can be formed in situ from iso-FPP and IPP without addition of GGPPS. Through this approach the two compounds prenylpseudogermacrene C (**9**) and prenylpseudogermacrene D (**10**) were obtained (Tables S7 and S8, Figures S47–S62). With phomopsene synthase from *Nocardiopsis rhamnosiphilia* (NrPS,[30] Scheme 2B) iso-GGPP II gave besides the main product **8** (Figure S63) smaller amounts of **7**, **9** and **10**, and the new diterpene alcohol prenylpseudohedycaryol (**11**, Table S9, Figures S64–S71). Notably, as observed for SoS also AbVS and NrPS change the natural initial 1,11–10,14 cyclisation with GGPP (Schemes S5 and S6) to a 1,18-cyclisation with iso-GGPP II. Another minor product obtained from this enzyme was characterised as pseudodollabella-3,7,18-triene (**12**, Table S10, Figures S72–S79). This compound requires a 1,2-hydride shift to **D**, cyclisation and deprotonation.

Different patterns of compounds **1**, **2** and **5**–**12** were also observed among the products obtained from iso-GGPP II with several other bacterial DTSs. Especially the prenylpseudogermacrenes A–D (**7**–**10**) and prenylpseudohedycaryol (**11**) were frequently found (Figures S18, S27, S46, S63, S80–S82).

The absolute configurations of terpenes can be determined with stereoselectively deuterated precursors, setting additional stereogenic centers in the terpene synthase products of known configuration. The relative configuration of the naturally present stereogenic centers to the stereogenic centers at the deuterated carbons can be determined through NOESY spectroscopy and allows to conclude on the absolute configuration of the terpene. Our method makes use of additional ^{13}C-labels for a highly sensitive analysis by HSQC. For this purpose, the labelled probes (*R*)- and (*S*)-(1-^{13}C,1-^{2}H)IPP,[31] and (*E*)- and (*Z*)-(4-^{13}C,4-^{2}H)IPP[24] were developed that can be used to elongate FPP and its analogue iso-FPP with GGPPS through a known stereochemical course.[32] Unfortunately, this method is not always suitable for the determination of absolute configurations of macrocyclic ring compounds, because their conformational flexibility sometimes does not allow for an unambiguous interpretation of NOESY spectra. However, the absolute configurations of **1** and **2** could be tentatively assigned from their optical rotations (**1**: $[\alpha]_D^{25} = +11.4$, *c* 0.07, Me_2CO, **2**: $[\alpha]_D^{25} = +84.6$, *c* 0.13, Me_2CO) which are of opposite sign to the reported optical rotations of (*R*)-**3** ($[\alpha]_D^{25} = -46.3$, *c* 1.20, $CHCl_3$)[33] and (*R*)-**4** ($[\alpha]_D^{25} = -14.2$, *c* 0.48, $CHCl_3$)[34] from plants. For **5** NOESY based assignments of diastereotopic hydrogens were possible (Figure S19), and isotopic labelling experiments with (*E*)- and (*Z*)-(4-^{13}C,4-^{2}H)IPP (Figure S83) pointed to the absolute configuration as shown in Scheme 1. For compound **11** no assignment could be made from labelling experiments, but the results showed a high enantiomeric purity of **11** obtained with HdS (90 % *ee*, Figure S84), but only 70 % *ee* for **11** obtained with NrPS (Figure S85). For **12** the production was too low to gain conclusive insights into its absolute configuration from labelling experiments.

The conversion of iso-GGPP I with the C6=C7 double bond of GGPP shifted to C7=C14 with several DTSs resulted in the iso-compounds showing the corresponding double bond shift in comparison to the native products from GGPP. Specifically, β-pinacene synthase (PcS) from the protist *Dyctostelium discoideum*[35] gave iso-β-pinacene (**16**) as main product (Scheme 3A, Figure S86). Notably, most ^{1}H signals and the ^{13}C signals of the geminal Me groups of **16** show line broadening in the NMR spectra, even at an elevated temperature of 70 °C, and despite the fact that **16** is achiral each aliphatic methylene group shows distinct signals for the two hydrogens (Table S11, Figures S87–S94), suggesting that **16** exists in two enantiomeric slowly interconverting conformers. With 18-hydroxydolabella-3,7-diene synthase (HdS) from *Chitinophaga pinensis*[36] iso-GGPP I is

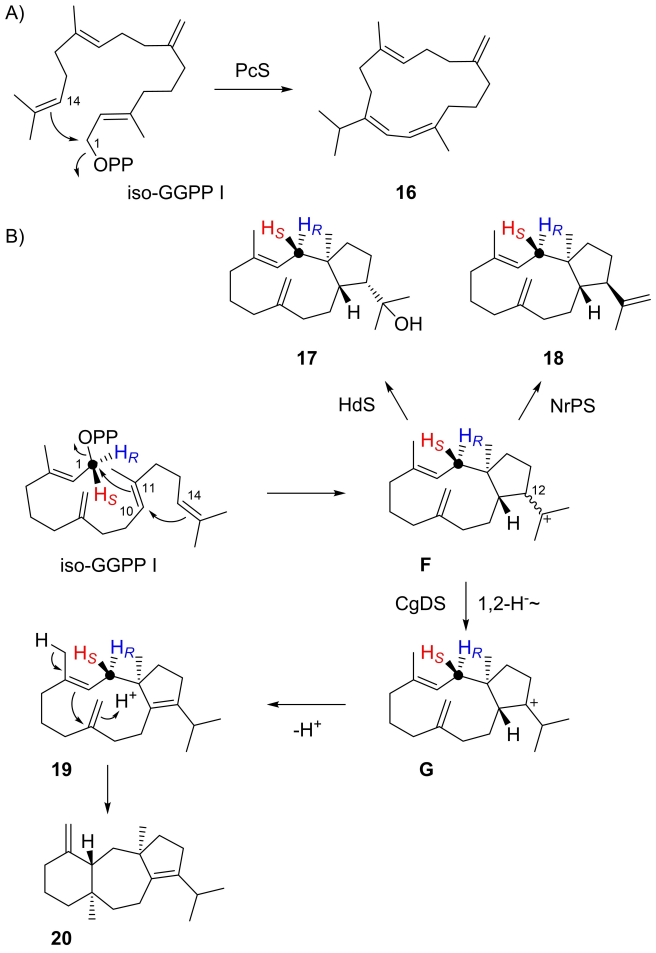

Scheme 3. Diterpenes from iso-GGPP I. A) Formation of **16** by PcS, B) formation of **17** by HdS, **18** by NrPS, and **19** and **20** by CgDS. Red and blue hydrogens are substituted with deuterium in the stereoselectively deuterated probes (*R*)- and (*S*)-(1-^{13}C,1-^{2}H)-iso-GGPP for determination of absolute configurations. Black dots represent ^{13}C-labelled carbons in these probes.

converted into 18-hydroxydolabella-3,8(17)-diene (**17**) as the main product (Scheme 3B, Table S12, Figures S95–S103). In both cases of **16** and **17** a cyclisation cascade is followed similar to that for the native enzyme products (Schemes S7 and S8). For a few other DTSs an interruption of the cyclisation cascade at an early intermediate was observed, e.g. with NrPS the bicyclic compound dolabella-3,8(17),18-triene (**18**) was obtained as the main product (Table S13, Figures S104–S112). Compounds **17** and **18** arise through cation **F**, but with different configurations at C12, which reflects in both cases the stereochemistry of the natural intermediate from GGPP (Schemes S6 and S8).

Incubation of iso-GGPP I with the bifunctional fungal PT-TS enzyme *Colletotrichum gloeosporioides* Dolasta-1(15),8-diene Synthase (CgDS)[37] gave a mixture of one diterpene alcohol (**25**) which will be explained below and several diterpene hydrocarbons (Scheme 3B, Figure S113). The hydrocarbon fraction contained **18**, besides two additional compounds that were isolated and identified as the new compound dolabella-3,8(17),11-triene (**19**, Table S14, Figures S114–S121) and dolasta-1(15),8-diene (**20**), the natural product of CgDS from GGPP.[37] Their formation can be explained by a 1,2-hydride shift from **F** to **G** and deprotonation to **19**, followed by reprotonation at the olefinic methylene carbon to induce a second ring closure to **20**. Notably, the mechanism towards **20** is very similar to its formation from GGPP, only with the reprotonated double bond in the neutral intermediate being located in a different position (Scheme S9).

With SaS iso-GGPP I was converted into the hydrocarbons isothunbergene A (**21**) and B (**22**), besides the diterpene alcohol albataxenol (**23**) as the main product (Tables S15–S17, Figures S122–S146). Notably, the NMR spectra of **23** recorded at 293 K showed line broadening, but sharper signals could be observed at 344 K. The isothunbergenes require 1,14-cyclisation of iso-GGPP I and two sequential 1,2-hydride shifts to **H**, in analogy to the reactions with the native substrate GGPP (Scheme S4). Subsequent deprotonation with formation of an (*E*,*E*) or (*E*,*Z*)-diene portion leads to **21** and **22** (Scheme 4A). If the cyclisation

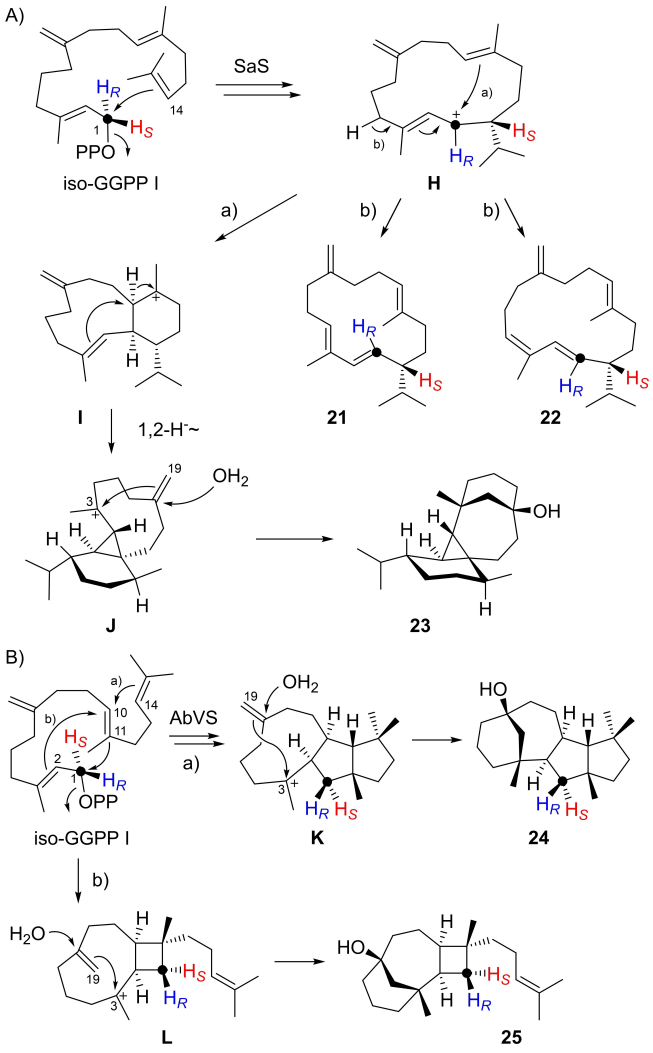

Scheme 4. Diterpenes from iso-GGPP I. A) Formation of **21**–**23** by SaS, B) formation of **24** and **25** by AbVS.

cascade is continued as for GGPP, another cyclisation leads to **I** which is followed by 1,2-hydride shift and cyclisation to **J**. At this stage the last remaining double bond becomes involved, which is the one that is shifted in iso-GGPP I, resulting in a change of the cyclisation mode with attack of water to give **23**. Its skeleton can only be reached from iso-GGPP I that can undergo 3,19-cyclisation, but not from GGPP with a Me19 group. The name albataxenol for **23** refers to the foreign nature of this compound (ancient Greek ξενοσ = strange, foreign).

With variediene synthase (AbVS) iso-GGPP I was converted into a complex mixture of several diterpene hydrocarbons and two alcohols (Figure S147). The alcohols were isolated and structurally characterised as variexenol A (**24**) and B (**25**, Tables S18 and S19, Figures S148–S163). Also in case of **24** the initial cyclisation steps towards **K** are analogous to those observed with GGPP (Scheme S5), but later the exo-methylene C19 takes part in a 3,19-cyclisation with attack of water, leading to new skeletons (Scheme 4B). For **25** the initial 1,11–10,14 cyclisation is modified to a 1,11–2,10 cyclisation to **L**, followed by 3,19-cyclisation and attack of water.

Similar findings have been made for cyclooctat-9-en-7-ol synthase (CotB2)[38] from *Streptomyces iakyrus* that converted iso-GGPP into 2,3,7-*triepi*-variexenol B (**26**), isoxeniaphyllene (**27**) and prenylisodauca-3,7(14)-diene (**28**, Tables S20–S22, Figures S164–S188). The name of **27** was assigned, because this compound exhibits the same skeleton as xeniaphyllenol (**29**, box in Scheme 5) from *Xenia macrospiculata*.[39] The formation of **26** and **27** can be explained through 1,11–2,10-cyclization to **M**, followed by another 3,19-cyclisation and attack of water to **26**, or by deprotonation to **27** (Scheme 5A). Compound **28** can be formed by 1,10-cyclisation of iso-GGPP I to **N**, followed by 1,3-hydride shift to **O**, rearrangement to **P** and 1,3-hydride shift with deprotonation from C1 (Scheme 5B). Incubation of (*R*)- and (*S*)-(1-^{13}C,1-^{2}H)-iso-GGPP I with CotB2 showed deprotonation from C1 with specific loss of the 1-*pro-S* and retainment of the 1-*pro-R* hydrogen (Figure S189). The cyclisation modes observed here for the three compounds **26**–**28** deviate from the natural 1,11–10,14-cyclisation of GGPP (Scheme S10).

With catenul-14-en-6-ol synthase from *Catenulispora acidiphila* (CaCS),[21b] iso-GGPP I was converted into one diterpene hydrocarbon and one alcohol (Figure S190). Their structures were elucidated as precatenulixenol (**30**) and catenulixenol (**31**, Tables S23 and S24, Figures S191–S206). Their formation follows the natural cyclisation cascade with GGPP closely (compare Scheme 6 and Scheme S11) and proceeds through 1,10-cyclisation of GGPP to **Q**, 1,3-hydride shift to **R**, and 1,14-cyclisation to **S**. Deprotonation yields **30**, which can undergo 3,19-cyclisation to **31**, instead of the naturally observed 2,7-cyclisation to catenul-14-en-6-ol.

Wanjudiene synthase from *Chryseobacterium wanjuense* (CwWS)[40] transformed iso-GGPP I into two diterpene hydrocarbons (Figure S207). Both compounds were isolated and identified as prewanjuxenene (**32**) and wanjuxenene (**33**, Tables S25 and S26, Figures S208–S223). Also in this

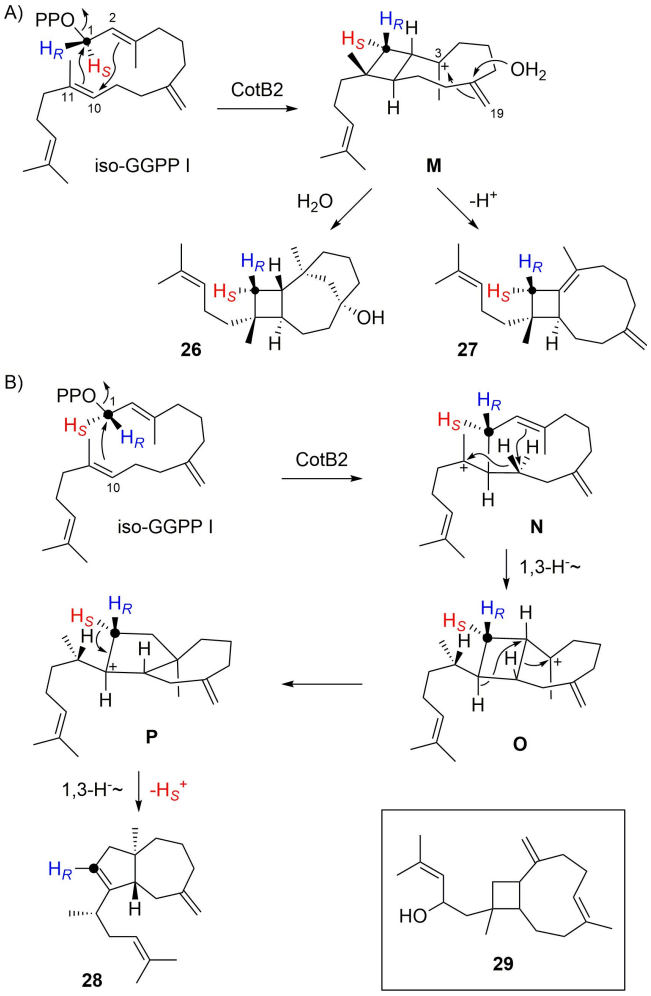

Scheme 5. Diterpenes from iso-GGPP I. A) Formation of **26** and **27** by CotB2, B) formation of **28** by CotB2. Box: structure of xeniaphyllenol (**29**).

case the cyclisation cascade follows in its initial steps the reactions towards natural wanjudiene (Scheme S12), starting with an isomerisation of iso-GGPP I to iso-geranyllinalyl diphosphate I (iso-GLPP I), followed by a 1,14-cyclisation to **T**, 1,3-hydride migration to **U** and 1,10-cyclisation to **V** (Scheme 7). Deprotonation of **V** yields **32**, or the cascade is continued through 1,2-hydride shift to **W** and 10,19-cyclisation to **X**. Here again the different double bond location in iso-GGPP I in comparison to GGPP leads to a distinct cyclisation mode towards a novel skeleton. A 1,2-hydride shift to **Y** and 2,19-cyclisation result in a secondary cation **Z** that may be a transient species that is stabilised by a 1,2-hydride shift to **Aa**. Its deprotonation finally leads to **33**. The 1,3-hydride shift from **T** to **U** was demonstrated by conversion of (*R*)- and (*S*)-(1-^{13}C,1-^{2}H)-iso-GGPP I and GC/MS analysis of the products, showing the cleavage of a deuterated iPr group from the *S*-configured substrate (Figure S224). Initially, the 1,2-hydride shift from **Z** to **Aa** was not taken into consideration, but rather a direct deprotonation of **Z** to **33** was assumed. However, the deuterium atoms from both substrates (*R*)- and (*S*)-(1-^{13}C,1-^{2}H)-iso-GGPP I

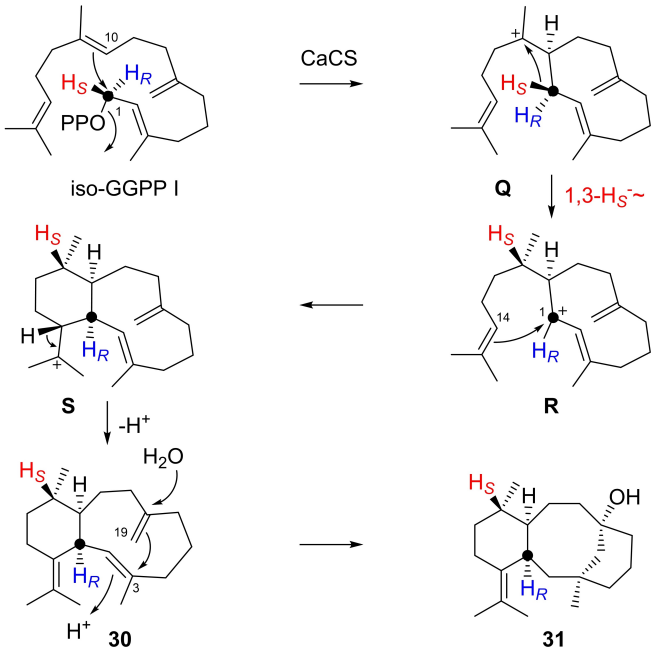

Scheme 6. Diterpenes from iso-GGPP I. Formation of **30** and **31** by CaCS.

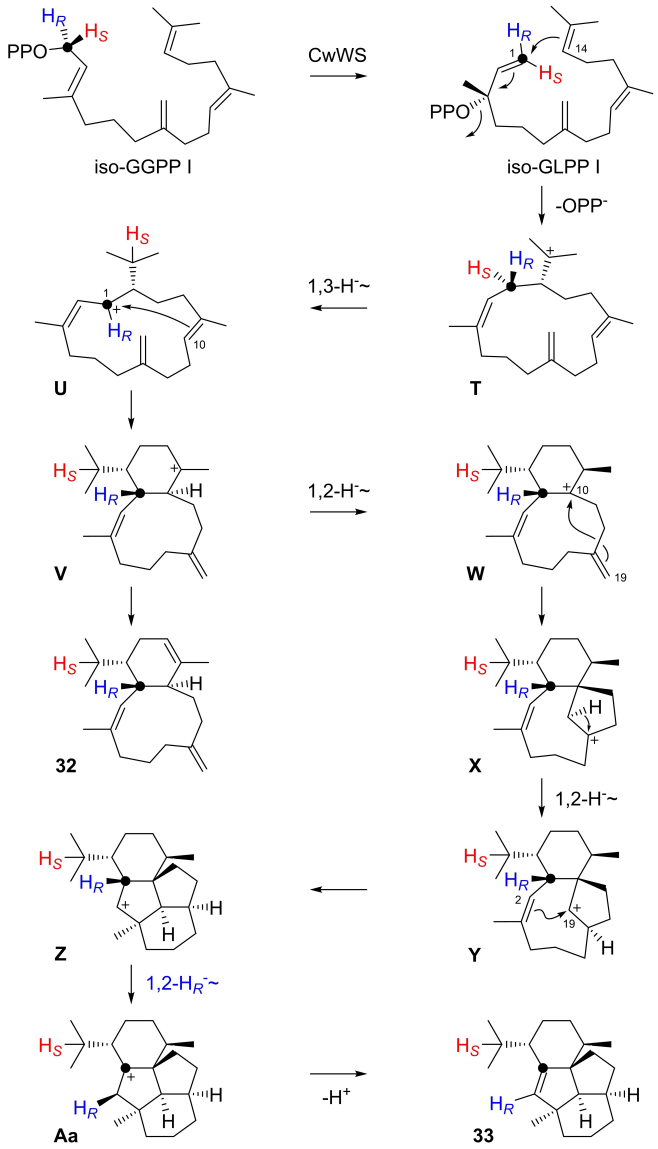

Scheme 7. Diterpenes from iso-GGPP I. Formation of **32** and **33** by CwWS.

remained in the product (Figure S224), with incorporation of deuterium from (*R*)-(1-^{13}C,1-^{2}H)-iso-GGPP I into a neighbouring position of C1 as indicated by a small upfield shift for the labelled carbon ($\Delta\delta = -0.1$ ppm, Figure S225). Remarkably, the olefinic methylene C19 in iso-GGPP I becomes involved in two cyclisation events towards **33**.

The enzyme reaction of iso-GGPP I with SpS[25] yielded a single diterpene hydrocarbon (Figure S226) whose structure was elucidated as that of isocneorubin Y (**34**, Table S27, Figures S227–S234). This compound can be formed by 1,10-cyclisation followed by deprotonation with cyclopropanation (Scheme 8). The hydrocarbon **34** is structurally related to cneorubin Y (**35**) that is a neutral intermediate towards the SpS product spata-13,17-diene (Scheme S2) and was first isolated from *Cneorum tricoccon*.[41] Interestingly, the same compound **34** was obtained from iso-GGPP I with SoS (Figure S226),[27] showing that in this case the structural

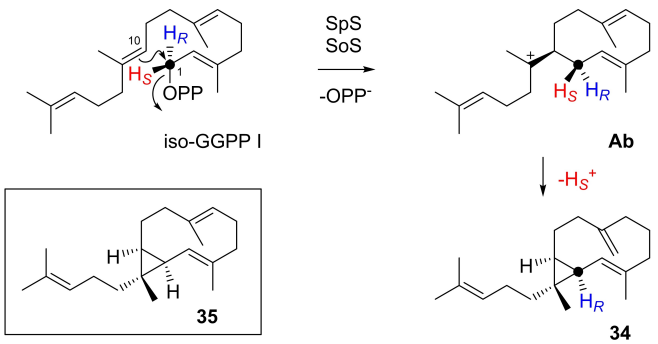

Scheme 8. Diterpenes from iso-GGPP I. Formation of **34** by SpS and SoS.

modification in the substrate changes the cyclisation mode from 1,11–10,14-cyclisation with GGPP (Scheme S3) to a 1,10-cyclisation.

The absolute configurations of the products derived from iso-GGPP I were also determined through the enantioselective labelling strategy. For this purpose, (*R*)- and (*S*)-(1-^{13}C,1-^{2}H)-iso-GGPP were synthesised (Scheme S13) and their enantiomeric purity was shown to be high by Mosher ester analysis (94 % ee and 96 % ee, respectively; Figure S235). Their conversion with HdS and HSQC analysis of the products allowed for the assignment of the absolute configuration of **17** (Figure S236). Analogously, the conversion with NrPS and CgDS revealed the absolute configuration of **18** (which is the same for both enzymes; Figure S237) and **19** (only obtained with CgDS, Figure S238). In the enzyme reactions with SaS one of the hydrogens at C1 migrates for all products so that no

stereogenic anchor can be introduced to allow a secure determination of absolute configurations. However, for **20** and **21** it is the same 1-*pro-S* hydrogen as for the natural enzyme product spiroalbatene that is shifted (Figures S239 and S240, Scheme S4) so that the absolute configurations should be analogous to the absolute configuration of spiroalbatene.[28] The transformation of (*R*)- and (*S*)-(1-^{13}C,1-^{2}H)-iso-GGPP with AbVS established the absolute configurations of **24** and **25** (Figure S241 and S242), and with CotB2 the absolute configurations of **26** and **27** were shown (Figure S243 and S244). For the enzyme reactions with CaCS to **30** and **31** one of the C1 hydrogens is migrating (1-*pro-S*, Figure S245 and S246), but again this is the same hydrogen that also migrates in catenul-14-en-6-ol biosynthesis (Scheme S11),[21b] suggesting that these compounds have analogous absolute configurations. For CwWS the 1-*pro-S* hydrogen is shifted into the iPr group in the formation of **32** (Figure S247) and **33** (Figure S224), which is the same hydrogen that also migrates in wanjudiene biosynthesis (Scheme S12).[40] Finally, the formation of **34** with both enzymes SpS and SoS proceeds with loss of the 1-*pro-S* hydrogen in the cyclopropanation (Figure S248), which is also observed for the SpS reaction to spata-13,17-diene (Scheme S2).[25] Therefore, the absolute configurations of **32**–**34** should also be analogous to their natural counterparts.

Conclusion

In conclusion, this work shows that diterpene synthases not only have a remarkable catalytic potential for the efficient conversion of the natural substrate GGPP, but also broadly accept substrate analogues, e.g. with altered double bond positions as used here. The product yields up to 9 % for a single isolated compound are satisfactory and comparable to the yields observed with GGPP. Acceptance of the substrate analogues iso-GGPP I and iso-GGPP II reveal a remarkable plasticity of terpene synthases. However, as shown in this study, many of the investigated diterpene synthases showed a conversion of the substrate analogues iso-GGPP I and iso-GGPP II through reactions that especially in the initial steps closely follow the cyclisation cascades observed with GGPP, suggesting that the substrate analogues in comparison to GGPP adopt very similar conformational folds in the active sites. Moreover, in iso-GGPP I and iso-GGPP II carbons C18 and C19, represented by non-reactive Me groups in GGPP, are activated so that they can directly get involved in the cyclisation cascades. Numerous examples in this study have shown that with iso-GGPP II 1,18- instead of 1,11–10,14-cyclisations can become possible, while with iso-GGPP I the initial cyclisation steps are often similar to those observed with GGPP, but later in the biosynthesis 3,19- or 10,19-cyclisations can occur. These changes in the cyclisation modes lead to skeletons that are unknown to nature and would be very difficult to make through chemical synthesis. The absolute configurations of all compounds reflect those of the natural enzyme products, which is not unexpected and further demonstrates that the substrate analogues with their minor structural differences compared to GGPP adopt a similar conformation in the enzymes' active sites as GGPP does. We will continue to investigate the enzymatic potential of terpene synthases with other specifically designed substrate analogues in our future research.

Acknowledgements

This work was funded by the DFG (DI1536/7-2). Open Access funding enabled and organized by Projekt DEAL.

Conflict of Interest

The authors declare no conflict of interest.

Data Availability Statement

The data that support the findings of this study are available in the supplementary material of this article.

Keywords: Configuration Determination · Enzymes · Isotopes · Substrate Analogues · Terpenoids

[1] M. Rohmer, *Nat. Prod. Rep.* **1999**, *16*, 565–574.
[2] R. Croteau, P. T. Purkett, *Arch. Biochem. Biophys.* **1989**, *271*, 524–535.
[3] F. Lynen, H. Eggerer, U. Henning, I. Kessel, *Angew. Chem.* **1958**, *70*, 738–742.
[4] D. L. Nandi, J. W. Porter, *Arch. Biochem. Biophys.* **1964**, *105*, 7–19.
[5] A. Tachibana, *FEBS Lett.* **1994**, *341*, 291–294.
[6] H. Tao, L. Lauterbach, G. Bian, R. Chen, A. Hou, T. Mori, S. Cheng, B. Hu, L. Lu, X. Mu, M. Li, N. Adachi, M. Kawasaki, T. Moriya, T. Senda, X. Wang, Z. Deng, I. Abe, J. S. Dickschat, T. Liu, *Nature* **2022**, *606*, 414–419.
[7] K. U. Wendt, G. E. Schulz, *Structure* **1998**, *6*, 127–133.
[8] D. E. Cane, I. Kang, *Arch. Biochem. Biophys.* **2000**, *376*, 354–364.
[9] P. Baer, P. Rabe, K. Fischer, C. A. Citron, T. A. Klapschinski, M. Groll, J. S. Dickschat, *Angew. Chem. Int. Ed.* **2014**, *53*, 7652–7656; *Angew. Chem.* **2014**, *126*, 7783–7787.
[10] D. E. Cane, J. H. Shim, Q. Xue, B. C. Fitzsimons, T. M. Hohn, *Biochemistry* **1995**, *34*, 2480–2488.
[11] D. J. Tantillo, *Angew. Chem. Int. Ed.* **2017**, *56*, 10040–10045; *Angew. Chem.* **2017**, *129*, 10172–10178.
[12] Y.-H. Wang, H. Xu, J. Zou, X.-B. Chen, Y.-Q. Zhuang, W.-L. Liu, E. Celik, G.-D. Chen, D. Hu, H. Gao, R. Wu, P.-H. Sun, J. S. Dickschat, *Nat. Catal.* **2022**, *5*, 128–135.
[13] H. Xu, J. S. Dickschat, *Synthesis* **2022**, *54*, 1551–1565.
[14] V. Harms, A. Kirschning, J. S. Dickschat, *Nat. Prod. Rep.* **2020**, *37*, 1080–1097.
[15] a) Y. Jin, D. C. Williams, R. Croteau, R. M. Coates, *J. Am. Chem. Soc.* **2005**, *127*, 7834–7842; b) D. J. Miller, F. Yu, R. K. Allemann, *ChemBioChem* **2007**, *8*, 1819–1825; c) D. J. Miller, F. Yu, D. W. Knight, R. K. Allemann, *Org. Biomol. Chem.* **2009**, *7*, 962–975; d) O. Cascón, S. Touchet, D. J. Miller, V. Gonzalez, J. A. Faraldos, R. K. Allemann, *Chem. Commun.* **2012**, *48*, 9702–9704.

[16] a) M. Demiray, X. Tang, T. Wirth, J. A. Faraldos, R. K. Allemann, *Angew. Chem. Int. Ed.* **2017**, *56*, 4347–4350; *Angew. Chem.* **2017**, *129*, 4411–4415; b) F. Huynh, D. J. Grundy, R. L. Jenkins, D. J. Miller, R. K. Allemann, *ChemBioChem* **2018**, *19*, 1834–1838; c) Z. Quan, A. Hou, B. Goldfuss, J. S. Dickschat, *Angew. Chem. Int. Ed.* **2022**, *61*, e202117273; *Angew. Chem.* **2022**, *134*, e202117273.
[17] a) A. Hou, J. S. Dickschat, *Chem. Eur. J.* **2021**, *27*, 15644–15649; b) L. Lauterbach, A. Hou, J. S. Dickschat, *Chem. Eur. J.* **2021**, *27*, 7923–7929.
[18] a) C. Oberhauser, V. Harms, K. Seidel, B. Schröder, K. Ekramzadeh, S. Beutel, S. Winkler, L. Lauterbach, J. S. Dickschat, A. Kirschning, *Angew. Chem. Int. Ed.* **2018**, *57*, 11802–11806; *Angew. Chem.* **2018**, *130*, 11976–11980; b) V. Harms, V. Ravkina, A. Kirschning, *Org. Lett.* **2021**, *23*, 3162–3166.
[19] a) A. Hou, L. Lauterbach, J. S. Dickschat, *Chem. Eur. J.* **2020**, *26*, 2178–2182; b) V. Harms, B. Schröder, C. Oberhauser, C. D. Tran, S. Winkler, G. Dräger, A. Kirschning, *Org. Lett.* **2020**, *22*, 4360–4365; c) L. Liang, J. S. Dickschat, *Chem. Eur. J.* **2022**, *28*, e202200095.
[20] H. Li, J. S. Dickschat, *Org. Chem. Front.* **2022**, *9*, 795–801.
[21] a) S. Y. Chow, H. J. Williams, Q. Huang, S. Nanda, A. I. Scott, *J. Org. Chem.* **2005**, *70*, 9997–10003; b) G. Li, Y.-W. Guo, J. S. Dickschat, *Angew. Chem. Int. Ed.* **2021**, *60*, 1488–1492; *Angew. Chem.* **2021**, *133*, 1510–1514.
[22] J. S. Dickschat, *Angew. Chem. Int. Ed.* **2019**, *58*, 15964–15976; *Angew. Chem.* **2019**, *131*, 16110–16123.
[23] P. Rabe, J. Rinkel, E. Dolja, T. Schmitz, B. Nubbemeyer, T. H. Luu, J. S. Dickschat, *Angew. Chem. Int. Ed.* **2017**, *56*, 2776–2779; *Angew. Chem.* **2017**, *129*, 2820–2823.
[24] L. Lauterbach, J. Rinkel, J. S. Dickschat, *Angew. Chem. Int. Ed.* **2018**, *57*, 8280–8283; *Angew. Chem.* **2018**, *130*, 8412–8415.
[25] J. Rinkel, L. Lauterbach, J. S. Dickschat, *Angew. Chem. Int. Ed.* **2017**, *56*, 16385–16389; *Angew. Chem.* **2017**, *129*, 16603–16607.
[26] Y. Kashman, A. Groweiss, *J. Org. Chem.* **1980**, *45*, 3814–3824.
[27] J. Rinkel, L. Lauterbach, J. S. Dickschat, *Angew. Chem. Int. Ed.* **2019**, *58*, 452–455; *Angew. Chem.* **2019**, *131*, 461–465.
[28] J. Rinkel, L. Lauterbach, P. Rabe, J. S. Dickschat, *Angew. Chem. Int. Ed.* **2018**, *57*, 3238–3241; *Angew. Chem.* **2018**, *130*, 3292–3296.
[29] J. Rinkel, S. T. Steiner, G. Bian, R. Chen, T. Liu, J. S. Dickschat, *ChemBioChem* **2020**, *21*, 486–491.
[30] J. Rinkel, S. T. Steiner, J. S. Dickschat, *Angew. Chem. Int. Ed.* **2019**, *58*, 9230–9233; *Angew. Chem.* **2019**, *131*, 9328–9332.
[31] J. Rinkel, J. S. Dickschat, *Org. Lett.* **2019**, *21*, 2426–2429.
[32] J. W. Cornforth, R. H. Cornforth, G. Popjak, L. Yengoyan, *J. Biol. Chem.* **1966**, *241*, 3970–3987.
[33] Y. Jin, R. M. Coates, *Chem. Commun.* **2006**, 2902–2904.
[34] I. Farkas, H. Pfander, *Helv. Chim. Acta* **1990**, *73*, 1980–1985.
[35] J. Rinkel, P. Rabe, X. Chen, T. G. Köllner, F. Chen, J. S. Dickschat, *Chem. Eur. J.* **2017**, *23*, 10501–10505.
[36] J. S. Dickschat, J. Rinkel, P. Rabe, A. Beyraghdar Kashkooli, H. J. Bouwmeester, *Beilstein J. Org. Chem.* **2017**, *13*, 1770–1780.
[37] G. Bian, J. Rinkel, Z. Wang, L. Lauterbach, A. Hou, Y. Yuan, Z. Deng, T. Liu, J. S. Dickschat, *Angew. Chem. Int. Ed.* **2018**, *57*, 15887–15890; *Angew. Chem.* **2018**, *130*, 16113–16117.
[38] a) S.-Y. Kim, P. Zhao, M. Igarashi, R. Sawa, T. Tomita, M. Nishiyama, T. Kuzuyama, *Chem. Biol.* **2009**, *16*, 736–743; b) A. Meguro, Y. Motoyoshi, K. Teramoto, S. Ueda, Y. Totsuka, Y. Ando, T. Tomita, S.-Y. Kim, T. Kimura, M. Igarashi, R. Sawa, T. Shinada, M. Nishiyama, T. Kuzuyama, *Angew. Chem. Int. Ed.* **2015**, *54*, 4353–4356; *Angew. Chem.* **2015**, *127*, 4427–4430.
[39] A. Groweiss, Y. Kashman, *Tetrahedron Lett.* **1978**, *19*, 2205–2208.
[40] L. Lauterbach, B. Goldfuss, J. S. Dickschat, *Angew. Chem. Int. Ed.* **2020**, *59*, 11943–11947; *Angew. Chem.* **2020**, *132*, 12041–12045.
[41] D. Trautmann, B. Epe, U. Oelbermann, A. Mondon, *Chem. Ber.* **1980**, *113*, 3848–3865.

Manuscript received: July 27, 2022
Accepted manuscript online: September 6, 2022
Version of record online: September 21, 2022

Appendices C

Enzymatic Synthesis of Diterpenoids from *iso*-GGPP III, a Geranylgeranyl Diphosphate Analog with Shifted Double Bond

Chem. Eur. J. **2024**, *30*, e202303560.

DOI: 10.1002/chem.202303560.

Chemistry–A European Journal
Research Article
doi.org/10.1002/chem.202303560
Chemistry Europe
European Chemical Societies Publishing
www.chemeurj.org

Enzymatic Synthesis of Diterpenoids from iso-GGPP III: A Geranylgeranyl Diphosphate Analog with a Shifted Double Bond

Heng Li[a] and Jeroen S. Dickschat*[a]

The analog of the diterpene precursor geranylgeranyl diphosphate with a double bond shifted from C14=C15 to C15=C16 (named iso-GGPP III) has been synthesized and enzymatically converted with six bacterial diterpene synthases; this allowed the isolation of nine unnatural diterpenes. For some of the enzyme-substrate combinations, the different reactivity implemented in the substrate analog iso-GGPP III opened reaction pathways that are not observed with natural GGPP, resulting in the formation of diterpenes with novel skeletons. A stereoselective deuteration strategy was used to assign the absolute configurations of the isolated diterpenes.

Introduction

Terpene synthases are remarkable biocatalysts that can convert structurally simple acyclic oligoprenyl diphosphates into terpene hydrocarbons or alcohols of high structural complexity.[1,2] This process is possible through multistep cationic cascade reactions that start with ionization of the substrate either through diphosphate abstraction (type I terpene synthases) or protonation (type II enzymes), which is followed by cyclization reactions through the attack of a remote alkene function to the cationic center, skeletal rearrangements, and hydride or proton shifts. Termination of the cascade proceeds either with deprotonation to yield a terpene hydrocarbon, or with water quenching to result in a terpene alcohol. Sometimes the initially formed product can encounter a reprotonation to initiate a second round of cyclization. The compounds obtained in this single enzymatic transformation are often polycyclic, contain several stereogenic centers, and are of high enantiomeric purity. Some terpene synthases are high-yielding, but even for enzymes with relatively low yields these reactions are still attractive, because an alternative total synthesis would usually require many consecutive steps to reach the same level of structural complexity.

Genome mining is an interesting strategy for the discovery of new enzymes to expand the known chemical space that can be reached through terpene synthase catalysis.[3] But we are not limited to nature's toolbox to create terpenoid compounds: Site-directed mutagenesis can lead to enzyme variants with changed product spectra which may potentially include new compounds that are not observed in a natural context.[4,5] However, the underlying changes in the amino acid sequence of a terpene synthase can of course also be introduced through natural mutation, meaning that the obtained compounds are likely present somewhere in nature, but yet undiscovered. A second approach that is more difficult to realize in nature, because it would require the establishment of new pathways requiring many new enzyme functions, are changes in the substrate structure, although some biosynthetic pathways are known that make use of noncanonical substrates.[6–11] This approach also offers an interesting playground for synthetic chemistry that can provide access to terpenoid substrate analogs with modified reactivity, leading to compounds with novel skeletons. Previous work has made use of fluorinated,[12] oxygenated[13,14] or sulfur-containing compounds,[15] substrate analogs with shifted methylation patterns,[15] containing cyclopropane rings,[16] or saturated double bonds.[17,18] We have recently shown that the geranylgeranyl diphosphate (GGPP) analogs iso-GGPP I and iso-GGPP II with shifted double bonds are accepted by many diterpene synthases.[19,20] Because the reactivity of these compounds resides in different positions compared to GGPP, diterpenes with novel skeletons can be obtained from these substrate analogs, for example, with spiroalbatene synthase (SaS)[21] iso-GGPP I can react in a late stage 3,19-cyclization to albataxenene (**1**), and with spata-13,17-diene synthase (SpS)[22] iso-GGPP II is converted through an initial 1,18-cyclization into pseudoobscuronatin (**2**; Scheme 1). In both cases the cyclization reactions involve carbons that are reactive in the iso-GGPPs, but not in GGPP (C18 and C19, respectively). Here we report on the synthesis of iso-GGPP III in which the C14=C15 double bond is shifted toward C15=C16 and its enzymatic conversion into diterpenes.

[a] H. Li, Prof. Dr. J. S. Dickschat
Kekulé-Institute for Organic Chemistry and Biochemistry
University of Bonn
Gerhard-Domagk-Straße 1, 53121 Bonn (Germany)
E-mail: dickschat@uni-bonn.de

Supporting information for this article is available on the WWW under https://doi.org/10.1002/chem.202303560

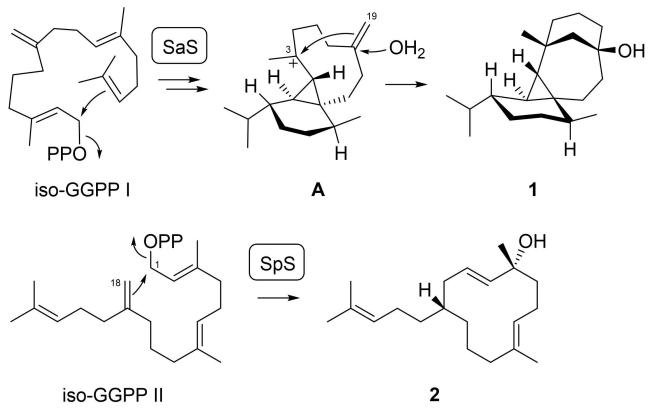

Scheme 1. Diterpenes with novel skeletons from iso-GGPP I and iso-GGPP II.

Results and Discussion

The synthesis of iso-GGPP III (Scheme 2) started with the conversion of isopentenol into isopentenyl iodide (**3**) that was used to alkylate ethyl acetoacetate to obtain **4**. Saponification and decarboxylation gave 6-methylhept-6-en-5-one (**5**) that was elongated through a Horner–Wadsworth–Emmons reaction to (*E*)- and (*Z*)-**6** that were separated by column chromatography. DIBAl-H reduction to **7** and phosphorylation made iso-GPP, the analog of GPP with the regular C6=C7 double bond shifted to C7=C8, available. Bromination of **7** and nucleophilic substitution with sodium benzenesulfinate yielded in **9**. Starting from geraniol (**10**) acetylation to **11**, SeO_2 oxidation to **12** and bromination gave **13** that was coupled with deprotonated **9** (BuLi) to obtain **14**. Saponification to **15** and reductive cleavage of the sulfinate group resulted in the geranylgeraniol isomer **16** that was brominated and phosphorylated under standard conditions to yield iso-GGPP III. A different approach to a deuterated analog of the alcohol **16** has been reported before that could be used for an alternative synthesis of unlabelled iso-GGPP III.[23]

Subsequently, test incubations of iso-GPP and isopentenyl diphosphate (IPP) with GGPP synthase (GGPPS) from *Streptomyces cyaneofuscatus*[24] and different diterpene synthases were performed (Table S1 in the Supporting Information), showing a good diterpene production with six enzymes, while with four enzymes including casbene synthase,[25] bonnadiene synthase,[26] wanjudiene synthase[27] and β-pinacene synthase[28] no efficient product formation was observed. Alternatively, iso-GGPP III was converted only with diterpene synthases. While the synthesis of iso-GPP is much shorter than the route toward iso-GGPP III, usage of the latter compound generally showed a better diterpene production as compared to iso-GPP, and no addition of GGPPS is required. Surprisingly, in all six cases also the formation of the natural product derived from GGPP was observed. The dephosphorylation of iso-GGPP III with calf intestinal phosphatase (CIP) in the same buffer and GC/MS analysis of the products showed the isomerization of the C15=C16 double bond under the incubation conditions, that is, the partial isomerization of iso-GGPP III to GGPP, explaining this observation.

The conversion of iso-GGPP III with the 18-hydroxydolabella-3,7-diene synthase (HdS) from *Chitinophaga pinensis*[29] resulted in the formation of four major compounds, two of which could be isolated (Figure S1). The main compound showed strong line broadening in the NMR spectra even at an elevated temperature (343 K) preventing its structure elucidation, while the second compound was structurally characterized as (11*E*)-12-isopentenyl-α-selinene (**18**; Scheme 3A, Figures S2–

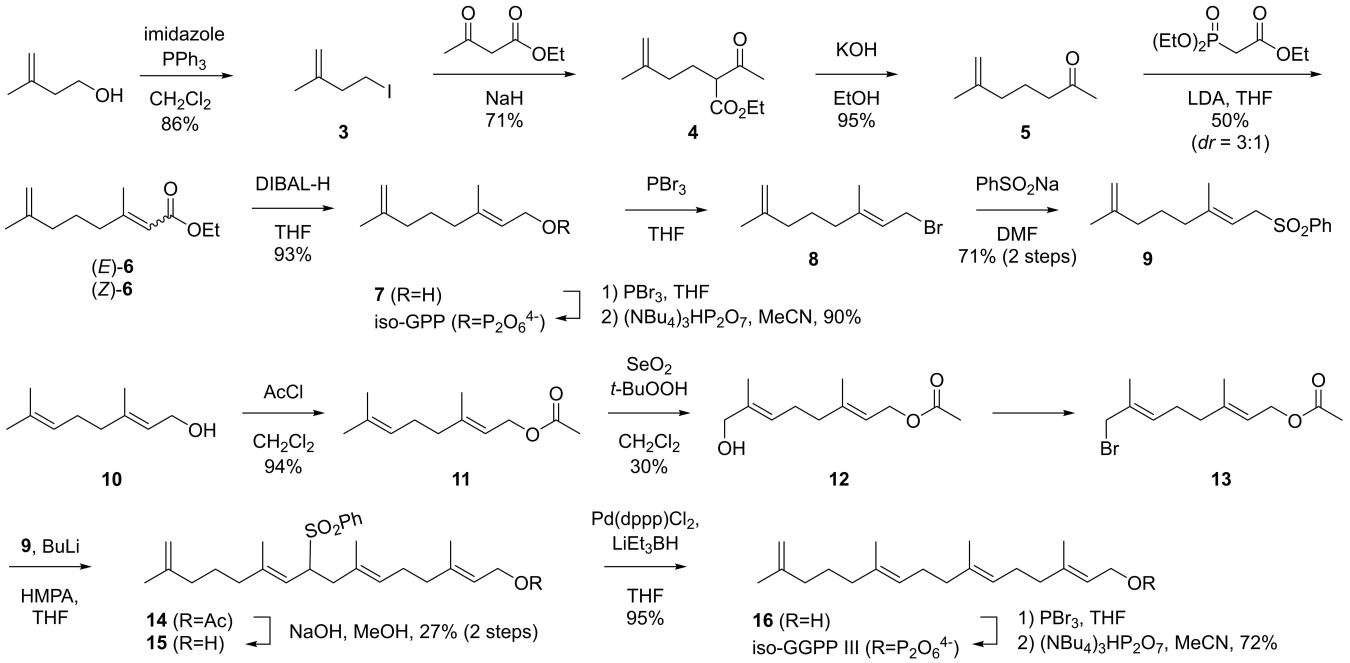

Scheme 2. Synthesis of iso-GPP and iso-GGPP III.

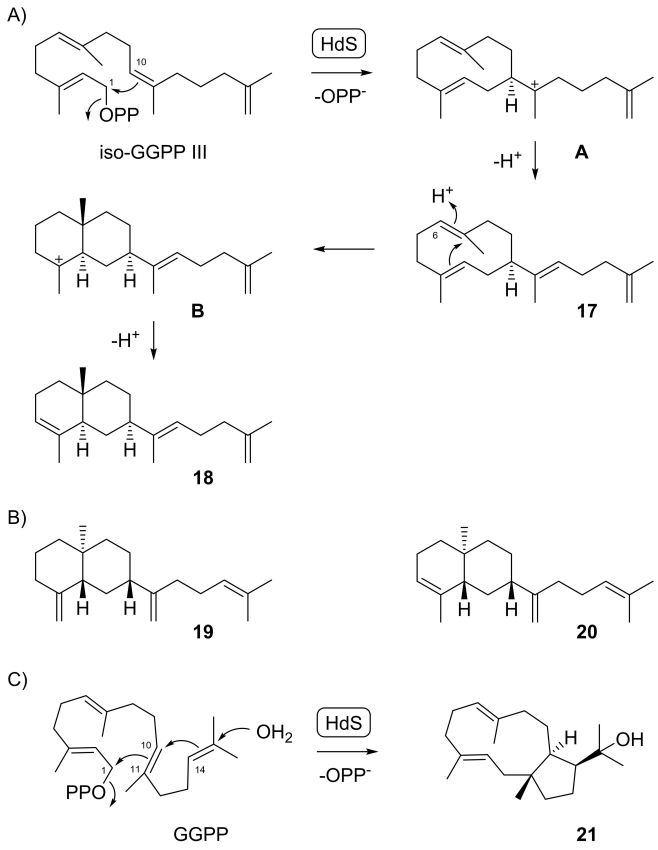

Scheme 3. 18-Hydroxydolabella-3,7-diene synthase (HdS). A) Cyclization of iso-GGPP III via **17** to **18**, B) structures of the related compounds **19** and **20**, and C) cyclization of GGPP to **21**.

S9, Table S2), a diterpene hydrocarbon that has structural similarity with the known compounds lobophytumins C (**19**) and D (**20**) from the soft coral *Lobophytum cristatum* (Scheme 3B).[30] A hypothetical cyclization mechanism from iso-GGPP to **18** starts with the abstraction of diphosphate and 1,10-cyclization to intermediate **A** that is deprotonated to **17**, a derivative of germacrene A[31] with an elongated side chain. Germacrene A is well known as a biosynthetic intermediate to many eudesmane and guaiane sesquiterpenes and can undergo a second cyclization cascade upon reprotonation.[32] Analogously, compound **17** can be reprotonated at C6 to initiate a second cyclization to **18** through intermediate **B** (Scheme 3A). Naturally, HdS catalyses the conversion of GGPP via 1,11-10,14-cyclization into 18-hydroxydolabella-3,7-diene (**21**; Scheme 3C). Herein, both cyclization events are likely concerted to avoid a free secondary cation as intermediate. With the shifted double bond in iso-GGPP III the 10,14-cyclization is no longer possible, and the 1,11-cyclization changes to a 1,10-cyclization in order to form the more stable tertiary cation **A**.

The hydropyrene synthase (HpS) from *Streptomyces clavuligerus*[33] catalyses the the formation of hydropyrene (**23**) and hydropyrenol (**24**) through a 1,10-cyclization of GGPP to **C**, followed by a 1,3-hydride migration to **D**, 1,14-cyclization and deprotonation to prehydropyrene (**22**). Its reprotonation at C6 can initiate two more cyclizations, and a final deprotonation or attack of water results in **23** or **24**, respectively (Scheme 4A).[28] On a second reaction path that operates in parallel HpS converts GGPP into elisabethatriene (**25**). This path proceeds through isomerization of GGPP to geranyllinalyl diphosphate (GLPP), followed by a 1,10-cyclization to **E**, a 1,3-hydride shift to **F**, 1,6-cyclization to **G**, and a 1,2-hydride shift and deprotonation to **25** (Scheme 4B). The incubation of iso-GGPP III with HpS resulted in the formation of a complex mixture of several diterpene hydrocarbons (Figure S10) from which two compounds were isolated. The first one was structurally identified as (11*Z*)-12-isopentenyl-α-selinene (**27**; Figures S11–S18, Table S3). Its formation can be understood starting from a similar conformational fold as for GGPP towards **23** and **24** (compare Schemes 4A and C). The initial 1,10-cyclization leads to **H**, but at this stage the cascade is interrupted and does not proceed with the 1,3-hydride shift as observed for the step from **C** to **D**. A possible reason could be that the remote C14=C15 double bond may assist in the 1,3-hydride shift from **C** to **D** (as indicated by the dashed lines in the structure of **C**). If this double bond is shifted to C15=C16, such an assistance in the 1,3-hydride shift may not be possible, with the consequence of deprotonation to **26**. The *Z* configuration of the double bond formed in this deprotonation step is explainable from the substrate conformation required for the formation of the tetracyclic compounds **23** and **24**. The downstream cyclization of **26** via **I** to **27** follows a different stereochemical course as observed for the cyclization of **22**. Compound **27** is observed by GC/MS in the crude enzyme extract and is thus likely an enzyme product, but its formation from **26** may also partially be non-enzymatic during chromatographic purification on silica gel, similar to the known cyclization of germacrene A into selinenes.[31,34,35] The second isolated product was characterized as isoelisabethatriene C (**28**; Figures S19–S26, Table S4). Its biosynthesis from iso-GGPP III by HpS can proceed through an analogous series of steps as required for the biosynthesis of natural **25** (compare Schemes 4B and D).

The enzymatic conversion of iso-GGPP III with the bacterial phomopsene synthase from *Nocardia testacea* (NtPS)[36] resulted in the formation of three major diterpene hydrocarbons two of which could be isolated (Figure S27). The NMR based structure elucidation (Figures S28–S43, Tables S5 and S6) revealed the structure of isoxeniaphyllene II (**29**) and iso-β-springene (**30**). Compound **29** was named after its close structural similarity to xeniaphyllenol (**31**), a known natural product from *Xenia macrospiculata* (Scheme 5A).[37] Moreover, the related compound isoxeniaphyllene (**32**) was previously obtained[20] from the enzymatic conversion of iso-GGPP I with cyclooctat-9-en-7-ol synthase from *Streptomyces iakyrus* (SiCotB2).[38,39] NtPS catalyses a 1,11-10,14-cyclization of GGPP to initiate the cyclization cascade toward phomopsene (**33**) (Scheme 5B). With the shifted terminal double bond in iso-GGPP III the 1,11-cyclization can still take place, but the 10,14-cyclization is altered to a 2,10-cyclization (Scheme 5C). Along this cyclization cascade, the hypothetical secondary cation **K** may be a highly transient species and may be stabilized through π-coordination with the C2=C3 alkene unit.

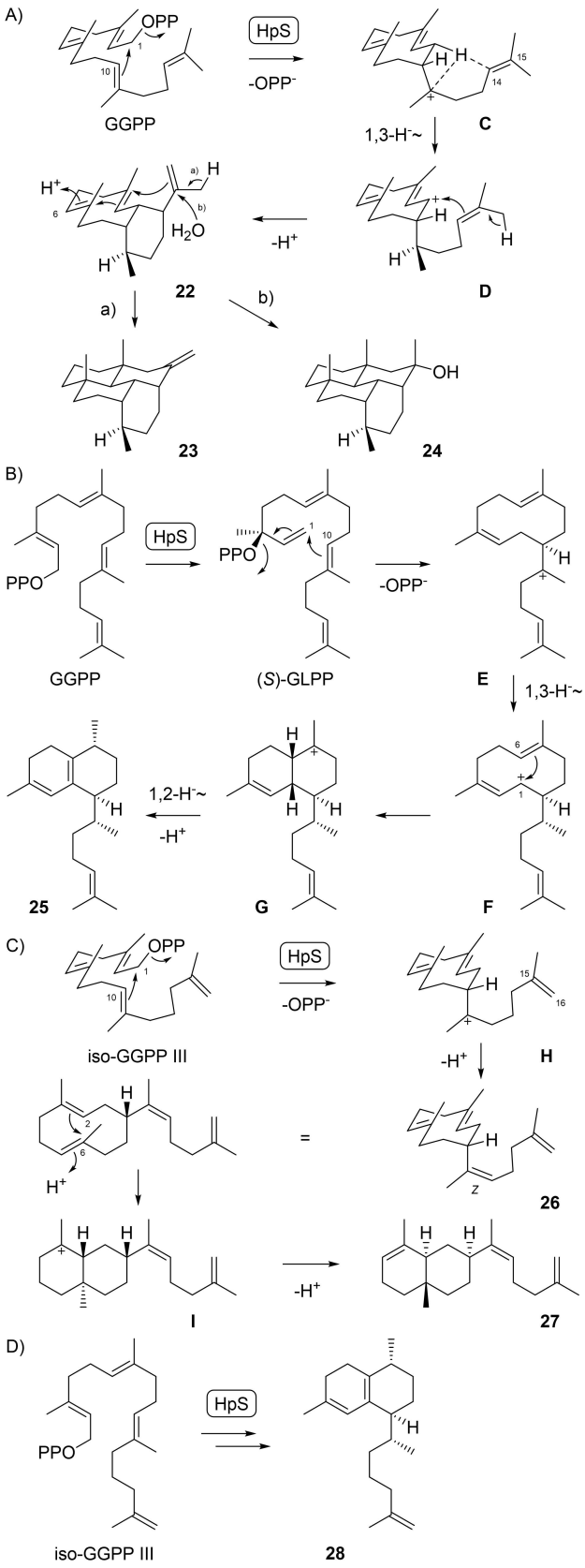

Scheme 4. Hydropyrene synthase (HpS). Cyclizations of GGPP A) to **23** and **24**, and B) to **25**. Analogous cyclizations of iso-GGPP III to C) **27** and D) **28**.

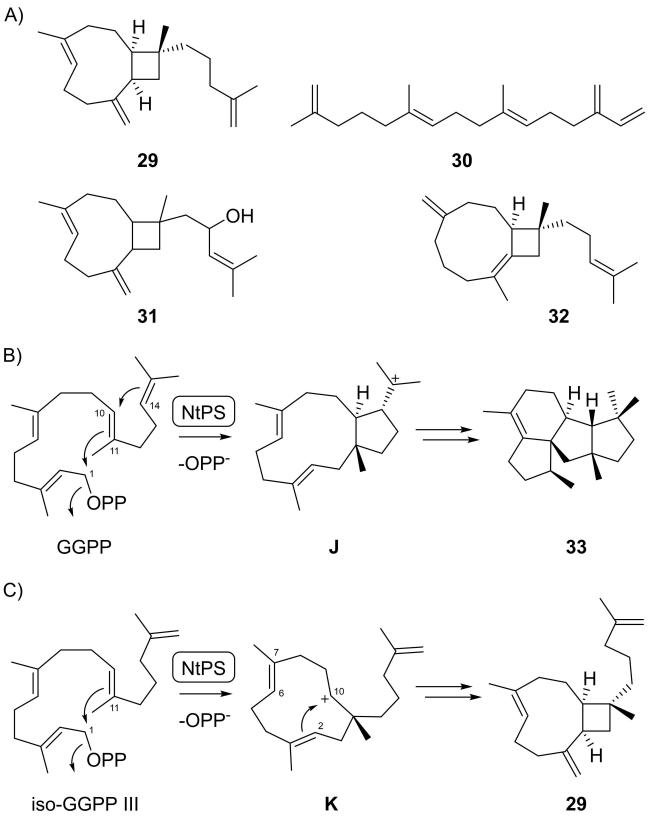

Scheme 5. *N. testacea* phomopsene synthase (NtPS). A) Structures of compounds **29–32**, B) initial cyclization of GGPP in the biosynthesis of **33**, C) initial cyclization of iso-GGPP III in the biosynthesis of **29**.

The catenul-14-en-6-ol synthase from *Catenulispora acidiphila* (CaCS)[40] naturally converts GGPP into the diterpene alcohol catenul-14-en-6-ol (**34**; Scheme 6A). This enzymatic reaction is initiated by the 1,10-cyclization of GGPP to **L** and a 1,3-hydride shift to **M**. A subsequent 1,14-cyclization to **N** and deprotonation lead to **O** that can be reactivated through protonation for another round of cyclization and capture with water to yield **34**. With the substrate iso-GGPP III the initial reactions to **P** and **Q** are analogous to those with GGPP, but then as a result of the shifted double bond the 1,14-cyclization cannot take place (Scheme 6B). Instead, a capture with water leads to isoobscuronatin (**35**; Figures S44–S51, Table S7), a double bond isomer of the diterpene alcohol obscuronatin (**37**) that is known from the sponge *Xenia obscuronata*.[41] During chromatographic purification on silica gel and upon the thermal impact during GC/MS analysis compound **35** decomposes to biflora-4,10(19),16-triene (**36**; Figure S52). This diterpene hydrocarbon was also isolated and structurally characterized (Figures S53–S60, Table S8).

The main product of the cyclooctat-9-en-7-ol synthase from *Streptomyces iakyrus* (SiCotB2),[39] a homolog of the previously characterized enzyme from *Streptomyces melanosporofaciens*,[38] is the diterpene alcohol **38** (Scheme 7A). This compound is formed through an initial 1,11-10,14-cyclization to **R** and a subsequent multistep cascade involving surprising skeletal rearrangements.[42] Remarkably, with iso-GGPP III as substrate

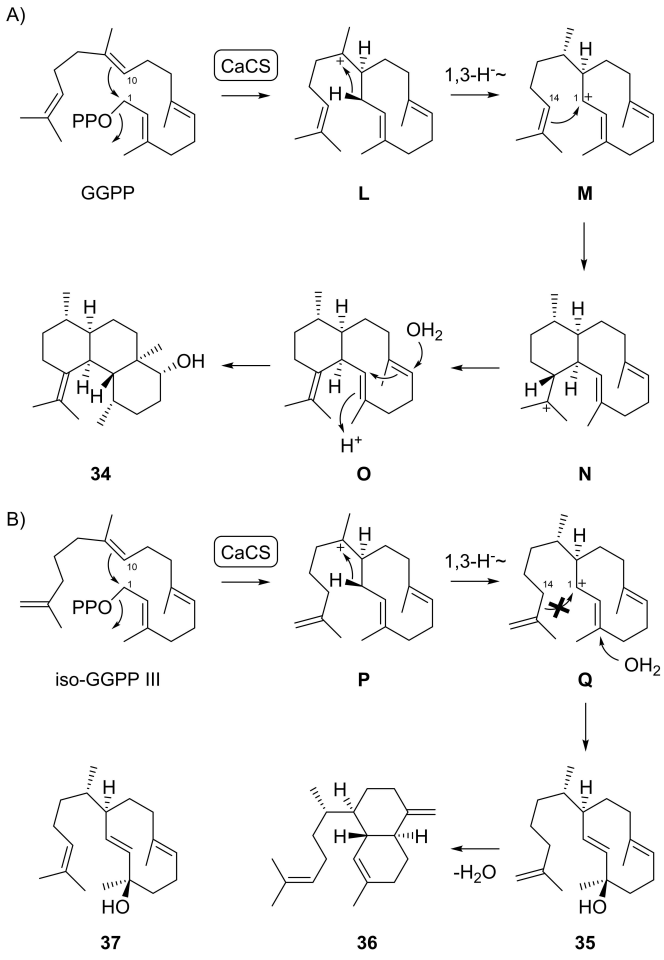

Scheme 6. *C. acidiphila* catenul-14-en-6-ol synthase (CaCS). A) Cyclization of GGPP to **34** by CaCS, B) cyclization of iso-GGPP III to **35** by CaCS, decomposition to **36** and structure of the related natural product **37**.

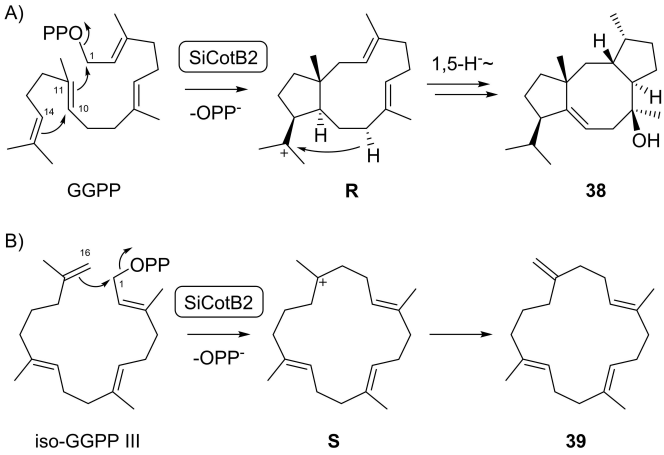

Scheme 7. *S. iakyrus* cyclooctat-9-en-7-ol synthase (SiCotB2). A) Cyclization of GGPP to **38**, B) cyclization of iso-GGPP III to **39**.

the cyclization mode changes to a 1,16-cyclization to **S** that upon deprotonation yields **39**, the main product obtained from iso-GGPP III (Scheme 7B, Figure S61). The shape of this molecule is reminiscent of a bucket wheel and therefore this compound was named bucket-wheelene (Figures S62–S69, Table S9).

The dolasta-1(15),8-diene (**41**) synthase from *Colletotrichum gloeosporioides* (CgDS)[43] naturally converts GGPP into δ-araneosene (**40**) and **41** (Scheme 8A). The cyclization cascade towards these product starts with a 1,11-10,14-cyclization of GGPP to **T**, followed by a 1,2-hydride shift to **U** and deprotonation to the neutral intermediate **40**. Its reprotonation induces a 2,7-cyclization to **V** that upon deprotonation reacts to **41**. With iso-GGPP III the cyclization mode by CgDS is altered to a 1,10-11,16-cyclization, again with involvement of C16, leading to cation **W** (Scheme 8B). Its deprotonation results in the hypothetical neutral intermediate **42** that is like **40** reprotonated at C7 for a subsequent 2,7-cyclization. The resulting intermediate **X** is the precursor to dolastaxenene (**43**) by deprotonation (Figures S70–S78, Table S10), with a skeleton that is foreign to CgDS or any other diterpene synthase (Greek ξενοσ = foreign). The highly selective formation of this compound from iso-GGPP III is remarkable.

The absolute configurations of the terpene analogs were investigated through a stereoselective deuteration method. This strategy enzymatically introduces stereogenic centers of known absolute configuration from stereoselectively deuterated substrates. The relative orientation of the naturally present stereo-

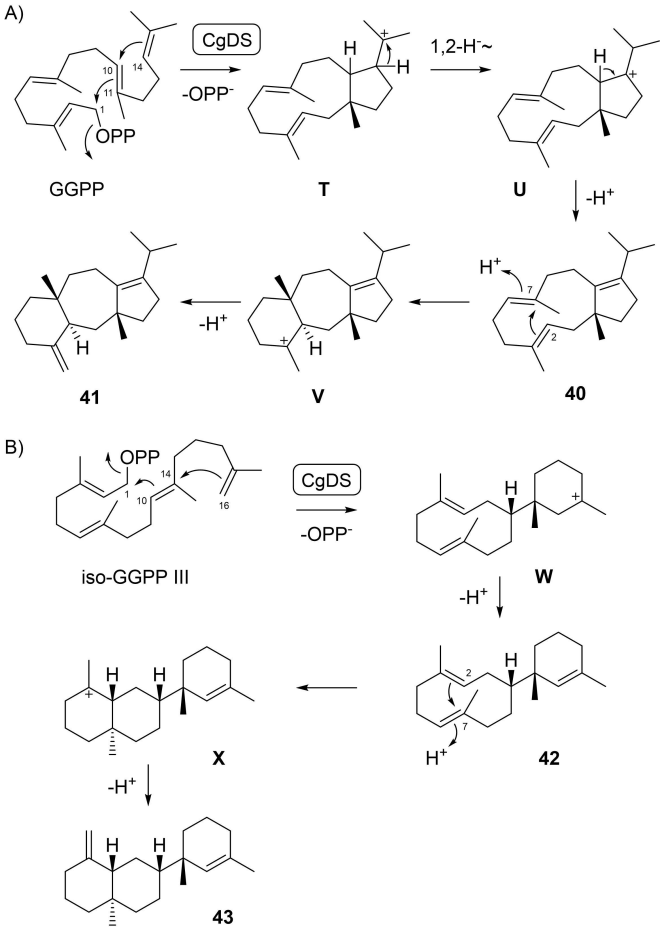

Scheme 8. *C. gloeosporioides* dolasta-1(15),8-diene synthase (CgDS). A) Cyclization of GGPP to **40** and **41**, B) cyclization of iso-GGPP III to **43**.

genic centers toward the stereogenic centers at the deuterated carbons give insight into the absolute configuration of the enzyme products. For this purpose, iso-GPP was elongated with (*R*)- or (*S*)-(1-^{13}C,1-^{2}H)IPP[44] using *Streptomyces cyaneofuscatus* GGPP synthase (GGPPS)[24] and then converted with the diterpene synthases used in this study into the corresponding terpene analogs. Furthermore, iso-GPP was used together with (*E*)- or (*Z*)-(4-^{13}C,4-^{2}H)IPP[26] and the same enzyme mixtures. The additionally introduced ^{13}C-labels enable a highly sensitive detection of the remaining hydrogen at the –CDH– groups through HSQC spectroscopy.

The data obtained allowed to conclude on the absolute configuration of **28** from the stereoselective deuteration at C8, while no conclusive NOESY correlations were observed for the hydrogens at C4 and C5 (Figures S79 and S80). The absolute configuration of **29** was conclusively assigned from the incorporations at C1, C4 and C8 (Figures S81 and S82), while for the determination of the absolute configuration of **35** the incorporations at C1, C4, C5 and C8 all gave unambiguous results (Figures S83 and S84). No signals were observed in these experiments for the degradation product **36** that is only obtained after column chromatography on silica gel, but its absolute configuration can be deduced from that of **35**. Also for **43** all four labelled positions allowed for conclusive insights into its absolute configuration (Figures S85 and S86).

Conclusions

After our previous reports on the biosynthesis of diterpene analogs from GGPP isomers with shifted double bonds,[19,20] we have shown in this study that iso-GGPP III can also serve as a substrate of diterpene synthases, leading to the formation of structurally complex diterpene hydrocarbons or alcohols. In some cases, for example, with HdS, highly complex mixtures of compounds were obtained making product isolation a tedious and highly challenging problem, but in other cases, such as with CgDS, a remarkable product selectivity was still observed. Some of the isolated compounds exhibit novel skeletons, as exemplified by the beautiful monocyclic compound bucket-wheelene or the tricyclic compound dolastaxenene. An alternative approach to obtaining new compounds by using terpene synthases is enzyme engineering through site-directed mutagenesis, but this approach cannot lead to inherently divergent terpene cyclization reactions. In contrast, changes in the substrate structure can lead to a changed reactivity that allows the formation of fundamentally different compounds that are usually not obtained from natural oligoprenyl diphosphates. In some of the cases reported here, the obtained yields, despite being comparably lower than with the natural substrate GGPP, are satisfying, especially when taking into account the high structural complexity that is introduced in a single enzymatic transformation by terpene synthases. We will continue to study the enzymatic transformations of terpenoid substrate analogs in our future experiments.

Experimental Section

Mass spectrometry. GC/MS analyses were carried out on a 7890B/5977A series gas chromatography/mass selective detector (Agilent). The GC was equipped with an HP5-MS fused silica capillary column (30 m, 0.25 mm i.d., 0.50 μm film; Agilent) and operated using the settings 1) inlet pressure: 77.1 kPa, He at 23.3 mL min^{-1}, 2) injection volume: 1–2 μL, 3) temperature program: 5 min at 50 °C then increasing 5 °C min^{-1} to 320 °C, 4) 60 s valve time, and 5) carrier gas: He at 1.2 mL min^{-1}. The MS was operated with settings 1) source: 230 °C, 2) transfer line: 250 °C, 3) quadrupole: 150 °C and 4) electron energy: 70 eV. High resolution mass spectra (APCI) were recorded on an Orbitrap XL instrument (Thermo Fisher Scientific) or using a 7890B/7200 series gas chromatography/accurate mass Q-ToF detector system (Agilent). The GC was equipped with a HP5-MS fused silica capillary column (30 m, 0.25 mm i.d., 0.50 mm film). GC settings were 1) injection volume: 1 μL, 2) temperature program: 5 min at 50 °C, increasing 10 °C min^{-1} to 320 °C, 3) split ratio: 5:1, 60 s valve time and 4) carrier gas flow: He at 1 mL min^{-1}. MS settings were 1) inlet pressure: 83.2 kPa, He flow at 24.6 mL min^{-1}, 2) transfer line temperature: 250 °C, 3) ionization energy: 70 eV.

Spectroscopic methods. NMR spectra were recorded at 298 K on a Bruker Avance III HD Cryo (700 and 500 MHz) NMR spectrometer. Spectra were measured in C_6D_6 and referenced against solvent signals (^{1}H NMR, residual proton signal: $\delta = 7.16$ ppm; ^{13}C NMR: $\delta = 128.06$ ppm).[45] Coupling constants are given in Hz. IR spectra were recorded on a Bruker α infrared spectrometer with a diamond ATR probehead. Peak intensities are given as s (strong), m (medium), w (weak) and br (broad).

Optical rotations. Optical rotations were recorded on a Modular Compact Polarimeter MCP 100 (Anton Paar, Graz, Austria). The temperature setting was 25 °C; the wavelength of the light used was 589 nm (sodium D line); the path-length was 10 cm, the compound concentrations *c* are given in g per 100 mL.

Synthesis of 4-iodo-2-methylbut-1-ene (3).[46] A solution of imidazole (16.7 g, 248 mmol, 1.20 equiv.) and PPh_3 (65.4 g, 248 mmol, 1.20 equiv.) in CH_2Cl_2 (400 mL) was mixed with I_2 (63 g, 248 mmol, 1.20 equiv.) and the 3-methylbut-3-en-1-ol (17.8 g, 207 mmol, 1.00 equiv.) subsequently. After stirring for 1 h at room temperature (TLC showed the starting material was consumed), the reaction mixture was quenched by the addition of sat. aqueous NH_4Cl and then extracted three times with Et_2O. The combined organic layers were dried with $MgSO_4$ and concentrated under reduced pressure. The residue was taken up in pentane, the precipitate was filtered off, and pentane was removed in vacuo. The product was purified by column chromatography (petroleum ether) to yield the **3** as a pink oil (35 g, 179 mmol, 86%). TLC (petroleum ether): $R_f = 0.64$. GC (HP5-MS): $I = 901$. EI-MS (70 eV): *m/z* (%) = 41 (0.4), 69 (1), 127 (0.1), 196 (0.1). ^{1}H NMR (C_6D_6, 500 MHz): 4.71 (m, 1H), 4.57 (m, 1H), 2.75 (m, 2H), 2.19 (t, 1H, $J = 7.6$ Hz), 1.42 (m, 1H), 1.37 (m, 3H) ppm. ^{13}C NMR (C_6D_6, 125 MHz): 143.87 (C_q), 112.35 (CH_2), 41.94 (CH_2), 21.44 (CH_3), 3.15 (CH_2) ppm.

Synthesis of ethyl 2-acetyl-5-methylhex-5-enoate (4).[47] To a cooled solution of ethyl acetoacetate (11.5 g, 88 mmol, 2.00 equiv.) in THF (160 mL, 2 mL mmol^{-1}) was added NaH (3.5 g, 88 mmol, 2.00 equiv., 60% purity) in small portions. The reaction mixture was allowed to reach room temperature and stirred for 1 h. The iodide **3** was added dropwise and the reaction mixture was refluxed overnight, followed by cooling to room temperature. The cooled mixture was quenched by the addition of saturated aqueous NH_4Cl solution and then extracted with Et_2O. The combined organic layers were dried with $MgSO_4$ and concentrated under reduced pressure. The residue was subjected to column chromatography (petroleum ether/EtOAc, 12:1) to yield the β-keto ester **4** (6.2 g, 31 mmol, 71%)

as a colourless oil. TLC (petroleum ether/EtOAc, 10:1): R_f = 0.40. GC (HP5-MS): I = 1315. EI-MS (70 eV): m/z (%) = 43 (3), 55 (1), 68 (0.6), 85 (0.5), 130 (1), 155 (0.3), 180 (0.01). ^{1}H NMR (C_6D_6, 500 MHz): 4.74 (m, 1H), 4.72 (m, 1H), 3.88 (qd, 2H, J = 7.2, 1.3 Hz), 3.24 (dd, 1H, J = 7.8, 6.3 Hz), 1.97 (m, 4H), 1.87 (d, 3H, J = 0.4 Hz), 1.55 (dd, 3H, J = 1.4, 1.0 Hz), 0.88 (t, 3H, J = 7.1 Hz) ppm. ^{13}C NMR (C_6D_6, 125 MHz): 201.46 (C_q), 169.67 (C_q), 144.55 (C_q), 111.43 (CH_2), 61.03 (CH_2), 59.12 (CH), 35.63 (CH_2), 28.56 (CH_3), 26.24 (CH_2), 22.10 (CH_3), 14.02 (CH_3) ppm.

Synthesis of ethyl 6-methylhept-6-en-2-one (5).[48] The solution of the β-keto ester **4** (6.3 g, 32 mmol, 1.00 equiv.) in EtOH (64 mL, 2 mL mmol^{-1}) was mixed with an aqueous solution of KOH (5.3 g, 95 mmol, 3.00 equiv.; 2 M) and the reaction mixture was refluxed for 3 h before cooling to room temperature. The reaction mixture was slowly acidified with 2 M HCl solution until CO_2 developed. The resulting suspension was extracted with pentane (three times). The combined layers were dried with $MgSO_4$ and concentrated under reduced pressure. The residue was subjected to column chromatography (petroleum ether /Et_2O, 10:1) to yield pure **5** (3.8 g, 30 mmol, 95%) as a colourless oil. TLC (petroleum ether /Et_2O, 8:1): R_f = 0.46. GC (HP5-MS): I = 967. EI-MS (70 eV): m/z (%) = 43 (7), 58 (2), 68 (1.5), 108 (1), 126 (0.3). ^{1}H NMR (C_6D_6, 500 MHz): 4.76 (m, 1H), 4.72 (m, 1H), 1.89 (t, 2H, J = 7.3 Hz), 1.83 (m, 2H), 1.60 (m, 2H), 1.63 (s, 3H), 1.58 (m, 3H) ppm. ^{13}C NMR (C_6D_6, 125 MHz): 205.99 (C_q), 145.23 (C_q), 110.80 (CH_2), 42.51 (CH_2), 37.30 (CH_2), 29.38 (CH_3), 22.19 (CH_3), 21.72 (CH_2) ppm.

Synthesis of ethyl (*E*)-3,7-dimethylocta-2,7-dienoate (*E*)-6. A solution of diisopropylamine (5.1 g, 50 mmol, 1.05 equiv.) dissolved in dry THF (100 mL, 2 mL mmol^{-1}) was cooled to 0 °C. *n*BuLi (31.5 mL, 1.6 M in hexane, 1.05 equiv.) was added dropwise and the reaction was stirred for 1 h at 0 °C. The reaction mixture was cooled to −78 °C and triethyl phosphonoacetate (10.8 g, 48 mmol, 1.00 equiv.) was added. After stirring the reaction mixture for 1 h at −78 °C the methyl ketone **5** (6.1 g, 48 mmol, 1.00 equiv.) was added. The reaction mixture was allowed to warm to room temperature and stirred overnight. Water (50 mL) was added to quench the reaction. The aqueous phase was extracted three times with Et_2O, and the combined layers were dried with $MgSO_4$ and concentrated under reduced pressure. Purification by column chromatography (petroleum ether/EtOAc, 15:1) yielded pure (*E*)-**6** (3.6 g, 18 mmol, 38%) and (*Z*)-**6** (1.2 g, 6 mmol, 12%) as colourless oils. (*E*)-**6**:[49] TLC (petroleum ether/EtOAc, 10:1): R_f = 0.36. GC (HP5-MS): I = 1398. EI-MS (70 eV): m/z (%) = 39 (1), 41 (3), 55 (1), 67 (2), 81 (0.7), 95 (1.3), 123 (0.6), 153 (1), 181 (0.2), 196 (0.01). ^{1}H NMR (C_6D_6, 500 MHz): 5.80 (q, 1H, J = 1.2 Hz), 4.76 (m, 1H), 4.70 (m, 1H), 4.06 (d, 2H, J = 7.2 Hz), 2.18 (d, 3H, J = 1.4 Hz), 1.78 (m, 4H), 1.55 (m, 3H), 1.36 (m, 2H), 1.02 (t, 3H, J = 7.1 Hz) ppm. ^{13}C NMR (C_6D_6, 125 MHz): 166.48 (C_q), 159.54 (C_q), 145.10 (C_q), 116.36 (CH), 110.71 (CH_2), 59.41 (CH_2), 40.40 (CH_2), 37.36 (CH_2), 25.46 (CH_2), 22.30 (CH_3), 18.70 (CH_3), 14.46 (CH_3) ppm. (*Z*)-**6**:[50] TLC (petroleum ether/EtOAc, 10:1): R_f = 0.45. GC (HP5-MS): I = 1348. EI-MS (70 eV): m/z (%) = 39 (2), 41 (3), 55 (1.3), 67 (2.1), 81 (1.4), 95 (2), 123 (1), 153 (1), 181 (0.1), 196 (0.01). ^{1}H NMR (C_6D_6, 500 MHz): 5.74 (q, 1H, J = 0.7 Hz), 4.79 (m, 2H), 4.02 (d, 2H, J = 7.1 Hz), 2.69 (m, 2H), 2.05 (m, 2H), 1.66 (t, 3H, J = 1.2 Hz), 1.59 (m, 2H), 1.51 (d, 3H, J = 1.5 Hz), 1.00 (t, 3H, J = 7.1 Hz) ppm.^{13}C NMR (C_6D_6, 125 MHz): 166.00 (C_q), 160.05 (C_q), 145.56 (C_q), 116.89 (CH), 110.52 (CH_2), 59.37 (CH_2), 38.17 (CH_2), 33.27 (CH_2), 26.55 (CH_2), 24.87 (CH_3), 22.40 (CH_3), 14.42 (CH_3) ppm.

Synthesis of (*E*)-3,7-dimethylocta-2,7-dien-1-ol (7).[50] To a cooled (0 °C) solution of the corresponding ester (*E*)-**6** (3.6 g, 18 mmol, 1.00 equiv.) in THF (90 mL, 5 mL mmol^{-1}) was added DIBAL-H (44 mL, 44 mmol, 1 M in hexane, 2.40 equiv.) and the reaction mixture was stirred for 1 h at room temperature. The mixture was cooled to 0 °C again and a saturated solution of Na–K-tartrate was added. The resulting slurry was stirred for 2 h to dissolve the precipitate and the aqueous phase was extracted three times with Et_2O. The organic layers were dried with $MgSO_4$ and concentrated under reduced pressure. The residue was purified by column chromatography (petroleum ether/Et_2O, 3:1) to yield the desired colourless alcohol **7** (2.6 g, 17 mmol, 93%) as a colourless oil. TLC (petroleum ether/Et_2O, 2:1): R_f = 0.30. GC (HP5-MS): I = 1253. EI-MS (70 eV): m/z (%) = 43 (1), 55 (1.8), 69 (2), 81 (1), 96 (1), 109 (0.4), 121 (0.5), 136 (0.2). ^{1}H NMR (C_6D_6, 500 MHz): 5.38 (tq, 1H, J = 5.6, 1.2 Hz), 4.80 (m, 2H), 3.99 (m, 2H), 1.90 (m, 4H), 1.63 (t, 3H, J = 1.2 Hz), 1.48 (m, 2H), 1.45 (m, 3H) ppm. ^{13}C NMR (C_6D_6, 125 MHz): 145.65 (C_q), 138.11 (C_q), 125.02 (CH), 110.46 (CH_2), 59.36 (CH_2), 39.35 (CH_2), 37.65 (CH_2), 25.98 (CH_2), 22.46 (CH_3), 16.08 (CH_3) ppm.

Synthesis of (*E*)-3,7-dimethylocta-2,7-dien-1-yl diphosphate (iso-GPP). PBr_3 (422 mg, 1.6 mmol, 0.40 equiv.) was added dropwise to a cooled (0 °C) solution of **7** (600 mg, 3.9 mmol, 1.00 equiv.) in Et_2O (12 mL). The mixture was stirred for 1 h at 0 °C and then poured onto an ice/water mixture. The aqueous layer was extracted three times with Et_2O, the combined organic layers were dried with $MgSO_4$ and concentrated under reduced pressure to give the allyl bromide **8** (1.8 g) that was used for the next step without purification.

Tris(tetra-*n*-butylammonium) hydrogen diphosphate (4.2 g, 4.7 mmol, 1.20 equiv.) was dissolved in acetonitrile (20 mL, 4 mL mmol^{-1}) and the allyl bromide **8** (1.8 g) was added. Then the mixture was stirred at room temperature overnight. Acetonitrile was removed under reduced pressure and the resulting residue was dissolved in aqueous NH_4HCO_3 solution (0.25 M) and loaded onto a DOWEX 50WX8 ion-exchange column (NH_4^+ form, pH 7.0). The column was flushed slowly with 1.5 column volumes of NH_4HCO_3 buffer (25 mM, 5% *i*PrOH) and the eluate was lyophilised to yield the diphosphate as a colourless hygroscopic powder (1.5 g, 3.5 mmol, 90%). ^{1}H NMR (D_2O, 500 MHz): 5.32 (m, 1H), 4.60 (dt, 2H, J = 6.6, 1.7 Hz), 4.34 (q, 2H, J = 6.9 Hz), 1.89 (m, 4H), 1.59 (m, 3H), 1.55 (m, 3H), 1.43 (m, 2H) ppm. ^{13}C NMR (D_2O, 125 MHz): 146.69 (C_q), 142.61 (C_q), 119.53 (d, CH, $^3J_{C,P}$ = 8.6 Hz), 109.48 (CH_2), 62.61 (d, CH_2, $^3J_{C,P}$ = 5.4 Hz), 38.52 (CH_2), 36.79 (CH_2), 25.06 (CH_2), 21.71 (CH_3), 15.54 (CH_3) ppm. ^{31}P NMR (D_2O, 203 MHz): −9.16 (d, $^2J_{P,P}$ = 19.9 Hz), −10.63 (d, $^2J_{P,P}$ = 19.9 Hz) ppm. HRMS (ESI(−)): calc. for $[C_{10}H_{19}O_7P_2]^-$ m/z = 313.0611; found: m/z = 313.0617.

Synthesis of (*E*)-((3,7-dimethylocta-2,7-dien-1-yl)sulfonyl)benzene (9).[51] Sodium benzenesulfinate (3.0 g, 18.6 mmol, 1.30 equiv.) was dissolved in DMF (25 mL), followed by the addition of allyl bromide **8** (6 g, prepared as described above). The reaction was stirred overnight and then quenched by pouring into water. The aqueous phase was extracted three times with Et_2O, and the combined layers were dried with $MgSO_4$ and concentrated under reduced pressure. Purification by column chromatography (petroleum ether/EtOAc, 3:1) yielded **9** (2.8 g, 9 mmol, 71%) as a colourless oil. TLC (petroleum ether/EtOAc, 2:1): R_f = 0.32. GC (HP5-MS): I = 1714. EI-MS (70 eV): m/z (%) = 41 (1), 55 (1), 67 (1), 81 (7), 95 (2), 137 (1), 267 (0.01). ^{1}H NMR (C_6D_6, 500 MHz): 7.78 (m, 2H), 6.92 (m, 3H), 5.11 (ddq, 1H, J = 9.4, 8.0, 1.4 Hz), 4.79 (m, 1H), 4.74 (m, 1H), 3.47 (d, 2H, J = 8.0 Hz), 1.79 (m, 2H), 1.72 (m, 2H), 1.60 (m, 3H), 1.29 (m, 2H), 1.03 (d, 3H, J = 1.6 Hz) ppm. ^{13}C NMR (C_6D_6, 125 MHz): 145.41 (C_q), 145.36 (C_q), 140.18 (C_q), 132.94 (CH), 128.81 (CH, x4), 111.63 (CH), 110.59 (CH_2), 56.11 (CH_2), 39.31 (CH_2), 37.41 (CH_2), 25.70 (CH_2), 22.41 (CH_3), 15.90 (CH_3) ppm.

Synthesis of (*E*)-3,7-dimethylocta-2,6-dien-1-yl acetate (11).[52] To a CH_2Cl_2 (200 mL, 0 °C) solution of geraniol (**10**; 12.2 g, 80.00 mmol) and pyridine (8.9 g, 112 mmol, 1.40 equiv.) was added acetyl chloride (7.5 g, 24.0 mmol, 1.20 equiv.) dropwise. The reaction was stirred at 0 °C for 45 min, then quenched by the addition of H_2O (200 mL). The organic layer was separated and the aqueous layer was extracted with Et_2O (2 x 60 mL). The combined organic layers were dried with $MgSO_4$ and concentrated under reduced pressure.

The product **11** (14.8 g, 75.2 mmol, 94%) was obtained via silica gel chromatography (petroleum ether/EtOAC, 12:1) as a colourless oil. TLC (petroleum ether/EtOAc, 10:1): $R_f = 0.50$. GC (HP5-MS): $I = 1382$. EI-MS (70 eV): m/z (%) = 41 (5), 69 (3), 93 (1), 121 (0.7), 136 (1.5), 154 (0.01). ^{1}H NMR (C_6D_6, 500 MHz): 5.41 (ddt, J = 8.4, 5.8, 1.3 Hz), 5.11 (m, 1H), 4.59 (d, 2H, J = 7.1 Hz), 2.05 (m, 2H), 1.94 (m, 2H), 1.69 (d, 3H, J = 0.9 Hz), 1.63 (t, 3H, J = 1.4 Hz), 1.55 (dd, 6H, J = 5.0, 1.4 Hz) ppm. ^{13}C NMR (C_6D_6, 125 MHz): 170.08 (C_q), 141.60 (C_q), 131.58 (C_q), 124.36 (CH), 119.47 (CH), 61.19 (CH_2), 39.83 (CH_2), 26.69 (CH_2), 25.80 (CH_3), 20.59 (CH_3), 17.69 (CH_3), 16.32 (CH_3) ppm.

Synthesis of (2*E*,6*E*)-8-hydroxy-3,7-dimethylocta-2,6-dien-1-yl acetate (12).[53] To a CH_2Cl_2 (130 mL, room temperature) suspension of SeO_2 (832 mg, 7.5 mmol, 0.10 equiv.) was added *t*BuOOH (27.0 mL, 5.5 M in decane, 151 mmol, 2.00 equiv.) dropwise. The mixture was stirred at room temperature for 0.5 h, followed by the dropwise addition of **11** (14.8 g, 75.5 mmol, 1.00 equiv.). The reaction mixture was stirred at room temperature for 24 h. Then the reaction solution was concentrated under reduced pressure. The residue was dissolved in Et_2O. The organic layer was washed with sat. $NaHCO_3$, dried with $MgSO_4$ and concentrated under reduced pressure. The residue was dissolved in methanol/THF (1:4, 150 mL), and the mixture was cooled to 0 °C, then $NaBH_4$ (5.7 g, 151 mmol, 2.00 equiv.) was added in three batches. The reaction was stirred at 0 °C for 1 h, and then quenched by pouring into aq. NH_4Cl (50 mL sat. NH_4Cl with 100 mL ice/water). The product was extracted with Et_2O, and the extracts were dried with $MgSO_4$ and concentrated under reduced pressure. Purification by flash chromatography (petroleum ether/EtOAC, 3:1) provided compound **12** (4.8 g, 23 mmol, 30%) as colourless oil. TLC (petroleum ether/EtOAC, 2:1): $R_f = 0.19$. GC (HP5-MS): $I = 1640$. EI-MS (70 eV): m/z (%) = 43 (5), 68 (3), 84 (2), 119 (0.7), 134 (1), 152 (0.1). ^{1}H NMR (C_6D_6, 500 MHz): 5.38 (ttq, 1H, J = 6.8, 2.8, 1.3 Hz), 5.27 (tq, 1H, J = 7.1, 1.4 Hz), 4.57 (d, 2H, J = 7.4 Hz), 3.80 (s, 2H), 2.03 (m, 2H), 1.92 (m, 2H), 1.70 (s, 3H), 1.51 (s, 3H), 1.49 (s, 3H).^{13}C NMR (C_6D_6, 125 MHz): 179.34 (C_q), 141.25 (C_q), 135.93 (C_q), 124.60 (CH), 119.74 (CH), 68.68 (CH_2), 61.27 (CH_2), 39.40 (CH_2), 25.92 (CH_2), 20.60 (CH_3), 16.25 (CH_3), 13.64 (CH_3) ppm.

Synthesis of (2*E*,6*E*,10*E*)-3,7,11,15-tetramethyl-9-(phenylsulfonyl)hexadeca-2,6,10,15-tetraen-1-ol (15). To a cooled (0 °C) solution of **12** (1.0 g, 4.8 mmol, 1.00 equiv.) in Et_2O (20 mL) PBr_3 (517 mg, 1.9 mmol, 0.40 equiv.) was added dropwise. The mixture was stirred for 1 h at 0 °C and then poured onto an ice/water mixture. The aqueous layer was extracted three times with Et_2O, the organic layers were dried with $MgSO_4$ and concentrated under reduced pressure to yield allyl bromide **13** (1.5 g) that was used in the next step without purification.

Sulfone **9** (1.5 g, 5.3 mmol, 1.10 equiv.) was dissolved in THF/HMPA (4:1, 25 mL). After cooling the mixture to −78 °C, *n*BuLi (3.6 mL, 1.6 M in hexane, 5.7 mmol, 1.20 equiv.) was added dropwise. The mixture was stirred for 2 h, and the allyl bromide **13** (1.5 g) was added dropwise. The reaction solution was stirred overnight without further cooling. The reaction was quenched by pouring into an ice-cold aqueous NH_4Cl solution (40 mL sat. NH_4Cl with 100 mL ice/water). The product was extracted with Et_2O, the combined extracts were washed with sat. NaCl, dried with $MgSO_4$, and concentrated under reduced pressure to provide the crude compound **14** that was used in the next step without purification.

Sulfone **14** was dissolved in methanol (40 mL) and NaOH (10 mL, 1 M in H_2O) was added. The reaction mixture was stirred at room temperature for 4 h and monitored by TLC to confirm the reaction was completed. Then the reaction mixture was poured into ice/water, and the product was extracted with Et_2O. The combined extracts were washed with brine, dried with $MgSO_4$ and concentrated under reduced pressure. Purification by silica gel chromatography (petroleum ether/EtOAC, 2:1) gave product **15** (564 mg, 1.3 mmol, 27%) as a colourless oil. TLC (EtOAC/petroleum ether, 2:1): $R_f = 0.59$. HRMS (APCI): calc. for $[C_{26}H_{38}O_3S]^+$ m/z = 430.2542; found: m/z = 430.2551. ^{1}H NMR (C_6D_6, 500 MHz): 7.85 (m, 2H), 6.94 (m, 3H), 5.35 (tq, 1H, J = 6.7, 1.3 Hz), 5.09 (t, 1H, J = 7.9 Hz), 5.05 (dp, 1H, J = 10.1, 1.3 Hz), 4.80 (m, 1H), 4.75 (m, 1H), 3.97 (m, 3H), 3.14 (brd, 1H, J = 13.7 Hz), 2.47 (dd, 1H, J = 13.5, 11.1 Hz), 1.97 (m, 2H), 1.88 (m, 2H), 1.78 (m, 4H), 1.61 (t, 3H, J = 1.2 Hz), 1.43 (d, 3H, J = 1.4 Hz), 1.40 (s, 3H), 1.32 (m, 2H), 1.08 (d, 3H, J = 1.4 Hz) ppm. ^{13}C NMR (C_6D_6, 125 MHz): 145.42 (C_q), 144.31 (C_q), 139.41 (C_q), 137.73 (C_q), 132.91 (CH), 130.76 (C_q), 129.63 (CH, x2), 128.65 (CH, x2), 128.07 (CH), 125.08 (CH), 118.80 (CH), 110.63 (CH_2), 63.75 (CH), 59.34 (CH_2), 39.50 (CH_2), 39.42 (CH_2), 38.26 (CH_2), 37.49 (CH_2), 26.71 (CH_2), 25.90 (CH_2), 22.43 (CH_3), 16.25 (CH_3), 16.15 (CH_3), 15.87 (CH_3) ppm.

Synthesis of (2*E*,6*E*,10*E*)-3,7,11,15-tetramethylhexadeca-2,6,10,15-tetraen-1-ol (16).[23] Compound **15** (0.67 g, 1.6 mmol, 1.00 equiv.) and Pd(dppp)Cl_2 (936 mg, 0.15 mmol, 0.1 equiv.) were dissolved in THF (4 mL). The mixture was cooled to 0 °C, and $LiEt_3BH$ (4.7 mL, 1.0 M in THF, 4.7 mmol, 3.00 equiv.) was added dropwise. After stirring for 1.5 h, the reaction was quenched by pouring into aqueous NH_4Cl (40 mL sat. NH_4Cl with 100 mL ice/water). The product was extracted with Et_2O (3×60 mL). The combined extracts were dried with $MgSO_4$ and concentrated under reduced pressure. The product **16** (0.43 g, 1.5 mmol, 95%) was purified by column chromatography (petroleum ether/Et_2O, 3:1) and was obtained as a colourless oil. TLC (petroleum ether/Et_2O, 2:1): $R_f = 0.38$. GC (HP5-MS): $I = 2193$. EI-MS (70 eV): m/z (%) = 41 (4), 55 (5), 67 (4), 81 (15), 95 (7), 107 (2), 121 (2), 161 (1), 189 (0.5), 290 (0.01). ^{1}H NMR (C_6D_6, 500 MHz): 5.40 (ddt, 1H, J = 6.8, 5.4, 1.3 Hz), 5.25 (m, 2H), 4.82 (m, 2H), 3.97 (m, 2H), 2.19 (m, 2H), 2.12 (m, 4H), 1.99 (m, 6H), 1.66 (t, 3H, J = 1.2 Hz), 1.58 (m, 6H), 1.55 (m, 2H), 1.48 (d, 3H, J = 1.4 Hz) ppm. ^{13}C NMR (C_6D_6, 125 MHz): 148.86 (C_q), 138.15 (C_q), 135.28 (C_q), 135.06 (C_q), 124.98 (CH), 124.88 (CH), 124.56 (CH), 110.40 (CH_2), 59.40 (CH_2), 40.20 (CH_2), 39.91 (CH_2), 39.68 (CH_2), 37.71 (CH_2), 27.06 (CH_2), 26.79 (CH_2), 26.37 (CH_2), 22.52 (CH_3), 16.21 (CH_3), 16.11 (CH_3), 16.03 (CH_3) ppm.

Synthesis of (2*E*,6*E*,10*E*)-3,7,11,15-tetramethylhexadeca-2,6,10,15-tetraen-1-diphosphate (iso-GGPP III). To a cooled (0 °C) solution of **16** (400 mg, 1.4 mmol, 1.00 equiv.) in Et_2O (3 mL) PBr_3 (150 mg, 0.6 mmol, 0.40 equiv.) was added dropwise. The mixture was stirred for 1 h at 0 °C and was transferred directly to an ice/water mixture. The aqueous layer was extracted with Et_2O three times and the organic layers were dried with $MgSO_4$, concentrated under reduced pressure to give the crude bromide (600 mg).

To a solution of tris(tetra-*n*-butylammonium)hydrogen diphosphate (1.5 g, 1.7 mmol, 1.20 equiv.) in acetonitrile (4 mL) a solution of the allyl bromide was added and the mixture was stirred at room temperature overnight. Acetonitrile was removed under reduced pressure. The residue was dissolved in aqueous NH_4HCO_3 solution (0.25 M) and loaded onto a DOWEX 50WX8 ion-exchange column (NH_4^+ form, pH 7.0). The column was flushed slowly with 1.5 column volume of NH_4HCO_3 buffer (25 mM, 5% *i*PrOH) and the eluate was lyophilised to yield the diphosphate as colourless hygroscopic powder (500 mg, 1.0 mmol, 72%). ^{1}H NMR (C_6D_6, 500 MHz): 5.41 (t, 1H, J = 6.7 Hz), 5.10 (m, 2H), 4.65 (d, 2H, J = 13.6 Hz), 4.43 (t, 2H, J = 6.3 Hz), 2.11-1.89 (m, 12H), 1.69 (brs, 3H), 1.65 (brs, 3H), 1.58 (brs, 3H), 1.55 (m, 5H) ppm. ^{13}C NMR (C_6D_6, 125 MHz): 145.33 (C_q), 142.10 (C_q), 135.28 (C_q), 134.54 (C_q), 124.56 (CH), 124.17 (CH), 119.98 (d, CH, $^3J_{C,P}$ = 9.3 Hz), 110.01 (CH_2), 62.46 (d, CH_2, $^2J_{C,P}$ = 4.2 Hz), 39.80 (CH_2), 39.59 (CH_2), 39.22 (CH_2), 37.29 (CH_2), 26.75 (CH_2), 26.55 (CH_2), 25.85 (CH_2), 22.16 (CH_3), 16.07 (CH_3), 15.77 (CH_3), 15.69 (CH_3) ppm. HRMS (ESI(−)): calc. for $[C_{20}H_{35}O_7P_2]^-$ m/z = 449.1864; found: m/z = 449.1868.

Enzymatic conversions. Test enzymatic conversions of iso-GPP and IPP (1 mg each) were done in incubation buffer (1 mL; 50 mM Tris·HCl, 10 mM $MgCl_2$, 10% glycerol, 20 mM β-cyclodextrin, pH 8.2). Enzyme preparations were obtained as reported previously (Table S1), and enzymes were added at a concentration of 0.3 mg L^{-1}, followed by incubation for 16 h at 30 °C. The reaction mixtures were extracted with petroleum ether, the extracts were dried with $MgSO_4$ and analysed by GC/MS. These conditions were also used for isotopic labelling experiments, followed by extraction with C_6D_6 and analysis by NMR spectroscopy.

Preparative-scale enzymatic conversions of the trisammonium salts of iso-GGPP III or of iso-GPP and IPP (for amounts, see Table S1) were done in incubation buffer at a substrate concentration of 1 mmol L^{-1} for 16 h at 30 °C. Enzymes were added at a concentration of 0.3 mg L^{-1}, followed by incubation for 16 h at 30 °C. The reaction mixtures were extracted with *n*-hexane, the extracts were dried with $MgSO_4$ and the solvent was evaporated, followed by compound isolation through column chromatography on silica gel or on on silica gel activated with silver nitrate.

(11*E*)-12-Isopentenyl-α-selinene (18). This compound was isolated by column chromatography on silica gel with *n*-pentane. Yield: 0.4 mg (1.1 μmol, 0.4%). TLC (n-pentane): $R_f = 0.68$, $[\alpha]_D^{25} = +12.5$ (*c* 0.04, acetone), HRMS (EI): $[M]^+$ calcd. for $C_{20}H_{32}^+$ *m/z* 272.2498; found *m/z* 272.2503. GC (HP5-MS): $I = 2021$. IR (diamond ATR): $\tilde{\nu}/cm^{-1} = 3192$ (w), 2921 (s), 2851 (s), 1741 (m), 1657 (m), 1632 (w), 1538 (w), 1467 (w), 1454 (w), 1375 (w), 1260 (w), 1096 (w), 1022 (w), 885 (w), 798 (w). For NMR data, see Table S2.

(11*Z*)-12-Isopentenyl-α-selinene (27). This compound was isolated by column chromatography on silica gel with *n*-pentane. Yield: 0.2 mg (0.7 μmol, 0.8%). TLC (*n*-pentane): $R_f = 0.70$, $[\alpha]_D^{25} = -20.0$ (*c* 0.02, acetone), HRMS (EI): $[M]^+$ calcd. for $C_{20}H_{32}^+$ *m/z* 272.2498; found *m/z* 272.2491. GC (HP5-MS): $I = 1957$. IR (diamond ATR): $\tilde{\nu}/cm^{-1} = 3360$ (w), 2959 (m), 2923 (s), 2853 (m), 1735 (w), 1659 (w), 1633 (w), 1453 (m), 1376 (w), 1260 (w), 1083 (w), 1019 (w), 968 (w), 886 (w), 807 (m), 703 (w). For NMR data, see Table S3.

Isoelisabethatriene C (28). This compound was isolated by column chromatography on silica gel with *n*-pentane. Yield: 0.5 mg (1.8 μmol, 2.0%). TLC (*n*-pentane): $R_f = 0.70$, $[\alpha]_D^{25} = -14.3$ (*c* 0.04, acetone), HRMS (EI): $[M]^+$ calcd. for $C_{20}H_{32}^+$ *m/z* 272.2498; found *m/z* 272.2501. GC (HP5-MS): $I = 1948$. IR (diamond ATR): $\tilde{\nu}/cm^{-1} = 3355$ (w), 2958 (m), 2923 (s), 2853 (m), 2175 (w), 1736 (m), 1658 (m), 1632 (m), 1458 (m), 1260 (m), 1094 (m), 1025 (m), 885 (m), 803 (m). For NMR data, see Table S4.

Isoxeniaphyllene II (29). This compound was isolated by column chromatography on silica gel (activated with silver nitrate) with Et_2O. Yield: 1.1 mg (4.0 μmol, 5.0%). TLC (*n*-pentane): $R_f = 0.54$, $[\alpha]_D^{25} = +83.0$ (*c* 0.1, acetone), HRMS (EI): $[M]^+$ calcd. for $C_{20}H_{32}^+$ *m/z* 272.2498; found *m/z* 272.2510. GC (HP5-MS): $I = 1981$. IR (diamond ATR): $\tilde{\nu}/cm^{-1} = 3071$ (w), 2924 (s), 2853 (m), 1738 (m), 1649 (w), 1453 (m), 1374 (m), 1228 (m), 1216 (m), 884 (m), 840 (w). For NMR data, see Table S5.

Iso-β-springene (30). This compound was isolated by column chromatography on silica gel with *n*-pentane. Yield: 0.7 mg (2.6 μmol, 3.3%). TLC (n-pentane): $R_f = 0.50$, HRMS (EI): $[M]^+$ calcd. for $C_{20}H_{32}^+$ *m/z* 272.2498; found *m/z* 272.2503. GC (HP5-MS): $I = 1919$. IR (diamond ATR): $\tilde{\nu}/cm^{-1} = 3080$ (w), 2924 (s), 2852 (m), 2015 (w), 1738 (w), 1648 (w), 1594 (w), 1453 (w), 1378 (w), 1241 (w), 1153 (w), 1098 (w), 989 (w), 889 (m). For NMR data, see Table S6.

Isoobscuronatin (35). This compound was isolated by column chromatography on silica gel with *n*-pentane/$Et_2O = 3:1$. Yield: 0.4 mg (1.4 μmol, 0.6%). TLC (n-pentane/$Et_2O = 2:1$): $R_f = 0.60$, $[\alpha]_D^{25} = +42.9$ (*c* 0.04, acetone), HRMS (EI): $[M]^+$ calcd. for $C_{20}H_{34}O^+$ *m/z* 290.2604; found *m/z* 290.2610. GC (HP5-MS): $I = 2059$. IR (diamond ATR): $\tilde{\nu}/cm^{-1} = 3362$ (w), 3199 (w), 2959 (m), 2923 (s), 2853 (m), 1731 (w), 1659 (w), 1632 (w), 1509 (m), 1456 (w), 1410 (w), 1376 (w), 1258 (m), 1196 (w), 1088 (m), 1014 (s), 883 (w), 794 (s), 702 (w). For NMR data, see Table S7.

Biflora-4,10(19),16-triene (36). This compound was isolated by column chromatography on silica gel (activated with silver nitrate) with *n*-pentane/$Et_2O = 10:1$. Yield: 1.5 mg (5.5 μmol, 2.4%). TLC (n-pentane): $R_f = 0.50$, $[\alpha]_D^{25} = -12.3$ (*c* 0.15, acetone), HRMS (EI): $[M]^+$ calcd. for $C_{20}H_{32}^+$ *m/z* 272.2498; found *m/z* 272.2511. GC (HP5-MS): $I = 1991$. IR (diamond ATR): $\tilde{\nu}/cm^{-1} = 3076$ (w), 2961 (m), 2929 (s), 2856 (m), 1738 (w), 1649 (m), 1451 (m), 1376 (w), 1021 (w), 885 (s), 792 (w). For NMR data, see Table S8.

Bucket-wheelene (38). This compound was isolated by column chromatography on silica gel with *n*-pentane. Yield: 0.6 mg (2.2 μmol, 1.9%). TLC (*n*-pentane): $R_f = 0.40$, HRMS (EI): $[M]^+$ calcd. for $C_{20}H_{32}^+$ *m/z* 272.2498; found *m/z* 272.2499. GC (HP5-MS): $I = 2070$. IR (diamond ATR): $\tilde{\nu}/cm^{-1} = 2961$ (m), 2924 (s), 2853 (m), 1642 (w), 1438 (w), 1382 (w), 1260 (s), 1092 (s), 1019 (s), 885 (w), 800 (s), 693 (w). For NMR data, see Table S9.

Dolastaxenene (43). This compound was isolated by column chromatography on silica gel with. Yield: 0.6 mg (2.2 μmol, 3.2%). TLC (*n*-pentane): $R_f = 0.76$, $[\alpha]_D^{25} = +34.6$ (*c*, acetone), HRMS (EI): $[M]^+$ calcd. for $C_{20}H_{32}^+$ *m/z* 272.2498; found *m/z* 272.2489. GC (HP5-MS): $I = 2067$. IR (diamond ATR): $\tilde{\nu}/cm^{-1} = 3077$(w), 2961 (s), 2927 (s), 2866 (s), 2841 (s), 1738 (m), 1645 (m), 1440 (m), 1372 (m), 1260 (m), 1093 (m), 883 (s), 799 (s). For NMR data, see Table S10.

Acknowledgements

This work was supported by the Deutsche Forschungsgemeinschaft DFG (project no. 513548540). Open Access funding enabled and organized by Projekt DEAL.

Conflict of Interests

The authors declare no conflict of interest.

Data Availability Statement

The data that support the findings of this study are available in the supplementary material of this article.

Keywords: biosynthesis · enzyme mechanisms · isotopes · NMR spectroscopy · terpenes

[1] J. S. Dickschat, *Nat. Prod. Rep.* **2016**, *33*, 87–110.
[2] D. W. Christianson, *Chem. Rev.* **2017**, *117*, 11570–11648.
[3] X. Lin, R. Hopson, D. E. Cane, *J. Am. Chem. Soc.* **2006**, *128*, 6022–6023.
[4] M. Seemann, G. Zhai, J.-W. de Kraker, C. M. Paschall, D. W. Christianson, D. E. Cane, *J. Am. Chem. Soc.* **2002**, *124*, 7681–7689.
[5] H. Xu, J. S. Dickschat, *Synthesis* **2022**, *54*, 1551–1565.
[6] D. A. Schooley, K. J. Judy, B. J. Bergot, M. S. Hall, J. B. Siddall, *Proc. Natl. Acad. Sci. USA* **1973**, *70*, 2921–2925.
[7] C.-M. Wang, D. E. Cane, *J. Am. Chem. Soc.* **2008**, *130*, 8908–8909.
[8] T. Ozaki, S. S. Shinde, L. Gao, R. Okuizumi, C. Liu, Y. Ogasawara, X. Lei, T. Dairi, A. Minami, H. Oikawa, *Angew. Chem. Int. Ed.* **2018**, *57*, 6629–6632; *Angew. Chem.* **2018**, *130*, 6739–6742.

[9] S. von Reuss, D. Domik, M. C. Lemfack, N. Magnus, M. Kai, T. Weise, B. Piechulla, *J. Am. Chem. Soc.* **2018**, *140*, 11855–11862.
[10] X. Xu, L. Lauterbach, B. Goldfuss, G. Schnakenburg, J. S. Dickschat, *Nat. Chem.* **2023**, *15*, 1164–1171.
[11] Y.-T. Duan, A. Koutsaviti, M. Harizani, C. Ignea, V. Roussis, Y. Zhao, E. Ioannou, S. C. Kampranis, *Nat. Chem. Biol.* **2023**, *19*, 1532–1539.
[12] Y. Jin, D. C. Williams, R. Croteau, R. M. Coates, *J. Am. Chem. Soc.* **2005**, *127*, 7834–7842.
[13] M. Demiray, X. Tang, T. Wirth, J. A. Faraldos, R. K. Allemann, *Angew. Chem. Int. Ed.* **2017**, *56*, 4347–4350; *Angew. Chem.* **2017**, *129*, 4411–4415.
[14] C. Oberhauser, V. Harms, K. Seidel, B. Schröder, K. Ekramzadeh, S. Beutel, S. Winkler, L. Lauterbach, J. S. Dickschat, *Angew. Chem. Int. Ed.* **2018**, *57*, 11802–11806; *Angew. Chem.* **2018**, *130*, 11976–11980.
[15] V. Harms, B. Schröder, C. Oberhauser, C. D. Tran, S. Winkler, G. Dräger, A. Kirschning, *Org. Lett.* **2020**, *22*, 4360–4365.
[16] C. D. Tran, G. Dräger, H. F. Struwe, L. Siedenberg, S. Vasisth, J. Grunenberg, A. Kirschning, *Org. Biomol. Chem.* **2022**, *20*, 7833–7839.
[17] S. Y. Chow, H. J. Williams, Q. Huang, S. Nanda, A. I. Scott, *J. Org. Chem.* **2005**, *70*, 9997–10003.
[18] B. Gu, J. S. Dickschat, *Angew. Chem. Int. Ed.* **2023**, *62*, e202307006; *Angew. Chem.* **2023**, *135*, e202307006.
[19] H. Li, J. S. Dickschat, *Org. Chem. Front.* **2022**, *9*, 795–801.
[20] H. Li, J. S. Dickschat, *Angew. Chem. Int. Ed.* **2022**, *61*, e202211054; *Angew. Chem.* **2022**, *134*, e202211054.
[21] J. Rinkel, L. Lauterbach, P. Rabe, J. S. Dickschat, *Angew. Chem. Int. Ed.* **2018**, *57*, 3238–3241; *Angew. Chem.* **2018**, *130*, 3292–3296.
[22] J. Rinkel, L. Lauterbach, J. S. Dickschat, *Angew. Chem. Int. Ed.* **2017**, *56*, 16385–16389; *Angew. Chem.* **2017**, *129*, 16603–16607.
[23] T. Eguchi, Y. Nishimura, K. Kakinuma, *Tetrahedron Lett.* **2003**, *44*, 3275–3279.
[24] P. Rabe, J. Rinkel, E. Dolja, T. Schmitz, B. Nubbemeyer, T. H. Luu, J. S. Dickschat, *Angew. Chem. Int. Ed.* **2017**, *56*, 2776–2779; *Angew. Chem.* **2017**, *129*, 2820–2823.
[25] A. M. Hill, D. E. Cane, C. J. D. Mau, C. A. West, *Arch. Biochem. Biophys.* **1996**, *336*, 283–289.
[26] L. Lauterbach, J. Rinkel, J. S. Dickschat, *Angew. Chem. Int. Ed.* **2018**, *57*, 8280–8283; *Angew. Chem.* **2018**, *130*, 8412–8415.
[27] L. Lauterbach, B. Goldfuss, J. S. Dickschat, *Angew. Chem. Int. Ed.* **2020**, *59*, 11943–11947; *Angew. Chem.* **2020**, *132*, 12041–12045.
[28] J. Rinkel, P. Rabe, X. Chen, T. G. Köllner, F. Chen, J. S. Dickschat, *Chem. Eur. J.* **2017**, *23*, 10501–10505.
[29] J. S. Dickschat, J. Rinkel, P. Rabe, A. Beyraghdar Kashkooli, H. J. Bouwmeester, *Beilstein J. Org. Chem.* **2017**, *13*, 1770–1780.
[30] L. Li, L. Sheng, C.-Y. Wang, Y.-B. Zhou, H. Huang, X.-B. Li, J. Li, E. Mollo, M. Gavagnin, Y.-W. Guo, *J. Nat. Prod.* **2011**, *74*, 2089–2094.
[31] A. J. Weinheimer, W. W. Youngblood, P. H. Washecheck, T. K. B. Karns, L. S. Ciereszko, *Tetrahedron Lett.* **1970**, *26*, 497–500.
[32] H. Xu, J. S. Dickschat, *Chem. Eur. J.* **2020**, *26*, 17318–17341.
[33] Y. Yamada, T. Kuzuyama, M. Komatsu, K. Shin-ya, S. Omura, D. E. Cane, H. Ikeda, *Proc. Natl. Acad. Sci. USA* **2015**, *112*, 857–862.
[34] W. S. Bowers, C. Nishino, M. E. Montgomery, L. R. Nault, M. W. Nielson, *Science* **1977**, *196*, 196–197.
[35] J.-W. de Kraker, M. C. R. Franssen, A. de Groot, W. A. König, H. J. Bouwmeester, *Plant Physiol.* **1998**, *117*, 1381–1392.
[36] J. Rinkel, S. T. Steiner, J. S. Dickschat, *Angew. Chem. Int. Ed.* **2019**, *58*, 9230–9233; *Angew. Chem.* **2019**, *131*, 9328–9332.
[37] A. Groweiss, Y. Kashman, *Tetrahedron Lett.* **1978**, *19*, 2205–2208.
[38] S.-Y. Kim, P. Zhao, M. Igarashi, R. Sawa, T. Tomita, M. Nishiyama, T. Kuzuyama, *Chem. Biol.* **2009**, *16*, 736–743.
[39] K. A. Taizoumbe, S. T. Steiner, J. S. Dickschat, *Chem. Eur. J.* **2023**, *29*, e202302469.
[40] G. Li, Y.-W. Guo, J. S. Dickschat, *Angew. Chem. Int. Ed.* **2021**, *60*, 1488–1492; *Angew. Chem.* **2021**, *133*, 1510–1514.
[41] Y. Kashman, A. Groweiss, *J. Org. Chem.* **1980**, *45*, 3814–3824.
[42] A. Meguro, Y. Motoyoshi, K. Teramoto, S. Ueda, Y. Totsuka, Y. Ando, T. Tomita, S.-Y. Kim, T. Kimura, M. Igarashi, R. Sawa, T. Shinada, M. Nishiyama, T. Kuzuyama, *Angew. Chem. Int. Ed.* **2015**, *54*, 4353–4356; *Angew. Chem.* **2015**, *127*, 4427–4430.
[43] G. Bian, J. Rinkel, Z. Wang, L. Lauterbach, A. Hou, Y. Yuan, Z. Deng, T. Liu, J. S. Dickschat, *Angew. Chem. Int. Ed.* **2018**, *57*, 15887–15890; *Angew. Chem.* **2018**, *130*, 16113–16117.
[44] J. Rinkel, J. S. Dickschat, *Org. Lett.* **2019**, *21*, 2426–2429.
[45] G. R. Fulmer, A. J. M. Miller, N. H. Sherden, H. E. Gottlieb, A. Nudelman, B. M. Stoltz, J. E. Bercaw, K. I. Goldberg, *Organometallics* **2010**, *29*, 2176–2179.
[46] K. H. Yong, J. A. Lotoski, J. M. Chong, *J. Org. Chem.* **2001**, *66*, 8248–8251.
[47] K. Zukowska, L. Paczek, K. Grela, *ChemCatChem* **2016**, *8*, 2817–2823.
[48] N. A. Braun, M. Meier, G. Schmaus, B. Hölscher, W. Pickenhagen, *Helv. Chim. Acta* **2003**, *86*, 2698–2708.
[49] V. Singh, S. Chaudhary, V. Sapehiyia, I. Kaur, G. L. Kad, J. Singh, *Ind. J. Chem.* **2004**, *43B*, 1950–1953.
[50] U. P. Dhoke, A. S. Rao, *Synth. Commun.* **1988**, *18*, 811–822.
[51] A. G. Ibragimov, D. L. Minsker, R. A. Saraev, U. M. Dzhemilev, *Izv. Akad. Nauk SSSR Ser. Khim.* **1983**, 2333–2336.
[52] K. Mori, Y. Nakazono, *Liebigs Ann. Chem.* **1988**, 167–174.
[53] E. R. Lee, I. Lakomy, P. Bigler, R. Scheffold, *Helv. Chim. Acta* **1991**, *74*, 146–162.

Manuscript received: October 27, 2023
Accepted manuscript online: November 10, 2023
Version of record online: December 14, 2023

Appendices D

Enzyme-Catalysed Formation of Hydrocarbon Scaffolds from Geranylgeranyl Diphosphate Analogs with Shifted Double Bonds

Chem. Eur. J. **2025**, *31*, e202500712.

DOI: 10.1002/chem.202500712.

Chemistry–A European Journal
Research Article
doi.org/10.1002/chem.202500712
Chemistry Europe
European Chemical Societies Publishing
www.chemeurj.org

VIP *Very Important Paper*

Enzyme-Catalysed Formation of Hydrocarbon Scaffolds from Geranylgeranyl Diphosphate Analogs with Shifted Double Bonds

Heng Li,[a] Bernd Goldfuss,[b] and Jeroen S. Dickschat*[a]

Four analogs of geranylgeranyl diphosphate (GGPP) with shifted double bonds were synthesised and enzymatically converted with 14 diterpene synthases of previously reported function, including two newly characterised homologs of the benditerpe-2,6,15-triene synthase Bnd4 and the venezuelaene synthase VenA. In successful cases the products were isolated and structurally characterised by NMR spectroscopy, revealing the formation of various diterpenoids with skeletons that have not been reported from natural sources. Isotopic labelling experiments in conjunction with DFT calculations were performed to give insights into hydride migrations in the biosynthesis of the non-natural diterpenes benditerpe-2,7(19),15-triene and venezuelaxenene and their natural counterparts from GGPP.

Introduction

Terpene synthases are remarkable biocatalysts that can turn structurally simple substrates such as geranyl diphosphate (GPP), farnesyl diphosphate (FPP), geranylgeranyl diphosphate (GGPP) and even longer oligoprenyl diphosphates into a large diversity of terpene hydrocarbons or alcohols.[1,2] The products of these reactions frequently contain multiple rings and stereogenic centres. During terpene cyclisation usually more than half of the carbons of the substrate undergo a change in the hybridisation and bonding state,[3] with several carbon-carbon bonds being formed. Overall, terpene cyclisations belong to the most complex transformations in nature catalysed by a single enzyme.

Recent research has demonstrated that terpene synthases cannot only act on their natural substrates, but many structural modifications realised in synthetic substrate analogs are tolerated. This includes hydroxylated oligoprenyl diphosphates,[4,5] epoxides,[6] compounds with heteroatoms inserted into the chain,[7,8] ketones[9,10] and halogenated[11–14] and methoxy-substituted[15] compounds. Also the double bond functions have been manipulated, represented by partially saturated substrate analogs[16–19] or derivatives with a shifted double bond.[20] In addition, compounds with a changed alkylation pattern[21,22] and cyclopropyl derivatives[23] have been employed.

In an alternative approach, Tiefenbacher has used supramolecular capsules to convert analogs of terpene precursors.[24] This method can also start from terpenoid acetate esters[25] of even alcohols[26] instead of diphosphate esters required by enzymes.

We have recently demonstrated that substrate analogs with shifted double bonds can because of their changed reactivity result in very interesting compounds with novel skeletons, e.g. *iso*-GGPP I, a GGPP isomer with a shifted C6=C7 double bond, can yield several unusual products with various type I terpene synthases. For instance, spiroalbatene synthase from *Allokutzneria albata* (SaS) generates spiroalbatene (**1**) from natural GGPP,[27] but albataxenene (**2**) from *iso*-GGPP I,[28] or wanjudiene synthase from *Chryseobacterium wanjuense* (CwWS) converts GGPP into wanjudiene (**3**),[29] but *iso*-GGPP I into wanjuxenene[28] ("xenene" after gr. ξενοσ = foreighn indicates the unusual carbon skeletons that cannot be formed from GGPP, Scheme 1). Furthermore, the dolasta-1(15),8-diene synthase from *Colletotrichum gloeosporioides* (CgDS) catalyses the formation of dolasta-1(15),8-diene (**5**) from GGPP,[30] while *iso*-GGPP III with a shifted C14=C15 double bond leads to dolastaxenene (**6**).[31] Here we report on the synthesis of four more GGPP derivatives with two or even three shifted double bonds and on several new diterpenoids obtained enzymatically from these substrate analogs.

Results and Discussion

The synthesis of *iso*-GGPP IV (**17**, Scheme 2A) started from prenyl bromide (**7**) that underwent nucleophilic substitution to **9** with the dianion of isoprenol generated with two equivalents of BuLi in the presence of TMEDA.[32] Conversion into the iodide **10** with iodine, PPh_3 and imidazole was followed by another coupling with **8** to yield **11**. After transformation into the iodide **12** a nucleophilic substitution with the enolate anion of ethyl

[a] H. Li, Prof. Dr. J. S. Dickschat
Kekulé-Institute for Organic Chemistry and Biochemistry
University of Bonn
Gerhard-Domagk-Straße 1, 53121 Bonn, Germany
E-mail: dickschat@uni-bonn.de
[b] Prof. Dr. B. Goldfuss
Department for Chemistry
University of Cologne
Greinstraße 4, 50939 Cologne, Germany

Supporting information for this article is available on the WWW under https://doi.org/10.1002/chem.202500712

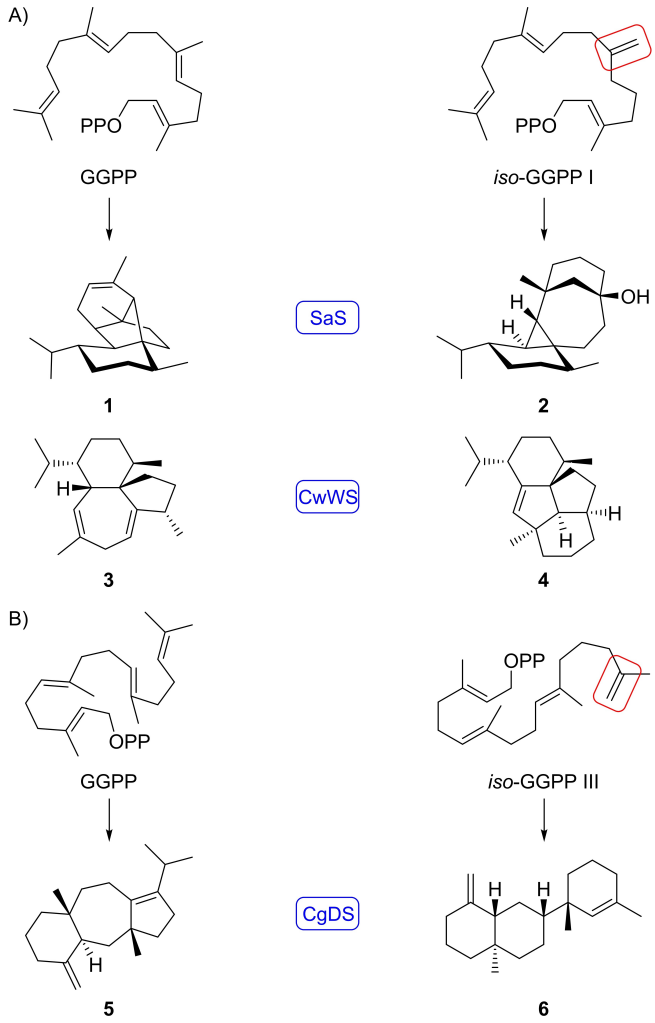

Scheme 1. Diterpene hydrocarbons previously obtained from GGPP and its analogs with shifted double bonds. A) Diterpene hydrocarbons obtained from GGPP (left) and from *iso*-GGPP I (right). B) Diterpene hydrocarbons obtained from GGPP (left) and *iso*-GGPP III (right). The blue boxes indicate the enzymes used and the red boxes highlight the shifted double bonds in the substrate analogs.

acetoacetate resulted in **13** that was saponified with spontaneous decarboxylation of the β-keto acid to **14**. A Horner-Wadsworth-Emmons (HWE) reaction with triethyl phosphonoacetate gave access to **15** that was reduced with DIBAlH to **16** and subsequently converted into the target compound **17** through bromination and phosphorylation. The diphosphate **17** was obtained with a yield of 6% over ten sequential steps.

Using a similar strategy, *iso*-GGPP V (**25**, Scheme 2B) was prepared from known alcohol **18**.[31] Bromination and elongation with **8** furnished alcohol **19** that was converted into the corresponding iodide **20**. This material was used to alkylate ethyl acetoactetat to yield ester **21** that was saponified with decarboxylation to **22**. A HWE reaction to **23**, DIBAlH reduction to **24**, bromination and phosphorylation completed the synthesis of **25** with an overall yield of 5% through nine linear steps.

The third target compound *iso*-GGPP VI (**33**, Scheme 3A) was made accessible in a combined synthetic and enzymatic approach. The C_{15} compound *iso*-FPP III (**32**) was obtained from known alcohol **26**[32,33] through conversion into the iodide **27** for the alkylation of ethyl acetoacetate to β-ketoester **28**, followed by saponification and decarboxylation to **29**. Subsequent standard transformations furnished the diphosphate **32** that can be elongated with isopentenyl diphosphate (IPP) to **33** using the GGPP synthase (GGPPS) from *Streptomyces cyaneofuscatus*.[34] The substrate analog **32** was obtained over seven sequential steps with a yield of 23%.

The fourth compound *iso*-GGPP VII (**40**, Scheme 3B) was likewise prepared from known alcohol **26**.[32,33] After conversion into the iodide **27** and elongation with **8** to **34** through the dianion method another iodination to **35** allowed for the alkylation of ethyl acetoactetate to β-ketoester **36**. Saponification and decarboxylation to **37**, HWE elongation to **38**, reduction and phosphorylation gave access to **40**. The material was made available with a yield of 14% over nine transformations.

All four synthetic substrate analogs were screened for their conversion by various diterpene synthases (Table S1). While for *iso*-GGPP V and *iso*-GGPP VII no successful cases were observed with any of the tested diterpene synthases, *iso*-GGPP IV and *iso*-GGPP VI were accepted by several enzymes. Furthermore, the previously reported substrate analog *iso*-GGPP I[20] was converted by two newly characterised bacterial diterpene synthases. This included the benditerpe-2,6,15-triene synthase Bnd4 from *Streptomyces iakyrus* NRRL ISP-5482 (accession number WP 033312626), which is a homolog of the previously reported Bnd4 from *Streptomyces* sp. CL12-4,[35] exhibiting a pairwise amino acid sequence identity of 92%. The incubation of GGPP with the purified enzyme from *S. iakyrus* (Figure S1) showed the formation of one major thermally instable compound by GC/MS (Figure S2) that was isolated and structurally characterised by NMR spectroscopy as benditerpe-2,6,15-triene (**41**),[35] a compound that can undergo a Cope rearrangement explaining its behaviour under the thermal impact during GC/MS analysis.

The biosynthesis of **41** has been demonstrated to proceed through a 1,3-hydride shift (Scheme 4A) through incubation of (1,1-$^2H_2$)GGPP with Bnd4 from *Streptomyces* sp. CL12-4, product isolation and NMR spectroscopy, and by DFT computations.[36] A simpler experiment makes use of a double labelling strategy with deuterium labelling at C1 and a ^{13}C-labelling at the target position of the migrating deuterium (C11), using the substrate (11-^{13}C,1,1-$^2H_2$)GGPP that can be prepared in situ from (7-^{13}C)FPP and (1,1-$^2H_2$)IPP using GGPP synthase (GGPPS). Furthermore, it has not been investigated experimentally which of the two enantiotopic hydrogens at C1 of GGPP is migrating, which can be investigated using stereoselectively deuterated substrates. In the present case the experiment with (7-^{13}C)FPP[37] and (1,1-$^2H_2$)IPP[38] was unsuccessful for two reasons: First, the signal for the deuterated carbon (C11) is expected to split into a triplet and will have a lower intensity compared to the signal of a non-deuterated carbon as a result of the nuclear quadrupole moment that causes prolonged spin relaxation times. Second,

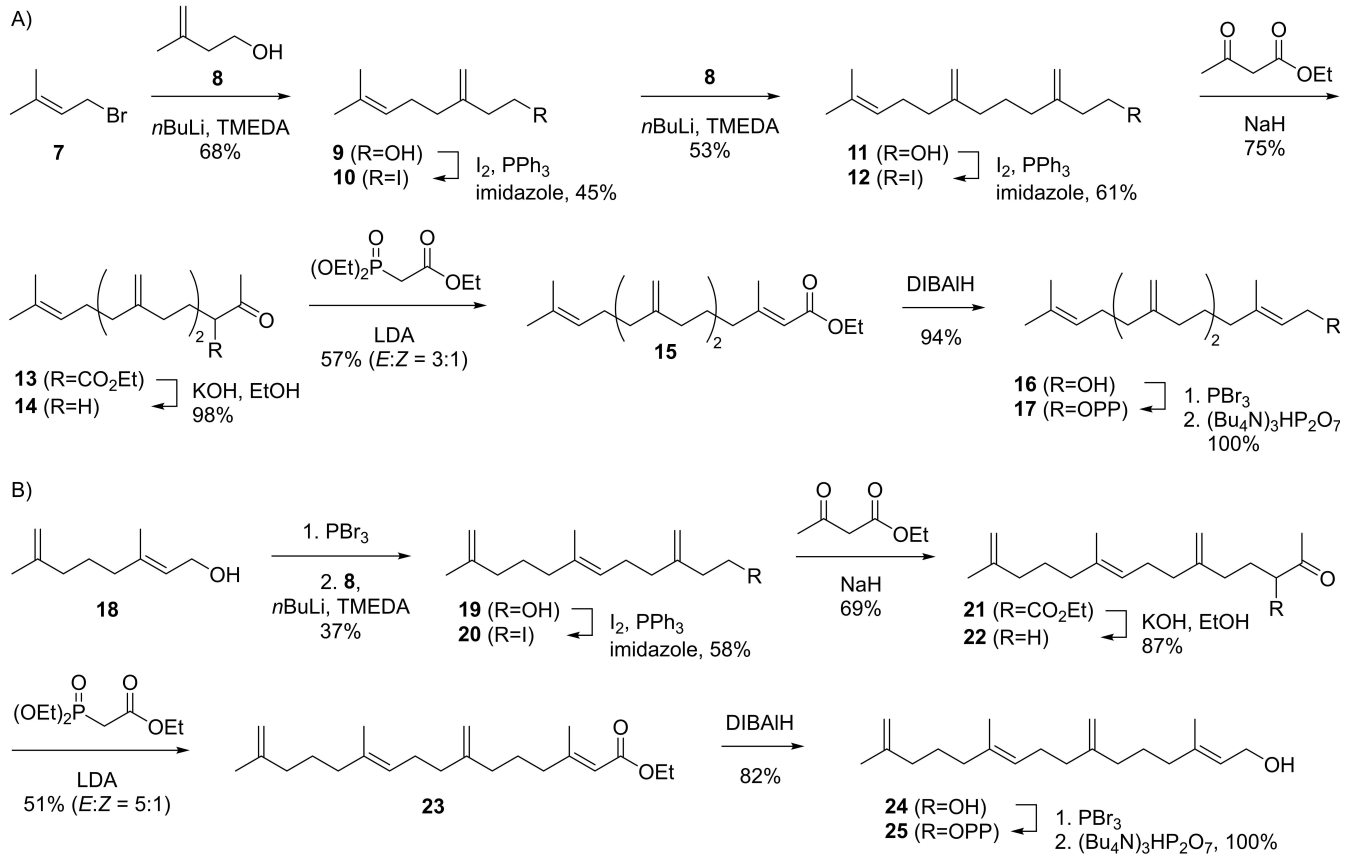

Scheme 2. Synthesis of *iso*-GGPP IV (**17**) and *iso*-GGPP V (**25**).

the special molecular mechanics of **41** cause a line broadening in the ^{13}C-NMR even at elevated temperature (343 K). Both effects together made it impossible to detect the triplet signal to confirm the 1,3-hydride shift. To overcome the second problem of line broadening, we tried to rigidify the skeleton of **41** through a derivatisation with N-bromosuccinimide (NBS) that resulted in the formation of three compounds (**42**–**44**, Schemes 4A and 4B, Tables S2 – S4, Figures S3 – S25). While the major products **42** and **43** were expected, the minor formation of **44** was surprising.

Quantum chemical calculations (Table S5, Figure S26) showed two barrierless cyclisations from **E** via **F** to **G** towards **42** and **43**, while **44** was more difficult to explain. Its formation can be understood from the bromonium adduct **H** that can undergo two asynchronous concerted cyclisations to **J** through a low barrier. An almost barrierless rearrangement to **K** opens the path to a ring-opening with simultaneous rearrangement to **L** that can undergo deprotonation to yield **44**. The high activation barrier for the **K**-to-**L** reaction of 30.7 kcal/mol explains the minor formation of **44**.

The first problem of the lowered signal intensity of a deuterated carbon was addressed by a change of strategy. The substrate combination of (7-^{13}C,6-^{2}H)FPP and IPP was converted with *Streptomyces cyaneofuscatus* GGPPS[34] and Bnd4, followed by NBS treatment to obtain labelled **42** (labelling experiments are summarised in Table S6). If the 1,3-hydride shift from **B** to **C** takes place in the biosynthesis of **41**, a proton will migrate from C1 to C11, while deuterium will stay at C10 and slightly influence the chemical shift of the neigbouring labelled carbon C11. The alternative of two sequential 1,2-hydride shifts (box in Scheme 4A) would require intermediate **B'**, the enantiomer of **B**, to explain the correct configuration at C11 in **C'**, and would result in a triplet for C11 of **42**. In the experiment an upfiled shifted singlet for C11 of **42** was observed ($\Delta\delta = -0.06$ ppm) revealing a deuterium effect from the neighboring position (Figure S27).

Bnd4 from *S. iakyrus* was also incubated with the substrate analog *iso*-GGPP I,[20] resulting in its conversion into one major diterpene hydrocarbon (Figure S28). This compound was isolated and structurally characterised by NMR spectroscopy as benditerpe-2,7(19),15-triene (**45**) (Table S7, Figures S29–S36). Its biosynthesis may proceed through ionisation of *iso*-GGPP I to **A**, followed by a 1,10-cyclisation to **B**, a 1,3-hydride shift to **C**, 1,14-cyclisation to **D** and deprotonation (Scheme 4C), closely resembling the cyclisation mechanism from GGPP to benditerpe-2,6,15-triene (Scheme 4A). Notably, the shifted double bond in **45** disrupts the Cope system and consequently this compound is – in contrast to the natural product **41** – thermally stable. The stereochemical course of the 1,3-hydride shift in the biosynthesis of **45** was investigated throught the incubation of (*R*)- and (*S*)-(1-^{13}C,1-^{2}H)*iso*-GGPP I[28] with Bnd4, indicating retainment of the 1-*pro-R* hydrogen at C1 ($\Delta\delta = -0.51$ ppm, $^{1}J_{C,D} =$

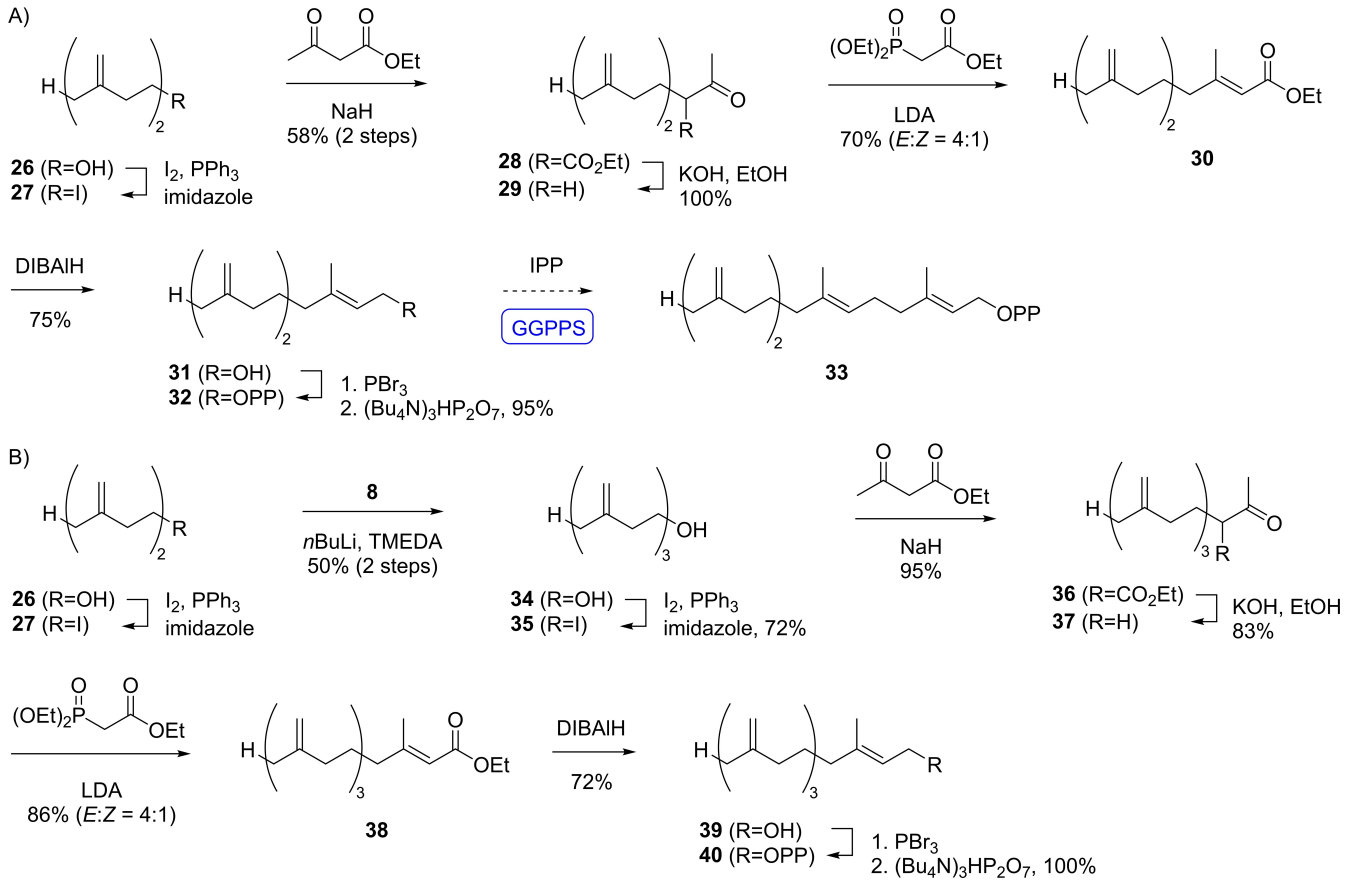

Scheme 3. Synthesis of *iso*-FPP III (**32**) and *iso*-GGPP VII (**40**).

18.8 Hz) and migration of the 1-*pro-S*, that resulted in an upfield shift of $\Delta\delta = -0.08$ ppm (Figure S37). This upfield shift is larger than usually observed for deuterium located two positions away ($\Delta\delta \approx -0.01$ ppm), but similar to the expected upfield shift for deuterium located at a directly neighbouring carbon ($\Delta\delta \approx -0.10$ ppm), questioning whether deuterium was located at C11 as a result of a direct 1,3-hydride shift or at C10 through two sequential 1,2-hydride shifts. However, two sequential hydride shifts would not only proceed through **B2′**, the enantiomer of **B2**, but also in the step from **C2′** to **D2′** the 1-*pro-R* hydrogen would have to migrate to set the correct stereochemistry at C10, which is not experimentally observed. The 1-*pro-R* and 1-*pro-S* hydrogens could swap their roles, if the absolute configuration of **45** and consequently also of **41** would be inverted, but stereoselective deuteration experiments with DMAPP and (*E*)- or (*Z*)-(4-^{13}C,4-^{2}H)IPP,[39] GGPPS and Bnd4, followed by conversion of the product with NBS into **42** (Figure S38) confirmed the published absolute configuration of **41**.[35] These experiments make use of the introduction of artificial stereogenic centres at the deuterated carbons of known configuration, simplifying the problem of absolute configuration determination to one of solving the relative configuration of the naturally present stereogenic centres with respect to the artificially introduced anchors. The additional ^{13}C-labels at the deuterated carbons allow for a highly sensitive detection of deuterium incorporation through HSQC spectroscopy. These experiments require a detailed knowledge about the stereochemical course of the GGPP biosynthesis from the terpene monomers.[40]

The second investigated diterpene synthase is a VenA homolog from *Streptomyces exfoliatus* DSM 41693, exhibiting an amino sequence identity of 97% to the previously characterised enzyme from *Streptomyces venezuelae* ATCC 15439.[41] Incubation of the purified enzyme (Figure S1) with GGPP resulted in the formation of one major diterpene hydrocarbon (Figure S39) that was isolated and its structure identified as venezuelaene A (**46**).[41] The proposed biosynthesis of **46** starts with substrate ionisation to **M** and 1,10-cyclisation to **N** (Scheme 5A). Next, a 1,3-hydride shift to **P** has been suggested,[41] but this step has not been experimentally verified and may also be substituted by two sequential 1,2-hydride shifts through **O**. A subsequent 1,14-cyclisation to **P** followed by a 3,15- and 2,6-cyclisation then lead to **R** as the direct precursor of **46** by deprotonation.

To distinguish between the possible 1,3- or the two sequential 1,2-hydride shifts in the biosynthesis of **46** isotopic labelling experiments were performed. The incubation of (7-^{13}C,6-^{2}H)FPP and IPP with GGPPS and VenA resulted in an upfield shifted triplet for C11 ($\Delta\delta = -0.52$ ppm, $^{1}J_{C,D} = 19.4$ Hz), which supports the sequence of two 1,2-hydride migrations and disfavours the single 1,3-hydride transfer (Figure S40). Furthermore, the conversion of (3-^{13}C)GPP[42] and (1,1-^{2}H$_2$)IPP[38] with GGPPS and VenA resulted in a slightly upfield shifted

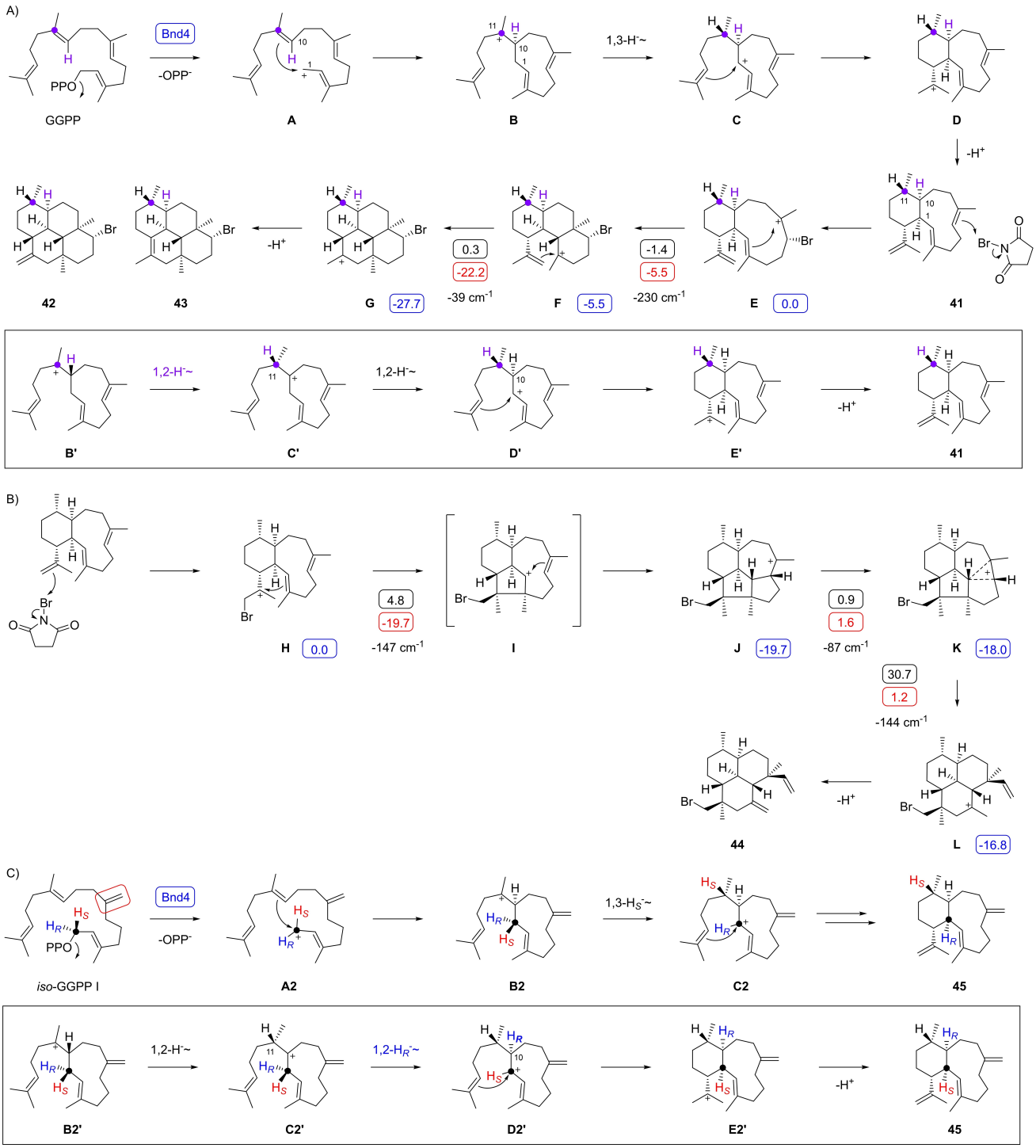

Scheme 4. The diterpene synthase Bnd4 from *S. iakyrus*. A) Cyclisation mechanism for the cyclisation of GGPP to benditerpe-2,6,15-triene (**41**) with a 1,3-hydride shift and formation of bromination products **42** and **43** with NBS. Box: Hypothetical sequence with two 1,2-hydride shifts that is disfavoured by labelling experiments. B) Formation of bromination product **44**. Blue boxes indicate computed relative energies to **E** or **H** (set to 0.0 kcal/mol), black boxes indicate reaction barriers, and red boxes show Gibbs free energies (computed with the mPW1PW91/6-311 + G(d,p)//B97D3/6-31G(d,p) method at 298 K). Imaginary frequencies of computationally localised transition state structures are given in cm^{-1} for each step. C) Cyclisation mechanism from *iso*-GGPP I to **45**. Box: Hypothetical sequence with two 1,2-hydride shifts. Purple and black dots indicate ^{13}C-labelled carbons.

singlet for C11 of **46** ($\Delta\delta = -0.12$ ppm), indicating deuterium in a neighbouring position and thus pointing into the same direction (Figure S41).

The conversion of *iso*-GGPP I with VenA also yielded one major diterpene hydrocarbon (Figure S42) that was isolated and identified as venezuelaxenene (**47**) (Table S8, Figures S43–50). In this case the skeleton of **47** is very different to that of **46**,

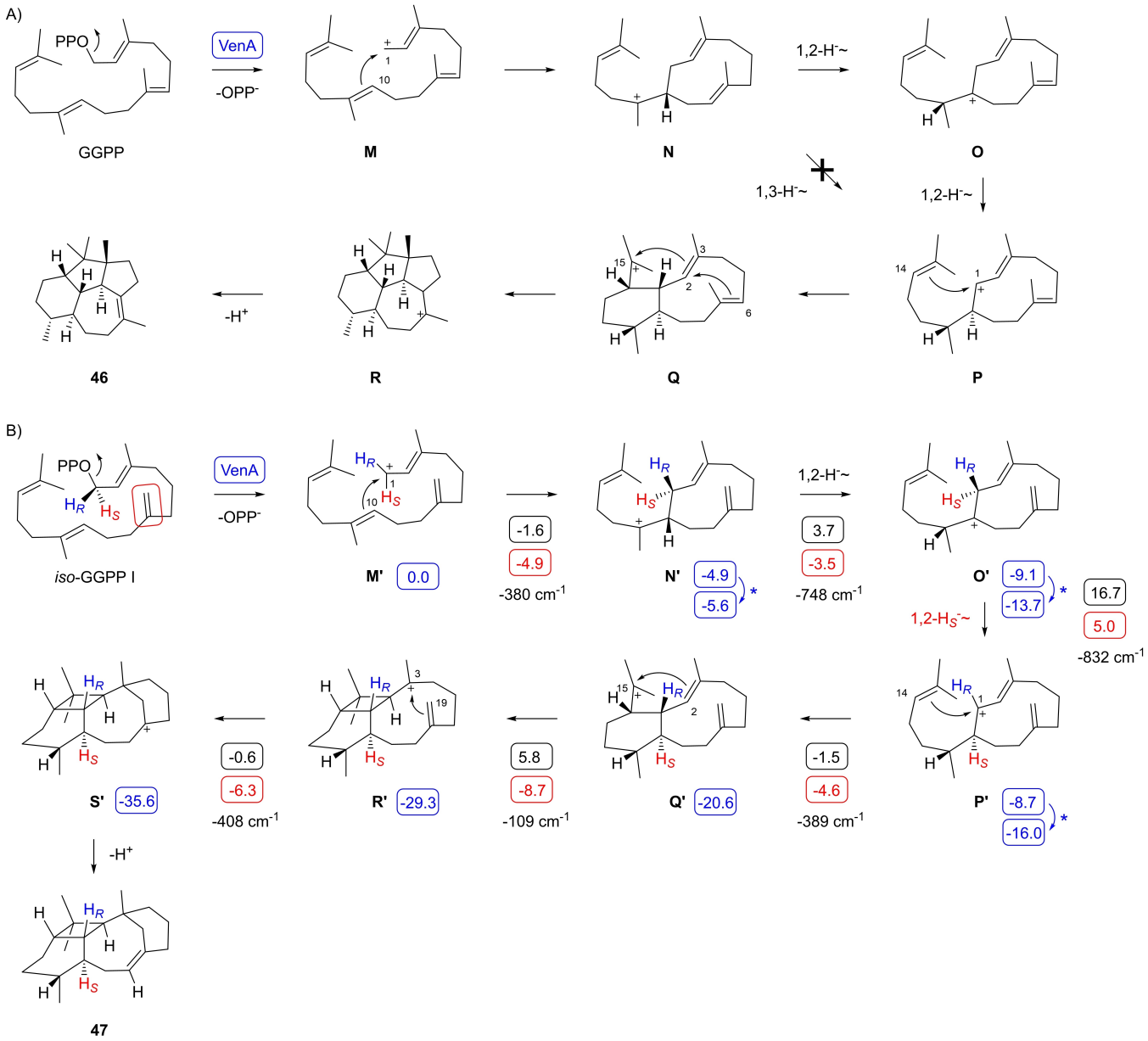

Scheme 5. The diterpene synthase VenA from *S. exfoliatus.* A) Cyclisation mechanism from GGPP to **46**. Cyclisation mechanism from *iso*-GGPP I to **47**. Blue boxes indicate computed relative energies to **M′** (set to 0.0 kcal/mol), black boxes indicate reaction barriers, and red boxes show Gibbs free energies (computed with the mPW1PW91/6-311 + G(d,p)//B97D3/6-31G(d,p) method at 298 K). Imaginary frequencies of computationally localised transition state structures are given in cm^{-1} for each step.

which is a result of the C7 = C19 double bond in *iso*-GGPP I that participates in the cyclisation reaction. After substrate ionisation to **M′** a 1,10-cyclisation to **N′** and two sequential 1,2-hydride shifts lead via **O′** to **P′** (Scheme 5B). A subsequent 1,14-cyclisation to **Q′** and another 2,15-cyclisation result in **R′** in which C19 is close enough to the cationic centre to initiate a 3,19-cyclisation to **S′**. A terminal deprotonation results in **47**. While the initial steps towards **P′** are the same as those towards **P** in the biosynthesis of **46** (Scheme 5A), the late stage transformations deviate and yield the unusual skeleton of **47**.

For **47** the same sequence of two 1,2-hydride shifts as experimentally verified for **46** can be assumed. To investigate the stereochemical course of this process, (*R*)- and (*S*)-(1-^{13}C,1-^{2}H)*iso*-GGPP I were incubated with VenA. The observed upfield shifted singlet peak for C1 with the substrate (*S*)-(1-^{13}C,1-^{2}H)*iso*-GGPP I ($\Delta\delta = -0.10$ ppm) illustrated the hydride migration of the 1-*pro-S* hydrogen into the neighbouring position C10, while the upfield shifted triplet obtained from (*R*)-(1-^{13}C,1-^{2}H)*iso*-GGPP I ($\Delta\delta = -0.54$ ppm, $^{1}J_{C,D} = 20.1$ Hz) demonstrated retainment of the 1-*pro-R* hydrogen at C1 (Figure S51).

The cyclisation mechanims of *iso*-GGPP I to **47** was also investigated computationally (Scheme 5B, Table S9, Figure S52). After a smooth cyclisation from **M′** to **N′** the DFT calculations in particular confirmed the sequence of two 1,2-hydride shifts to **P′**, while a single 1,3-hydride transfer could not be realised. The second 1,2-hydride shift proceeds with migration of the 1-*pro-S*

hydrogen and is with an activation barrier of 16.7 kcal/mol the rate limiting step. All subsequent cyclisation steps towards **S'** exhibit low activation barriers or are even barrierless, and the whole cascade is with $\Delta G = -35.6$ kcal/mol strongly exergonic.

The substrate analog *iso*-GGPP IV was efficiently converted by three of the tested enzymes (Table S1). The 18-hydroxydolabella-3,7-diene synthase from *Chitinophaga pinensis* (HdS)[43] converted *iso*-GGPP IV into one main product (Figure S53). Isolation and NMR-based structure elucidation revealed the structure of a macrocyclic diterpene hydrocarbon (**48**) (Table S10, Figures S54–S61). Because of the structural similarity to cembrene A with two shifted double bonds this compound was named diisocembrene A (Scheme 6A). Its formation requires substrate ionisation to **T**, cyclisation to **U** and deprotonation. Also the variediene synthase from *Aspergillus brasiliensis* (AbVS) and the dolasta-1(15),8-diene synthase from *C. gloeosporioides* (CgDS)[30] converted *iso*-GGPP IV into one major diterpene hydrocarbon (Figure S62). Compound isolation and structure elucidation by NMR spectroscopy (Table S11, Figures S63–S70) revealed the structure of prenylisopseudogermacrene B (**49**). Its formation proceeds through ionisation of *iso*-GGPP IV to **V**, followed by a 1,18-cyclisation to **W** and deprotonation (Scheme 6B). Compound **49** is an isomer with a shifted double bond of prenylpseudogermacrene B (**50**) that was previously obtained from *iso*-GGPP II[28] using the spiroalbatene synthase from *A. albata*[27] (Scheme 6C).

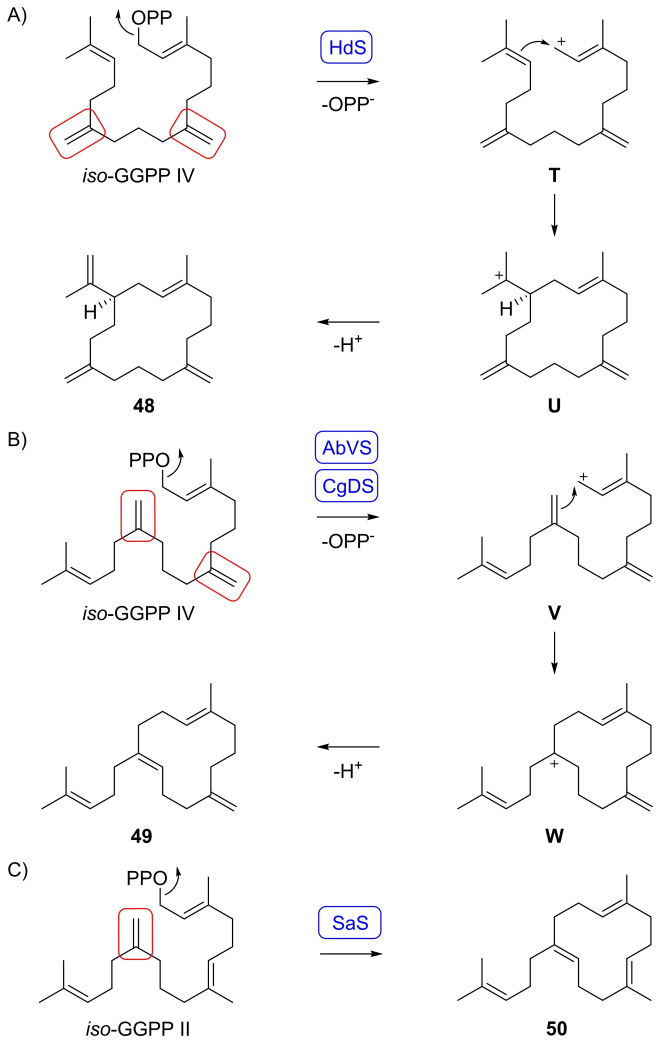

Scheme 6. Cyclisation mechanisms from *iso*-GGPP IV to A) **48** by HdS and to B) **49** by AbVS and CgDS, and C) of *iso*-GGPP II to **50** by SaS.

The substrate analog *iso*-GGPP VI, enzymatically prepared in situ from *iso*-FPP III and IPP with GGPPS, was accepted by many different diterpene synthases, in some cases with conversion into one major product, but in other cases complex product mixtures were obtained (Scheme 7, Table S1, Figures S71–S73). In total, seven different products were isolated from enzymatic reactions in which the compounds were formed as major products. The structures of all seven isolated compounds were determined by NMR spectroscopy (Tables S12–S18, Figures S74–S129). Isopentenylpseudogermacrene A (**51**) was isolated from an incubation of *iso*-FPP III and IPP with GGPPS and spinodiene synthase from *Saccharopolyspora spinosa* (SoS).[44] The same compound is also formed by the phomopsene/allokutznere synthase from *A. albata* (PmS),[39] the catenul-14-en-6-ol synthase from *Catenulispora acidiphila* (CaCS),[17] and (in traces) by CgDS (Scheme 7, Figure S71).

This compound is formed from *iso*-GGPP VI by substrate ionisation to **X**, 1,18-cyclisation to **Y** and deprotonation. Its regioisomer isopentenylpseudogermacrene B (**52**) is produced by all investigated enzymes but SoS, albeit in different quantities, and arises from **Y** by alternative deprotonation. This compound was isolated from the cattleyene synthase from *Streptomyces cattleya* (CyS)[45] that converts *iso*-GGPP VI into **52** almost as a single product. Isopentenylpseudogermacrene C (**53**) also arises from **Y** and is a stereoisomer of **52**. This compound is only formed by CyS, PmS and the spiroviolene synthase from *Streptomyces violens*.[34] SvS is the best producing enzyme of **53** and thus this enzyme was used for a preparative scale incubation for its isolation. Two more compounds coeluted in the GC/MS analysis, but were separable by column chromatography and identified as the regioisomers α-spirocattleyaxenene (**54**), isolated as a minor product from CyS, and β-spirocattleyaxenene (**55**) that was isolated from PmS in which larger amounts are produced. Their formation can be explained through a second cyclisation from **Y** to **Z** and deprotonation. Compounds **54** and **55** show similar mass spectra and coelute in the GC/MS analysis, so that it is impossible to decide based on GC/MS data which of these compounds is formed by which enzyme. Therefore, isotopic labelling experiments were performed, introducing a ^{13}C label at C1 with the substrate combination of *iso*-FPP III and (1-^{13}C)IPP, that were converted with GGPPS and the different diterpene synthases producing **54** and/or **55**. ^{13}C-NMR analysis of the product mixture allowed to distinguish the production of these compounds by each enzyme (Figure S130). Mixtures of **54** and **55** are formed by almost all investigated enzymes, albeit in different proportions, with the exceptions of SoS and cyclooctat-9-en-7-ol synthase from *S. iakyrus* (*Si*CotB2),[46] a recently reported homolog of CotB2 from *Streptomyces melanosporofaciens* (*Sm*CotB2).[47] Instead, *Si*CotB2 produced two other interesting compounds, namely isobucketwheelene (**56**) and iakyroxenene (**57**). Their

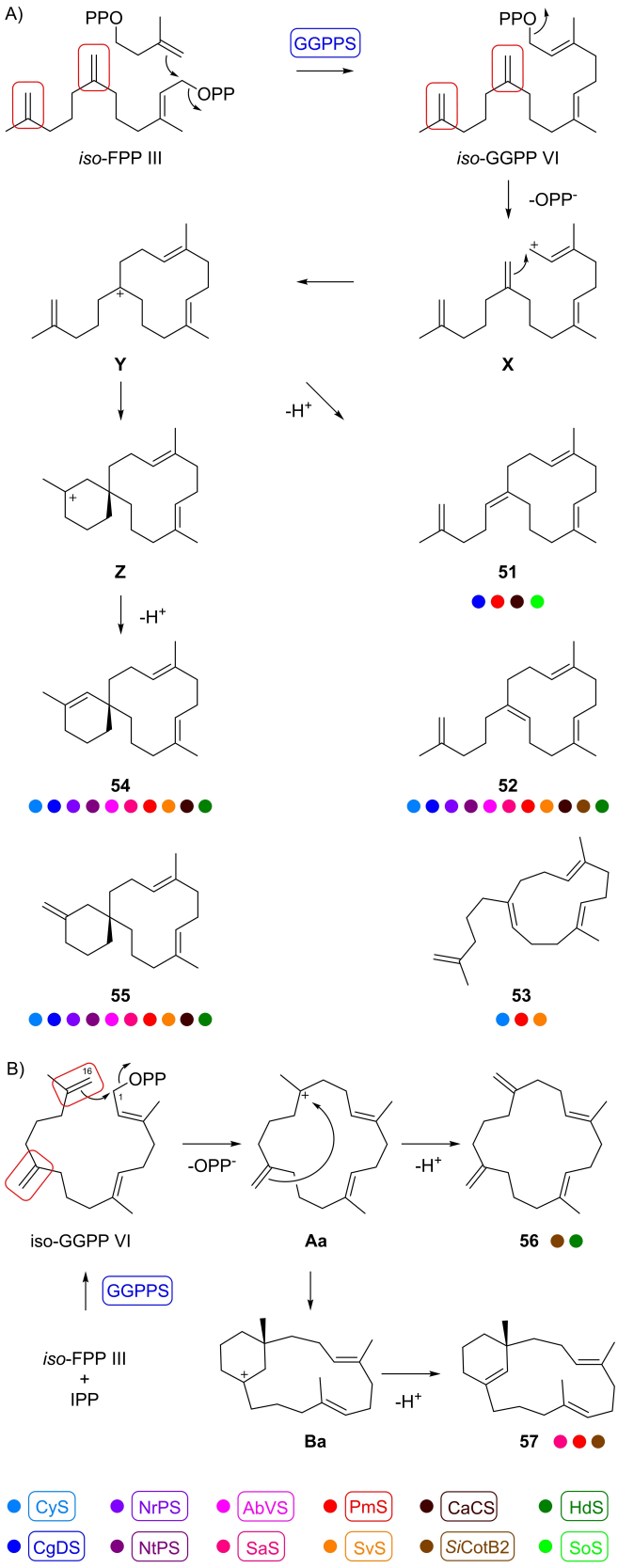

Scheme 7. A) Cyclisation mechanism from *iso*-GGPP VI to **51**–**55** by various diterpene synthases. B) Cyclisation mechanism from *iso*-GGPP VI to **56** and **57** by *Si*CotB2. Coulored dots indicate compound production by enzymes according to the colour code at the bottom of the scheme.

biosynthesis can be explained by a 1,16-cyclisation to **Aa** and deprotonation (to **56**), while another 15,18-cyclisation from **Aa** to **Ba** and deprotonation result in **57**. Compound **56** is a double bond isomer of the previously reported bucketwheelene;[31] both compounds were named because of their molecular shape that is reminiscent of a bucket wheel. The absolute configurations of **55** and **57** was determined through stereoselective deuteration experiments using *iso*-FPP III and (*R*)- or (*S*)-(1-^{13}C,1-^{2}H)IPP[48] with GGPPS and PmS or *Si*CotB2, respectively (Figures S131 and S132).

Conclusions

After our previous reports on the biosynthesis of diterpene analogs from different GGPP isomers with shifted double bonds, we now report the synthesis of four more GGPP isomers named *iso*-GGPP IV–VII. While *iso*-GGPP V and VII were not accepted by any of the tested diterpene synthases, the analogs *iso*-GGPP IV and VI can serve as efficient substrates in several cases. This often leads to the formation of compounds with complex skeletons that are as a consequence of the changed reactivity in the substrate analogs different to naturally observed skeletons. Two newly investigated enzymes, Bnd4 from *S. iakyrus* and VenA from *S. exfoliates*, that are homologs of previously reported enzymes exhibiting the same function,[35,41] were converted with *iso*-GGPP I to benditerpe-2,7(19),15-triene (**45**) and venezuelaxenene (**47**), and their biosynthesis was investigated through isotopic labelling experiments, showing an early stage 1,3-hydride shift for **45**, but two sequential 1,2-hydride shifts for **47**, respectively. The same findings were made for the natural products of these enzymes obtained from GGPP, i.e. benditerpe-2,6,15-triene (**41**) and venezuelaene A (**46**). Due to severe line broadening in the NMR spectra of **41** interpretation of the results from the labelling experiments for this compound required NBS derivatization to obtain compounds with rigidified skeleton.

The observation that minor structural changes in terpenoid substrates can result in previously unknown skeletons using the enzymatic approach in this study is of high interest, because this method outcompetes total synthesis approaches for the rapid structural diversification of terpene skeletons. Future work on oxidative and other modifications of the obtained diterpene hydrocarbons will be of interest to gain access to potentially bioactive compounds.

Experimental Section

General methods. Chemicals were purchased from Sigma Aldrich Chemie GmbH (Steinheim, Germany), Carbolution Chemicals GmbH (St. Ingbert, Germany), or Carl Roth (Karlsruhe, Germany) and used without purification. Solvents for column chromatography were purchased in p.a. grade and purified by distillation. Thin-layer chromatography (TLC) was performed with 0.2 mm precoated plastic sheets Polygram Sil G/UV254 purchased from Machery-Nagel (Düren, Germany). Column chromatography was performed using silica gel 60 purchased from Merck (Darmstadt, Germany).

GC/MS. GC/MS analyses were performed on a 5977 A GC/MSD system (Agilent, Santa Clara, CA, USA) with a 7890B GC and a 5977 A mass selective detector. The GC was equipped with a HP5-MS fused silica capillary column (30 m, 0.25 mm i. d., 0.50 μm film). Specific GC settings were 1) inlet pressure: 77.1 kPa, He at 23.3 mL min^{-1}, 2) injection volume: 1 μL, 3) temperature program: 5 min at 50 °C increasing at 10 °C min^{-1} to 320 °C, 4) 60 s valve time, and 5) carrier gas: He at 1.2 mL min^{-1}. MS settings were 1) source: 230 °C, 2) transfer line: 250 °C, 3) quadrupole: 150 °C and 4) electron energy: 70 eV. Retention indices (*I*) were determined from retention times in comparison to the retention times of *n*-alkanes (C_7-C_{40}).

HRMS. High resolution mass spectra were recorded on an Orbitrap XL instrument (APCI; Thermo Fisher Scientific, Waltham, MA, USA) or using a 7890B/7200 series gas chromatography/accurate mass Q-ToF detector system (Agilent). The GC was equipped with a HP5-MS fused silica capillary column (30 m, 0.25 mm i. d., 0.50 μm film). GC settings were 1) injection volume: 1 μL, 2) temperature program: 5 min at 50 °C, increasing 10 °C min^{-1} to 320 °C, 3) split ratio: 5:1, 60 s valve time and 4) carrier gas flow: He at 1 mL min^{-1}. MS settings were 1) inlet pressure: 83.2 kPa, He flow at 24.6 mL min^{-1}, 2) transfer line temperature: 250 °C, 3) ionization energy: 70 eV.

HPLC. Analytical scale HPLC seperation was carried out using a EUROPA HPLC system (Knauer, Berlin, Germany), equipped with UV/Vis-DAD detector (190–900 nm) and a KNAUER Eurospher II 100–3 C18 column (3.0 μm, 2.0 mm ×100 mm). The UV-Vis absorption was monitored at 190–600 nm. Preparative scale HPLC purification was performed on an Azura series HPLC system (Knauer, Berlin, Germany) with a multi wavelength detector MWL 2.1 L (190 – 700 nm) using a Macherey-Nagel Nucleodur 100–5 Gravity C18 column (5 μm, 10 x 250 mm).

NMR spectroscopy. NMR spectra were recorded on a Bruker (Billerica, MA, USA) Avance I (300 MHz), Avance I (400 MHz), Avance I (500 MHz), Avance III HD Prodigy (500 MHz) or an Avance III HD Cryo (700 MHz) NMR spectrometer. Spectra were measured in C_6D_6 and referenced against solvent signals (^{1}H-NMR, residual proton signal: δ = 7.16 ppm; ^{13}C-NMR: δ = 128.06 ppm).[49]

IR spectroscopy. IR spectra were recorded on a Bruker α infrared spectrometer with a diamond ATR probehead. Peak intensities are given as s (strong), m (medium), w (weak) and br (broad).

Optical rotations. Optical rotations were recorded on a Modular Compact Polarimeter MCP 100 (Anton Paar, Graz, Austria). The temperature setting was 25 °C, the wavelength of the light used was 589 nm (sodium D line), the path-length was 10 cm, and the compound concentrations *c* are given in g 100 mL^{-1}.

General procedure for synthesis of allyl bromides. To a cooled (0 °C) solution of alcohol (1.00 eq) in Et_2O (3 mL $mmol^{-1}$) PBr_3 (0.40 eq) was added dropwise. The mixture was stirred for 1 h at 0 °C and was transferred directly to an ice/water mixture. The aqueous layer was extracted with Et_2O three times and the organic layers were dried with $MgSO_4$, concentrated under reduced pressure and the bromides were directly used for subsequent reactions without purification.

General procedure for nucleophilic substitution with the dianion of isopentenol. To a solution of *n*Buli (1.6 M in hexane, 2.00 eq) in hexane (0.75 mL $mmol^{-1}$, −15 °C) was added TMEDA (2.00 eq) and the mixture was stirred for 0.5 h at −23 °C. The mixture was warmed to room temperature and isopentenol (**8**, 1.00 eq) was added dropwise. After 6 h stirring, HMPA (3 mL) and a solution of the corresponding allyl bromide or alkyl iodides (1.00 eq) in Et_2O was added at −78 °C, and the mixture was allowed to warm to room temperature overnight. The reaction was quenched by the addition of 1 M HCl and extracted with Et_2O three times. The combined organic layers were dried with $MgSO_4$, evaporated under reduced pressure and subjected to column chromatography (petroleum ether/Et_2O, 3:1) to yield the desired alcohols.

7-Methyl-3-methyleneoct-6-en-1-ol (**9**).[50] Prepared from prenyl bromide (**7**). Yield: 7.28 g (47 mmol, 68 %) TLC (pentane:Et_2O = 2:1): R_f = 0.35. GC (HP-5): *I* = 1219. ^{1}H-NMR (C_6D_6, 500 MHz): δ = 5.15 (thept, *J* = 6.9, *J* = 1.4, 1H), 4.83 (m, 1H), 4.77 (m, 1H), 3.48 (m, 2H), 2.10 (m, 4H), 1.97 (m, 2H), 1.65 (d, *J* = 1.2, 3H), 1.52 (br s, 3H) ppm. ^{13}C-NMR (C_6D_6, 125 MHz): δ = 146.48 (C_q), 131.54 (C_q), 124.57 (CH), 111.45 (CH_2), 60.78 (CH_2), 39.74 (CH_2), 36.36 (CH_2), 26.80 (CH_2), 25.82 (CH_3), 17.74 (CH_3) ppm.

11-Methyl-3,7-dimethylenedodec-10-en-1-ol (**11**). Prepared from the iodide **10**. Yield: 586 mg (2.64 mmol, 53 %) TLC (pentane:Et_2O = 2:1): R_f = 0.30. GC (HP-5): *I* = 1690. ^{1}H-NMR (C_6D_6, 500 MHz): δ = 5.23 (ddq, 1H, *J* = 8.4, 5.5, 1.4 Hz), 4.88 (dhept, 1H, *J* = 2.1, 0.8 Hz), 4.85 (m, 1H), 4.81 (m, 1H), 4.76 (m, 1H), 3.47 (td, 2H, *J* = 6.6, 5.4 Hz), 2.19 (m, 2H), 2.07 (m, 4H), 1.98 (m, 2H), 1.90 (m, 2H), 1.67 (m, 3H), 1.56 (d, 3H, *J* = 1.4 Hz), 1.53 (m, 2H) ppm. ^{13}C-NMR (C_6D_6, 125 MHz): δ = 149.39 (C_q), 146.56 (C_q), 131.43 (C_q), 124.77 (CH), 111.43 (CH_2), 109.60 (CH_2), 60.77 (CH_2), 39.62 (CH_2), 36.47 (CH_2), 36.10 (CH_2), 35.95 (CH_2), 26.95 (CH_2), 26.17 (CH_2), 25.85 (CH_3), 17.75 (CH_3) ppm. IR (diamond ATR): $\tilde{\nu}$ = 3345 (br), 3073 (m), 2966 (s), 2903 (m), 1738 (m), 1644 (m), 1440 (m), 1375 (m), 1216 (w), 1045 (m), 888 (s), 820 (w) cm^{-1}. HR-MS (Q-TOF, 70 eV): calc. $[C_{15}H_{26}O]^{+\bullet}$ *m/z* = 222.1979, found: *m/z* = 222.1982.

(*E*)-7,11-Dimethyl-3-methylenedodeca-6,11-dien-1-ol (**19**). Prepared from the bromide corresponding to **18**. Yield: 1.04 g (4.68 mmol, 37 %) TLC (pentane:Et_2O = 1:1): R_f = 0.52. GC (HP-5): *I* = 1691. ^{1}H-NMR (C_6D_6, 500 MHz): δ = 5.19 (ddq, 1H, *J* = 8.4, 7.0, 1.3 Hz), 4.81 (m, 4H), 3.48 (td, 2H, *J* = 6.6, 3.7 Hz), 2.12 (m, 4H), 1.98 (m, 6H), 1.66 (m, 3H), 1.54 (m, 3H) ppm. ^{13}C-NMR (C_6D_6, 125 MHz): δ = 146.46 (C_q), 145.82 (C_q), 135.38 (C_q), 124.53 (CH), 111.50 (CH_2), 110.40 (CH_2), 60.78 (CH_2), 39.72 (CH_2), 39.61 (CH_2), 37.68 (CH_2), 36.38 (CH_2), 26.66 (CH_2), 26.30 (CH_2), 22.52 (CH_3), 16.02 (CH_3) ppm. IR (diamond ATR): $\tilde{\nu}$ = 3345 (br), 3073 (m), 2966 (m), 2933 (s), 2861 (m), 1738 (m), 1646 (m), 1442 (m), 1373 (m), 1216 (w), 1044 (m), 886 (s), 821 (w) cm^{-1}. HR-MS (Q-TOF, 70 eV): calc. $[C_{15}H_{26}O]^{+\bullet}$ *m/z* = 222.1979, found: *m/z* = 222.1977.

7-Methyl-3-methyleneoct-7-en-1-ol (**26**). Prepared from isopentenyl iodide. Yield: 4.64 g (30.1 mmol, 60 %) TLC (pentane:Et_2O = 2:1): R_f = 0.26. GC (HP-5): *I* = 1239. ^{1}H-NMR (C_6D_6, 500 MHz): δ = 4.80 (dt, 2H, *J* = 2.1, 1.1 Hz), 4.77 (ddt, 2H, *J* = 9.0, 2.0, 1.1 Hz), 3.47 (t, 2H, *J* = 6.6 Hz), 2.07 (td, 2H, *J* = 6.6, 1.4 Hz), 1.89 (m, 2H), 1.62 (m, 3H), 1.47 (m, 2H) ppm. ^{13}C-NMR (C_6D_6, 125 MHz): δ = 146.54 (C_q), 145.57 (C_q), 111.40 (CH_2), 110.50 (CH_2), 60.78 (CH_2), 39.61 (CH_2), 37.65 (CH_2), 35.82 (CH_2), 25.95 (CH_2), 22.42 (CH_3) ppm. IR (diamond ATR): $\tilde{\nu}$ = 3346 (br), 3073 (w), 2934 (s), 2884 (m), 1646 (m), 1443 m), 1373 (w), 1045 (s), 885 (s) cm^{-1}. HR-MS (Q-TOF, 70 eV): calc. $[C_{10}H_{18}O]^{+\bullet}$ *m/z* = 154.1353, found: *m/z* = 154.1350.

11-Methyl-3,7-dimethylenedodec-11-en-1-ol (**34**). Prepared from the iodide **27**. Yield: 3.49 g (15.7 mmol, 52 %) TLC (pentane:Et_2O = 1:1): R_f = 0.51. GC (HP-5): *I* = 1677. ^{1}H-NMR (C_6D_6, 500 MHz): δ = 4.84 (m, 2H), 4.81 (m, 3H), 4.77 (m, 1H), 3.48 (t, 2H, *J* = 5.8 Hz), 2.09 (t, 2H, *J* = 6.6 Hz), 1.96 (m, 6H), 1.90 (m, 2H), 1.64 (d, 3H, *J* = 1.2 Hz), 1.55 (m, 4H) ppm. ^{13}C-NMR (C_6D_6, 125 MHz): δ = 149.43 (C_q), 146.57 (C_q), 145.65 (C_q), 111.42 (CH_2), 110.50 (CH_2), 109.61 (CH_2), 60.79 (CH_2), 39.62 (CH_2), 37.76 (CH_2), 35.95 (CH_2), 35.92 (CH_2), 26.16 (CH_2), 26.10 (CH_2), 22.46 (CH_3) ppm. IR (diamond ATR): $\tilde{\nu}$ = 3335 (br), 3073 (m), 2934 (m), 1646 (m), 1442 (w), 1373 (w), 1044 (m), 885 (s) cm^{-1}. HR-MS (Q-TOF, 70 eV): calc. $[C_{15}H_{26}O]^{+\bullet}$ *m/z* = 222.1979, found: *m/z* = 222.1980.

Synthesis of *iso*-GGPP IV

Synthesis of 8-iodo-2-methyl-6-methyleneoct-2-ene (10).[20] A solution of imidazole (2.61 g, 38.4 mmol, 1.20 eq) and PPh_3 (10.08 g, 38.4 mmol, 1.20 eq) in CH_2Cl_2 (90 mL) was mixed with I_2 (9.77 g, 38.4 mmol, 1.20 eq) and the corresponding alcohol **9** (4.97 g, 32 mmol, 1.00 eq) subsequently. After stirring for 4 h at room temperature, the reaction mixture was quenched by the addition of sat. aqueous NH_4Cl and then extracted with Et_2O (150 mL) three times. The combined organic layers were dried with $MgSO_4$ and concentrated under reduced pressure. The residue was taken up in petroleum ether, the precipitate was filtered off, and the petroleum ether was removed in vacuum. The product was purified by column chromatography (petroleum ether) to yield the iodide **10** (5.98 g, 23 mmol, 71%) as a pink oil. 5.98 g (23 mmol, 71%) TLC (pentane: Et_2O = pentane): R_f = 0.50. GC (HP-5): I = 1401. ^{1}H-NMR (C_6D_6, 500 MHz): δ = 5.09 (thept, J = 7.0, J = 1.4, 1H), 4.78 (m, 1H), 4.62 (m, 1H), 2.82 (t, J = 7.4, 2H), 2.29 (t, J = 7.4, 2H), 2.00 (m, 2H), 1.83 (m, 2H), 1.65 (d, J = 1.2, 3H), 1.49 (br s, 3H) ppm. ^{13}C-NMR (C_6D_6, 125 MHz): δ = 147.88 (C_q), 131.63 (C_q), 124.35 (CH), 111.34 (CH_2), 40.66 (CH_2), 35.59 (CH_2), 26.58 (CH_2), 25.81 (CH_3), 17.73 (CH_3), 3.28 (CH_2) ppm.

Synthesis of 12-iodo-2-methyl-6,10-dimethylenedodec-2-ene (12). A solution of imidazole (0.88 g, 13.0 mmol, 1.20 eq) and PPh_3 (3.41 g, 13.0 mmol, 1.20 eq) in CH_2Cl_2 (30 mL) was mixed with I_2 (3.31 g, 13.0 mmol, 1.20 eq) and the corresponding alcohol **11** (2.40 g, 10.8 mmol, 1.00 eq) subsequently. After stirring for 4 h at room temperature, the reaction mixture was quenched by the addition of sat. aqueous NH_4Cl and then extracted with Et_2O (150 mL) three times. The combined organic layers were dried with $MgSO_4$ and concentrated under reduced pressure. The residue was taken up in petroleum ether, the precipitate was filtered off, and the petroleum ether was removed in vacuum. The product was purified by column chromatography (petroleum ether) to yield the iodide **12** (2.20 g, 6.6 mmol, 61%) as a pink oil. 2.20 g (6.6 mmol, 61%) TLC (pentane): R_f = 0.54. GC (HP-5): I = 1880. ^{1}H-NMR (C_6D_6, 500 MHz): δ = 5.22 (tp, 1H, J = 7.0, 1.5 Hz), 4.86 (qt, 2H, J = 1.5, 0.7 Hz), 4.82 (qt, 2H, J = 1.5, 0.7 Hz), 4.77 (qt, 2H, J = 1.4, 0.7 Hz), 4.62 (tp, 2H, J = 1.4, 0.6 Hz), 2.82 (t, 3H, J = 7.4 Hz), 2.28 (m, 4H), 2.18 (m, 2H), 2.05 (m, 2H), 1.92 (m, 2H), 1.76 (m, 2H), 1.67 (m, 3H), 1.56 (m, 3H), 1.43 (m, 2H) ppm. ^{13}C-NMR (C_6D_6, 125 MHz): δ = 149.23 (C_q), 147.91 (C_q), 131.48 (C_q), 124.73 (CH), 111.32 (CH_2), 109.67 (CH_2), 40.53 (CH_2), 36.45 (CH_2), 35.99 (CH_2), 35.17 (CH_2), 26.94 (CH_2), 25.93 (CH_2), 25.86 (CH_3), 17.78 (CH_3), 3.28 (CH_2) ppm. IR (diamond ATR): $\tilde{\nu}$ = 3406 (w), 3076 (m), 2966 (s), 2856 (m), 1737 (m), 1671 (m), 1441 (m), 1376 (w), 1232 (w), 1169 (m), 1105 (w), 1043 (w), 889 (s), 820 (w) cm^{-1}. HR-MS (Q-TOF, 70 eV): calc. $[C_{15}H_{25}I]^{+\bullet}$ m/z = 332.0996, found: m/z = 332.0995.

Synthesis of ethyl 2-acetyl-13-methyl-5,9-dimethylenetetradec-12-enoate (13). To a cooled solution of ethyl acetoacetate (1.71 g, 13.2 mmol, 2.00 eq) in THF (30 mL) was added NaH (0.53 g, 13.2 mmol, 2.00 eq, 60% in mineral oil) in small portions. The reaction mixture was allowed to warm to room temperature and stirred for 1 h. The corresponding iodide **12** (2.20 g, 6.6 mmol, 1.00 eq) was added dropwise and the reaction mixture was refluxed overnight, followed by cooling to room temperature. The cooled mixture was quenched by the addition of sat. aqueous NH_4Cl solution and then extracted with Et_2O (50 mL) three times. The combined organic layers were dried with $MgSO_4$ and concentrated under reduced pressure. The residue was subjected to column chromatography (petroleum ether/EtoAc, 10:1) to yield **13** (1.64 g, 4.9 mmol, 75%) as a colourless oil. TLC (pentane:Et_2O = 8:1): R_f = 0.70. GC (HP-5): I = 2219. ^{1}H-NMR (C_6D_6, 500 MHz): δ = 5.23 (tdq, 1H, J = 7.0, 2.7, 1.4 Hz), 4.87 (m, 2H), 4.81 (m, 2H), 3.89 (qd, 2H, J = 7.2, 1.9 Hz), 3.28 (ddd, 1H, J = 7.8, 4.7, 1.8 Hz), 2.19 (m, 2H), 2.02 (m, 12H), 1.87 (s, 3H), 1.67 (m, 3H), 1.56 (m, 3H), 0.88 (t, 3H, J = 7.2 Hz) ppm. ^{13}C-NMR (C_6D_6, 125 MHz): δ = 201.42 (C_q), 169.69 (C_q), 149.40 (C_q), 148.50 (C_q), 131.40 (C_q), 124.80 (CH), 110.50 (CH_2), 109.61 (CH_2), 61.05 (CH_2), 59.26 (CH), 36.48 (CH_2), 36.10 (CH_2), 35.68 (CH_2), 33.97 (CH_2), 28.55 (CH_3), 26.95 (CH_2), 26.15 (CH_2), 25.85 (CH_3), 17.76 (CH_3), 14.04 (CH_3) ppm. IR (diamond ATR): $\tilde{\nu}$ = 3074 (w), 2977 (m), 2932 (m), 2858 (m), 1740 (s), 1716 (s), 1644 (m), 1444 (m), 1358 (m), 1241 (m), 1215 (m), 1177 (m), 1147 (w), 1096 (w), 1023 (w), 887 (m) cm^{-1}. HR-MS (Q-TOF, 70 eV): calc. $[C_{21}H_{34}O_3]^{+\bullet}$ m/z = 334.2503, found: m/z = 334.2500.

Synthesis of 14-methyl-6,10-dimethylenepentadec-13-en-2-one (14). To a solution of β-keto ester **13** (2.70 g, 8.0 mol, 1.00 eq) in EtOH (40 mL) was added an aqueous solution of KOH (1.34 g dissolved in 8 mL of water, 24 mmol, 3.00 eq) and the reaction mixture was stirred under reflux for 3 h before cooling to room temperature. The reaction mixture was slowly acidified with 2 M HCl solution until CO_2 developed. The resulting mixture was extracted with Et_2O (100 mL) three times. The combined layers were dried with $MgSO_4$ and concentrated under reduced pressure. The residue was subject to column chromatography (petroleum ether/EtOAc, 15:1) to yield the desired methyl ketone **14** (2.05 g, 7.8 mmol, 98%) as a colourless oil. TLC (pentane:Et_2O = 8:1): R_f = 0.40. GC (HP-5): I = 1917. ^{1}H-NMR (C_6D_6, 500 MHz): δ = 5.23 (tdp, 1H, J = 7.0, 2.9, 1.4 Hz), 4.88 (ddt, 2H, J = 4.3, 2.1, 1.3 Hz), 4.80 (m, 2H), 2.20 (m, 2H), 2.10 (m, 2H), 1.95 (m, 10H), 1.67 (m, 3H), 1.64 (m, 3H), 1.60 (m, 2H), 1.56 (m, 3H) ppm. ^{13}C-NMR (C_6D_6, 125 MHz): δ = 205.99 (C_q), 149.47 (C_q), 149.13 (C_q), 131.40 (C_q), 124.80 (CH), 109.89 (CH_2), 109.59 (CH_2), 42.64 (CH_2), 36.50 (CH_2), 36.17 (CH_2), 35.82 (CH_2), 35.61 (CH_2), 29.40 (CH_3), 26.97 (CH_2), 26.24 (CH_2), 25.85 (CH_3), 21.95 (CH_2), 17.76 (CH_3) ppm. IR (diamond ATR): $\tilde{\nu}$ = 3072 (w), 2930 (s), 2858 (m), 1717 (s), 1644 (m), 1441 (m), 1364 (m), 1158 (w), 888 (s) cm^{-1}. HR-MS (Q-TOF, 70 eV): calc. $[C_{18}H_{30}O]^{+\bullet}$ m/z = 262.2292, found: m/z = 262.2292.

Synthesis of ethyl (*E*)-3,15-dimethyl-7,11-dimethylenehexadeca-2,14-dienoate (15). A solution of diisopropylamine (828 mg, 8.2 mmol, 1.05 eq) dissolved in dry THF (30 mL) was cooled to 0 °C. *n*Buli (5.1 mL, 8.2 mmol, 1.6 M in hexane, 1.05 eq) was added dropwise and the reaction mixture was stirred for 1 h at 0 °C. The reaction was cooled to −78 °C and triethyl phosphonaacetate (1.78 g, 7.8 mmol, 1.00 eq) was added. After stirring the reaction mixture for 1 h at −78 °C the methyl ketone **14** (2.05 g, 7.8 mmol, 1.00 eq) was added. The reaction mixture was allowed to warm to room temperature and stirred overnight. Water (15 mL) was added to quench the reaction. The aqueous phase was extracted with Et_2O (80 mL, 3 times), and the combined layers were dried with $MgSO_4$ and concentrated under reduced pressure. Purification by column chromatography (petroleum ether/EtOAc, 15:1) yielded pure (*E*)-**15** and (*Z*)-**15** as colourless oils.

(*E*)-**15**. Yield: 1.12 g (3.4 mmol, 44%). TLC (pentane:Et_2O = 10:1): R_f = 0.59. GC (HP-5): I = 2324. ^{1}H-NMR (C_6D_6, 500 MHz): δ = 5.82 (h, 1H, J = 1.3 Hz), 5.24 (tdp, J = 7.0, 4.3, 1.4 Hz), 4.88 (m, 2H), 4.79 (m, 2H), 4.06 (q, 2H, J = 7.2 Hz), 2.20 (m, 5H), 2.09 (m, 2H), 2.02 (m, 2H), 1.94 (m, 2H), 1.84 (m, 2H), 1.67 (m, 3H), 1.59 (m, 2H), 1.56 (m, 3H), 1.41 (m, 2H), 1.02 (t, 3H, J = 7.1 Hz) ppm. ^{13}C-NMR (C_6D_6, 125 MHz): δ = 166.47 (C_q), 159.53 (C_q), 149.43 (C_q), 148.98 (C_q), 131.44 (C_q), 124.76 (CH), 116.38 (CH), 109.82 (CH_2), 109.62 (CH_2), 59.41 (CH_2), 40.52 (CH_2), 36.51 (CH_2), 36.16 (CH_2), 35.91 (CH_2), 35.71 (CH_2), 26.96 (CH_2), 26.23 (CH_2), 25.85 (CH_3), 25.68 (CH_2), 18.73 (CH_3), 17.76 (CH_3), 14.46 (CH_3) ppm. IR (diamond ATR): $\tilde{\nu}$ = 3074 (w), 3046 (w), 2978 (m), 2932 (w), 1715 (s), 1645 (s), 1442 (m), 1377 (w), 1321 (w), 1270 (s), 1220 (s), 1141 (s), 1096 (w), 1074 (w), 1040 (m), 886 (s), 819 (w) cm^{-1}. HR-MS (Q-TOF, 70 eV): calc. $[C_{22}H_{36}O_2]^{+\bullet}$ m/z = 332.2712, found: m/z = 332.2712.

(*Z*)-**15**. Yield: 370 mg (1.1 mmol, 14%). TLC (pentane:Et_2O = 10:1): R_f = 0.64. GC (HP-5): I = 2261. ^{1}H-NMR (C_6D_6, 500 MHz): δ = 5.75 (dt, 1H, J = 1.4, 0.7 Hz), 5.23 (ddq, 1H, J = 8.4, 5.6, 1.5 Hz), 4.87 (m, 4H),

4.03 (q, 2H, J = 7.2 Hz), 2.72 (m, 2H), 2.19 (m, 3H), 2.10 (m, 4H), 2.03 (m, 3H), 1.67 (m, 3H), 1.62 (m, 4H), 1.56 (m, 3H), 1.53 (d, 3H, J = 1.4 Hz), 1.01 (t, 3H, J = 7.1 Hz) ppm. ^{13}C-NMR (C_6D_6, 125 MHz): δ = 166.02 (C_q), 160.05 (C_q), 149.52 (C_q), 149.46 (C_q), 131.33 (C_q), 124.85 (CH), 116.93 (CH), 109.60 (CH_2), 109.55 (CH_2), 59.38 (CH_2), 36.51 (CH_2), 36.49 (CH_2), 36.21 (CH_2), 36.04 (CH_2), 33.40 (CH_2), 26.97 (CH_2), 26.81 (CH_2), 26.28 (CH_2), 25.85 (CH_2), 24.89 (CH_2), 17.76 (CH_2), 14.43 (CH_2) ppm. IR (diamond ATR): $\tilde{\nu}$ = 3074 (w), 3045 (w), 2978 (m), 2932 (w), 1714 (s), 1643 (s), 1442 (m), 1377 (w), 1322 (w), 1270 (s), 1220 (s), 1141 (s), 1096 (w), 1074 (w), 1040 (m), 886 (s), 821 (w) cm^{-1}. HR-MS (Q-TOF, 70 eV): calc. $[C_{22}H_{36}O_2]^{+\bullet}$ m/z = 332.2712, found: m/z = 332.2715.

Synthesis of (*E*)-3,15-dimethyl-7,11-dimethylenehexadeca-2,14-dien-1-ol (16). To a cooled (0 °C) solution of the ester (*E*)-**15** (1.0 g, 3.1 mmol, 1.00 eq) in THF (15 mL) was added DIBAL–H (7.4 mL, 7.4 mmol, 1.0 M in hexane, 2.40 eq) and the reaction mixture was stirred for 1 h at room temperature. The mixture was cooled to 0 °C and a saturated solution of Na–K-tartrate (15 mL) was added. The resulting slurry was stirred for 2 h to dissolve the precipitate and the aqueous phase was extracted with Et_2O (50 mL, 3 times). The organic layers were dried with $MgSO_4$ and concentrated under reduced pressure. The residue was purified by column chromatography (petroleum ether/Et_2O, 3:1) to yield the alcohol **16** (836 mg, 2.9 mmol, 94%) as a colourless oil. TLC (pentane:Et_2O = 2:1): R_f = 0.35. GC (HP-5): I = 2193. ^{1}H-NMR (C_6D_6, 500 MHz): δ = 5.39 (tp, 1H, J = 6.7, 1.3 Hz), 5.23 (ddq, 1H, J = 8.4, 5.5, 1.4 Hz), 4.87 (m, 4H), 3.97 (d, 2H, J = 6.7 Hz), 2.20 (m, 2H), 2.09 (m, 2H), 1.98 (m, 8H), 1.67 (d, 3H, J = 1.4 Hz), 1.62 (m, 2H), 1.56 (d, 3H, J = 1.2 Hz), 1.52 (m, 2H), 1.46 (s, 3H) ppm. ^{13}C-NMR (C_6D_6, 125 MHz): δ = 149.52 (C_q), 149.49 (C_q), 138.15 (C_q), 131.42 (C_q), 125.04 (CH), 124.79 (CH), 109.59 (2x CH_2), 59.37 (CH_2), 39.46 (CH_2), 36.51 (CH_2), 36.21 (CH_2), 36.09 (CH_2), 35.96 (CH_2), 26.97 (CH_2), 26.32 (CH_2), 26.20 (CH_2), 25.85 (CH_3), 17.76 (CH_3), 16.10 (CH_3) ppm. IR (diamond ATR): $\tilde{\nu}$ = 3316 (br), 3072 (m), 2966 (s), 2859 (m), 1644 (m), 1441 (m), 1371 (w), 1217 (w), 1102 (w), 1001 (m), 887 (s), 822 (w) cm^{-1}. HR-MS (Q-TOF, 70 eV): calc. $[C_{20}H_{34}O]^{+\bullet}$ m/z = 290.2604, found: m/z = 290.2600.

Synthesis of (*E*)-3,15-dimethyl-7,11-dimethylenehexadeca-2,14-dien-1-yl diphosphate (17). To a solution of tris(tetra-n-butylammonium)hydrogen diphosphate (1.64 g, 1.82 mmol, 1.30 eq) in acetonitrile (5 mL) a solution of the allyl bromide (made from 1.00 eq of alcohol **16** followed by general procedure) was added. The mixture was stirred at room temperature overnight. Acetonitrile was removed under reduced pressure. The residue was dissolved in aqueous NH_4HCO_3 solution (1.0 mL, 0.25 M) and loaded onto a DOWEX 50WX8 ion-exchange column (NH_4^+ form, pH 7.0). The column was flushed slowly with 1.5 volumes of NH_4HCO_3 buffer (25 mM, 5% iPrOH) and the eluate was lyophilized to yield the diphosphate **17** as a colourless hygroscopic powder (1.0 g, 2.0 mmol, 100%). ^{1}H-NMR (D_2O, 500 MHz): δ = 5.42 (m, 1H), 5.10 (m, 1H), 4.72 (m, 4H), 4.48 (m, 2H), 2.04 (m, 12H), 1.70 (m, 3H), 1.65 (m, 4H), 1.59 (m, 3H), 1.38 (m, 5H) ppm. ^{13}C-NMR (D_2O, 125 MHz): δ = 149.36 (C_q), 149.01 (C_q), 140.93 (C_q), 131.05 (C_q), 124.27 (CH), 120.89 (d, CH, $^3J_{C,P}$ = 7.6 Hz), 109.02 (CH_2), 108.89 (CH_2), 62.47 (d, CH_2, $^2J_{C,P}$ = 4.1 Hz), 39.31 (CH_2), 36.10 (CH_2), 35.82 (CH_2), 35.78 (2x CH_2), 26.48 (CH_2), 25.90 (CH_2), 25.78 (CH_2), 25.49 (CH_3), 17.45 (CH_3), 15.90 (CH_3) ppm. ^{31}P-NMR (D_2O, 203 MHz): δ = –8.60 (d, $^2J_{P,P}$ = 16.7 Hz), –10.63 (d, $^2J_{P,P}$ = 18.1 Hz) ppm. HR-MS (APCI): calc. for $[C_{20}H_{35}O_7P_2]^-$ m/z = 449.1863; found: m/z = 449.1868.

Synthesis of *iso*-GGPP V

Synthesis of (*E*)-12-iodo-2,6-dimethyl-10-methylenedodeca-1,6-diene (20). A solution of imidazole (1.27 g, 18.6 mmol, 1.20 eq) and PPh_3 (4.89 g, 18.6 mmol, 1.20 eq) in CH_2Cl_2 (45 mL) was mixed with I_2 (4.71 g, 18.6 mmol, 1.20 eq) and the corresponding alcohol **19** (3.45 g, 15.5 mmol, 1.00 eq) subsequently. After stirring for 4 h at room temperature, the reaction mixture was quenched by the addition of sat. aqueous NH_4Cl and then extracted with Et_2O (100 mL) three times. The combined organic layers were dried with $MgSO_4$ and concentrated under reduced pressure. The residue was taken up in petroleum ether, the precipitate was filtered off, and the petroleum ether was removed under reduced pressure. The product was purified by column chromatography (petroleum ether) to yield the iodide **20** (3.1 g, 9.3 mmol, 60%) as a pink oil. TLC (pentane): R_f = 0.60. GC (HP-5): I = 1884. ^{1}H-NMR (C_6D_6, 500 MHz): δ = 5.13 (tq, 1H, J = 6.9, 1.3 Hz), 4.83 (dt, 2H, J = 2.1, 1.0 Hz), 4.79 (m, 1H), 4.63 (m, 1H), 2.83 (t, 2H, J = 7.6 Hz), 2.30 (td, 2H, J = 7.7, 1.4 Hz), 2.03 (m, 2H), 1.96 (m, 4H), 1.85 (m, 2H), 1.66 (t, 3H, J = 1.3 Hz), 1.55 (m, 2H), 1.51 (d, 3H, J = 1.4 Hz) ppm. ^{13}C-NMR (C_6D_6, 125 MHz): δ = 147.88 (C_q), 145.78 (C_q), 135.49 (C_q), 124.31 (CH), 111.39 (CH_2), 110.43 (CH_2), 40.64 (CH_2), 39.60 (CH_2), 37.69 (CH_2), 35.62 (CH_2), 26.47 (CH_2), 26.30 (CH_2), 22.53 (CH_3), 16.02 (CH_3), 3.02 (CH_2) ppm. IR (diamond ATR): $\tilde{\nu}$ = 3404 (w), 3075 (m), 2965 (s), 2856 (m), 1737 (m), 1670 (m), 1441 (m), 1376 (w), 1232 (w), 1169 (m), 1110 (w), 1043 (w), 886 (s), 820 (w) cm^{-1}. HR-MS (Q-TOF, 70 eV): calc. $[C_{15}H_{25}I]^{+\bullet}$ m/z = 332.0996, found: m/z = 332.0991.

Synthesis of ethyl (*E*)-2-acetyl-9,13-dimethyl-5-methylenetetradeca-8,13-dienoate (21). To a cooled solution of ethyl acetoacetate (2.43 g, 18.7 mmol, 2.00 eq) in THF (35 mL) was added NaH (0.45 g, 18.7 mmol, 2.00 eq, 60% in mineral oil) in small portions. The reaction mixture was allowed to warm to room temperature and stirred for 1 h. The corresponding iodide **20** (3.1 g, 9.3 mmol, 1.00 eq) was added dropwise and the reaction mixture was stirred under reflux overnight, followed by cooling to room temperature. The cooled mixture was quenched by the addition of sat. aqueous NH_4Cl solution and then extracted with Et_2O (100 mL) three times. The combined organic layers were dried with $MgSO_4$ and concentrated under reduced pressure. The residue was subjected to column chromatography (petroleum ether/EtoAc, 10:1) to yield **21** (2.30 g, 6.9 mmol, 74%) as a colourless oil. TLC (pentane:Et_2O = 5:1): R_f = 0.45. GC (HP-5): I = 2223. ^{1}H-NMR (C_6D_6, 500 MHz): δ = 5.21 (tq, 1H, J = 7.0, 1.3 Hz), 4.83 (m, 4H), 3.89 (qd, 2H, J = 7.1, 1.6 Hz), 3.28 (m, 1H), 2.16 (m, 2H), 2.02 (m, 12H), 1.87 (s, 3H), 1.66 (s, 3H), 1.56 (m, 3H), 0.88 (t, 3H, J = 7.1 Hz) ppm. ^{13}C-NMR (C_6D_6, 125 MHz): δ = 201.43 (C_q), 169.69 (C_q), 148.40 (C_q), 145.83 (C_q), 135.38 (C_q), 124.54 (CH), 110.57 (CH_2), 110.39 (CH_2), 61.04 (CH_2), 59.26 (CH), 39.63 (CH_2), 37.70 (CH_2), 36.12 (CH_2), 34.06 (CH_2), 28.55 (CH_3), 26.64 (CH_2), 26.55 (CH_2), 26.31 (CH_2), 22.52 (CH_3), 16.03 (CH_3), 14.03 (CH_3) ppm. IR (diamond ATR): $\tilde{\nu}$ = 3072 (w), 2968 (m), 2933 (s), 2859 (m), 1738 (m), 1646 (m), 1434 (m), 1373 (m), 1229 (m), 1216 (m), 1169 (w), 887 (s) cm^{-1}. HR-MS (Q-TOF, 70 eV): $[C_{21}H_{34}O_3]^{+\bullet}$ m/z = 334.2503, found: m/z = 334.2500.

Synthesis of (*E*)-10,14-dimethyl-6-methylenepentadeca-9,14-dien-2-one (22). To a solution of β-keto ester **21** (2.30 g, 6.9 mol, 1.00 eq) in EtOH (20 mL) was added an aqueous solution of KOH (1.16 g dissolved in 5 mL of water, 20.7 mmol, 3.00 eq) and the reaction mixture was stirred under reflux for 3 h before cooling to room temperature. The reaction mixture was slowly acidified with 2 M HCl solution until CO_2 developed. The resulting mixture was extracted with Et_2O (100 mL) three times. The combined organic layers were dried with $MgSO_4$ and concentrated under reduced pressure. The residue was subjected to column chromatography (petroleum ether/EtOAc, 13:1) to yield the desired methyl ketone **22** (1.73 g, 6.6 mmol, 96%) as a colourless oil. TLC (pentane:Et_2O = 8:1): R_f = 0.45. GC (HP-5): I = 1913. ^{1}H-NMR (C_6D_6, 500 MHz): δ = 5.25 (ddq, 1H, J = 8.4, 7.0, 1.4 Hz), 4.82 (m, 4H), 2.19 (m, 2H), 2.06 (m, 2H), 1.94 (m, 8H), 1.65 (m, 8H), 1.58 (m, 3H), 1.55 (m, 2H) ppm. ^{13}C-NMR (C_6D_6, 125 MHz): δ = 205.98 (C_q), 149.04 (C_q), 145.83 (C_q), 135.29 (C_q), 124.68 (CH), 110.39 (CH_2), 109.94 (CH_2), 42.65 (CH_2), 39.64 (CH_2), 37.70 (CH_2), 36.26 (CH_2), 35.72 (CH_2), 29.40 (CH_3), 26.74 (CH_2), 26.33

(CH_2), 22.52 (CH_3), 21.96 (CH_2), 16.04 (CH_3) ppm. IR (diamond ATR): $\tilde{\nu}$ = 3073 (w), 2934 (s), 2856 (m), 1716 (s), 1644 (m), 1442 (m), 1364 (m), 1158 (w), 884 (s) cm^{-1}. HR-MS (Q-TOF, 70 eV): calc. $[C_{18}H_{30}O]^{+\bullet}$ m/z = 262.2292, found: m/z = 262.2296.

Synthesis of ethyl (2*E*,10*E*)-3,11,15-trimethyl-7-methylenehexadeca-2,10,15-trienoate (23). NaH (406 mg, 10.2 mmol, 2.00 eq, 60% in mineral oil) suspended in dry THF (25 mL) was cooled to 0 °C. Triethyl phosphonoacetate (2.50 g, 11.1 mmol, 2.20 eq) was added. After stirring the reaction mixture for 1 h at 0 °C, the reaction mixture was cooled to −78 °C and the methyl ketone **22** (1.33 g, 5.3 mmol, 1.00 eq) was added. The reaction mixture was allowed to warm to room temperature and stirred overnight. Water (10 mL) was added to quench the reaction. The aqueous phase was extracted with Et_2O (100 mL, 3 times), and the combined layers were dried with $MgSO_4$ and concentrated under reduced pressure. Purification by column chromatography (petroleum ether/EtOAc, 15 : 1) yielded pure (*E*)-**23** and (*Z*)-**23** as colourless oils.

(*E*)-**23**. Yield: 740 mg (2.3 mmol, 43%). TLC (pentane:Et_2O = 8 : 1): R_f = 0.65. GC (HP-5): I = 2314. ^{1}H-NMR (C_6D_6, 500 MHz): δ = 5.82 (q, 1H, J = 1.3 Hz), 5.24 (qd, 1H, J = 5.6, 1.4 Hz), 4.81 (m, 4H), 4.06 (q, 2H, J = 7.1 Hz), 2.20 (d, 3H, J = 1.2 Hz), 2.17 (m, 2H), 2.00 (m, 6H), 1.85 (m, 4H), 1.66 (t, 3H, J = 1.2 Hz), 1.57 (m, 5H), 1.42 (m, 2H), 1.02 (t, 3H, J = 7.1 Hz) ppm. ^{13}C-NMR (C_6D_6, 125 MHz): δ = 166.28 (C_q), 159.35 (C_q), 148.71 (C_q), 145.61 (C_q), 135.12 (C_q), 124.46 (CH), 116.18 (CH), 110.22 (CH_2), 109.65 (CH_2), 59.21 (CH_2), 40.34 (CH_2), 39.44 (CH_2), 37.50 (CH_2), 36.16 (CH_2), 35.61 (CH_2), 26.54 (CH_2), 26.13 (CH_2), 25.49 (CH_2), 22.32 (CH_3), 18.54 (CH_3), 15.84 (CH_3), 14.27 (CH_3) ppm. IR (diamond ATR): $\tilde{\nu}$ = 3074 (w), 2978 (m), 2933 (s), 2861 (m), 1716 (s), 1647 (s), 1443 (m), 1381 (m), 1348 (w), 1271 (w), 1220 (s), 1142 (s), 1096 (w), 1072 (m), 1039 (m), 885 (s) cm^{-1}. HR-MS (Q-TOF, 70 eV): calc. $[C_{22}H_{36}O_2]^{+\bullet}$ m/z = 332.2711, found: m/z = 332.2714.

(*Z*)-**23**. Yield: 151 mg (0.45 mmol, 8%). TLC (pentane:Et_2O = 8 : 1): R_f = 0.70. GC (HP-5): I = 2257. ^{1}H-NMR (C_6D_6, 500 MHz): δ = 5.75 (m, 1H), 5.26 (m, 1H), 4.83 (m, 4H), 4.03 (q, 1H, J = 7.2 Hz), 2.73 (m, 2H), 2.22 (m, 2H), 2.12 (m, 4H), 1.98 (m, 4H), 1.65 (s, 3H), 1.58 (s, 3H), 1.55 (m, 2H), 1.53 (m, 3H), 1.01 (t, 3H, J = 7.1 Hz) ppm. ^{13}C-NMR (C_6D_6, 125 MHz): δ = 166.02 (C_q), 159.99 (C_q), 149.40 (C_q), 145.86 (C_q), 135.15 (C_q), 124.87 (CH), 116.96 (CH), 110.36 (CH_2), 109.63 (CH_2), 59.37 (CH_2), 39.66 (CH_2), 37.72 (CH_2), 36.59 (CH_2), 36.49 (CH_2), 33.42 (CH_2), 26.85 (CH_2), 26.80 (CH_2), 26.36 (CH_2), 24.87 (CH_3), 22.51 (CH_3), 16.03 (CH_3), 14.43 (CH_3) ppm. IR (diamond ATR): $\tilde{\nu}$ = 3076 (w), 2978 (m), 2932 (s), 2860 (m), 1714 (s), 1644 (s), 1444 (m), 1381 (m), 1348 (m), 1271 (w), 1221 (s), 1142 (s), 1096 (w), 1072 (m), 1039 (m), 886 (s) cm^{-1}. HR-MS (Q-TOF, 70 eV): calc. $[C_{22}H_{36}O_2]^{+\bullet}$ m/z = 332.2711, found: m/z = 332.2719.

Synthesis of (2*E*,10*E*)-3,11,15-trimethyl-7-methylenehexadeca-2,10,15-trien-1-ol (24). To a cooled (0 °C) solution of the ester (*E*)-**23** (740 mg, 2.2 mmol, 1.00 eq) in THF (10 mL) was added DIBAL–H (5.3 mL, 5.3 mmol, 1.0 M in hexane, 2.40 eq) and the reaction mixture was stirred for 1 h at room temperature. The mixture was cooled to 0 °C and a saturated solution of Na–K-tartrate (10 mL) was added. The resulting slurry was stirred for 2 h to dissolve the precipitate and the aqueous phase was extracted with Et_2O (50 mL, 3 times). The organic layers were dried with $MgSO_4$ and concentrated under reduced pressure. The residue was purified by column chromatography (petroleum ether/Et_2O, 3 : 1) to yield the alcohol **24** (530 mg, 1.8 mmol, 82%) as a colourless oil. TLC (pentane:Et_2O = 2 : 1): R_f = 0.30. ^{1}H-NMR (C_6D_6, 500 MHz): δ = 5.38 (tq, 1H, J = 6.7, 1.4 Hz), 5.27 (tq, 1H, J = 7.0, 1.3 Hz), 4.88 (m, 2H), 4.82 (m, 2H), 3.97 (dq, 2H, J = 6.7, 0.8 Hz), 2.22 (m, 2H), 2.10 (m, 2H), 1.99 (m, 6H), 1.91 (m, 2H), 1.66 (m, 3H), 1.58 (m, 3H), 1.54 (m, 4H), 1.45 (m, 3H) ppm. ^{13}C-NMR (C_6D_6, 125 MHz): δ = 149.43 (C_q), 145.83 (C_q), 138.17 (C_q), 135.26 (C_q), 125.01 (CH), 124.74 (CH), 110.40 (CH_2), 109.61 (CH_2), 59.37 (CH_2), 39.65 (CH_2), 39.47 (CH_2), 37.69 (CH_2), 36.52 (CH_2), 36.07 (CH_2), 26.81 (CH_2), 26.32 (CH_2), 26.21 (CH_2), 22.52 (CH_3), 16.10 (CH_3), 16.04 (CH_3) ppm. IR (diamond ATR): $\tilde{\nu}$ = 3357 (br), 3073 (w), 2965 (m), 2933 (s), 2860 (m), 1727 (w), 1667 (w), 1646 (m), 1441 (m), 1375 (w), 1302 (w), 1097 (w), 1000 (m), 886 (s) cm^{-1}. HR-MS (Q-TOF, 70 eV): calc. $[C_{20}H_{34}O]^{+\bullet}$ m/z = 290.2605, found: m/z = 290.2604.

Synthesis of (2*E*,10*E*)-3,11,15-trimethyl-7-methylenehexadeca-2,10,15-trien-1-yl diphosphate (25). To a solution of tris(tetra-n-butylammonium)hydrogen diphosphate (1.67 g, 1.86 mmol, 1.20 eq) in acetonitrile (6 mL) a solution of the allyl bromide (made from 1.00 eq of alcohol **24** followed by the above mentioned general procedure) was added and the mixture was stirred at room temperature overnight. Acetonitrile was removed under reduced pressure. The residue was dissolved in aqueous NH_4HCO_3 solution (1.0 mL, 0.25 M) and loaded onto a DOWEX 50WX8 ion-exchange column (NH_4^+ form, pH 7.0). The column was flushed slowly with 1.5 volumes of NH_4HCO_3 buffer (25 mM, 5% iPrOH) and the eluate was lyophilized to yield the diphosphate **25** as a colourless hygroscopic powder (1.1 g, 2.0 mmol, 100%). ^{1}H-NMR (C_6D_6, 500 MHz): δ = 5.36 (q, 1H, J = 7.5 Hz), 5.06 (m, 1H), 4.64 (m, 4H), 4.41 (m, 2H), 1.96 (m, 12H), 1.64 (m, 3H), 1.61 (s, 3H), 1.52 (m, 4H), 1.34 (m, 3H) ppm. ^{13}C-NMR (C_6D_6, 125 MHz): δ = 149.55 (C_q), 145.42 (C_q), 140.44 (C_q), 134.73 (C_q), 124.56 (CH), 121.45 (CH, $^3J_{P,C}$ = 7.5 Hz), 110.05 (CH_2), 108.98 (CH_2), 62.41 (CH_2, $^2J_{P,C}$ = 3.8 Hz), 39.39 (CH_2), 39.26 (CH_2), 37.30 (CH_2), 36.30 (CH_2), 35.89 (CH_2), 26.39 (CH_2), 26.01 (CH_2), 25.90 (CH_2), 22.24 (CH_3), 15.96 (CH_3), 15.76 (CH_3) ppm. ^{31}P-NMR (D_2O, 203 MHz): δ = −8.49 (d, $^2J_{P,P}$ = 19.1 Hz), −10.78 (d, $^2J_{P,P}$ = 19.8 Hz) ppm. HR-MS (APCI): calc. for $[C_{20}H_{35}O_7P_2]^-$ m/z = 449.1863; found: m/z = 449.1860.

Synthesis of *iso*-FPP III

Synthesis of 8-iodo-2-methyl-6-methyleneoct-1-ene (27). A solution of imidazole (5.47 g, 80.4 mmol, 1.20 eq) and PPh_3 (21.1 g, 80.4 mmol, 1.20 eq) in CH_2Cl_2 (150 mL) was mixed with I_2 (20.3 g, 80.4 mmol, 1.20 eq) and the corresponding alcohol **26** (10.39 g, 67.0 mmol, 1.00 eq) subsequently. After stirring for 2 h at room temperature, the reaction mixture was quenched by the addition of sat. aqueous NH_4Cl and then extracted with Et_2O (200 mL) three times. The combined organic layers were dried with $MgSO_4$ and concentrated under reduced pressure. The residue was taken up in petroleum ether, the precipitate was filtered off, and the petroleum ether was removed under reduced pressure. The product was purified by column chromatography (petroleum ether) to yield the iodide **27** (17.2 g, 65.2 mmol, 97%) as a pink oil. TLC (pentane): R_f = 0.52. GC (HP-5): I = 1422. ^{1}H-NMR (C_6D_6, 500 MHz): δ = 4.77 (m, 2H), 4.68 (m, 2H), 2.82 (t, 2H, J = 7.6 Hz), 2.26 (td, 2H, J = 7.7, 1.4 Hz), 1.85 (td, 2H, J = 7.6, 1.4 Hz), 1.73 (m, 2H), 1.60 (m, 3H), 1.37 (m, 2H) ppm. ^{13}C-NMR (C_6D_6, 125 MHz): δ = 147.89 (C_q), 145.41 (C_q), 111.31 (CH_2), 110.58 (CH_2), 40.52 (CH_2), 37.54 (CH_2), 35.05 (CH_2), 25.72 (CH_2), 22.41 (CH_3), 3.28 (CH_2) ppm. IR (diamond ATR): $\tilde{\nu}$ = 3073 (w), 2966 (m), 2934 (s), 2862 (m), 1647 (m), 1443 (m), 1373 (w), 1350 (w), 1232 (w), 1169 (m), 887 (s) cm^{-1}. HR-MS (Q-TOF, 70 eV): calc. $[C_{10}H_{17}I]^{+\bullet}$ m/z = 264.0371, found: m/z = 264.0365.

Synthesis of ethyl 2-acetyl-9-methyl-5-methylenedec-9-enoate (28). To a cooled solution of ethyl acetoacetate (5.21 g, 40.0 mmol, 2.00 eq) in THF (40 mL) was added NaH (1.60 g, 40.0 mmol, 2.00 eq, 60% in mineral oil) in small portions. The reaction mixture was allowed to reaction room temperature and stirred for 1 h. The corresponding iodide **27** (5.28 g, 20.0 mmol, 1.00 eq) was added dropwise and the reaction mixture was refluxed overnight, followed by cooling to room temperature. The cooled mixture was quenched by the addition of sat. aqueous NH_4Cl solution and then extracted with Et_2O (150 mL) three times. The combined organic layers were dried with $MgSO_4$ and concentrated under reduced pressure. The residue was subjected to column chromatography (petroleum

ether/EtoAc, 10:1) to yield **28** (3.10 g, 11.7 mmol, 60%) as a colourless oil. TLC (pentane:Et_2O = 8:1): R_f = 0.39. GC (HP-5): I = 1798. ^{1}H-NMR (C_6D_6, 500 MHz): δ = 4.80 (m, 4H), 3.89 (qd, 2H, J = 7.1, 1.9 Hz), 3.28 (m, 1H), 2.03 (m, 4H), 1.92 (dd, 4H, J = 9.1, 5.6 Hz), 1.87 (s, 3H), 1.63 (s, 3H), 1.52 (m, 2H) 0.88 (t, 3H, J = 7.1 Hz) ppm. ^{13}C-NMR (C_6D_6, 125 MHz): δ = 201.42 (C_q), 169.69 (C_q), 148.47 (C_q), 145.57 (C_q), 110.52 (CH_2), 110.48 (CH_2), 61.05 (CH_2), 59.25 (CH), 37.66 (CH_2), 35.56 (CH_2), 33.94 (CH_2), 28.55 (CH_3), 26.52 (CH_2), 25.93 (CH_2), 22.44 (CH_3), 14.03 (CH_3) ppm. IR (diamond ATR): $\tilde{\nu}$ = 3073 (w), 2970 (m), 2937 (m), 2877 (w), 1741 (s), 1716 (s), 1646 (w), 1446 (m), 1367 (m), 1242 (m), 1215 (m), 1148 (m), 1095 (w), 1041 (w), 888 (m) cm^{-1}. HR-MS (Q-TOF, 70 eV): calc. $[C_{16}H_{26}O_3]^{+\bullet}$ m/z = 266.1877, found: m/z = 266.1880.

Synthesis of 10-methyl-6-methyleneundec-10-en-2-one (29). To a solution of β-keto ester **28** (3.10 g, 11.7 mol, 1.00 eq) in EtOH (40 mL) was added an aqueous solution of KOH (1.96 g dissolved in 10 mL of water, 35.0 mmol, 3.00 eq) and the reaction mixture was stirred under reflux for 3 h before cooling to room temperature. The reaction mixture was slowly acidified with 2 M HCl solution until CO_2 developed. The resulting mixture was extracted with Et_2O (150 mL) three times. The combined layers were dried with $MgSO_4$ and concentrated under reduced pressure. The residue was subjected to column chromatography (petroleum ether/EtOAc, 13:1) to yield the desired methyl ketone **29** (2.74 g, 11.7 mmol, 100%, solvent containing) as a colourless oil. TLC (pentane:Et_2O = 8:1): R_f = 0.30. GC (HP-5): I = 1435. ^{1}H-NMR (C_6D_6, 500 MHz): δ = 4.81 (m, 2H), 4.78 (m, 2H), 1.92 (m, 10H), 1.64 (m, 6H), 1.55 (m, 2H) ppm. ^{13}C-NMR (C_6D_6, 125 MHz): δ = 206.00 (C_q), 149.11 (C_q), 145.65 (C_q), 110.50 (CH_2), 109.87 (CH_2), 42.64 (CH_2), 37.74 (CH_2), 35.69 (CH_2), 35.60 (CH_2) 29.40 (CH_3), 26.02 (CH_2), 22.46 (CH_3), 21.95 (CH_2) ppm. IR (diamond ATR): $\tilde{\nu}$ = 3073 (w), 2935 (m), 1716 (s), 1646 (m), 1413 (m), 1365 (m), 1225 (w), 1158 (w), 865 (s) cm^{-1}. HR-MS (Q-TOF, 70 eV): calc. $[C_{13}H_{22}O]^{+\bullet}$ m/z = 194.1666, found: m/z = 194.1665.

Synthesis of ethyl (*E*)-3,11-dimethyl-7-methylenedodeca-2,11-dienoate (30). A solution of diisopropylamine (1.23 g, 12.2 mmol, 1.05 eq) dissolved in dry THF (40 mL) was cooled to 0 °C. *n*Buli (7.6 mL, 12.2 mmol, 1.6 m in hexane, 1.05 eq) was added dropwise and the reaction mixture was stirred for 1 h at 0 °C. The reaction was cooled to −78 °C and triethyl phosphonoacetate (2.61 g, 11.7 mmol, 1.00 eq) was added. After stirring the reaction mixture for 1 h at −78 °C the methyl ketone **29** (2.74 g, 11.7 mmol, 1.00 eq) was added. The reaction mixture was allowed to warm to room temperature and stirred overnight. Water (25 mL) was added to quench the reaction. The aqueous phase was extracted with Et_2O (150 mL, 3 times), and the combined layers were dried with $MgSO_4$ and concentrated under reduced pressure. Purification by column chromatography (petroleum ether/EtOAc, 15:1) yielded pure (*E*)-**30** and (*Z*)-**30** as colourless oils.

(*E*)-**30**. Yield: 1.75 g (6.6 mmol, 57%) TLC (pentane:Et_2O = 8:1): R_f = 0.68. GC (HP-5): I = 1850. ^{1}H-NMR (C_6D_6, 500 MHz): δ = 5.82 (h, 1H, J = 1.3 Hz), 4.79 (m, 4H), 4.06 (q, 2H, J = 7.2 Hz), 2.20 (d, 3H, J = 1.4 Hz), 1.89 (m, 8H), 1.64 (t, 3H, J = 1.2 Hz), 1.53 (m, 2H), 1.40 (m, 2H), 1.02 (t, 3H, J = 7.2 Hz) ppm. ^{13}C-NMR (C_6D_6, 125 MHz): δ = 166.46 (C_q), 159.53 (C_q), 148.95 (C_q), 145.60 (C_q), 116.38 (CH), 110.53 (CH_2), 109.80 (CH_2), 59.42 (CH_2) 40.50 (CH_2), 37.72 (CH_2), 35.78 (CH_2), 35.67 (CH_2), 26.02 (CH_2), 25.66 (CH_2), 22.45 (CH_3), 18.73 (CH_3), 14.46 (CH_3) ppm. IR (diamond ATR): $\tilde{\nu}$ = 3073 (w), 2979 (m), 2937 (m), 2879 (w), 1716 (s), 1648 (m), 1444 (w), 1367 (w), 1322 (w), 1272 (s), 1221 (s), 1040 (w), 886 (m) cm^{-1}. HR-MS (Q-TOF, 70 eV): calc. $[C_{17}H_{28}O_2]^{+\bullet}$ m/z = 264.2084, found: m/z = 264.2090.

(*Z*)-**30**. Yield: 370 mg (1.6 mmol, 14%) TLC (pentane:Et_2O = 8:1): R_f = 0.74. GC (HP-5): I = 1791. ^{1}H-NMR (C_6D_6, 500 MHz): δ = 5.75 (dhept, 1H, J = 1.4, 0.7 Hz), 4.83 (m, 4H), 4.02 (q, J = 7.1 Hz), 2.73 (m, 2H), 2.10 (m, 2H), 1.99 (m, 2H), 1.64 (m, 3H), 1.58 (m, 2H), 1.53 (d, 3H, J = 1.4 Hz), 1.00 (t, 3H, J = 7.1 Hz) ppm. ^{13}C-NMR (C_6D_6, 125 MHz): δ = 166.03 (C_q), 160.06 (C_q), 149.45 (C_q), 145.71 (C_q), 116.93 (CH), 110.45 (CH_2), 109.59 (CH_2), 59.38 (CH_2), 37.79 (CH_2), 36.47 (CH_2), 35.92 (CH_2), 33.39 (CH_2), 26.81 (CH_2), 24.88 (CH_3), 22.46 (CH_3), 14.42 (CH_3) ppm. IR (diamond ATR): $\tilde{\nu}$ = 3073 (w), 2977 (m), 2935 (s), 2865 (m), 1715 (s), 1647 (s), 1444 (m), 1375 (m), 1270 (s), 1227 (s), 1153 (s), 1077 (w), 1057 (w), 1036 (w), 886 (s), 858 (m) cm^{-1}. HR-MS (Q-TOF, 70 eV): calc. $[C_{17}H_{28}O_2]^{+\bullet}$ m/z = 264.2084, found: m/z = 264.2080.

Synthesis of (*E*)-3,11-dimethyl-7-methylenedodeca-2,11-dien-1-ol (31). To a cooled (0 °C) solution of the ester (*E*)-**30** (1.50 g, 5.7 mmol, 1.00 eq) in THF (25 mL) was added DIBAL–H (15.9 mL, 15.9 mmol, 1.0 M in hexane, 2.40 eq) and the reaction mixture was stirred for 1 h at room temperature. The mixture was cooled to 0 °C and a saturated solution of Na–K-tartrate (15 mL) was added. The resulting slurry was stirred for 2 h to dissolve the precipitate and the aqueous phase was extracted with Et_2O (100 mL, 3 times). The organic layers were dried with $MgSO_4$ and concentrated under reduced pressure. The residue was purified by column chromatography (petroleum ether/Et_2O, 3:1) to yield the alcohol **31** (943 mg, 4.2 mmol, 75%) as a colourless oil. TLC (pentane:Et_2O = 2:1): R_f = 0.25. GC (HP-5): I = 1715. ^{1}H-NMR (C_6D_6, 500 MHz): δ = 5.39 (tq, 1H, J = 6.7, 1.4 Hz), 4.83 (m, 4H), 3.98 (d, 2H, J = 6.7 Hz), 1.94 (m, 8H), 1.64 (s, 3H), 1.54 (m, 4H), 1.45 (m, 3H) ppm. ^{13}C-NMR (C_6D_6, 125 MHz): δ = 149.50 (C_q), 145.66 (C_q), 138.15 (C_q), 125.02 (CH), 110.50 (CH_2), 109.57 (CH_2), 59.37 (CH_2), 39.46 (CH_2), 37.77 (CH_2), 35.95 (CH_2), 26.19 (CH_2), 26.10 (CH_2), 22.46 (CH_3), 16.10 (CH_3) ppm. IR (diamond ATR): $\tilde{\nu}$ = 3323 (br), 3073 (w), 2969 (m), 2934 (s), 2863 (m), 1738 (m), 1668 (w), 1646 (m), 1442 (m), 1374 (m), 1230 (w), 1099 (s), 1000 (s), 885 (s) cm^{-1}. HR-MS (Q-TOF, 70 eV): calc. $[C_{15}H_{26}O]^{+\bullet}$ m/z = 222.1979, found: m/z = 222.1970.

Synthesis of (*E*)-3,11-dimethyl-7-methylenedodeca-2,11-dien-1-yl diphosphate (32). To a solution of tris(tetra-n-butylammonium)hydrogen diphosphate (4.50 g, 5.0 mmol, 1.20 eq) in acetonitrile (20 mL) a solution of the allyl bromide (made from 1.00 eq of alcohol **31** following the above mentioned general procedure) was added and the mixture was stirred at room temperature overnight. Acetonitrile was removed under reduced pressure. The residue was dissolved in aqueous NH_4HCO_3 solution (1.0 mL, 0.25 M) and loaded onto a DOWEX 50WX8 ion-exchange column (NH_4^+ form, pH 7.0). The column was flushed slowly with 1.5 volumes of NH_4HCO_3 buffer (25 mM, 5% iPrOH) and the eluate was lyophilized to yield the diphosphate **32** as a colourless hygroscopic powder (1.75 g, 4.0 mmol, 95%). ^{1}H-NMR (C_6D_6, 500 MHz): δ = 5.46 (t, 1H, J = 7.2 Hz), 4.79 (m, 2H, overlapped with the signal of D_2O), 4.74 (m, 2H), 4.47 (t, 2H, J = 6.6 Hz), 2.04 (m, 8H), 1.71 (s, 6H), 1.57 (m, 4H) ppm. ^{13}C-NMR (C_6D_6, 125 MHz): δ = 151.40 (C_q), 147.63 (C_q), 143.00 (C_q), 119.86 (d, CH, $^3J_{C,P}$ = 8.7 Hz), 109.56 (CH_2), 108.69 (CH_2), 62.63 (d, CH_2, $^2J_{C,P}$ = 5.2 Hz), 38.76 (CH_2), 36.98 (CH_2), 35.17 (CH_2), 35.09 (CH_2), 25.39 (CH_2), 25.27 (CH_2), 21.74 (CH_3), 15.65 (CH_3) ppm. ^{31}P-NMR (D_2O, 203 MHz): δ = −7.41 (d, $^2J_{P,P}$ = 21.5 Hz), −10.30 (d, $^2J_{P,P}$ = 21.0 Hz) ppm. HR-MS (APCI): calc. for $[C_{15}H_{27}O_7P_2]^-$ m/z = 381.1237; found: m/z = 381.1238.

Synthesis of *iso*-GGPP VII

Synthesis of 12-iodo-2-methyl-6,10-dimethylenedodec-1-ene (35). A solution of imidazole (1.29 g, 18.9 mmol, 1.20 eq) and PPh_3 (4.96 g, 18.9 mmol, 1.20 eq) in CH_2Cl_2 (45 mL) was mixed with I_2 (4.78 g, 18.9 mmol, 1.20 eq) and the corresponding alcohol **34** (3.49 g, 15.7 mmol, 1.00 eq) subsequently. After stirring for 2 h at room temperature, the reaction mixture was quenched by the addition of sat. aqueous NH_4Cl and then extracted with Et_2O (150 mL) three times. The combined organic layers were dried with $MgSO_4$ and concentrated under reduced pressure. The residue was

taken up in petroleum ether, the precipitate was filtered off, and the petroleum ether was removed under reduced pressure. The product was purified by column chromatography (petroleum ether) to yield the iodide **35** (3.75 g, 11.2 mmol, 71%) as a pink oil. TLC (pentane): $R_f = 0.70$. GC (HP-5): $I = 1871$. ^{1}H-NMR (C_6D_6, 500 MHz): δ = 4.82 (m, 4H), 4.77 (m, 1H), 4.62 (m, 1H), 2.83 (t, 2H, J = 7.6 Hz), 2.28 (td, 2H, J = 7.6, 1.4 Hz), 1.93 (m, 6H), 1.76 (m, 2H), 1.65 (br s, 3H), 1.56 (m, 2H), 1.42 (m, 2H) ppm. ^{13}C-NMR (C_6D_6, 125 MHz): δ = 149.27 (C_q), 147.90 (C_q), 145.61 (C_q), 111.34 (CH_2), 110.55 (CH_2), 109.68 (CH_2), 40.53 (CH_2), 37.75 (CH_2), 35.90 (CH_2), 35.85 (CH_2), 35.18 (CH_2), 26.08 (CH_2), 25.93 (CH_2), 22.48 (CH_3), 3.26 (CH_2) ppm. IR (diamond ATR): $\tilde{\nu}$ = 3070 (w), 2966 (m), 2933 (s), 2855 (m), 1743 (m), 1636 (m), 1454 (m), 1373 (m), 1216 (w), 1140 (w), 880 (s) cm^{-1}. HR-MS (Q-TOF, 70 eV): calc. $[C_{15}H_{25}I]^{+\bullet}$ m/z = 332.0996, found: m/z = 332.0992.

Synthesis of ethyl 2-acetyl-13-methyl-5,9-dimethylenetetradec-13-enoate (36). To a cooled solution of ethyl acetoacetate (2.92 g, 22.4 mmol, 2.00 eq) in THF (40 mL) was added NaH (537 mg, 22.4 mmol, 2.00 eq, 60% in mineral oil) in small portions. The reaction mixture was allowed to warm to room temperature and stirred for 1 h. The corresponding iodide **35** (3.75 g, 11.2 mmol, 1.00 eq) was added dropwise and the reaction mixture was stirred under reflux overnight, followed by cooling to room temperature. The cooled mixture was quenched by the addition of sat. aqueous NH_4Cl solution and then extracted with Et_2O (150 mL) three times. The combined organic layers were dried with $MgSO_4$ and concentrated under reduced pressure. The residue was subjected to column chromatography (petroleum ether/EtoAc, 10:1) to yield **36** (3.55 g, 10.6 mmol, 95%) as a colourless oil. TLC (pentane:Et_2O = 5:1): $R_f = 0.47$. GC (HP-5): $I = 2209$. ^{1}H-NMR (C_6D_6, 500 MHz): δ = 4.82 (m, 6H), 3.89 (qd, 2H, J = 7.1, 1.8 Hz), 3.28 (ddd, 1H, J = 7.8, 4.6, 1.9 Hz), 1.99 (m, 12H), 1.88 (s, 3H), 1.65 (m, 3H), 1.57 (m, 4H), 0.88 (t, 3H, J = 7.2 Hz) ppm. ^{13}C-NMR (C_6D_6, 125 MHz): δ = 201.42 (C_q), 169.68 (C_q), 149.44 (C_q), 148.50 (C_q), 145.67 (C_q), 110.50 (CH_2), 110.49 (CH_2), 109.62 (CH_2), 61.06 (CH_2), 59.25 (CH), 37.77 (CH_2), 35.97 (CH_2), 35.93 (CH_2), 35.68 (CH_2), 33.97 (CH_2), 28.56 (CH_3), 26.54 (CH_2), 26.14 (CH_2), 26.11 (CH_2), 22.47 (CH_3), 14.04 (CH_3) ppm. IR (diamond ATR): $\tilde{\nu}$ = 3068 (w), 2967 (m), 2933 (s), 2859 (m), 1746 (m), 1630 (m), 1444 (m), 1372 (m), 1229 (m), 1169 (w), 880 (s) cm^{-1}. HR-MS (Q-TOF, 70 eV): $[C_{21}H_{34}O_3]^{+\bullet}$ m/z = 334.2503, found: m/z = 334.2499.

Synthesis of 14-methyl-6,10-dimethylenepentadec-14-en-2-one (37). To a solution of β-keto ester **36** (3.55 g, 10.6 mol, 1.00 eq) in EtOH (40 mL) was added an aqueous solution of KOH (1.78 g dissolved in 10 mL of water, 35.0 mmol, 3.00 eq) and the reaction mixture was stirred under reflux for 3 h before cooling to room temperature. The reaction mixture was slowly acidified with 2 M HCl solution until CO_2 developed. The resulting mixture was extracted with Et_2O (150 mL) three times. The combined organic layers were dried with $MgSO_4$ and concentrated under reduced pressure. The residue was subjected to column chromatography (petroleum ether/EtOAc, 13:1) to yield the desired methyl ketone **37** (2.31 g, 8.8 mmol, 83%) as a colourless oil. TLC (pentane:Et_2O = 8:1): R_f = 0.40. GC (HP-5): $I = 1894$. ^{1}H-NMR (C_6D_6, 500 MHz): δ = 4.82 (m, 6H), 1.95 (m, 12H), 1.65 (m, 8H), 1.58 (m, 4H) ppm. ^{13}C-NMR (C_6D_6, 125 MHz): δ = 206.00 (C_q), 149.51 (C_q), 149.13 (C_q), 145.67 (C_q), 110.49 (CH_2), 109.90 (CH_2), 109.60 (CH_2), 42.64 (CH_2), 37.77 (CH_2), 36.04 (CH_2), 35.95 (CH_2), 35.81 (CH_2), 35.62 (CH_2), 29.41 (CH_3), 26.23 (CH_2), 26.12 (CH_2), 22.47 (CH_3), 21.96 (CH_2) ppm. IR (diamond ATR): $\tilde{\nu}$ = 3073 (w), 2934 (s), 2865 (m), 1716 (s), 1644 (m), 1442 (m), 1364 (m), 1158 (w), 884 (s) cm^{-1}. HR-MS (Q-TOF, 70 eV): calc. $[C_{18}H_{30}O]^{+\bullet}$ m/z = 262.2292, found: m/z = 262.2290.

Synthesis of ethyl (*E*)-3,15-dimethyl-7,11-dimethylenehexadeca-2,15-dienoate (38). NaH (704 mg, 17.6 mmol, 2.00 eq, 60% in mineral oil) suspended in dry THF (30 mL) was cooled to 0 °C. Triethyl phosphonoacetate (4.34 g, 19.4 mmol, 2.20 eq) was added. After stirring the reaction mixture for 1 h at 0 °C, the reaction mixture was cooled to −78 °C and the methyl ketone **37** (2.31 g, 8.8 mmol, 1.00 eq) was added. The reaction mixture was allowed to warm to room temperature and stirred overnight. Water (15 mL) was added to quench the reaction. The aqueous phase was extracted with Et_2O (100 mL, 3 times), and the combined organic layers were dried with $MgSO_4$ and concentrated under reduced pressure. Purification by column chromatography (petroleum ether/EtOAc, 15:1) yielded pure (*E*)-**38** and (*Z*)-**38** as colourless oils.

(*E*)-**38**. Yield: 1.97 g (5.9 mmol, 67%) TLC (pentane:Et_2O = 8:1): R_f = 0.65. GC (HP-5): $I = 2305$. ^{1}H-NMR (C_6D_6, 500 MHz): δ = 5.82 (q, 1H, J = 1.3 Hz), 4.81 (m, 6H), 4.06 (q, 2H, J = 7.1 Hz), 2.20 (d, 3H, J = 1.4 Hz), 1.97 (m, 8H), 1.84 (m, 4H), 1.65 (t, 3H, J = 1.2 Hz), 1.57 (m, 4H), 1.42 (m, 2H), 1.02 (t, 3H, J = 7.1 Hz) ppm. ^{13}C-NMR (C_6D_6, 125 MHz): δ = 166.46 (C_q), 159.51 (C_q), 149.47 (C_q), 148.97 (C_q), 145.63 (C_q), 116.39 (CH), 110.52 (CH_2), 109.83 (CH_2), 109.64 (CH_2), 59.41 (CH_2), 40.52 (CH_2), 37.77 (CH_2), 36.02 (CH_2), 35.95 (CH_2), 35.91 (CH_2), 35.71 (CH_2), 26.23 (CH_2), 26.11 (CH_2), 25.68 (CH_2), 22.46 (CH_3), 18.73 (CH_3), 14.46 (CH_3) ppm. IR (diamond ATR): $\tilde{\nu}$ = 3073 (w), 2979 (m), 2935 (s), 2872 (w), 1716 (s), 1647 (s), 1443 (w), 1368 (w), 1272 (s), 1221 (s), 1143 (s), 1040 (w), 886 (s), 858 (w) cm^{-1}. HR-MS (Q-TOF, 70 eV): calc. $[C_{22}H_{36}O_2]^{+\bullet}$ m/z = 332.2710, found: m/z = 332.2700.

(*Z*)-**38**. Yield: 558 mg (1.7 mmol, 19%) TLC (pentane:Et_2O = 8:1): R_f = 0.73. GC (HP-5): $I = 2292$. ^{1}H-NMR (C_6D_6, 500 MHz): δ = 5.75 (q, 1H, J = 1.0 Hz), 4.84 (m, 6H), 4.03 (q, 2H, J = 7.2 Hz), 2.73 (m, 2H), 2.11 (m, 2H), 2.00 (m, 8H), 1.61 (m, 9H), 1.53 (d, 3H, J = 1.4 Hz), 1.01 (t, 3H, J = 7.1 Hz) ppm. ^{13}C-NMR (C_6D_6, 125 MHz): δ = 166.03 (C_q), 160.05 (C_q), 149.56 (C_q), 149.46 (C_q), 145.69 (C_q), 116.93 (CH), 110.47 (CH_2), 109.61 (CH_2), 109.56 (CH_2), 59.39 (CH_2), 37.78 (CH_2), 36.49 (CH_2), 36.07 (CH_2), 36.04 (CH_2), 35.97 (CH_2), 33.40 (CH_2), 26.82 (CH_2), 26.27 (CH_2), 26.12 (CH_2), 24.89 (CH_3), 22.47 (CH_3), 14.43 (CH_3) ppm. IR (diamond ATR): $\tilde{\nu}$ = 3073 (w), 2978 (m), 2935 (s), 2862 (m), 1716 (s), 1647 (s), 1444 (m), 1375 (m), 1227 (m), 1154 (s), 1070 (w), 1037 (w), 886 (s), 858 (w) cm^{-1}. HR-MS (Q-TOF, 70 eV): calc. $[C_{22}H_{36}O_2]^{+\bullet}$ m/z = 332.2710, found: m/z = 332.2715.

Synthesis of (*E*)-3,15-dimethyl-7,11-dimethylenehexadeca-2,15-dien-1-ol (39). To a cooled (0 °C) solution of the ester (*E*)-**38** (1.97 g, 5.9 mmol, 1.00 eq) in THF (10 mL) was added DIBAL–H (11.9 mL, 11.9 mmol, 1.0 M in hexane, 2.00 eq) and the reaction mixture was stirred for 1 h at room temperature. The mixture was cooled to 0 °C and a saturated solution of Na–K-tartrate (15 mL) was added. The resulting slurry was stirred for 2 h to dissolve the precipitate and the aqueous phase was extracted with Et_2O (100 mL, 3 times). The organic layers were dried with $MgSO_4$ and concentrated under reduced pressure. The residue was purified by column chromatography (petroleum ether/Et_2O, 3:1) to yield the alcohol **39** (1.24 g, 4.3 mmol, 73%) as a colourless oil. TLC (pentane:Et_2O = 2:1): R_f = 0.30. GC (HP-5): $I = 2176$. ^{1}H-NMR (C_6D_6, 500 MHz): δ = 5.40 (ddq, 1H, J = 7.9, 6.7, 1.4 Hz), 4.86 (m, 4H), 4.80 (m, 2H), 3.99 (d, 2H, J = 6.7 Hz), 1.96 (m, 12 H), 1.64 (s, 3H), 1.57 (m, 6H), 1.47 (d, 3H, J = 1.4 Hz) ppm. ^{13}C-NMR (C_6D_6, 125 MHz): δ = 149.53 (C_q), 149.52 (C_q), 145.66 (C_q), 138.14 (C_q), 125.04 (CH), 110.50 (CH_2), 109.60 (2x CH_2), 59.36 (CH_2), 39.48 (CH_2), 37.77 (CH_2), 36.08 (CH_2), 36.07 (CH_2), 35.98 (CH_2), 35.96 (CH_2), 26.31 (CH_2), 26.21 (CH_2), 26.11 (CH_2), 22.47 (CH_3), 16.12 (CH_3) ppm. IR (diamond ATR): $\tilde{\nu}$ = 3358 (br), 3073 (w), 2965 (m), 2933 (s), 2860 (m), 1727 (w), 1667 (w), 1656 (m), 1444 (m), 1375 (w), 1302 (w), 1021 (m), 886 (s) cm^{-1}. HR-MS (Q-TOF, 70 eV): calc. $[C_{20}H_{34}O]^{+\bullet}$ m/z = 290.2605, found: m/z = 290.2600.

Synthesis of (*E*)-3,15-dimethyl-7,11-dimethylenehexadeca-2,15-dien-1-yl diphosphate (40). To a solution of tris(tetra-n-butylammonium)hydrogen diphosphate (4.53 g, 5.0 mmol, 1.20 eq) in acetonitrile (12 mL) a solution of the allyl bromide (made from 1.00 eq of alcohol **39** following the above mentioned general procedure) was added and the mixture was stirred at room

temperature overnight. Acetonitrile was removed under reduced pressure. The residue was dissolved in aqueous NH_4HCO_3 solution (1.0 mL, 0.25 M) and loaded onto a DOWEX 50WX8 ion-exchange column (NH_4^+ form, pH 7.0). The column was flushed slowly with 1.5 volumes of NH_4HCO_3 buffer (25 mM, 5% iPrOH) and the eluate was lyophilized to yield the diphosphate **40** as a colourless hygroscopic powder (3.1 g, 6.2 mmol, 100%). ^{1}H-NMR (C_6D_6, 500 MHz): δ = 5.41 (t, 1H, J = 6.7 Hz), 4.70 (m, 6H), 4.47 (m, 2H), 1.98 (m, 12H), 1.68 (s, 3H), 1.55 (m, 6H), 1.38 (m, 3H) ppm. ^{13}C-NMR (C_6D_6, 125 MHz): δ = 149.12 (C_q), 148.83 (C_q), 144.87 (C_q), 140.47 (C_q), 120.90 (d, CH, $^3J_{C,P}$ = 9.2 Hz), 110.05 (CH_2), 109.03 (CH_2), 108.81 (CH_2), 62.46 (d, $^2J_{C,P}$ = 3.8 Hz), 39.28 (CH_2), 37.30 (CH_2), 35.78 (CH_2), 35.99 (CH_2), 35.74 (CH_2), 35.53 (CH_2),25.85 (CH_2), 25.71 (CH_2), 25.56 (CH_2), 22.13 (CH_3), 15.87 (CH_3) ppm. ^{31}P-NMR (D_2O, 203 MHz): δ = −9.75 (d, $^2J_{P,P}$ = 19.8 Hz), −10.94 (d, $^2J_{P,P}$ = 19.1 Hz) ppm. HR-MS (APCI): calc. for $[C_{20}H_{35}O_7P_2]^-$ m/z = 449.1863; found: m/z = 449.1869.

Strains and culture conditions. *Streptomyces iakyrus* DSM 40482 and *Streptomyces exfoliatus* DSM 41693 were obtained from the Leibniz Institute DSMZ – German Collection of Microorganisms and Cell Cultures GmbH. Both strains were cultivated in 65 medium (4.0 g glucose, 4.0 g yeast extract, 10.0 g malt extract dissolved in 1 L of distilled water, pH 7.2) at 28 °C. For agar plates $CaCO_3$ (2.0 g L^{-1}) and agar (20.0 g L^{-1}) were added to the medium. *Saccharomyces cerevisiae* FY834 was grown on SM-URA agar (425 mg yeast nitrogen base, 1.25 g ammonium sulfate, 5 g glucose, 192.5 mg nutritional supplement minus uracil (Carl Roth GmbH, Karlsruhe, Germany), 5 g agar, 250 mL water).

Buffers. The buffers used for protein purification and incubation experiments were: binding buffer (20 mM Na_2HPO_4, 500 mM NaCl, 20 mm imidazole, 1 mM $MgCl_2$, pH = 7.4), washing buffer (20 mM Na_2HPO_4, 500 mM NaCl, 100 mM imidazole, 1 mM $MgCl_2$, pH = 7.4), elution buffer (20 mM Na_2HPO_4, 500 mM NaCl, 500 mM imidazole, 1 mM $MgCl_2$, pH = 7.4), incubation buffer (50 mM Tris/HCl, 10 mM $MgCl_2$, 10% glycerol, 20 mM β-cyclodextrin, pH = 8.2) and substrate buffer (25 mM aq. NH_4HCO_3).

Gene cloning. The target genes coding for Bnd4 (accession number WP_033312626) from *S. iakyrus* DSM 40482 and VenA (WP_024756998) from *S. exfoliatus* DSM 41693 were amplified from gDNA by PCR using Q5 High-fidelity DNA polymerase (New England Biolabs, Ipswich, MA, USA) and the primer pairs (homology arms are in bold and underlined; Bnd4-Fw: **GGCAGCCATATGGCTAGCAT-GACTGGTGGA**GTGATCA-CCGACGCCGATCT; Bnd4-Rv: **TCTCAGTGGTGGTGGTGGTGGTGCT-CGAGTG**TCAAAC-CAGCGGTCGGGTGG; VenA–Fw: **GGCAGCCATAT-GGCTAGCAT-GACTGGTGGA**ATGACGACCATCCCGAAGCC; VenA–Rv: **TCTCAGTGGTGGTGGTGGTGGTGCTCGAGTG**TCACGCGGGCA-CCTCCGTGC). Yeast homologous recombination of the PCR products with the linearised (BamHI and HindIII digestion) pYE-Express shuttle vector[51] was carried out through the standard protocol using LiOAc, polyethylene glycol and salmon sperm DNA.[52] After transformation of *Saccharomyces cerevisiae* FY834 cultures were grown on SM-URA agar at 28 °C for 3 days. The recombinant plasmids were isolated from grown yeast colonies using the Zymoprep Yeast Plasmid Miniprep II kit (Zymo Research, Irvine, CA, USA) and subsequently used for transformation of *Escherichia coli* BL21 (DE3) electrocompetent cells. Cells were plated on LB agar plates amended with kanamycin sulfate (50 μg mL^{-1}) followed by incubation at 37 °C overnight. Single colonies were selected and used to inoculate LB medium (6 mL) liquid cultures with kanamycin sulfate (6 μL; 50 mg mL^{-1}). After 24 h growth plasmid DNA was isolated and checked for correct insertion of the desired gene by PCR amplification of the inserted DNA sequence using the T7 primer pair and by sequencing. The obtained plasmids were named pYE-Bnd4 and pYE-VenA.

Gene expression and protein purification. Small scale cultures of *Escherichia coli* BL21 (DE3) transformed with the plasmid pYE-Bnd4 or pYE-VenA were grown in LB medium (10 mL) containing kanamycin sulfate (50 mg L^{-1}) overnight with shaking at 37 °C. A large scale expression culture in LB medium (1 L) containing kanamycin sulfate was inoculated with the grown overnight culture (2%). Culturing was continued with shaking at 37 °C until an OD_{600} = 0.4–0.6 was reached. After cooling the culture to 18 °C, enzyme expression was induced by the addition of IPTG solution (100 mm, 1‰). The cultures were shaken at 18 °C for 18 h. Cells were harvested via centrifugation (1,500 g, 40 min, 4 °C), resuspended in binding buffer (30 mL, 4 °C) and lysed by ultrasonication (10x 1 min) on ice. The cell debris was removed by centrifugation (14,600 g, 10 min, 4 °C) and the supernatant was loaded on a Ni^{2+}-NTA superflow affinity chromatography column (Qiagen, Venlo, Netherlands) equilibrated with binding buffer. The column was washed with binding buffer (2 column volumes, CV, 4 °C) and washing buffer (2 CV, 4 °C). The desired protein was eluted with elution buffer (1 CV, 4 °C). Protein purity was checked by SDS-PAGE analysis (Figure S1) and protein concentrations were determined through Bradford assay.[53]

Preparative scale incubation of substrate analogs with recombinant diterpene synthases and compound isolation. For preparative scale enzymatic conversions the enzyme-substrate combinations as detailed in Table S1 were used (for expression and purification of the enzymes cf. the references given in Table S1).

Compounds from *iso*-GGPP I. A solution of the trisammonium salt of *iso*-GGPP I (60 mg, 120 μmol) in substrate buffer (20 mL) was added to incubation buffer (130 mL) containing Bnd4 or VenA (0.3 mg L^{-1}), followed by incubation for 16 h at 30 °C. The reaction mixtures were extracted with n-hexane, the extracts were dried with $MgSO_4$ and the solvent was evaporated, followed by compound isolation through column chromatography on silica gel to yield the pure compounds **45** and **47**.

Compounds from *iso*-GGPP IV. A solution of the trisammonium salt of *iso*-GGPP IV (60 mg, 120 μmol for HdS; 80 mg, 160 μmol for AbVS) in substrate buffer (10 mL) was added to incubation buffer (105 mL for HdS; 80 mL for AbVS) containing HdS (0.52 mg L^{-1}, containing 60 mg of protein in total) or AbVS (0.35 mg L^{-1}, 40 mg), followed by incubation for 16 h at 30 °C. The reaction mixtures were extracted with n-hexane, the extracts were dried with $MgSO_4$ and the solvent was evaporated, followed by compound isolation through column chromatography on silica gel to give compounds **48** and **49**.

Compounds from *iso*-GGPP VI. A solution of the trisammonium salts of *iso*-FPP III (70 mg, 162 μmol) and IPP (60 mg, 203 μmol) (as precursors of *iso*-GGPP VI using GGPP synthase, GGPPS) in substrate buffer (10 mL) was added to incubation buffer (65 mL) containing SoS (1.06 mg L^{-1}, 80 mg) and GGPPS (0.86 mg L^{-1}, 60 mg) followed by incubation for 16 h at 30 °C. The reaction mixture was extracted with n-hexane, the extract was dried with $MgSO_4$ and the solvent was evaporated, followed by compound isolation through column chromatography on silica gel to give compound **51**.

A solution of the trisammonium salts of *iso*-FPP III (70 mg, 162 μmol) and IPP (70 mg, 296 μmol) in substrate buffer (10 mL) was added to incubation buffer (70 mL) containing CyS (1.56 mg L^{-1}, 125 mg) and GGPPS (0.94 mg L^{-1}, 80 mg) followed by incubation for 16 h at 30 °C. The reaction mixture was extracted with n-hexane, the extract was dried with $MgSO_4$ and the solvent was evaporated, followed by compound isolation through column chromatography on silica gel to give compounds **52** and **54**.

A solution of the trisammonium salts of *iso*-FPP III (90 mg, 208 μmol) and IPP (100 mg, 338 μmol) in substrate buffer (20 mL) was

added to incubation buffer (150 mL) containing SvS (0.59 mg L^{-1}, 100 mg) and GGPPS (0.47 mg L^{-1}, 80 mg) followed by incubation for 16 h at 30 °C. The reaction mixture was extracted with n-hexane, the extract was dried with $MgSO_4$ and the solvent was evaporated, followed by compound isolation through column chromatography on silica gel to give compound **53** and a mixture of **54** and **55**. Compounds **54** and **55** were further separated on $AgNO_3$ coated silica gel (for its preparation 50 g of silica gel were suspended in a solution of $AgNO_3$ (10.0 g) in methanol (150 mL) overnight, followed by rigorous evaporation of the solvent).

A solution of the trisammonium salts mixture of *iso*-FPP III (100 mg, 231 μmol) and IPP (100 mg, 338 μmol) in substrate buffer (30 mL) was added to incubation buffer (245 mL) containing *Si*CotB2 (0.54 mg L^{-1}, 150 mg) and GGPPS (0.36 mg L^{-1}, 100 mg) followed by incubation for 16 h at 30 °C. The reaction mixture was extracted with n-hexane, the extract was dried with $MgSO_4$ and the solvent was evaporated, followed by compound isolation through column chromatography on silica gel. A mixture of **56** and **57** was obtained that was further separated on $AgNO_3$ coated silica gel to obtain pure **57**. The purity of **56** was further improved by HPLC.

Benditerpe-2,7(19),15-triene (45). Yield: 4.3 mg (15.8 μmol, 13%). TLC (pentane): $R_f = 0.60$. GC (HP-5MS): $I = 1928$. MS (EI, 70 eV): *m/z* (%) = 39 (1), 41 (4), 55 (5), 67 (6), 79 (9), 91 (11), 105 (9), 107 (7), 119 (6), 133 (6), 147 (4), 161 (4), 173 (3), 187 (5), 201 (4), 216 (2), 229 (2), 257 (9), 272 (1). IR (diamond ATR): $\tilde{\nu} = 3071$ (w), 2924 (s), 2867 (s), 1639 (w), 1452 (m), 1375 (w), 884 (s), 846 (w), 805 (w) cm^{-1}. HR-MS (Q-TOF, 70 eV): calc. $[C_{20}H_{32}]^{+\bullet}$ *m/z* = 272.2499; found: *m/z* = 272.2495. Optical rotation: $[\alpha]_D^{25} = +24.8$ (*c* 0.4, acetone). NMR data are given in Table S7.

Venezuelaxenene (47). Yield: 2.0 mg (7.4 μmol, 6%). TLC (pentane): $R_f = 0.84$. GC (HP-5MS): $I = 2001$. MS (EI, 70 eV): *m/z* (%) = 41 (1), 55 (2), 67 (2), 79 (3), 91 (4), 105 (4), 107 (3), 119 (3), 133 (3), 147 (3), 161 (2), 173 (2), 187 (3), 201 (2), 229 (11), 257 (2), 272 (3). IR (diamond ATR): $\tilde{\nu} = 2924$ (s), 2866 (m), 1731 (w), 1672 (w), 1463 (m), 1373 (m), 1312 (m), 1260 (w), 1228 (m), 1081 (m), 1025 (m), 893 (w), 800 (m) cm^{-1}. HR-MS (Q-TOF, 70 eV): calc. $[C_{20}H_{32}]^{+\bullet}$ *m/z* = 272.2499; found: *m/z* = 272.2503. Optical rotation: $[\alpha]_D^{25} = +18.5$ (*c* 0.2, CH_2Cl_2). NMR data are given in Table S8.

Diisocembrene A (48). Yield: 0.63 mg (2.3 μmol, 1.9%). TLC (pentane): $R_f = 0.42$. GC (HP-5MS): $I = 1986$. MS (EI, 70 eV): *m/z* (%) = 39 (2), 41 (6), 43 (1), 67 (8), 79 (9), 81 (10), 93 (8), 107 (6), 121 (5), 133 (4), 159 (1), 175 (1), 189 (1), 229 (1), 257 (1), 272 (1). IR (diamond ATR): $\tilde{\nu} = 3070$ (w), 2928 (s), 2854 (m), 2180 (w), 1734 (w), 1643 (m), 1439 (m), 1374 (w), 1260 (w), 1093 (w), 1022 (w), 887 (s), 802 (w) cm^{-1}. HR-MS (Q-TOF, 70 eV): calc. $[C_{20}H_{32}]^{+\bullet}$ *m/z* = 272.2499; found: *m/z* = 272.2502. Optical rotation: $[\alpha]_D^{25} = +30.0$ (*c* 0.06, acetone). NMR data are given in Table S10.

Prenylisopseudogermacrene B (49). Yield: 0.40 mg (1.5 μmol, 0.9%). TLC (pentane): $R_f = 0.54$. GC (HP-5MS): $I = 2058$. MS (EI, 70 eV): *m/z* (%) = 41 (18), 53 (5), 67 (9), 69 (14), 79 (7), 93 (22), 107 (5), 109 (2), 121 (3), 135 (4), 147 (2), 161 (2), 175 (1), 187 (1), 203 (1), 229 (1), 257 (1), 272 (1). IR (diamond ATR): $\tilde{\nu} = 2958$ (br), 2932 (br), 2852 (m), 2315 (s), 1644 (w), 1375 (s), 1259 (w), 1200 (w), 1083 (w), 1021 (w), 884 (w), 789 (m) cm^{-1}. HR-MS (Q-TOF, 70 eV): calc. $[C_{20}H_{32}]^{+\bullet}$ *m/z* = 272.2499; found: *m/z* = 272.2495. NMR data are given in Table S11.

Isopentenylpseudogermacrene A (51). Yield: 4.0 mg (14.7 μmol, 9.1%). TLC ($AgNO_3$ activated TLC plate, pentane:Et_2O = 8:1): R_f = 0.32. GC (HP-5MS): $I = 2042$. MS (EI, 70 eV): *m/z* (%) = 39 (3), 41 (13), 55 (7), 67 (10), 69 (8), 79 (12), 93 (11), 107 (9), 109 (3), 121 (4), 135 (2), 147 (3), 161 (3), 175 (2), 190 (2), 203 (4), 229 (1), 257 (1), 272 (1). IR (diamond ATR): $\tilde{\nu} = 3368$ (w), 2922 (s), 2852 (m), 2268 (w), 1650 (w), 1633 (w), 1443 (w), 1382 (w), 1259 (w), 886 (w), 831 (w) cm^{-1}. HR-MS (Q-TOF, 70 eV): calc. $[C_{20}H_{32}]^{+\bullet}$ *m/z* = 272.2499; found: *m/z* = 272.2501. NMR data are given in Table S12.

Isopentenylpseudogermacrene B (52). Yield: 2.0 mg (7.4 μmol, 4.6%). TLC (pentane): $R_f = 0.38$. GC (HP-5MS): $I = 2013$. MS (EI, 70 eV): *m/z* (%) = 39 (3), 41 (10), 55 (7), 68 (16), 69 (3), 79 (10), 93 (11), 107 (8), 109 (2), 121 (9), 133 (4), 147 (3), 161 (3), 175 (1), 189 (3), 201 (2), 216 (2), 229 (1), 257 (2), 272 (1). IR (diamond ATR): $\tilde{\nu} = 3352$ (w), 2924 (s), 2851 (m), 2144 (w), 1991 (w), 1739 (w), 1657 (w), 1632 (w), 1443 (w), 1381 (w), 1259 (w), 1215 (w), 1097 (w), 1081 (w), 1027 (w), 814 (w) cm^{-1}. HR-MS (Q-TOF, 70 eV): calc. $[C_{20}H_{32}]^{+\bullet}$ *m/z* = 272.2499; found: *m/z* = 272.2497. NMR data are given in Table S13.

Isopentenylpseudogermacrene C (53). Yield: 1.3 mg (4.8 μmol, 2.3%). TLC (pentane): $R_f = 0.48$. GC (HP-5MS): $I = 2036$. MS (EI, 70 eV): *m/z* (%) = 39 (6), 41 (13), 55 (10), 67 (19), 79 (11), 93 (8), 107 (5), 121 (5), 133 (4), 147 (2), 161 (2), 173 (1), 189 (7), 201 (2), 216 (1), 257 (3), 272 (1). IR (diamond ATR): $\tilde{\nu} = 3074$ (w), 2917 (s), 2852 (m), 1744 (w), 1649 (w), 1445 (m), 1375 (w), 1259 (w), 1099 (w), 885 (w), 829 (w) cm^{-1}. HR-MS (Q-TOF, 70 eV): calc. $[C_{20}H_{32}]^{+\bullet}$ *m/z* = 272.2499; found: *m/z* = 272.2508. NMR data are given in Table S14.

α-Spirocattleyaxenene (54). Yield: 0.4 mg (1.5 μmol, 0.9%). TLC (pentane): $R_f = 0.48$. GC (HP-5MS): $I = 2118$. MS (EI, 70 eV): *m/z* (%) = 39 (3), 41 (9), 53 (5), 55 (9), 67 (12), 79 (10), 81 (11), 93 (9), 105 (11), 107 (5), 121 (5), 135 (2), 147 (2), 161 (1), 189 (1), 201 (1), 272 (4). IR (diamond ATR): $\tilde{\nu} = 2923$ (s), 2850 (m), 1739 (w), 1442 (m), 1377 (w), 1258 (m), 1216 (w), 1090 (m), 1014 (m), 924 (w), 885 (w), 794 (s), 702 (w) cm^{-1}. HR-MS (Q-TOF, 70 eV): calc. $[C_{20}H_{32}]^{+\bullet}$ *m/z* = 272.2499; found: *m/z* = 272.2503. Optical rotation: $[\alpha]_D^{25} = -20.0$ (*c* 0.04, acetone, obtained with CyS); $[\alpha]_D^{25} = +7.5$ (*c* 0.04, acetone, obtained with SvS). NMR data are given in Table S15.

β-Spirocattleyaxenene (55). Yield: 0.4 mg (1.5 μmol, 0.7%). TLC ($AgNO_3$ activated TLC plate, pentane:Et_2O = 8:1): $R_f = 0.52$. GC (HP-5MS): $I = 2113$. MS (EI, 70 eV): *m/z* (%) = 39 (2), 41 (7), 53 (4), 55 (6), 67 (9), 79 (11), 81 (10), 93 (8), 105 (5), 107 (6), 121 (8), 135 (3), 147 (3), 161 (2), 189 (2), 201 (3), 216 (1), 229 (1), 243 (1), 257 (1), 272 (4). IR (diamond ATR): $\tilde{\nu} = 3361$ (w), 2969 (m), 2924 (s), 2851 (w), 1738 (s), 1656 (w), 1438 (w), 1365 (m), 1228 (m), 1216 (m), 1206 (m), 885 (w), 527 (w) cm^{-1}. HR-MS (Q-TOF, 70 eV): calc. $[C_{20}H_{32}]^{+\bullet}$ *m/z* = 272.2499; found: *m/z* = 272.2494. Optical rotation: $[\alpha]_D^{25} = +5.0$ (*c* 0.06, acetone, obtained with CyS); $[\alpha]_D^{25} = -2.5$ (*c* 0.04, acetone, obtained with SvS). NMR data are given in Table S16.

Isobucketwheelene (56). Yield: 3.0 mg (11.0 μmol, 4.8%). TLC ($AgNO_3$ activated TLC plate, pentane:Et_2O = 15:1): $R_f = 0.28$. GC (HP-5MS): $I = 2062$. MS (EI, 70 eV): *m/z* (%) = 39 (3), 41 (9), 53 (6), 55 (7), 67 (10), 79 (12), 81 (13), 93 (9), 105 (4), 107 (6), 121 (6), 133 (5), 147 (2), 161 (2), 175 (1), 189 (1), 201 (1), 257 (1), 272 (1). IR (diamond ATR): $\tilde{\nu} = 3071$ (w), 2978 (m), 2931 (s), 2849 (m), 1731 (w), 1643 (m), 1439 (m), 1381 (w), 1229 (w), 1217 (w), 1099 (w), 887 (s), 831 (w) cm^{-1}. HR-MS (Q-TOF, 70 eV): calc. $[C_{20}H_{32}]^{+\bullet}$ *m/z* = 272.2499; found: *m/z* = 272.2505. NMR data are given in Table S17.

Iakyroxenene (57). Yield: 1.8 mg (6.6 μmol, 3.3%). TLC ($AgNO_3$ activated TLC plate, pentane:Et_2O = 15:1): $R_f = 0.28$. GC (HP-5MS): $I = 2092$. MS (EI, 70 eV): *m/z* (%) = 39 (2), 41 (6), 53 (4), 55 (5), 67 (9), 79 (10), 81 (7), 91 (7), 93 (9), 108 (8), 121 (14), 135 (3), 147 (2), 161 (2), 175 (3), 189 (3), 201 (1), 215 (1), 229 (1), 243 (1), 257 (2), 272 (2). IR (diamond ATR): $\tilde{\nu} = 2925$ (s), 2845 (m), 1737 (w), 1441 (w), 1381 (w), 1368 (w), 1229 (w), 1216 (w), 852 (w) cm^{-1}. HR-MS (Q-TOF, 70 eV): calc. $[C_{20}H_{32}]^{+\bullet}$ *m/z* = 272.2499; found: *m/z* = 272.2503. Optical rotation: $[\alpha]_D^{25} = +98.0$ (*c* 0.3, acetone). NMR data are given in Table S18.

Conversion of 41 with NBS. To a solution of **41** (11.3 mg, 41.6 μmol, 1.0 eq) in CH_2Cl_2 was added *N*-bromosuccinimide (7.4 mg, 41.6 μmol, 1.0 eq) at −78 °C under argon atmosphere. After stirring

at −78 °C for 20 min, the reaction mixture warmed to room temperature over 1 h and stirring was continued for another 1 h. The reaction was quenched by the addition of sat. $NaHCO_3$ soultion and extracted with n-pentane (3×20 mL). The combined organic layers were dried with $MgSO_4$ and concentrated under reduced pressure. The residues was subjected to column chromatography (n-pentane) to yield **42** (0.7 mg, 2.00 μmol, 5%), **43** (0.6 mg, 1.71 μmol, 4%) and **44** (0.3 mg, 0.85 μmol, 2%).

Bromide **42**. $R_f = 0.31$ (n-pentane). GC (HP-5MS): $I = 2473$. IR (diamond ATR): $\tilde{\nu} = 2924$ (s), 2853 (m), 1754 (w), 1655 (w), 1634 (w), 1463 (w), 1385 (w), 1170 (w), 888 (w), 795 (w) cm^{-1}. Optical rotation: $[\alpha]_D^{25} = -42.5$ (*c* 0.03, CH_2Cl_2). HRMS (APCI): $[M–Br]^+$ calc. for $[C_{20}H_{31}]^+$ $m/z = 271.2421$, found $m/z = 271.2418$. NMR data are given in Table S2.

Bromide **43**. TLC (n-pentane): $R_f = 0.50$. GC (HP-5MS): $I = 2460$. IR (diamond ATR): $\tilde{\nu} = 2922$ (s), 2853 (s), 1677 (w), 1465 (m), 1441 (m), 1383 (m), 1260 (m), 1090 (m), 1018 (m), 867 (w), 795 (m), 701 (w) cm^{-1}. Optical rotation: $[\alpha]_D^{25} = +43.3$ (*c* 0.06, CH_2Cl_2). HRMS (APCI): $[M–Br]^+$ calc. for $[C_{20}H_{31}]^+$ $m/z = 271.2421$, found $m/z = 271.2415$. NMR data are given in Table S3.

Bromide **44**. $R_f = 0.42$ (n-pentane). GC (HP-5MS): $I = 2285$. IR (diamond ATR): $\tilde{\nu} = 2923$ (s), 2853 (m), 2172 (w), 2023 (w), 1720 (w), 1634 (w), 1454 (w), 1259 (w), 1077 (w), 1024 (w), 907 (w), 799 (w) cm^{-1}. Optical rotation: $[\alpha]_D^{25} = +56.7$ (*c* 0.03, CH_2Cl_2). HRMS (APCI): $[M–Br]^+$ calc. for $[C_{20}H_{31}]^+$ $m/z = 271.2421$, found $m/z = 271.2426$. NMR data are given in Table S4.

Acknowledgements

This work was supported by the Deutsche Forschungsgemeinschaft DFG (project number 513548540), and by the computing center of the University of Cologne (RRZK), providing CPU time on the DFG-funded supercomputer RAMSES. We thank Andreas Schneider for HPLC purifications. Open Access funding enabled and organized by Projekt DEAL.

Conflict of Interests

The authors declare no conflict of interest.

Data Availability Statement

The data that support the findings of this study are available in the supplementary material of this article.

Keywords: biosynthesis · enzyme mechanisms · isotopes · substrate analogs · terpenes

[1] J. S. Dickschat, *Nat. Prod. Rep.* **2016**, *33*, 87–110.
[2] A. Minami, T. Ozaki, C. Liu, H. Oikawa, *Nat. Prod. Rep.* **2018**, *35*, 1330–1346.
[3] D. W. Christianson, *Chem. Rev.* **2017**, *117*, 11570–11648.
[4] M. Demiray, X. Tang, T. Wirth, J. A. Faraldos, R. K. Allemann, *Angew. Chem.* **2017**, *129*, 4411–4415; *Angew. Chem. Int. Ed.* **2017**, *56*, 4347–4350.
[5] Z. Quan, A. Hou, B. Goldfuss, J. S. Dickschat, *Angew. Chem. Int. Ed.* **2022**, *61*, e202117273; *Angew. Chem.* **2022**, *134*, e202117273.
[6] F. Huynh, D. J. Grundy, R. L. Jenkins, D. J. Miller, R. K. Allemann, *ChemBioChem* **2018**, *19*, 1834–1838.
[7] C. Oberhauser, V. Harms, K. Seidel, B. Schröder, K. Ekramzadeh, S. Beutel, S. Winkler, L. Lauterbach, J. S. Dickschat, A. Kirschning, *Angew. Chem. Int. Ed.* **2018**, *57*, 11802–11806; *Angew. Chem.* **2018**, *130*, 11976–11980.
[8] H. Struwe, H. Li, F. Schrödter, L. Höft, J. Fohrer, J. S. Dickschat, A. Kirschning, *Org. Lett.* **2024**, *26*, 5888–5892.
[9] A. Hou, J. S. Dickschat, *Chem. Eur. J.* **2021**, *27*, 15644–15649.
[10] L. Lauterbach, A. Hou, J. S. Dickschat, *Chem. Eur. J.* **2021**, *27*, 7923–7929.
[11] Y. Jin, D. C. Williams, R. Croteau, R. M. Coates, *J. Am. Chem. Soc.* **2005**, *127*, 7834–7842.
[12] D. J. Miller, F. Yu, R. K. Allemann, *ChemBioChem* **2007**, *8*, 1819–1825.
[13] D. J. Miller, F. Yu, D. W. Knight, R. K. Allemann, *Org. Biomol. Chem.* **2009**, *7*, 962–975.
[14] O. Cascón, S. Touchet, D. J. Miller, V. Gonzalez, J. A. Faraldos, R. K. Allemann, *Chem. Commun.* **2012**, *48*, 9702–9704.
[15] M. Moeller, D. Dhar, G. Dräger, M. Özbasi, H. Struwe, M. Wildhagen, M. D. Davari, S. Beutel, A. Kirschning, *J. Am. Chem. Soc.* **2024**, *146*, 17838–17846.
[16] S. Y. Chow, H. J. Williams, Q. Huang, S. Nanda, A. I. Scott, *J. Org. Chem.* **2005**, *70*, 9997–10003.
[17] G. Li, Y.-W. Guo, J. S. Dickschat, *Angew. Chem. Int. Ed.* **2021**, *60*, 1488–1492; *Angew. Chem.* **2021**, *133*, 1510–1514.
[18] B. Gu, J. S. Dickschat, *Angew. Chem. Int. Ed.* **2023**, *62*, e202307006; *Angew. Chem.* **2023**, *135*, e202307006.
[19] G. B. Tabekoueng, H. Li, B. Goldfuss, G. Schnakenburg, J. S. Dickschat, *Angew. Chem. Int. Ed.* **2024**, *63*, e202413860; *Angew. Chem.* **2024**, *136*, e202413860.
[20] H. Li, J. S. Dickschat, *Org. Chem. Front.* **2022**, *9*, 795–801.
[21] V. Harms, B. Schröder, C. Oberhauser, C. D. Tran, S. Winkler, G. Dräger, A. Kirschning, *Org. Lett.* **2020**, *22*, 4360–4365.
[22] A. Hou, L. Lauterbach, J. S. Dickschat, *Chem. Eur. J.* **2020**, *26*, 2178–2182.
[23] C. D. Tran, G. Dräger, H. F. Struwe, L. Siedenberg, S. Vasisth, J. Grunenberg, A. Kirschning, *Org. Biomol. Chem.* **2022**, *20*, 7833–7839.
[24] I. Nemethova, D. Schmid, K. Tiefenbacher, *Angew. Chem. Int. Ed.* **2023**, *62*, e202218625; *Angew. Chem.* **2023**, *135*, e202218625.
[25] Q. Zhang, J. Rinkel, B. Goldfuß, J. S. Dickschat, K. Tiefenbacher, *Nat. Catal.* **2018**, *1*, 609–615.
[26] G. Persiani, D. Sokolova, R. Ivanov, S. Merget, T. Maintok, D. Häussinger, K. Tiefenbacher, *Eur. J. Org. Chem.* **2024**, *27*, e202400923.
[27] J. Rinkel, L. Lauterbach, P. Rabe, J. S. Dickschat, *Angew. Chem. Int. Ed.* **2018**, *57*, 3238–3241; *Angew. Chem.* **2018**, *130*, 3292–3296.
[28] H. Li, J. S. Dickschat, *Angew. Chem. Int. Ed.* **2022**, *61*, e202211054; *Angew. Chem.* **2022**, *134*, e202211054.
[29] L. Lauterbach, B. Goldfuss, J. S. Dickschat, *Angew. Chem. Int. Ed.* **2020**, *59*, 11943–11947; *Angew. Chem.* **2020**, *132*, 12041–12045.
[30] G. Bian, J. Rinkel, Z. Wang, L. Lauterbach, A. Hou, Y. Yuan, Z. Deng, T. Liu, J. S. Dickschat, *Angew. Chem. Int. Ed.* **2018**, *57*, 15887–15890; *Angew. Chem.* **2018**, *130*, 16113–16117.
[31] H. Li, J. S. Dickschat, *Chem. Eur. J.* **2024**, *30*, e202303560.
[32] L. Poppe, L. Novak, C. Szantay, *Synth. Commun.* **1987**, *17*, 173–179.
[33] R. J. Anderson, H. R. Chinn, K. Gill, C. A. Henrick, *J. Chem. Ecol.* **1979**, *5*, 919–927.
[34] P. Rabe, J. Rinkel, E. Dolja, T. Schmitz, B. Nubbemeyer, T. H. Luu, J. S. Dickschat, *Angew. Chem. Int. Ed.* **2017**, *56*, 2776–2779; *Angew. Chem.* **2017**, *129*, 2820–2823.
[35] C. Zhu, B. Xu, D. A. Adpressa, J. D. Rudolf, S. Loesgen, *Angew. Chem. Int. Ed.* **2021**, *60*, 14163–14170; *Angew. Chem.* **2021**, *133*, 14282–14289.
[36] B. Xu, D. J. Tantillo, J. D. Rudolf, *Angew. Chem. Int. Ed.* **2021**, *60*, 23156–23163; *Angew. Chem.* **2021**, *133*, 23343–23347.
[37] P. Rabe, L. Barra, J. Rinkel, R. Riclea, C. A. Citron, T. A. Klapschinski, A. Janusko, J. S. Dickschat, *Angew. Chem. Int. Ed.* **2015**, *54*, 13448–13451; *Angew. Chem.* **2015**, *127*, 13649–13653.
[38] J. Rinkel, P. Rabe, X. Chen, T. G. Köllner, F. Chen, J. S. Dickschat, *Chem. Eur. J.* **2017**, *23*, 10501–10505.
[39] L. Lauterbach, J. Rinkel, J. S. Dickschat, *Angew. Chem. Int. Ed.* **2018**, *57*, 8280–8283; *Angew. Chem.* **2018**, *130*, 8412–8415.
[40] J. W. Cornforth, R. H. Cornforth, G. Popjak, L. Yengoyan, *J. Biol. Chem.* **1966**, *241*, 3970–3987.
[41] Z. Li, Y. Jiang, X. Zhang, Y. Chang, S. Li, X. Zhang, S. Zheng, C. Geng, P. Men, L. Ma, Y. Yang, Z. Gao, Y.-J. Tang, S. Li, *ACS Catal.* **2020**, *10*, 5846–5851.
[42] T. Lou, A. Li, H. Xu, J. Pan, B. Xing, R. Wu, J. S. Dickschat, D. Yang, M. Ma, *J. Am. Chem. Soc.* **2023**, *145*, 8474–8485.

[43] J. S. Dickschat, J. Rinkel, P. Rabe, A. Beyraghdar Kashkooli, H. J. Bouwmeester, *Beilstein J. Org. Chem.* **2017**, *13*, 1770–1780.
[44] J. Rinkel, L. Lauterbach, J. S. Dickschat, *Angew. Chem. Int. Ed.* **2019**, *58*, 452–455; *Angew. Chem.* **2019**, *131*, 461–465.
[45] J. Rinkel, S. T. Steiner, J. S. Dickschat, *Angew. Chem. Int. Ed.* **2019**, *58*, 9230–9233; *Angew. Chem.* **2019**, *131*, 9328–9332.
[46] K. A. Taizoumbe, S. T. Steiner, J. S. Dickschat, *Chem. Eur. J.* **2023**, *29*, e202302469.
[47] S.-Y. Kim, P. Zhao, M. Igarashi, R. Sawa, T. Tomita, M. Nishiyama, T. Kuzuyama, *Chem. Biol.* **2009**, *16*, 736–743.
[48] J. Rinkel, J. S. Dickschat, *Org. Lett.* **2019**, *21*, 2426–2429.
[49] G. R. Fulmer, A. J. M. Miller, N. H. Sherden, H. E. Gottlieb, A. Nudelman, B. M. Stoltz, J. E. Bercaw, K. I. Goldberg, *Organometallics* **2010**, *29*, 2176–2179.
[50] H. C. Brown, K. P. Singh, B. J. Garner, *J. Organomet. Chem.* **1963**, *1*, 2–7.
[51] J. S. Dickschat, K. A. K. Pahirulzaman, P. Rabe, T. A. Klapschinski, *ChemBioChem* **2014**, *15*, 810–814.
[52] R. D. Gietz, R. H. Schiestl, *Nat. Protoc.* **2007**, *2*, 31–34.
[53] M. M. Bradford, *Anal. Biochem.* **1976**, *72*, 248–254.

Manuscript received: February 24, 2025
Accepted manuscript online: March 11, 2025
Version of record online: March 21, 2025

Appendices E

Mechanistic Characterisation of the Diterpene Synthase for Clitopilene and Identification of Isopentalenene Synthase from the fungus *Clitopilus passeckerianus*

ChemComm. **2024**, *60,* 7041-7044.

DOI: 10.1039/D4CC02286F

ChemComm

COMMUNICATION

View Article Online
View Journal | View Issue

Cite this: *Chem. Commun.*, 2024, **60**, 7041

Received 10th May 2024,
Accepted 17th June 2024

DOI: 10.1039/d4cc02286f

rsc.li/chemcomm

Mechanistic characterisation of the diterpene synthase for clitopilene and identification of isopentalenene synthase from the fungus *Clitopilus passeckerianus*†

Heng Li,[a] Bernd Goldfuss [b] and Jeroen S. Dickschat *[a]

Two terpene synthases from the pleuromutilin producing fungus *Clitopilus passeckerianus* were functionally characterised. The first enzyme CpTS1 produces the new diterpene clitopilene with a novel 6-6-5-5 tetracyclic skeleton, while the second enzyme CpTS2 makes the new sesquiterpene isopentalenene. The CpTS1 reaction mechanism was studied in depth using experimental and theoretical approaches.

Terpenoids constitute the largest class of natural products with about 100 000 known representatives. Many terpenoids exhibit a potent bioactivity and are thus beneficial for human health. Prominent examples include the anticancer drug taxol from the Pacific yew *Taxus brevifolia*,[1] a highly oxidised compound that is derived from the parent hydrocarbon taxa-4(5),11(12)-diene,[2] the antimalaria drug artemisinin from *Artemisia annua*[3] that originates from amorphadiene,[4,5] and ingenol mebutate[6] used to treat actinic keratosis that occurs in different *Euphorbia* spp. and arises from the diterpene hydrocarbon casbene.[7,8] Also fungal compounds can be of interest such as the antibacterial drug pleuromutilin from *Clitopilus passeckerianus*,[9] that is formed from premutilin.[10,11] Besides the premutilin synthase, an enzyme that has been studied for its mechanism,[12,13] several more terpene synthase homologs are encoded in the genome of *C. passeckerianus* DSM 1602.[14] Here we report on the identification of two terpene synthases for the novel diterpene clitopilene and the sesquiterpene isopentalenene, and an in-depth mechanistic study of the clitopilene synthase through isotopic labelling experiments and DFT calculations.

The coding sequence of two terpene synthase candidates was obtained through isolation of the mRNA from a *C. passeckerianus* agar plate culture and PCR amplification using reverse transcriptase (RT-PCR). The genes were cloned into the expression vector pYE-Express and expressed in *Escherichia coli* BL21 (DE3). For testing of enzyme functions, the purified proteins (Fig. S1, ESI†) were then incubated with the trisammonium salts of geranyl (GPP), farnesyl (FPP), geranylgeranyl (GGPP) and geranylfarnesyl pyrophosphate (GFPP) that were synthesised from the corresponding alcohols according to Poulter's standard protocol.[15]

The first enzyme (CpTS1, accession no. PP777465) exhibited all highly conserved motifs of type I terpene synthases including the Asp-rich motif ^{88}DDMVE, the pyrophosphate sensor Arg180, the NSE triad ^{225}NDFFSYEVE and the ^{329}RY pair (Fig. S2, ESI†). The substrate screening only showed a diterpene synthase activity with GGPP, but no conversion of GPP, FPP or GFPP (Fig. S3, ESI†). The diterpene hydrocarbon was isolated and its structure was elucidated through NMR spectroscopy as the new compound clitopilene (**1**) with a novel 6-6-5-5 tetracyclic skeleton (Scheme 1 and Table S2, Fig. S4–S11, ESI†).

The proposed biosynthesis of **1** starts with the ionisation and 1,11-10,14-cyclisation of GGPP to **A**. After ring expansion to **B** a ring opening leads to **C** in which the cation at C11 is stabilised through cation-π interaction with the C10=C14 double bond. Subsequent ring closures lead to **D** and **E** that is a common intermediate to biosynthetically related diterpenes including phomopsene,[16–18] spiroviolene,[19] allokutznerene,[17] the cyclopiane-type diterpene,[20] cattleyene[18] and variediene.[21] These steps were shown to be energetically feasible through DFT computations by Hong and Tantillo.[22] Subsequent reactions specific to the pathway towards **1** include a 1,2-hydride shift from **E** to **F**, a cyclisation to **G**, and another 1,2-hydride migration to **H**. At this point an unusual 1,3-hydride shift to the secondary cation **I** may be possible that can undergo a skeletal rearrangement to **J** and deprotonation to **1**. This proposal is in full agreement with our results from DFT calculations (Table S3 and Fig. S12, ESI†). Repeated calculations for the first steps gave a good agreement with the data obtained by Hong and Tantillo,[22] while for all steps low reaction barriers were found (the highest barrier is 12.0 kcal mol^{-1} for the ring expansion

[a] *Kekulé-Institute for Organic Chemistry and Biochemistry, University of Bonn, Gerhard-Domagk-Straße 1, 53121 Bonn, Germany. E-mail: dickschat@uni-bonn.de*
[b] *Department for Chemistry, University of Cologne, Greinstraße 4, 50939 Cologne, Germany*

† Electronic supplementary information (ESI) available. See DOI: https://doi.org/10.1039/d4cc02286f

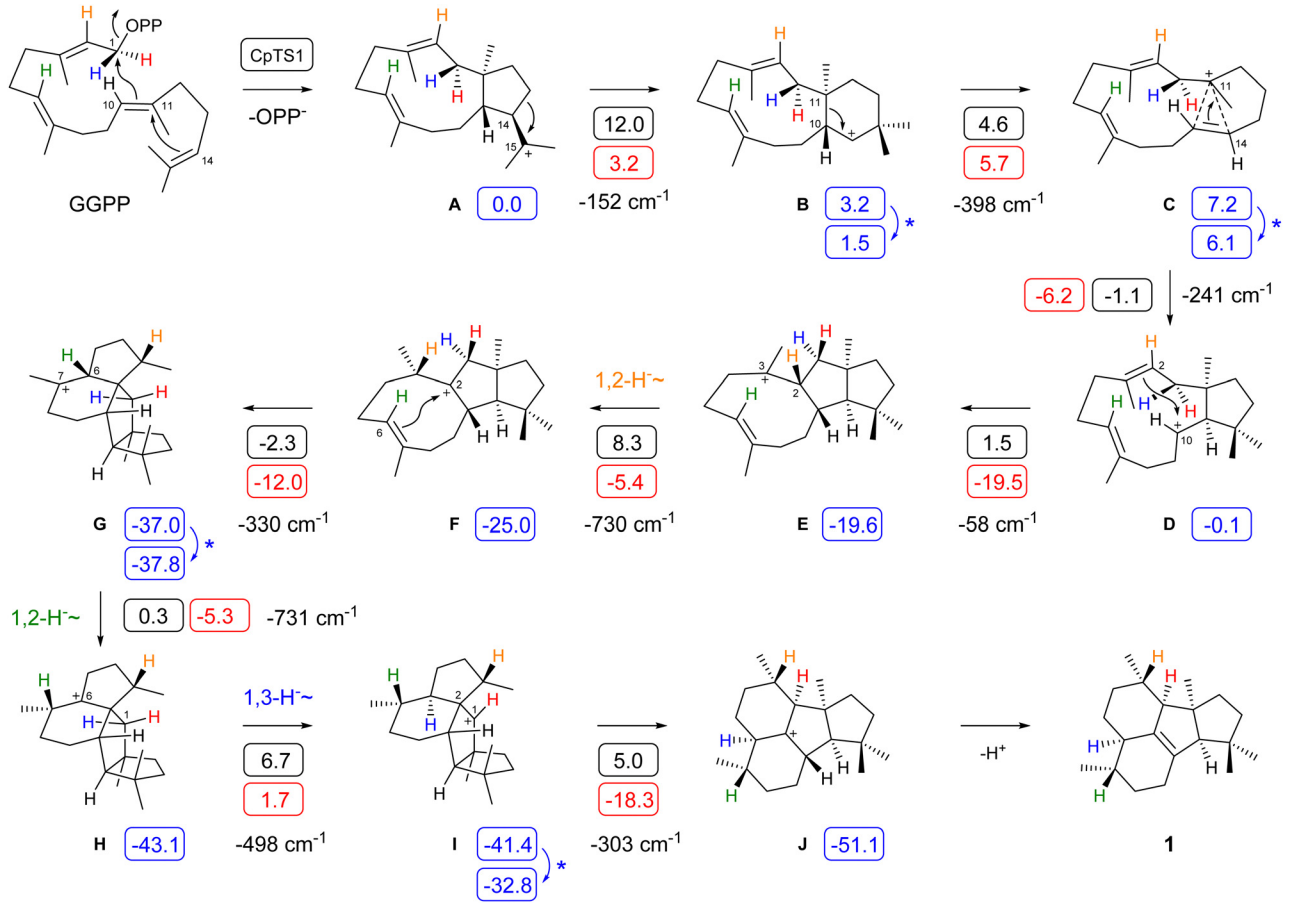

Scheme 1 Cyclisation mechanisms from GGPP to clitopilene (**1**) by CpTS1. The numbers in blue boxes are computed energies relative to **A** (set as 0.0 kcal mol^{-1}), numbers in black boxes are reaction barriers, and numbers in red boxes are Gibbs free energies (all in kcal mol^{-1}, mPW1PW91/6-311+G(d,p)//B97D3/6-31g(d,p), 298 K). For each step imaginary frequences of transition states are given. Blue asterisks mark minor conformational changes between the computed product of one step and the reactant structure for the next step.

from **A** to **B**) and the overall process is strongly exergonic (ΔG = −51.1 kcal mol^{-1} for the transformations from **A** to **J**). Notably, both secondary cations **B** and **I** are well stabilised through C–C hyperconjugation and not much higher in energy than their direct precursors.

The biosynthesis of **1** was also investigated in a series of isotopic labelling experiments (Table S4, ESI†). First, the biosynthetic origin of each carbon was determined through enzymatic conversion of all 20 isotopomers of (^{13}C)GGPP that were obtained through synthesis[19,23] or enzymatically from correspondingly labelled shorter oligoprenyl pyrophosphates.[24] In all cases the incorporation of labelling was observed into positions in line with the above mechanism, which particularly confirms the skeletal rearrangements in the biosynthesis of **1** (Fig. S13 and S14, ESI†). Furthermore, the three hydride shifts along the cyclisation cascade were investigated using a strategy in which the migrating hydrogen was substituted with deuterium and its target position with ^{13}C in the same labelled GGPP precursor molecule. This should lead to a product in which deuterium is directly bound to ^{13}C yielding a moderately upfield shifted triplet signal for the labelled carbon in the ^{13}C-NMR spectrum as a result of ^{13}C–^{2}H spin coupling. The first 1,2-hydride shift from **E** to **F** was confirmed through conversion of (3-^{13}C,2-^{2}H)GGPP[19] with CpTS1, showing the expected triplet for C3 ($\Delta\delta$ = −0.50 ppm, $^{1}J_{C,D}$ = 19.2 Hz, Fig. 1A). Along similar lines, the 1,2-hydride shift from **G** to **H** was evident from an incubation of (7-^{13}C,6-^{2}H)GGPP, enzymatically prepared from (3-^{13}C,2-^{2}H)FPP[25] and IPP with *Streptomyces cyaneofuscatus* GGPP synthase (GGPPS),[19] with CpTS1 ($\Delta\delta$ = −0.54 ppm, $^{1}J_{C,D}$ = 19.5 Hz, Fig. 1B). In these two experiments, the residual signals at the original chemical shifts of C3 and C7, respectively, are due to incomplete substrate deuteration. Finally, the 1,3-hydride shift from **H** to **I** was demonstrated with (6-^{13}C,1,1-^{2}H$_2$)GGPP, obtained from (2-^{13}C)FPP and (1,1-^{2}H$_2$)IPP with GGPPS ($\Delta\delta$ = −0.52 ppm, $^{1}J_{C,D}$ = 19.0 Hz, Fig. 1C). In this case, the residual signal resulting from incomplete deuteration of the substrate shows a minor upfield shift influenced by deuterium at C1.

For the 1,3-hydride transfer from **H** to **I** also the question about the precise stereochemical course arises, *i.e.*, which of the two enantiotopic hydrogens at C1 of GGPP is migrating. This question was investigated using the stereoselectively deuterated precursors (*R*)- and (*S*)-(1-^{13}C,1-^{2}H)IPP[26] that were converted with *E. coli* isopentenyl diphosphate isomerase (IDI),[27] GGPPS and CpTS1. Product analysis through HSQC spectroscopy

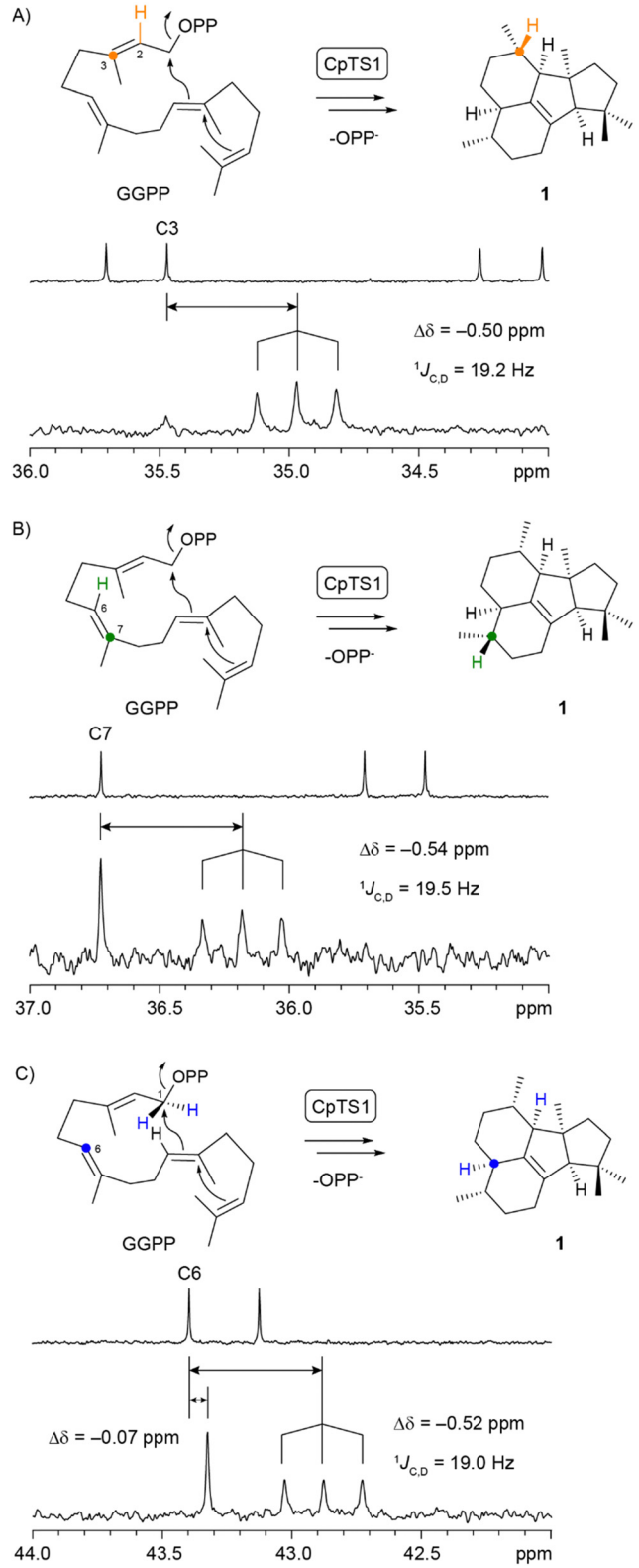

Fig. 1 The hydride shifts in the biosynthesis of **1**. (A) The 1,2-hydride shift from **E** to **F** investigated with (3-^{13}C,2-^{2}H)GGPP, (B) the 1,2-hydride shift from **G** to **H** determined with (7-^{13}C,6-^{2}H)GGPP, and (C) the 1,3-hydride migration from **H** to **I** experimentally confirmed with (6-^{13}C,1,1-^{2}H$_2$)GGPP. The upfield shifted triplets as a result of ^{13}C–^{2}H spin coupling in each experiment give evidence for the proposed hydride shifts.

revealed the specific migration of the 1-*pro-R* hydrogen of GGPP (blue in Scheme 1), while the 1-*pro-S* hydrogen (red) remains bound to C1 (Fig. S15, ESI†).

The same experiment also introduced stereoselective deuterations at C5, C9 and C13 of **1**, resulting in artificial stereogenic centres of known configurations[28] at these carbons. The NOESY based assignments for the relative orientations of the hydrogens with respect to the naturally present stereogenic centres in **1** allowed to conclude on its absolute configuration that is represented by the structure in Scheme 1 (Fig. S16, ESI†). Additional experiments using DMAPP and (*E*)- or (*Z*)-(4-^{13}C,4-^{2}H)IPP[17] introduced stereoselective deuterations at C4, C8 and C12, leading to a confirmation for the absolute configuration of **1** (Fig. S17, ESI†).

The second enzyme (CpTS2, accession no. PP777466) contained the Asp-rich motif ^{86}DEYSD, the pyrophosphate sensor Arg178, the NSE triad ^{222}NDLYSYNVE and the ^{312}RY pair (Fig. S18, ESI†). This enzyme did not accept GPP or GFPP as a substrate, but efficiently converted FPP, resulting in the formation of an unknown sesquiterpene (**2**) besides minor amounts of pentalenene (**3**) and other trace compounds (Table S5 and Fig. S19, ESI†). Furthermore, a small production of a diterpene hydrocarbon from GGPP was observed, but was insufficient for compound isolation. The main product from FPP was isolated and structurally characterised as the new sesquiterpene isopentalenene (Scheme 2 and Table S6 and Fig. S20–S27, ESI†). Its absolute configuration was determined through stereoselective deuteration experiments with (*E*)- and (*Z*)-(4-^{13}C,4-^{2}H)IPP (Fig. S28, ESI†). The biosynthesis of **3** has intensively been studied,[29–38] and compound **2** is the alternative deprotonation product from the terminal intermediate to **3**.

In summary, we have investigated two new terpene synthases from the pleuromutilin producing fungus *Clitopilus passeckerianus*. The first enzyme CpTS1 is a diterpene synthase for clitopilene, a diterpene hydrocarbon with a novel skeleton. Its biosynthesis was deeply studied through isotopic labelling experiments and DFT calculations. While the first steps are analogous to those catalysed by other cyclopentane forming diterpene synthases,[39] the later steps are specific to CpTS1 and proceed through a remarkable

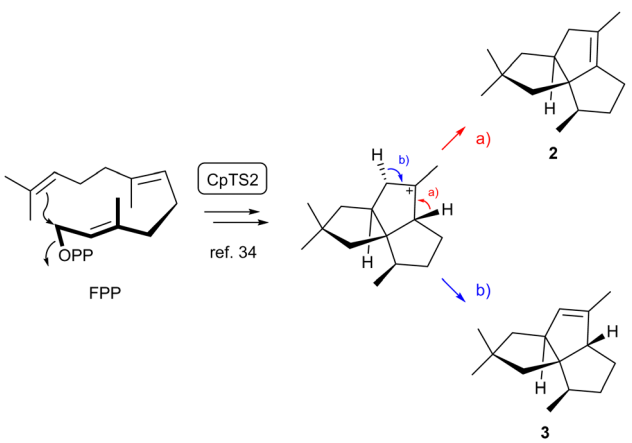

Scheme 2 Conversion of FPP into isopentalenene (**2**, main product) and pentalenene (3, minor product) by CpTS2.

1,3-hydride shift leading to a well stabilised secondary cation, followed by skeletal rearrangement.

The second enzyme CpTS2 was characterised as a sesquiterpene synthase for the new compound isopentalenene, a double bond isomer of pentalenene known from *Streptomyces exfoliatus*. One of the trace products of this enzyme was identified as the biosynthetically related compound protoillud-6-ene. Notably, CpTS2 shows amino acid sequence identities between 52% and 48% to previously described protoillud-6-ene synthases from *Stereum hirsutum* (accession numbers P9WEW0 and P9WEW1)[40] and from *Agrocybe aegerita* (QGA30882 and QGA30883),[41] suggesting a common ancestor of these fungal enzymes.

This work was funded by the Deutsche Forschungsgemeinschaft (project number 513548540) and by the computing center of the University of Cologne (RRZK), providing CPU time on the DFG-funded supercomputer CHEOPS.

Data availability

The data supporting this article have been included as part of the ESI.†

Conflicts of interest

There are no conflicts to declare.

References

1 M. C. Wani, H. L. Taylor, M. E. Wall, P. Coggon and A. T. McPhail, *J. Am. Chem. Soc.*, 1971, **93**, 2325–2327.
2 A. E. Koepp, M. Hezari, J. Zajicek, B. Stofer Vogel, R. E. LaFever, N. G. Lewis and R. Croteau, *J. Biol. Chem.*, 1995, **270**, 8686–8690.
3 J.-M. Liu, M.-Y. Ni, J.-F. Fan, Y.-Y. Tu, Z.-H. Wu, Y.-L. Wu and W.-S. Chou, *Acta Chim. Sin.*, 1979, **37**, 129–143.
4 Y.-J. Chang, S.-H. Song, S.-H. Park and S.-U. Kim, *Arch. Biochem. Biophys.*, 2000, **383**, 178–184.
5 T. E. Wallaart, H. J. Bouwmeester, J. Hille, L. Poppinga and N. C. A. Maijers, *Planta*, 2001, **212**, 460–465.
6 M. D. Sayed, A. Riszk, F. M. Hammouda, M. M. El-Missiry, E. M. Williamson and F. J. Evans, *Experientia*, 1980, **36**, 1206–1207.
7 C. J. Mau and C. A. West, *Proc. Natl. Acad. Sci. U. S. A.*, 1994, **91**, 8497–8501.
8 A. J. King, G. D. Brown, A. D. Gilday, T. R. Larson and I. A. Graham, *Plant Cell*, 2014, **26**, 3286–3298.
9 F. H. Kavanagh, A. Hervey and W. J. Robbins, *Proc. Natl. Acad. Sci. U. S. A.*, 1951, **37**, 570–574.
10 M. Yamane, A. Minami, C. Liu, T. Ozaki, I. Takeuchi, T. Tsukagoshi, T. Tokiwano, K. Gomi and H. Oikawa, *ChemBioChem*, 2017, **18**, 2317–2322.
11 F. Albertini, K. Khairudin, E. R. Venegas, J. A. Davies, P. M. Hayes, C. L. Willis, A. M. Bailey and G. D. Foster, *Nat. Commun.*, 2017, **8**, 1831.
12 M. Xu, M. Jia, Y. J. Hong, X. Yin, D. J. Tantillo, P. J. Proteau and R. J. Peters, *Org. Lett.*, 2018, **20**, 1200–1202.
13 C. Lemke, O. Whitham and R. J. Peters, *Org. Biomol. Chem.*, 2020, **18**, 5586–5588.
14 T. Schafhauser, D. Wibberg, A. Binder, C. Rückert, T. Busche, W. Wohlleben and J. Kalinowski, *J. Fungi*, 2022, **8**, 862.
15 V. M. Dixit, F. M. Laskovics, W. I. Noall and C. D. Poulter, *J. Org. Chem.*, 1981, **46**, 1967–1969.
16 T. Toyomasu, A. Kaneko, T. Tokiwano, Y. Kanno, Y. Kanno, R. Niida, S. Miura, T. Nishioka, C. Ikeda, W. Mitsuhashi, T. Dairi, T. Kawano, H. Oikawa, N. Kato and T. Sassa, *J. Org. Chem.*, 2009, **74**, 1541–1548.
17 L. Lauterbach, J. Rinkel and J. S. Dickschat, *Angew. Chem., Int. Ed.*, 2018, **57**, 8280–8283.
18 J. Rinkel, S. T. Steiner and J. S. Dickschat, *Angew. Chem., Int. Ed.*, 2019, **58**, 9230–9233.
19 P. Rabe, J. Rinkel, E. Dolja, T. Schmitz, B. Nubbemeyer, T. H. Luu and J. S. Dickschat, *Angew. Chem., Int. Ed.*, 2017, **56**, 2776–2779.
20 T. Mitsuhashi, T. Kikuchi, S. Hoshino, M. Ozeki, T. Awakawa, S.-P. Shi, M. Fujita and I. Abe, *Org. Lett.*, 2018, **20**, 5606–5609.
21 B. Qin, Y. Matsuda, T. Mori, M. Okada, Z. Quan, T. Mitsuhashi, T. Wakimoto and I. Abe, *Angew. Chem., Int. Ed.*, 2016, **55**, 1658–1661.
22 Y. J. Hong and D. J. Tantillo, *Aust. J. Chem.*, 2017, **70**, 362–366.
23 Z. Quan and J. S. Dickschat, *Org. Biomol. Chem.*, 2020, **18**, 6072–6076.
24 P. Rabe, L. Barra, J. Rinkel, R. Riclea, C. A. Citron, T. A. Klapschinski, A. Janusko and J. S. Dickschat, *Angew. Chem., Int. Ed.*, 2015, **54**, 13448–13451.
25 T. A. Klapschinski, P. Rabe and J. S. Dickschat, *Angew. Chem., Int. Ed.*, 2016, **55**, 10141–10144.
26 J. Rinkel and J. S. Dickschat, *Org. Lett.*, 2019, **21**, 2426–2429.
27 F. M. Hahn, A. P. Hurlburt and C. D. Poulter, *J. Bacteriol.*, 1999, **181**, 4499–4504.
28 J. W. Cornforth, R. H. Cornforth, G. Popjak and L. Yengoyan, *J. Biol. Chem.*, 1966, **241**, 3970–3987.
29 D. E. Cane, C. Abell, R. Lattman, C. T. Kane, B. R. Hubbard and P. H. M. Harrison, *J. Am. Chem. Soc.*, 1988, **110**, 4081–4082.
30 D. E. Cane, J. S. Oliver, P. H. M. Harrison, C. Abell, B. R. Hubbard, C. T. Kane and R. Lattman, *J. Am. Chem. Soc.*, 1988, **110**, 5922–5923.
31 D. E. Cane, J. S. Oliver, P. H. M. Harrison, C. Abell, B. R. Hubbard, C. T. Kane and R. Lattman, *J. Am. Chem. Soc.*, 1990, **112**, 4513–4524.
32 D. E. Cane, J.-K. Sohng, C. R. Lamberson, S. M. Rudnicki, Z. Wu, M. D. Lloyd, J. S. Oliver and B. R. Hubbard, *Biochemistry*, 1994, **33**, 5846–5857.
33 D. E. Cane and A. M. Tillman, *J. Am. Chem. Soc.*, 1983, **105**, 122–124.
34 P. Gutta and D. J. Tantillo, *J. Am. Chem. Soc.*, 2006, **128**, 6172–6179.
35 M. W. Lodewyk, D. Willenbring and D. J. Tantillo, *Org. Biomol. Chem.*, 2014, **12**, 887–894.
36 M. Seemann, G. Zhai, K. Umezawa and D. E. Cane, *J. Am. Chem. Soc.*, 1999, **121**, 591–592.
37 L. Zu, M. Xu, M. W. Lodewyk, D. E. Cane, R. Peters and D. J. Tantillo, *J. Am. Chem. Soc.*, 2012, **134**, 11369–11371.
38 H. Xu, T. G. Köllner, F. Chen and J. S. Dickschat, *Org. Biomol. Chem.*, 2024, **22**, 1360–1364.
39 A. Minami, T. Ozaki, C. Liu and H. Oikawa, *Nat. Prod. Rep.*, 2018, **35**, 1330–1346.
40 M. B. Quin, C. M. Flynn, G. T. Wawrzyn, S. Choudhary and C. Schmidt-Dannert, *ChemBioChem*, 2013, **14**, 2480–2491.
41 C. Zhang, X. Chen, A. Orban, S. Shukal, F. Birk, H.-P. Too and M. Rühl, *ACS Chem. Biol.*, 2020, **15**, 1268–1277.

Appendices F

A Hydrophobic Tunnel and a Gatekeeper at the Active Site Entrance in Two Type I Terpene Synthases

ACS Catal. **2025**, *15*, 6209–6215.

DOI: 10.1021/acscatal.5c01540.

ACS Catalysis

pubs.acs.org/acscatalysis Letter

A Hydrophobic Tunnel and a Gatekeeper at the Active Site Entrance in Two Type I Terpene Synthases

Heng Li,[▽] Zhaoye Bai,[▽] Georges B. Tabekoueng, Baiying Xing, Bernd Goldfuss, Ming Ma, Donghui Yang,* and Jeroen S. Dickschat*

Cite This: *ACS Catal.* 2025, 15, 6209–6215 Read Online

ACCESS | Metrics & More | Article Recommendations | Supporting Information

ABSTRACT: The diterpene synthase *Sx*SpS is known to produce spata-13,17-diene from geranylfarnesyl diphosphate (GGPP), but can also convert farnesyl diphosphate (FPP) and GFPP into structurally similar terpenes. Here we demonstrate that *Sx*SpS is even able to produce a triterpene from FFPP. This behavior is explained by a hydrophobic tunnel observed crystallograpghically that is connected to the active site and can accommodate nonreacting spectator isoprenoid units, as demonstrated by extensive docking studies. The tunnel is contoured by three small amino acid residues, and their systematic exchange against larger residues disrupts the acceptance of higher oligoprenyl diphosphates. A similar tunnel in selina-4(15),7(11)-diene synthase (SdS) is blocked by a gatekeeper, but its opening through site-directed mutagenesis leads to formation of a diterpene.

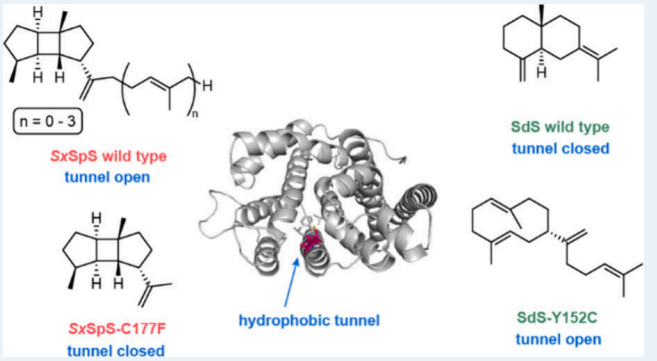

KEYWORDS: *enzyme engineering, substrate promiscuity, terpenes, protein crystallography, MD simulations*

INTRODUCTION

Terpene synthases (TSs) are remarkable biocatalysts that can introduce unprecedented structural complexity into structurally simple terpene precursors in just one enzymatic step. These reactions proceed with a change of hybridization and bonding status of often more than half of the carbons.[1] This is explainable by cationic cascade reactions, i.e., the processes inside the active site cavity of a TS are in fact multistep transformations, and the intermediates can—as a consequence of their short lifetimes and low concentrations—neither be observed nor isolated. Therefore, mechanistic investigations rely on indirect strategies, including isotopic labeling experiments,[2] the enzymatic transformation of substrate analogues with blocked or changed reactivity,[3] and structure-based site-directed mutagenesis,[4] or on computational data.[5]

For the modular type of polyketide biosynthesis, a sequence of logic and stepwise transformations is catalyzed by domains and modules that are arranged like pearls on a string. Enzyme functional and thus structural predictions for the products of polyketide synthases can today be made with some confidence.[6] In contrast, it is still impossible to predict the structure of a TS product from the enzyme's amino acid sequence. Several recent studies have focused on engineering approaches to rationally alter the product profiles of terpene synthases,[7−21] including changes of the substrate tolerance. Despite the insights gained from these studies, predictions about the preferred substrate of TSs are difficult, and some enzymes have the potential to accept several terpenoid substrates. An example is the bacterial spatadiene synthase from *Streptomyces xinghaiensis* (*Sx*SpS) that makes the main product spata-13,17-diene (**1b**) from geranylgeranyl diphosphate (GGPP, C_{20}), besides small amounts of prenylkelsoene (**2b**) and cneorubin Y (**3b**) (Figure 1).[7] The biosynthesis of these products is explained by a 1,10-cyclization of GGPP to **A**, followed by a deprotonation with cyclopropanation to **3b**. A reprotonation induced cyclization to **B**, and sacrificial carbocyclization with opening of the cyclopropane ring can lead to **C** and **D** as the direct precursors of **1b** and **2b**, respectively.

Also, farnesyl (FPP, C_{15}) and geranylfarnesyl diphosphate (GFPP, C_{25}) are converted by *Sx*SpS through analogous reactions, albeit with lower efficiency, while geranyl diphosphate (GPP, C_{10}) is not accepted. In the present study, we solved the X-ray structure of *Sx*SpS in the open conformation, revealing a hydrophobic tunnel between helices C and F that explains the observed remarkable substrate tolerance. The precise role of this tunnel was investigated through docking

Received: March 5, 2025
Revised: March 28, 2025
Accepted: March 31, 2025
Published: April 2, 2025

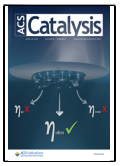

https://doi.org/10.1021/acscatal.5c01540
ACS Catal. 2025, 15, 6209−6215

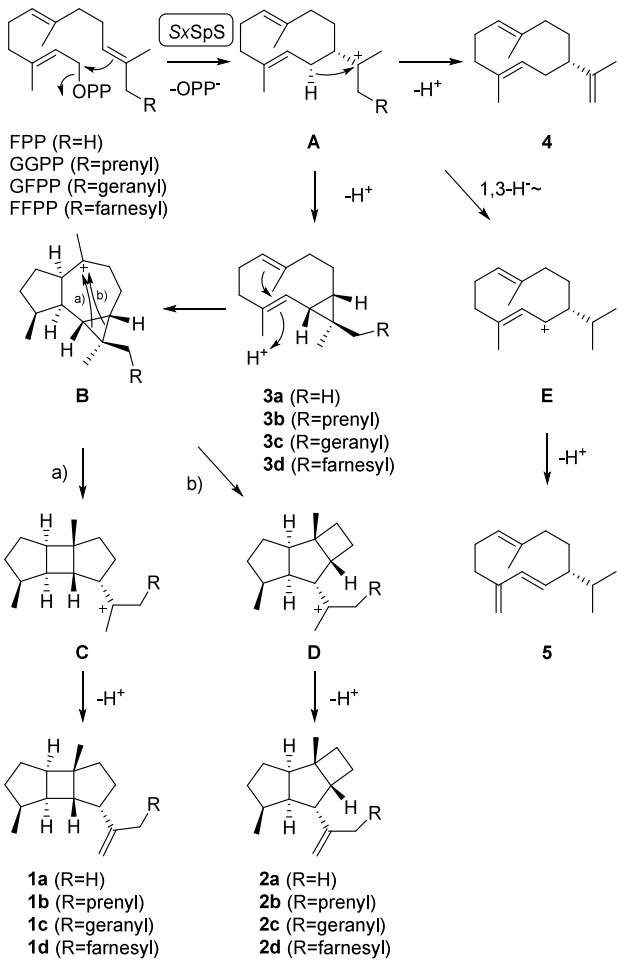

Figure 1. Products and cyclization mechanism of *Sx*SpS.

studies and site-directed mutagenesis experiments. A similar tunnel is observed in selina-4(15),7(11)-diene synthase (SdS), but here the tunnel is blocked by a gatekeeper residue. Enzyme engineering through opening of this tunnel widened the substrate scope of SdS for the conversion of GGPP.

RESULTS AND DISCUSSION

For the current study, a TS homologue from *Streptomyces platensis* DSM 40041 (accession number WP_085926110) was investigated. This enzyme is closely related to the *epi*-cubenol synthase from *Streptomyces griseus* NBRC 13350[22] (Figure S1) and shows all highly conserved motifs required for enzyme function (Figure S2), including the Asp-rich motif (^{77}DDQLDD),[23] the NSE triad (^{224}NDVYSLAKE),[24] the ^{312}RY pair,[25] and the pyrophosphate sensor (Arg178).[26] Its gene was cloned into the expression vector pYE-Express,[27] and the purified recombinant enzyme (Figure S3) was tested with substrates GPP, FPP, GGPP, and GFPP (Figures S4 and S5, Table S2). The highest activity was observed with GGPP that was converted into spata-13,17-diene (**1b**) as the main product and prenylkelsoene (**2b**) as a side product, identifying the enzyme from *S. platensis* as a spata-13,17-diene synthase (*Sp*SpS). This result was unexpected because *Sp*SpS is monophyletic to *epi*-cubenol synthases and polyphyletically separated from *Sx*SpS (Figure S6) and because *Sp*SpS and *Sx*SpS showed only 53% amino acid sequence identity. Also, some previous cases of phylogenetically distant TSs are known that make the same product. For instance, the (+)-*epi*-cubenol synthases from *Streptomyces griseus* NBRC 13350[22] and *Nonomuraea coxensis* DSM 45129[28] show an amino acid sequence identity of only 28%, and the (+)-T-muurolol synthases from *Streptomyces clavuligerus* ATCC 27064[29] and *Roseiflexus castenholzii* DSM 13941[30] exhibit only 31% amino acid sequence identity. Good production by *Sp*SpS was also observed with GFPP as the substrate, yielding prenylspata-13,17-diene (**1c**) and geranylkelsoene (**2c**), which were both isolated and characterized by NMR spectroscopy (Tables S3 and S4, Figures S7−S22). Compound **2c** was previously tentatively identified by GC/MS as a product of *Sx*SpS but has not been isolated before. *Sp*SpS showed a similar product pattern as *Sx*SpS with FPP, including bicyclogermacrene (**3a**), germacrene A (**4**), and germacrene D (**5**), and only formed acyclic products besides traces of limonene from GPP (Figure S4, Table S2).

We recently discovered three fungal nonsqualene triterpene synthases that convert farnesylfarnesyl diphosphate (FFPP, C_{30}) into triterpenes.[31] The substrate tolerance of *Sx*SpS ranging from FPP to GFPP prompted the question of whether FFPP can also be converted by this enzyme. Remarkably, FFPP was indeed accepted but only converted sluggishly into a triterpene hydrocarbon (Figure S23), likely because FFPP is poorly soluble in the aqueous medium. Nevertheless, the product was formed in sufficient amount for compound isolation, allowing its structural characterization as geranylspata-13,17-diene (**1d**) (Table S5, Figures S24−S30). Furthermore, farnesylkelsoene (**2d**) was tentatively identified as a side product by GC/MS (Figure S23) The substrate flexibility of *Sx*SpS was further demonstrated by the conversion of *iso*-GGPP III, a synthetic GGPP analogue with a shifted double bond,[32] resulting in the formation of *iso*-spata-13,17-diene (**6**) (Figure 2, Table S6, Figures S31−S38).

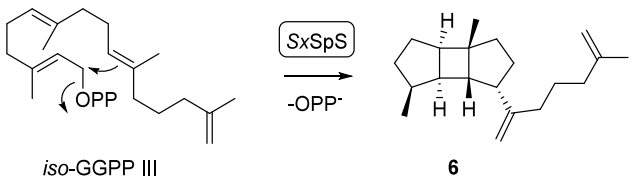

Figure 2. Conversion of *iso*-GGPP III by *Sx*SpS.

All compounds produced by *Sx*SpS from the substrates FPP, GGPP, GFPP, FFPP, and *iso*-GGPP III are formed with participation of only the first three isoprene units in the cyclization cascade, while eventually attached further units are only present as spectators not directly involved in the reaction. To investigate this interesting phenomenon in depth, an X-ray crystal structure of *Sx*SpS was obtained in the open conformation in complex with one Mg^{2+} bound to the NSE triad, named *Sx*SpS-Mg^{2+} (Figure 3A, Table S7). This structure showed the typical α-helical fold of type I terpene synthases first reported for avian farnesyl diphosphate synthase[33] and the unique helix G break motif with the effector triad ^{207}GAI involved in substrate ionization. The first 28 amino acid residues of *Sx*SpS-Mg^{2+} appeared disordered (Figure S39) and may represent an anchor to an unknown cellular target. Notably, removal of these residues did not affect enzyme activity (Figure S40), and MD simulations of the protein in a periodic water box of 1 000 000 Å^3 over 10 ps at 298.15 K gave no hints that the disordered loop structure may

https://doi.org/10.1021/acscatal.5c01540
ACS Catal. 2025, 15, 6209−6215

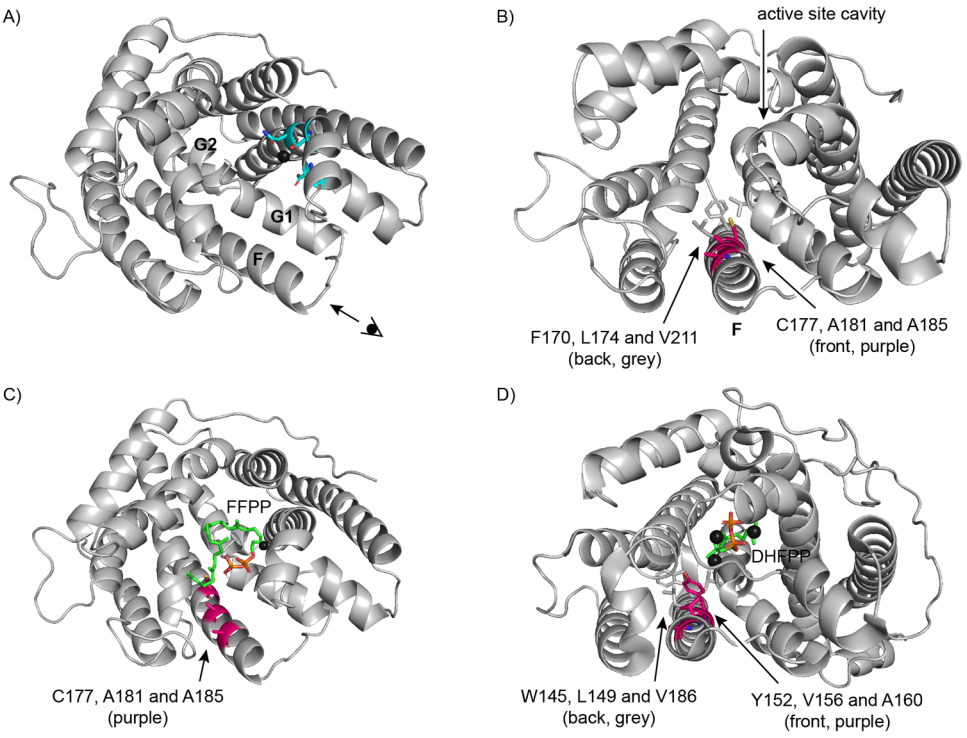

Figure 3. X-ray crystal structure of *Sx*SpS-Mg^{2+}. (A) Open conformation in complex with one Mg^{2+} (*Sx*SpS-Mg^{2+}). The NSE triad binding to Mg^{2+} is shown in cyan. The stylized eye and the arrow indicate the view into the substrate tunnel. (B) View into the substrate tunnel that is limited at the bottom by F170, L174, and V211 (gray). The small residues C177, A181, and A185 (purple) create the space to accommodate spectator isoprene units. (C) Docking of FFPP to *Sx*SpS shows that its tail stretches out into the hydrophobic tunnel. (D) Crystal structure of SdS (PDB: 4OKZ) showing the analogous residues Y152, V156, and A160 (purple). The gatekeeper Y152 blocks the entrance to the hydrophobic tunnel. Mg^{2+} are shown as black spheres, DHFPP = 1,2-dihydro-FPP.

close the observed substrate tunnel (Supporting Movie 1). Even prolonged simulations over 10 ns at 373.15 K did not lead to major conformational changes (Supporting Movie 2).

The *Sx*SpS-Mg^{2+} crystal structure revealed the presence of a hydrophobic tunnel along helix F that is directly connected to the active site and closed at the back by the three residues, namely, F170, L174, and V211 (Figure 3B). This tunnel is kept open by three aligned small residues (C177, A181 and A185) and is ca. 12 Å long and 5 Å in diameter, exhibiting a space of ~250 $Å^3$, which is sufficient to accommodate up to three isoprene units (the calculated van der Waals volume of one isoprene is 74 $Å^3$).[15,34] Thus, the tunnel may take up the spectator units and explain their nonparticipation in the cyclization reaction. This hypothesis was tested by docking the substrate FFPP into the *Sx*SpS-Mg^{2+} structure, revealing that its tail can indeed stretch out into the hydrophobic tunnel (Figure 3C). Analogously, docking of GFPP and GGPP resulted in the binding of the substrate tails to the substrate tunnel (Figure S41).

A comparison of the *Sx*SpS-Mg^{2+} structure to the X-ray structure of selina-4(15),7(11)-diene synthase in complex with three Mg^{2+} ions and the substrate analogue 1,2-dihydro-FPP (SdS, PDB: 4OKZ)[26] reveals that the positions of the spacious substrate tunnel are in two cases occupied by larger residues (Y152 and V156), while the most distant residue from the active site is in both cases Ala (compare Figures 3B and D). Thus, in SdS the tunnel entrance is blocked by the gatekeeper Y152, and as a consequence SdS can only catalyze the conversion of FPP into selina-4(15),7(11)-diene (**10**, Figure 4) but does not accept larger substrates such as GGPP and GFPP. Interestingly, the position of C177 is highly conserved

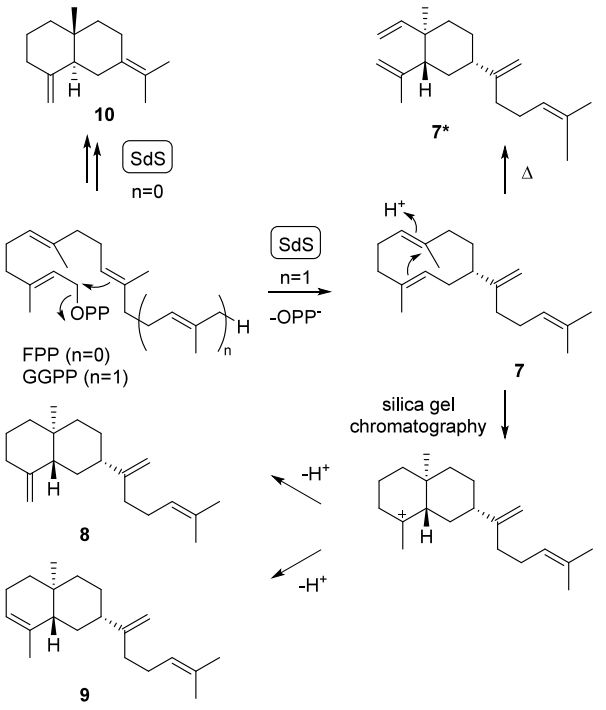

Figure 4. Conversion of FPP into **10** and of GGPP into **7** by SdS, followed by thermal rearrangement to **7*** or acid-induced cyclization to **8** and **9**.

in *Sx*SpS and 36 SpS homologues from other organisms (Figure S42), whereas all 212 *epi*-cubenol synthase homo-

https://doi.org/10.1021/acscatal.5c01540
ACS Catal. 2025, 15, 6209−6215

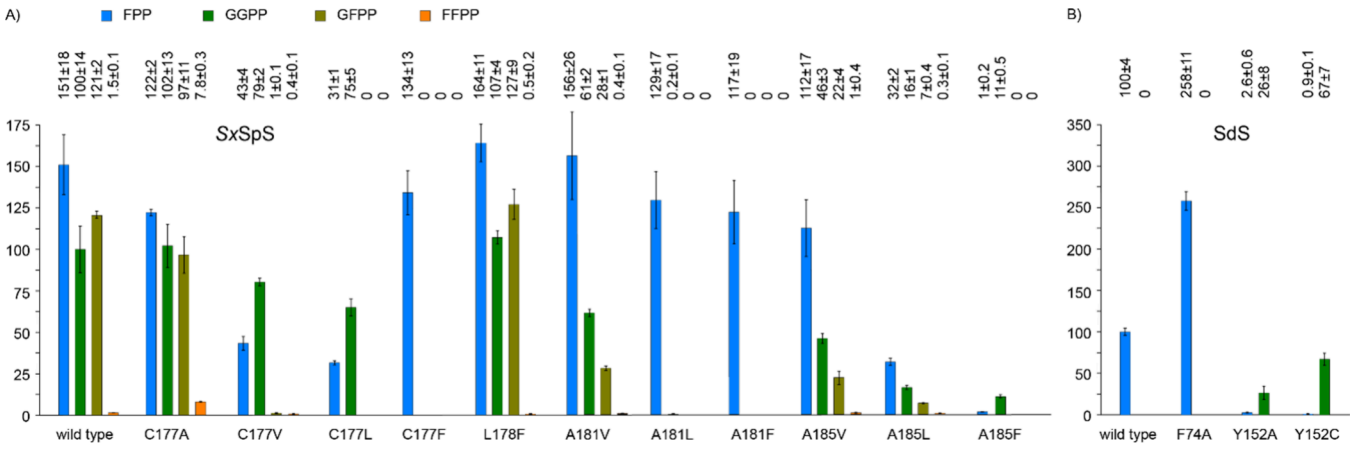

Figure 5. Relative terpene production of (A) *Sx*SpS and (B) SdS (wild type and enzyme variants). Blue bars represent products from FPP, green bars represent products from GGPP, olive bars represent products from GFPP, and orange bars represent products from FFPP. The sesquiterpene production of SdS and the diterpene production of *Sx*SpS were set to 100%. All data were obtained from triplicate (mean ± standard deviation, Tables S9 and S10).

logues included in the tree shown in Figure S6 contain a Tyr in this position (one exemplary sequence of the functionally characterized *epi*-cubenol synthase from *S. griseus*[22] was added to Figure S42), which may be an important structural difference to switch between the function as a synthase for sesquiterpenes or diterpenes and even higher terpenes.

The roles of the small tunnel residues in *Sx*SpS and of the gatekeeper in SdS were tested through a series of systematic site-directed mutagenesis experiments (Figure 5A, Tables S8–S10). Indeed, the C177F variant of *Sx*SpS completely lost the activity with GGPP and larger substrates, while sesquiterpene synthase activity was retained. The C177V and C177L enzyme variants lost sester- and triterpene synthase activity (only traces were observed in the C177V variant) but retained sesqui- and diterpene production. The exchange of C177 against a smaller residue (C177A) showed the strongest effect for triterpene production, which was almost four times higher than with the wild type enzyme. Overall, there is a clear trend for position 177: the smaller the residue in this position is, the more effective larger substrates can be accepted.

The next position going outward from the active site is A181. If a large residue is introduced in this position (A181F), the enzyme can only convert FPP, but none of the larger substrates. For a smaller residue as in the A181L variant, traces of diterpenes can be formed from GGPP, and the A181V exchange only leads to reduced amounts of products from all substrates larger than FPP. Again, the same inverse correlation between the size of the residue and the tolerance toward large substrates is observed.

For the most exterior position A185, exchange against a large residue (A185F) leads to a loss of sester- and triterpene synthase activity, with reduced production of sesqui- and diterpenes. For the A185L variant, terpene production from all four substrates was reduced, and a similar but less pronounced effect was observed for the A185V variant. Also for this position, the introduction of large substrates had an especially negative impact for the production of terpenes from large substrates. The reason why sesquiterpene production is also strongly affected in the A185F variant is unclear, but a possible explanation may be a major structural disturbance.

The *Sx*SpS-Mg^{2+} structure aligned well with an AlphaFold2 model of *Sx*SpS with rmsd = 0.577, suggesting that docking studies with enzyme variants can be done with their AlphaFold2-generated structures. Such docking experiments with the *Sx*SpS-C177Y model and GGPP, GFPP, or FFPP did not lead to any meaningful enzyme−substrate complexes. Taken together, the introduction of large residues in all three positions of the hydrophobic tunnel had an especially negative impact on sester- and triterpene biosynthesis, in agreement with the hypothesis that this tunnel can occupy spectator units during terpene cyclization.

On the contrary, exchange of the gatekeeper Y152 in SdS against smaller residues (Y152A and Y152C) resulted in the acceptance of GGPP and its conversion into one diterpene hydrocarbon, which showed a thermal reaction during GC/MS analysis (Figures 5B and S43). This compound was isolated from the more productive Y152C variant and structurally characterized as prenylgermacrene A (**7**) (Figure 4, Table S11, Figures S44–S51). Germacrene A (**4**) is known to undergo a Cope rearrangement to *β*-elemene,[35−37] suggesting a rearrangement of **7** to prenyl-*β*-elemene (**7***) during GC/MS analysis.

Upon chromatographic purification, not only **7** but also known lobophytumin C (**8**)[38] and prenyl-*α*-selinene (**9**) were isolated (Tables S12 and S13, Figures S52–S67). These bicyclic hydrocarbons were formed during the contact with slightly acidic silica gel, similar to the reported behavior of **4** that reacts to *α*- and *β*-selinene upon column chromatographic purification.[35,39] Heating of a solution of **7** in Ph_2O to 180 °C in a pressurized tube gave access to the Cope rearrangement product **7*** (Table S14, Figures S68–S75).

The absolute configurations of **7**–**9** and **7*** were determined by comparing optical rotations to previously reported data for the same or structurally related compounds (Figure S76).[35,38,40,41] An independent method to establish the absolute configuration of **7** made use of a stereoselective deuteration strategy (labeling experiments are summarized in Table S15). Dimethylallyl diphosphate (DMAPP) plus (*R*)- or (*S*)-(1-^{13}C,1-^{2}H)IPP[37] were converted with *Streptomyces cyaneofuscatus* GGPP synthase (GGPPS)[42] and SdS-Y152C into **7** containing stereoselectively deuterated carbons of known configuration.[43] The relative orientation of the naturally present to the artificially introduced stereogenic centers allowed the identification of the absolute configuration of **7**

https://doi.org/10.1021/acscatal.5c01540
ACS Catal. 2025, 15, 6209−6215

(Figure S77). The additional ^{13}C-label in these experiments enabled a highly sensitive analysis through HSQC spectroscopy. Analogous experiments with DMAPP plus (*E*)- or (*Z*)-(4-^{13}C,4-^{2}H)IPP[44] demonstrated the same absolute configuration of **7** (Figure S78). Upon heating of the samples from all four labeling experiments the Cope rearrangement to **7*** was induced, and analysis through HSQC spectroscopy gave insights into its absolute configuration (Figure S79 and S80).

CONCLUSIONS

In conclusion, *Sx*SpS not only has sesqui-, di-, and sesterterpene synthase activity but also can convert FFPP into a triterpene hydrocarbon. After the discovery of three fungal enzymes,[31] *Sx*SpS represents the first bacterial non-squalene triterpene synthase. All substrates from FPP to FFPP are cyclized with participation of only the first three units, always leading to the same tricyclic core; additional terpene units have a spectator role and just remain attached as a tail. We have identified a hydrophobic tunnel linked to the active site that can explain this behavior: only the first three terpene units of each substrate can enter the active site, and they always adopt the same conformation, explaining analogous cyclization reactions for all substrates. Additional terpene units accommodate the hydrophobic tunnel and do not participate in the terpene cyclization process. This interpretation is supported by the effects upon closing the tunnel at its entrance: exchange of a small to a large residue (C177F) completely disrupts the activity for all substrates larger than FPP. A similar hydrophobic tunnel is observed in SdS, but here the entrance into this tunnel is naturally blocked by a large residue. Opening of the tunnel through exchange to a small residue enables the conversion of GGPP, with participation of only the first three terpene units.

Hydrophobic tunnels stretching out from the active site are also observed in *Streptomyces viridochromogenes* 7-*epi*-α-eudesmol synthase (*Sv*ES)[30,45] and *Streptomyces pratensis* (1(10)*E*,4*E*,6*S*,7*R*)-germacradien-6-ol synthase (*Sp*GdolS),[46] but in these enzymes the entrance into the tunnel is also blocked by large residues (Figure S81). We will investigate these and other type I TSs for the possibility to open these tunnels for expanded substrate acceptance in due course. Also, further structural work aiming at a ligated enzyme complex is ongoing to experimentally show the accommodation of spectator units by the hydrophobic tunnel of *Sx*SpS.

MATERIALS AND METHODS

Materials and methods are described in detail in the Supporting Information.

ASSOCIATED CONTENT

Supporting Information

The Supporting Information is available free of charge at https://pubs.acs.org/doi/10.1021/acscatal.5c01540.

Experimental details, phylogenetic tree of bacterial terpene synthases, X-ray structural data, detailed results of site-directed mutagenesis experiments, spectroscopic data, NMR spectra, and determination of the absolute configurations of isolated compounds (PDF)

Movie showing an MD simulation of *Sx*SpS with the following conditions: 10 ps at 298.15 K (MP4)

Movie showing an MD simulation of *Sx*SpS with the following conditions: 10 ns at 373.15 K (MP4)

AUTHOR INFORMATION

Corresponding Authors

Jeroen S. Dickschat − *Kekulé-Institute for Organic Chemistry and Biochemistry, University of Bonn, 53121 Bonn, Germany*; orcid.org/0000-0002-0102-0631; Email: dickschat@uni-bonn.de

Donghui Yang − *State Key Laboratory of Natural and Biomimetic Drugs, School of Pharmaceutical Sciences, Beijing University, Beijing 100191, China*; Email: ydhui@bjmu.edu.cn

Authors

Heng Li − *Kekulé-Institute for Organic Chemistry and Biochemistry, University of Bonn, 53121 Bonn, Germany*; orcid.org/0000-0002-6406-7269

Zhaoye Bai − *State Key Laboratory of Natural and Biomimetic Drugs, School of Pharmaceutical Sciences, Beijing University, Beijing 100191, China*

Georges B. Tabekoueng − *Kekulé-Institute for Organic Chemistry and Biochemistry, University of Bonn, 53121 Bonn, Germany*

Baiying Xing − *State Key Laboratory of Natural and Biomimetic Drugs, School of Pharmaceutical Sciences, Beijing University, Beijing 100191, China*

Bernd Goldfuss − *Department of Chemistry, University of Cologne, 50939 Cologne, Germany*; orcid.org/0000-0002-1814-8818

Ming Ma − *State Key Laboratory of Natural and Biomimetic Drugs, School of Pharmaceutical Sciences, Beijing University, Beijing 100191, China*; orcid.org/0000-0001-8311-3892

Complete contact information is available at: https://pubs.acs.org/10.1021/acscatal.5c01540

Author Contributions

[▽]H.L. and Z.B. contributed equally. J.S.D. designed the research, H.L. and G.B.T. performed all chemical and biochemical experiments, B.G. performed MD simulations, Z.B. and B.X. performed the crystallization and X-ray diffraction data collection, D.Y. and M.M. performed the crystal structure elucidation and analyzed the structure, and J.S.D. wrote the manuscript with contributions by all authors.

Notes

The authors declare no competing financial interest.

ACKNOWLEDGMENTS

This work was funded by the Deutsche Forschungsgemeinschaft (project number 513548540); by the computing center of the University of Cologne (RRZK), which provided CPU time on the DFG-funded supercomputer RAMSES; by the National Natural Science Foundation of China (grant numbers 82325046 and 22377004); and by the Alexander von Humboldt Foundation with a Georg Forster Research Fellowship (to G.B.T.).

REFERENCES

(1) Christianson, D. W. Structural and Chemical Biology of Terpenoid Cyclases. *Chem. Rev.* **2017**, *117*, 11570−11648.

(2) Dickschat, J. S. Bacterial Diterpene Biosynthesis. *Angew. Chem., Int. Ed.* **2019**, *58*, 15964−15976.

(3) Chow, S. Y.; Williams, H. J.; Huang, Q.; Nanda, S.; Scott, A. I. Studies on Taxadiene Synthase: Interception of the Cyclization Cascade at the Isocembrene Stage with GGPP Analogs. *J. Org. Chem.* **2005**, *70*, 9997−10003.

(4) Seemann, M.; Zhai, G.; Umezawa, K.; Cane, D. Pentalenene Synthase. Histidine-309 Is Not Required for Catalytic Activity. *J. Am. Chem. Soc.* **1999**, *121*, 591−592.
(5) Tantillo, D. J. Biosynthesis *via* carbocations: Theoretical studies on terpene formation. *Nat. Prod. Rep.* **2011**, *28*, 1035−1053.
(6) Weissman, K. J. Polyketide stereocontrol: a study in chemical biology. *Beilstein J. Org. Chem.* **2017**, *13*, 348−371.
(7) Rinkel, J.; Lauterbach, L.; Dickschat, J. S. Spata-13,17-diene Synthase, an Enzyme with Sesqui-, Di- and Sesterterpene Synthase Activity from *Streptomyces xinghaiensis*. *Angew. Chem., Int. Ed.* **2017**, *56*, 16385−16389.
(8) Yoshikuni, Y.; Martin, V. J. J.; Ferrin, T. E.; Keasling, J. D. Engineering Cotton (+)-δ-Cadinene Synthase to an Altered Function: Germacrene D-4-ol Synthase. *Chem. Biol.* **2006**, *13*, 91−98.
(9) Kampranis, S. C.; Ioannidis, D.; Purvis, A.; Mahrez, W.; Ninga, E.; Katerelos, N. A.; Anssour, S.; Dunwell, J. M.; Degenhardt, J.; Makris, A. M.; Goodenough, P. W.; Johnson, C. B. Rational Conversion of Substrate and Product Specificity in a Salvia Monoterpene Synthase: Structural Insights into the Evolution of Terpene Synthase Function. *Plant Cell* **2007**, *19*, 1994−2005.
(10) Faraldos, J. A.; Gonzalez, V.; Senske, M.; Allemann, R. K. Templating effects in aristolochene synthase catalysis: elimination *versus* cyclisation. *Org. Biomol. Chem.* **2011**, *9*, 6920−6923.
(11) Chen, M.; Chou, W. K. W.; Al-Lami, N.; Faraldos, J. A.; Allemann, R. K.; Cane, D. E.; Christianson, D. W. Probing the Role of Active Site Water in the Sesquiterpene Cyclization Reaction Catalyzed by Aristolochene Synthase. *Biochemistry* **2016**, *55*, 2864−2874.
(12) Bian, G.; Han, Y.; Hou, A.; Yuan, Y.; Liu, X.; Deng, Z.; Liu, T. Releasing the potential power of terpene synthases by a robust precursor supply platform. *Metab. Eng.* **2017**, *42*, 1−8.
(13) Hou, A.; Dickschat, J. S. Targeting Active Site Residues and Structural Anchoring Positions in Terpene Synthases. *Beilstein J. Org. Chem.* **2021**, *17*, 2441−2449.
(14) Schriever, K.; Saenz-Mendez, P.; Rudraraju, R. S.; Hendrikse, N. M.; Hudson, E. P.; Biundo, A.; Schnell, R.; Syren, P.-O. Engineering of Ancestors as a Tool to Elucidate Structure, Mechanism, and Specificity of Extant Terpene Cyclase. *J. Am. Chem. Soc.* **2021**, *143*, 3794−3807.
(15) Hou, A.; Goldfuss, B.; Dickschat, J. S. Functional Switch and Ethyl Group Formation in the Bacterial Polytrichastrene Synthase from *Chryseobacterium polytrichastri*. *Angew. Chem., Int. Ed.* **2021**, *60*, 20781−20785.
(16) Leferink, N. G. H.; Escorcia, A. M.; Ouwersloot, B. R.; Johanissen, L. O.; Hay, S.; van der Kamp, M. W.; Scrutton, N. S. Molecular Determinants of Carbocation Cyclisation in Bacterial Monoterpene Synthases. *ChemBioChem.* **2022**, *23*, No. e202100688.
(17) Xu, H.; Dickschat, J. S. Turning a Sesquiterpene Synthase into a Di- and Sesterterpene Synthase. *ACS Catal.* **2023**, *13*, 12723−12729.
(18) Srivastava, P. L.; Johns, S. T.; Walters, R.; Miller, D. J.; van der Kamp, M. W.; Allemann, R. K. Molecular Determinants of Carbocation Cyclisation in Bacterial Monoterpene Synthases. *ACS Catal.* **2023**, *13*, 14199−14204.
(19) Srivastava, P. L.; Johns, S. T.; Voice, A.; Morley, K.; Escorcia, A. M.; Miller, D. J.; Allemann, R. K.; van der Kamp, M. W. Simulation-Guided Engineering Enables a Functional Switch in Selinadiene Synthase toward Hydroxylation. *ACS Catal.* **2024**, *14*, 11034−11043.
(20) Liu, J.-Y.; Lin, F.-L.; Taizoumbe, K. A.; Lv, J.-M.; Wang, Y.-H.; Wang, G.-Q.; Chen, G.-D.; Yao, X.-S.; Hu, D.; Gao, H.; Dickschat, J. S. A Functional Switch Between Asperfumene and Fusicoccadiene Synthase and Entrance to Asperfumene Biosynthesis through a Vicinal Deprotonation-Reprotonation Process. *Angew. Chem., Int. Ed.* **2024**, *63*, No. e202407895.
(21) Johnson, L. A.; Allemann, R. K. Engineering terpene synthases and their substrates for the biocatalytic production of terpene natural products and analogues. *Chem. Commun.* **2025**, *61*, 2468.
(22) Nakano, C.; Tezuka, T.; Horinouchi, S.; Ohnishi, Y. Identification of the SGR6065 gene product as a sesquiterpene cyclase involved in (+)-epicubenol biosynthesis in *Streptomyces griseus*. *J. Antibiot.* **2012**, *65*, 551−558.
(23) Cane, D. E.; Xue, Q.; Fitzsimons, B. C. Trichodiene Synthase. Probing the Role of the Highly Conserved Aspartate-Rich Region by Site-Directed Mutagenesis. *Biochemistry* **1996**, *35*, 12369−12376.
(24) Cane, D. E.; Kang, I. Aristolochene Synthase: Purification, Molecular Cloning, High-Level Expression in *Escherichia coli*, and Characterization of the *Aspergillus terreus* Cyclase. *Arch. Biochem. Biophys.* **2000**, *376*, 354−364.
(25) Cane, D. E.; Shim, J. H.; Xue, Q.; Fitzsimons, B. C.; Hohn, T. M. Trichodiene Synthase. Identification of Active Site Residues by Site-Directed Mutagenesis. *Biochemistry* **1995**, *34*, 2480−2488.
(26) Baer, P.; Rabe, P.; Fischer, K.; Citron, C. A.; Klapschinski, T. A.; Groll, M.; Dickschat, J. S. Induced Fit Mechanism in Class I Terpene Cyclases. *Angew. Chem., Int. Ed.* **2014**, *53*, 7652−7656.
(27) Dickschat, J. S.; Pahirulzaman, K. A. K.; Rabe, P.; Klapschinski, T. A. An Improved Technique for the Rapid Chemical Characterisation of Bacterial Terpene Cyclases. *ChemBioChem.* **2014**, *15*, 810−814.
(28) Dickschat, J. S.; Quan, Z.; Schnakenburg, G. A Case of Convergent Evolution: The Bacterial Sesquiterpene Synthase for 1-*epi*-Cubenol from *Nonomuraea coxensis*. *ChemBioChem.* **2023**, *24*, No. e202300581.
(29) Hu, Y.; Chou, W. K. W.; Hopson, R.; Cane, D. E. Genome Mining in *Streptomyces clavuligerus*: Expression and Biochemical Characterization of Two New Cryptic Sesquiterpene Synthases. *Chem. Biol.* **2011**, *18*, 32−37.
(30) Rabe, P.; Dickschat, J. S. Rapid Chemical Characterisation of Bacterial Terpene Synthases. *Angew. Chem., Int. Ed.* **2013**, *52*, 1810−1812.
(31) Tao, H.; Lauterbach, L.; Bian, G.; Chen, R.; Hou, A.; Mori, T.; Cheng, S.; Hu, B.; Lu, L.; Mu, X.; Li, M.; Adachi, N.; Kawasaki, M.; Moriya, T.; Senda, T.; Wang, X.; Deng, Z.; Abe, I.; Dickschat, J. S.; Liu, T. Discovery of non-squalene triterpenes. *Nature* **2022**, *606*, 414−419.
(32) Li, H.; Dickschat, J. S. Enzymatic Synthesis of Diterpenoids from *iso*-GGPP III: A Geranylgeranyl Diphosphate Analog with Shifted Double Bond. *Chem.-Eur. J.* **2024**, *30*, No. e202303560.
(33) Tarshis, L. C.; Yan, M.; Poulter, C. D.; Sacchettini, J. C. Crystal structure of recombinant farnesyl diphosphate synthase at 2.6-A resolution. *Biochemistry* **1994**, *33*, 10871−10877.
(34) Zhao, Y. H.; Abraham, M. H.; Zissimos, A. M. Fast Calculation of van der Waals Volume as a Sum of Atomic and Bond Contributions and Its Application to Drug Compounds. *J. Org. Chem.* **2003**, *68*, 7368−7373.
(35) Weinheimer, A. J.; Youngblood, W. W.; Washecheck, P. H.; Karns, T. K. B.; Ciereszko, L. S. Isolation of the elusive (−)-germacrene A from the gorgonian, *Eunicea mammosa*. Chemistry of coelenterates. XVIII. *Tetrahedron Lett.* **1970**, *11*, 497−500.
(36) Faraldos, J. A.; Wu, S.; Chappell, J.; Coates, R. M. Conformational analysis of (+)-germacrene A by variable-temperature NMR and NOE spectroscopy. *Tetrahedron* **2007**, *63*, 7733−7742.
(37) Rinkel, J.; Dickschat, J. S. Addressing the Chemistry of Germacrene A by Isotope Labeling Experiments. *Org. Lett.* **2019**, *21*, 2426−2429.
(38) Li, L.; Sheng, L.; Wang, C.-Y.; Zhou, Y.-B.; Huang, H.; Li, X.-B.; Li, J.; Mollo, E.; Gavagnin, M.; Guo, Y.-W. Diterpenes from the Hainan Soft Coral *Lobophytum cristatum* Tixier-Durivault. *J. Nat. Prod.* **2011**, *74*, 2089−2094.
(39) de Kraker, J.-W.; Franssen, M. C. R.; de Groot, A.; König, W. A.; Bouwmeester, H. J. (+)-Germacrene A Biosynthesis. The Committed Step in the Biosynthesis of Bitter Sesquiterpene Lactones in Chicory. *Plant Physiol.* **1998**, *117*, 1381−1392.
(40) Nishino, C.; Bowers, W. S.; Montgomery, M. E.; Nault, L. R.; Nielson, M. W. Alarm pheromone of the spotted alfalfa aphid, *Therioaphis maculata* Buckton (Homoptera: Aphididae). *J. Chem. Ecol.* **1977**, *3*, 349−357.
(41) Maurer, B.; Grieder, A. Sesquiterpenoids from Costus Root Oil (*Saussurea lappa* Clarke). *Helv. Chim. Acta* **1977**, *60*, 2177−2190.

https://doi.org/10.1021/acscatal.5c01540
ACS Catal. 2025, 15, 6209−6215

(42) Rabe, P.; Rinkel, J.; Dolja, E.; Schmitz, T.; Nubbemeyer, B.; Luu, T. H.; Dickschat, J. S. Mechanistic investigantions on two bacterial diterpene cyclases: Spiroviolene Synthase and Tsukubadiene Synthase. *Angew. Chem., Int. Ed.* **2017**, *56*, 2776−2779.
(43) Cornforth, J. W.; Cornforth, R. H.; Popjak, G.; Yengoyan, L. Studies on the Biosynthesis of Cholesterol. *J. Biol. Chem.* **1966**, *241*, 3970−3987.
(44) Lauterbach, L.; Rinkel, J.; Dickschat, J. S. Two Bacterial Diterpene Synthases from *Allokutzneria albata* for Bonnadiene and for Phomopsene and Allokutznerene. *Angew. Chem., Int. Ed.* **2018**, *57*, 8280−8283.
(45) Rabe, P.; Schmitz, T.; Dickschat, J. S. Mechanistic Investigations on Six Bacterial Terpene Cyclases. *Beilstein J. Org. Chem.* **2016**, *12*, 1839−1850.
(46) Rabe, P.; Barra, L.; Rinkel, J.; Riclea, R.; Citron, C. A.; Klapschinski, T. A.; Janusko, A.; Dickschat, J. S. Conformational Analysis, Thermal Rearrangement and EI-MS-Fragmentation Mechanism of (1(10)*E*,4*E*,6*S*,7*R*)-Germacradien-6-ol by ^{13}C-Labeling Experiments. *Angew. Chem., Int. Ed.* **2015**, *54*, 13448−13451.

https://doi.org/10.1021/acscatal.5c01540
ACS Catal. 2025, 15, 6209−6215

Appendices G

On the Role of Hydrogen Migrations in the Taxadiene System

Angew. Chem. Int. Ed., **2025**, *64*, e202422788.

DOI: 10.1002/anie.202422788.

Angew. Chem. **2025**, *137*, e202422788.

DOI: 10.1002/ange.202422788.

How to cite: *Angew. Chem. Int. Ed.* **2025**, *64*, e202422788
doi.org/10.1002/anie.202422788

Natural Products

On the Role of Hydrogen Migrations in the Taxadiene System

*Heng Li, Bernd Goldfuss, and Jeroen S. Dickschat**

Abstract: Taxa-4,11-diene is made by the taxa-4,11-diene synthase (TxS) from *Taxus brevifolia.* The unique reactivity of the taxane system is characterised by long distance hydrogen migrations in the biosynthesis. This study demonstrates that selective long range hydrogen migrations also play a role in the high energy process of the EI-MS fragmentation of taxa-4,11-diene. A TxS enzyme variant was generated that produces cyclophomactene, a compound that is formed through a concerted process involving a long range proton shift and a ring closure that can also be described as the addition of a methylcarbinyl cation to an olefin. Based on a previous computational study the cyclisation mechanism towards taxa-4,11-diene was suggested to involve two long distance proton migrations instead of one direct transfer. A substrate analog with a shifted double bond was converted with TxS to obtain experimental evidence for this proposal.

Introduction

Taxol was first isolated from the stem bark of Pacific yew (*Taxus brevifolia*).[1] The compound exhibits a pronounced cytotoxicity by enhancing the polymerisation of tubulin[2] and is in clinical use for the treatment of various types of cancer. The low content in the bark and the slow growth of the tree lead to a supply problem that is addressed through genetic engineering of microbial strains,[3,4] which requires profound knowledge of the biosynthetic genes and enzymes involved in its biosynthesis.[5–14]

The first committed step is catalysed by taxa-4,11-diene (**1**) synthase (TxS, Scheme 1) that has originally been purified from *Taxus brevifolia*,[15] followed by cloning and heterologous expression of its coding nucleotide sequence and functional characterisation of the enzyme.[16] The crystal structure of TxS has been reported[17] and the enzyme has extensively been investigated through site-directed mutagenesis.[18,19] Initially suggested mechanisms[20,21] for the formation of **1** start with the abstraction of diphosphate from the diterpene precursor geranylgeranyl diphosphate (GGPP) to yield cation **A**. A subsequent 1,14-cyclisation to **B** and a 10,15-cyclisation result in **C** that were suggested to undergo a deprotonation from C10 to a neutral intermediate (verticillene) and its reprotonation to **E**.[20] However, incubation experiments with (10-^{2}H)GGPP revealed a retainment of deuterium with incorporation into H6α of **1**, leading to the suggestion that **C** may react in a direct 1,5-proton transfer from C10 to C6 to yield **E**.[21] The ultimate 2,7-cyclisation to **F** and deprotonation from C4 would then result in **1**.

Also several stereochemical details of the cyclisation process have been investigated. The stereospecificity of the terminal deprotonation step was investigated using (*R*)-(4-^{2}H)GGPP, showing selective removal of a proton from the *Re* face at C4.[21] Incubation experiments with stereoselectively deuterated (*R*)- and (*S*)-(1-^{2}H)GGPP revealed the inversion of configuration at C1 in the initial 1,14-cyclisation, and a selective deuterium labelling at Me16, realised in the substrate (16,16,16-$^2H_3$)GGPP, established a stereochemical course for the 10,15-cyclisation from **B** to **C** with attack at C15 from the *Re* face (for unlabelled GGPP, this is identical to the *Si* face of GGPP deuterated at C16).[22]

DFT calculations using the B3LYP/6-31+G(d,p) method reveiled that the situation for the intramolecular proton migrations is more complex than initially anticipated. Besides the direct conversion of **C** to **E** also two sequential 1,5-proton transfers with translocation of a proton from C10 to C2 (**C** to **D**) and then from C2 to C6 (**D** to **E**) are possible.[23,24] Interestingly, the energy barriers for the two-step process from **C** to **E** were lower than for the direct proton shift.[23,24] The existence of cation **D** was also supported by a docking study,[19] while QM/MM calculations in the environment of the enzyme by Major and co-workers suggested a slight energetic preference for the direct pathway.[25,26] In contrast, QM/MM calculations by Thiel and co-workers were in favour of the **C**-**D**-**E** transformation.[27,28]

The cyclisation cascade was further interrogated using substrate analogs with a reduced reactivity (Scheme 2). The enzymatic conversion of (*R*)- and (*S*)-10,11-dihydro-GGPP resulted in the corresponding stereoisomers of **9**,[29] while 6-fluoro-GGPP with an electronically buffered reactivity in the C6=C7 double bond yielded several fluorinated diterpenes including the main product **10**.[30] Also 7-desmethyl-GGPP has a reduced reactivity in the C6=C7 double bond,

[*] H. Li, Prof. Dr. J. S. Dickschat
Kekulé Institute of Organic Chemistry and Biochemistry
University of Bonn
Gerhard-Domagk-Straße 1, 53121 Bonn, Germany
E-mail: dickschat@uni-bonn.de
Prof. Dr. B. Goldfuss
Department for Chemistry
University of Cologne
Greinstrasse 4, 50939 Cologne, Germany

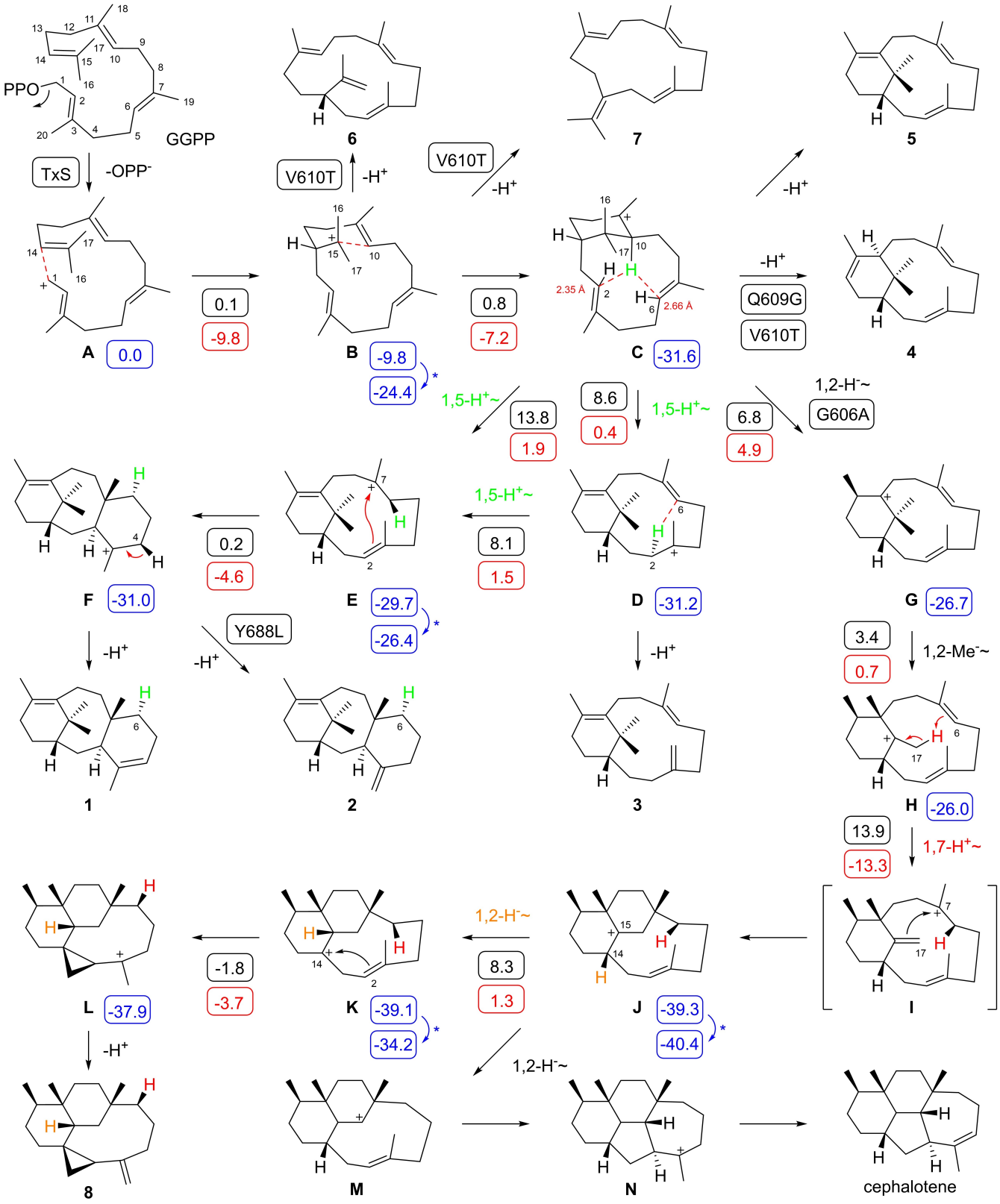

Scheme 1. Taxa-4,11-diene biosynthesis. A) Mechanism for the cyclisation of GGPP to **1** and biosynthetically related products by TxS and its enzyme variants. For isolated products the source enzymes are given in boxes. The numbers in boxes are computed energies (in kcal/mol) of intermediates relative to **A** (set to 0.0 kcal/mol, blue), reaction barriers (Gibbs free energies of activation at 298.15 K, black) and Gibbs free reaction energies (red) relative to each preceeding intermediate. All structures were computed using the mPW1PW91/6-311+G(d,p)//B97D3/6-31 G(d,p) method (298 K). Asterisks indicate conformational changes needed between the product of one transformation and the starting structure of the next step. All carbon numbers follow GGPP numbering, which is different to the accepted carbon numbering of taxanes.[15]

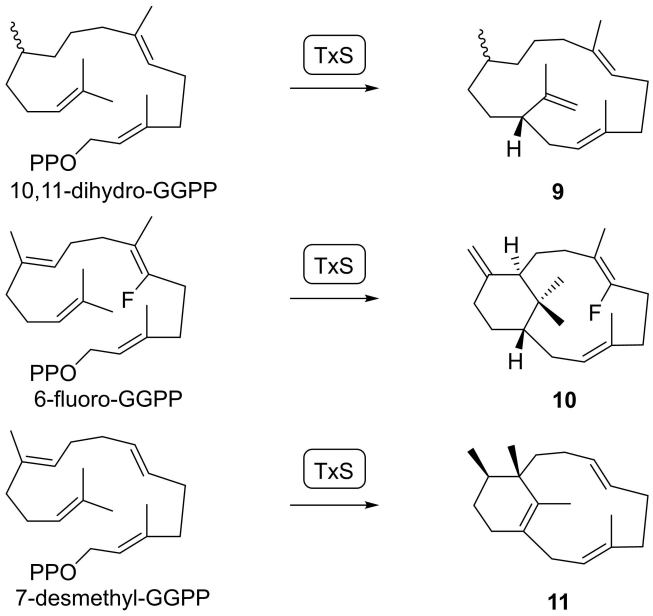

Scheme 2. Products obtained with TxS from GGPP derivatives.

because its participation in proton transfers or cyclisation reactions would lead to a secondary cation. Consequently, the bicyclic hydrocarbon **11** was isolated from this substrate.[31] While **9** and **10** represent the deprotonation products of the analogs of intermediates **B** and **C**, compound **11** arises from a **C** analog by hydride and methyl migrations and deprotonation.

Here we report on advanced isotopic labelling experiments to investigate the cyclisation cascade towards **1** and its EI-MS fragmentation mechanism. Site-directed mutagenesis and incubation experiments using a substrate analog with a shifted double bond gave additional insights into the unusual long-range proton shifts in the biosynthesis of **1** and related molecules.

Results and Discussion

All experiments performed in this study are based on a truncated and His-tagged taxadiene synthase lacking 78 amino acids at the N-terminus, further referred to as "TxS" in this study. This enzyme is known to give high yields of soluble protein in the expression in *Escherichia coli* (Figure S1) and exhibits a high activity in the in vitro conversion of GGPP into taxa-4,11-diene (**1**, 87 %) and its double bond isomer taxa-4(20),11-diene (**2**) (13 %).[32]

The isotopic labelling experiments performed in this study are summarised in Table S1. For interpretation of the results **1** and **2** were isolated from a preparative scale incubation of GGPP (Table S2), followed by a complete NMR assignment (Tables S3 and S4, Figures S2–S10). Compound **2** has initially been identified as a TxS product by GC/MS[33] in comparison to a synthetic authentic standard,[34] but has never been isolated before from an enzymatic reaction with TxS. For an unambiguous assignment of all diastereotopic hydrogen atoms incubation experiments with (*R*)- and (*S*)-(1-^{13}C,1-^{2}H)isopentenyl diphosphate (IPP),[35] and with dimethylallyl diphosphate (DMAPP) plus (*E*)- or (*Z*)-(4-^{13}C,4-^{2}H)IPP[36] were performed (Figures S11 and S12). These stereoselectively deuterated precursors were enzymatically converted into **1** with *E. coli* isopentenyl diphosphate isomerase (IDI,[37] only used for the substrates labelled at C1), *Streptomyces cyaneofuscatus* GGPP synthase (GGPPS)[38] and TxS, followed by HSQC analysis of the product, showing vanished crosspeaks for the hydrogens substituted by deuterium. As a result, a correction for the previous hydrogen assignment at C9 of **1**[20] is necessary (Table S3). These experiments require knowledge about the stereochemical course of the oligomerisation of the terpene precursor monomers[39] and about the absolute configuration of **1** that can be inferred from the absolute configuration of taxol[1] and has been established through enantioselective synthesis.[40]

The conversion of all twenty isotopomers of (^{13}C)GGPP, obtained through chemical synthesis[38,41] or by enzymatic preparation from its correspondingly labelled prenyl diphosphate precursors,[38,42–44] with TxS confirmed the general carbon skeleton assambly including the precise stereochemical course for the geminal Me groups C16 and C17 (Figures S13 and S14).[22] The EI mass spectrum of **1** exhibits a base peak ion at *m*/*z* 122 (Figure S15), and inspection of the mass spectra of its singly ^{13}C-labelled isotopomers showed an increase to *m*/*z* 123, if one of the carbons marked by the blue dots in Scheme 3 is substituted with ^{13}C, indicating that this fragment ion arises from the nine carbons in the eastern portion of **1** (Figures S16 and S17). Mechanistically, this is explainable by the ionisation of **1** to $\mathbf{A}^{+\bullet}$, which preferentially takes place at the highest substituted (most electron rich) double bond, followed by a retro-Diels–Alder (RDA) fragmentation to $\mathbf{B}^{+\bullet}$ and a hydrogen migration to $\mathbf{C}^{+\bullet}$. A subsequent hydrogen migration to $\mathbf{D}^{+\bullet}$ induces the neutral loss of ethylene by α-fragmentation to $\mathbf{E}^{+\bullet}$ that can undergo another hydrogen rearrangement to $\mathbf{F}^{+\bullet}$ and α-cleavage to $\mathbf{G}^{+\bullet}$ (*m*/*z* 122) (Scheme 3).

This fragmentation mechanism was further investigated through DFT calculations (Table S5, Figure S18), revealing the higest activation barrier (+35.8 kcal/mol) and a strongly positive Gibbs free energy (+36.1 kcal/mol) for the RDA, which can be overcome by the high ionisation energy used (70 eV ≈ 1614 kcal/mol) that leaves the molecule after ionisation in a highly excited state. $\mathbf{B}^{+\bullet}$ is obtained in a conformation that enables the next hydrogen transfer to $\mathbf{C}^{+\bullet}$ through a distance of 3.4 Å between H2 and C12 (Figure S19A) with a low reaction barrier (12.4 kcal/mol). Also $\mathbf{C}^{+\bullet}$ is formed with a short distance of 2.6 Å between C14 and H16 for the next hydrogen transfer to $\mathbf{D}^{+\bullet}$ (Figure S19B). In this case the barrier is much higher (31.8 kcal/mol), because the reaction leads to a primary radical cation. After α-cleavage of ethylene to $\mathbf{E}^{+\bullet}$ a conformational change is required to allow for the hydrogen migration to $\mathbf{F}^{+\bullet}$ (Figure S19C). The reaction barriers for both steps and the terminal α-fragmentation are with ca. 6 kcal/mol in all three cases low. A key step of this mechanism is the long range hydrogen migration from C2 to C12 ($\mathbf{B}^{+\bullet}$ to $\mathbf{C}^{+\bullet}$) that was

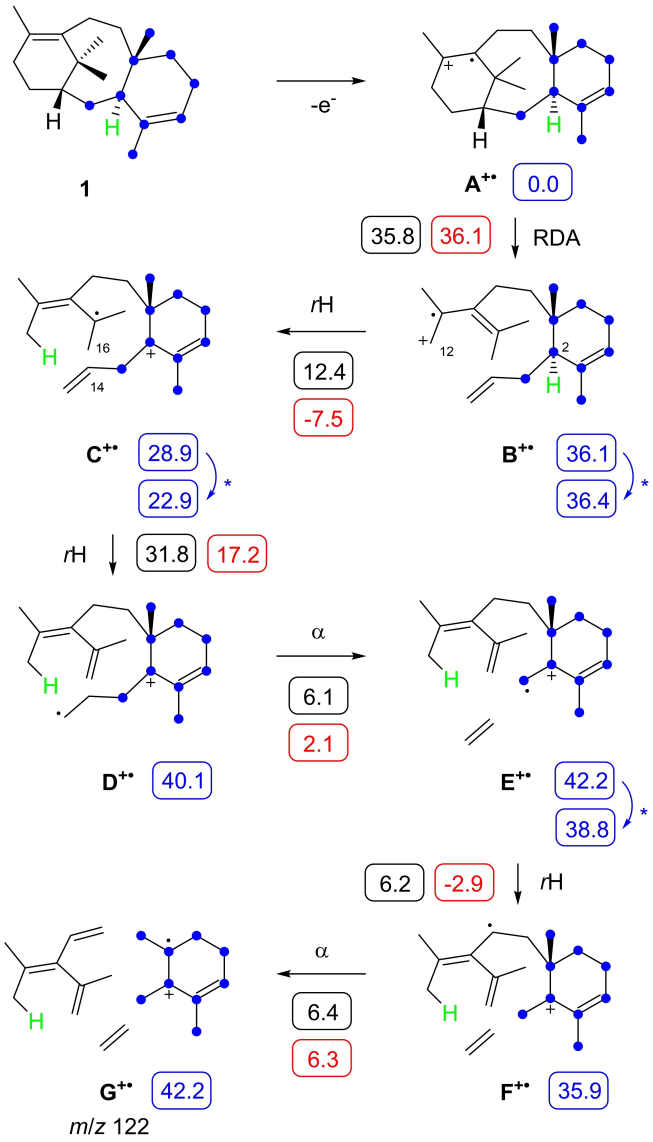

Scheme 3. EIMS fragmentation mechanism for the base peak ion *m/z* 122 of **1**. Blue dots indicate carbons for which a substitution with ^{13}C leads to an increase of the base peak ion to *m/z* 123. The numbers in boxes are computed energies (in kcal/mol) of intermediates relative to **A** (set to 0.0 kcal/mol, blue), reaction barriers (Gibbs free energies of activation at 298.15 K, black) and Gibbs free reaction energies (red) relative to each preceeding intermediate. All structures were computed using the mPW1PW91/6-311+G(d,p)//B97D3/6-31 G(d,p) method (298 K).

investigated through incubation of (2-^{2}H)GGPP[45] with TxS and analysis of the product **1** by GC/MS (Figure S20). Observation of the base peak at *m/z* 122 confirmed the loss of deuterium from the corresponding fragment ion and thus the long distance hydrogen migration during the fragmentation reaction.

TxS has been extensively studied through site-directed mutagenesis.[17,19] All previously reported enzyme variants have been designed based on the structure of the enzyme and have targeted active site residues. The results revealed that TxS is highly sensitive to reshaping of the active site, as many of the tested enzyme variants were inactive or exhibited a strongly reduced production (Tables S6–S8). Frequently observed products include, besides **1** and **2**, the hydrocarbons verticilla-4(20),7,11-triene (**3**),[46] verticilla-3,7,12-triene (**4**),[19] and cembrene A (**6**)[47] that can be explained as the deprotonation products of intermediates **B**, **C**, and **D**, respectively (Scheme 1). Also verticilla-3,7,11-triene (**5**) has tentatively been identified from wildtype TxS and various enzyme variants,[18,19] but has never been isolated and properly structurally characterised. Moreover, its isomer **3** has been isolated with NMR-based structure elucidation from various plant sources,[46,48] but its structure was confused with that of **5** in a later publication,[49] resulting in the assignment of a CAS number and a confusion about the identity of **5** as a TxS product. We tried to isolate this material from a large scale enzyme incubation, but unfortunately the production of **5** was too low for an unambiguous structure elucidation. Based on GC/MS data we can confirm the observation of the same compound as reported by Brück and co-workers,[19] but its identity remains at the end unclear. Notable discoveries are the selective formation of **4** by the Q609G variant and the good production of **2** by the Y688L variant.[18]

This work was expanded through the investigation of additional enzyme variants, addressing the active site residues shown in Figure 1A (the results are summarised in Figure 1B, Table S8 and Figure S21). Several of these residues have not been tested before, including E583, G606 and I848. All three enzyme variants E583D, E583M and E583A were inactive, demonstrating that amino acid exchanges in this position even against the structurally similar Asp are critical. A structural analysis revealed a hydrogen bond of E583 to a cluster of four water molecules at the enzyme surface (Figure S22), suggesting that E583 serves as a gatekeeper that blocks the entrance of water to the active site. The G606A variant showed a reduced productivity, but a good selectivity for **4**, giving access to an enzyme for the selective production of this compound. This variant also formed a side product that was isolated and structurally characterised as the new compound cyclophomactene (**8**) (Table S9, Figures S23–S30). The exchange of I848 against other hydrophobic residues gave surprising results: While the I848V variant only showed a moderately reduced activity, the I848L variant was completely inactive. A comparison of the X-ray structure with an AlphaFold2 model of the I848L variant reveals a strong disturbance of F834, a residue presumably involved in a cation-π stabilisation of Intermediate **B**, causing a rotation of F834 by ca. 90° and explaining the loss of acivity, while only a minor disturbance is observed in the I848V variant (Figure S31).

Additional enzyme variants targeted active site positions that were investigated before,[18,19] but with exchange to different residues than in the previous experiments. R580 adopts two alternative conformations. Its exchange against another basic residue in the R580K variant or against a large hydrophobic residue (R580M) resulted in inactivity. Aromatic active site residues are potentially involved in the stabilisation of cationic intermediates. The exchange of F602 and F834 against Tyr gave in both cases a lower productiv-

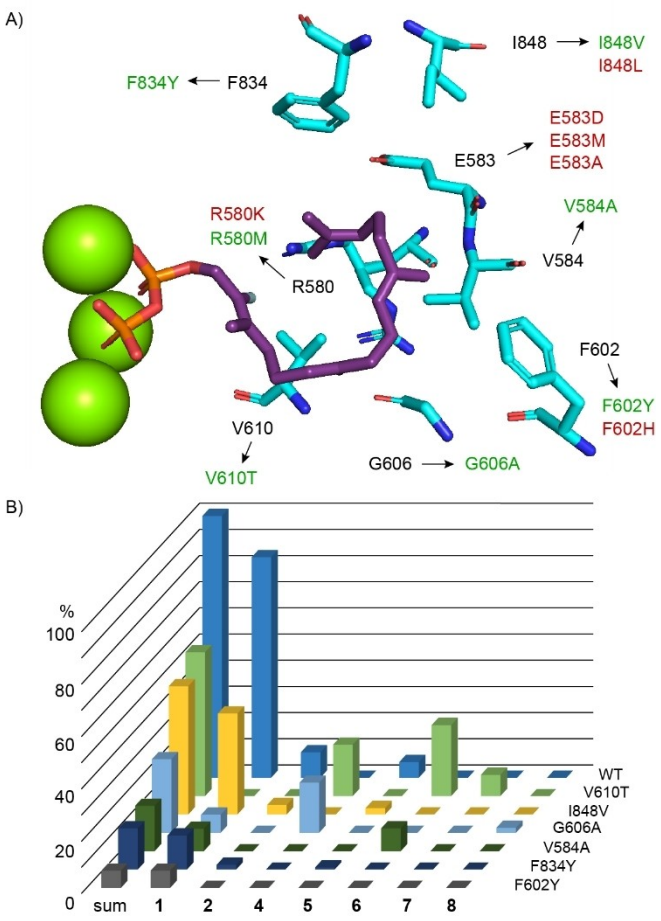

Figure 1. Site-directed mutagenesis of TxS. A) Active site residues targeted by site-directed mutagenesis in this study (based on the X-ray structure of TxS, PDB 3P5R). Enzyme variants shown in green were catalytically active, those shown in red were inactive. B) Relative production of enzyme variants. The sum of compounds produced by the wild-type (WT) was set to 100%. Bars represent means from triplicates. For standard deviations cf. Table S8.

ity, while the F602H variant was inactive. The V584A variant resulted in a substantially lower production of **1**, with additional formation of **6**. The most interesting results were obtained with the V610T variant that completely lost the ability to produce **1**. Instead, compounds **4** and **6** in addition to another diterpene hydrocarbon (**7**) that could not be identified by GC/MS were obtained. Compound **7** was isolated and identified as a known macrocyclic diterpene hydrocarbon for which we propose the name cembrene D (Figure S32, Table S10). The same hydrocarbon **7** was previously isolated from the soft coral *Sarcophyton glaucum*[50] and is a side product of the diterpene synthase DtcycA from *Streptomyces* sp. SANK 60404.[51]

The formation of the new compound **8** was investigated through DFT calculations using the advanced mPW1PW91/6-311+G(d,p)//B97D3/6-31G(d,p) method. These calculations showed similar results as previously obtained with three different methods (including B3LYP/6-31+G(d,p), mPW1PW91/6-31+G(d,p)//B3LYP/6-31+G(d,p) and MPWB1K/6-31+G(d,p)//B3LYP/6-31+G(d,p)) for the reactions from intermediate **A** to **F**[23,24] (Scheme 1, Table S11, Figure S33). In particular, the sequence of two 1,5-proton shifts (**C**-**D**-**E**) was favoured over the direct 1,5-proton shift from **C** to **E** by the lower reaction barriers. The pathway to **8** branches out from **C** by a 1,2-hydride shift to **G** and a 1,2-methyl group migration to **H**, the precursor of the fungal compound phomacta-1(14),3,7-triene for which recently a type I terpene synthase was discovered.[52,53] An intramolecular 1,7-proton transfer to **I** may then be followed by an unusual 7,17-cyclisation to **J**, a 1,2-hydride shift to **K**, a 2,14-cyclisation to **L** and deprotonation to yield **8**. The DFT calculations revealed an overall smooth energy profile for this biosynthetic process, but also uncovered a surprising direct transformation from **H** to **J** with skipping of the intermediate **I**, which shows with 13.9 kcal/mol the highest activation barrier and is thus the rate-limiting step towards **8**. The conversion of **H** into **J** can be understood as a direct addition of a C–H bond of Me17 to the olefinic C6=C7 bond. This unusual step was further investigated through an isotopic labelling experiment. For this purpose, (4,4,4,5,5,5-$^{2}H_6$)DMAPP was synthesised from ($^{2}H_6$)acetone (Scheme S1) and incubated with (2-^{13}C)IPP and GGPPS to obtain (2,6-$^{13}C_2$,16,16,16,17,17,17-$^{2}H_6$)GGPP. Its conversion with TxS-G606A resulted in a strongly reduced production of labelled **8** in comparison to the production from unlabelled GGPP (Figure S34), which is explained by the large computed kinetic isotope effect of $k_H/k_D = 7.2$ (Scheme 4A). As a consequence, the expected triplet signal in the ^{13}C NMR (as a result of ^{13}C-^{2}H spin coupling) for the $^{13}C^{2}H^{1}H$ group (C6) of **8** formed by the deuterium migration from C17 to C6 was not observed. However, GC/MS analysis of the product revealed that all six deuterium atoms of the substrate remained in the product **8** (Figure S34), giving experimental support for the C17-to-C6 proton transfer. The pronounced kinetic isotope effect for the **H**-to-**J** transformation in the biosynthesis of **8** compares to smaller computed values for the 1,5-proton shifts in the biosynthesis of **1** (Scheme 4B–D).

Based on isotopic labelling experiments, a similar 1,7-proton shift has also been suggested for the biosynthesis of cephalotene, the product of the diterpene synthase CsCTS from *Cephalotaxus sinensis*, whose biosynthesis also proceeds through intermediate **J**, then branching out to **M** and **N** (Scheme 1).[54] The results from the labelling experiments provided in this previous and in the present study support analogous long range proton migrations in the biosynthesis of **8** and cephalotene, while our DFT calculations clarify the unique mechanism for the formation of **J**.

We have recently demonstrated the efficient conversion of *iso*-GGPP I, an isomer of GGPP with the C6=C7 double bond shifted into the C7=C19 position, with a large variety of diterpene synthases. The minor structural changes in *iso*-GGPP I have resulted in unexpected reactivities leading to the formation of many new compounds with previously unknown skeletons.[55–57] The conversion of *iso*-GGPP I with TxS yielded the novel compound taxaxenene (**12**) as the major product (Figure S35) that was isolated and structurally characterised by NMR spectroscopy (Table S12, Figures S36–S43). Xenenes are a family of compounds from *iso*-

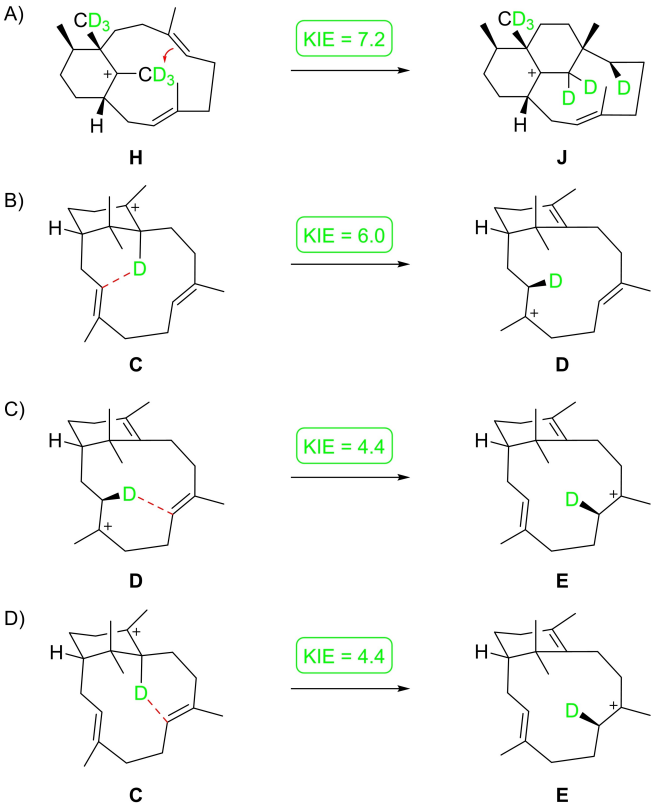

Scheme 4. Computed kinetic isotope effects (ratio of rate constants k_H/k_D) for long distance hydrogen migrations in the biosynthesis of **1** and **8**, determined with H/D exchange of only the migrating hydrogen. Kinetic isotope effects for A) the unusual cyclisation reaction in the biosynthesis of **8** and B–D) the 1,5-proton shifts in the biosynthesis of **1**.

GGPP I formed through a cyclisation mechanism with participation of the C6=C19 double bond, generally leading to compounds that are foreign to the enzyme used for their preparation (gr. ξενοσ=foreign). The formation of **12** from *iso*-GGPP I requires substrate ionisation to **A***, followed by 1,14- and 10,15-cyclisations to **B*** and **C*** (Scheme 5). At this stage a direct 1,5-proton shift can lead to **D*** that can undergo 3,19-cyclisation to **F*** and deprotonation to **12**. Similar to the situation in the biosynthesis of **1**, the direct 1,5-proton transfer from **C*** to **D*** may be substituted by two sequential 1,5-proton shifts mediated through **E***.

The biosynthesis of **12** was investigated through isotopic labelling experiments. The incubation of *iso*-GGPP I with TxS in a D_2O buffer showed no incorporation of deuterium (Figure S44), suggesting that the cyclisation cascade does not proceed through a neutral intermediate. To investigate the intramolecular proton shifts, (10-^{2}H)-*iso*-GGPP I was synthesised (Scheme S2) and converted with TxS, followed by the isolation of labelled **12**. The deuterium in the substrate may migrate directly to C2 in which case one of the signals for the hydrogens at C2 (H2α) should be vanished in the HSQC spectrum. On the contrary, if deuterium would first migrate to C19, a distribution of the three homotopic hydrogens in the Me group would be expected and a kinetic isotope effect should result in the preferential migration of a proton from C19 to C2. In this case crosspeaks for both hydrogens at C2 would be expected in the HSQC spectrum. For the unlabelled compound in C_6D_6 at 298 K one of the C2 crosspeaks overlaps with a strong signal for Me19, but after a change of the solvent and measuring the spectra at 238 K the signals were resolved. Analysis of the sample obtained with TxS from (10-^{2}H)-*iso*-GGPP revealed a vanished crosspeak for H2α (Figure S45), giving first experimental evidence for the proton transfer from C10 to C2 in a system that is structurally closely related to the natural taxadiene system. Most computational studies have favoured a two-step proton transfer from C10 to C6 using C2 as an intermediate springboard in the biosynthesis of **1**, but conclusive experimental evidence for this mechanistic hypothesis as provided here is difficult to obtain.

These experimental findings are also in line with computational data for the conversion of *iso*-GGPP I into **12** (Scheme 5, Table S13 and Figure S46). DFT calculations revealed a low reaction barrier of 5.5 kcal/mol for the direct conversion of **C1*** into **E***, while the step from **C2***, a conformer of **C1***, to **D*** exhibits a reaction barrier of 21.1 kcal/mol. All other transformations proceed through low reaction barriers and the overall cyclisation cascade is with −49.0 kcal/mol highly exergonic.

The V610T variant of TxS was selected for further study with *iso*-GGPP I as substrate, because this variant showed the best diterpene production of all variants created in this study. In addition, the V610T variant has a completely altered product profile in comparison to wild-type TxS, suggesting that the formation of products different to **12** may be expected from this variant. The incubation of *iso*-GGPP I with TxS-V610T resulted in the formation of four main compounds besides several side products (Figure S47). The main compounds were isolated and structurally characterised as isocembrene A2 (**13**), isocembrene C (**14**), verticilla-3,8(19),12(18)-triene (**15**) and taxasimplene (**16**) that are all new diterpenoid hydrocarbons (Tables S14–S17, Figures S48–S79). Compounds **13–15** are explainable as the deprotonation products of the cationic intermediates **B1*** and **C1***, while **16** requires a change in the initial cyclisation mode from the usually observed 1,14- to a 3,19-cyclisation, leading to the direct precursor **G***.

The absolute configurations of terpenes can be determined through chemical correlation using stereoselectively deuterated terpene precursors. To investigate the absolute configurations of **12**, **15** and **16**, the stereoselectively deuterated compounds (*R*)- and (*S*)-(1-^{13}C,1-^{2}H)-*iso*-GGPP I[56] were converted with TxS-V610T. In these reactions stereogenic centers of known configuration are introduced at the labelled carbons, allowing to conclude on the absolute configuration of the products by determination of the relative orientation. For **12** and **15** this approach uncovered the absolute configurations as shown in Scheme 5 (Figures S80 and S81). For compound **16** the argumentation is more complex: Starting from the usual conformational fold of *iso*-GGPP I that is analogous to the fold of GGPP leading to taxa-4,11-diene, diphosphate will leave to the front side to allow a 1,14-cyclisation of **A*** to **B1*** with inversion of configuration at C1 (S_N2 reaction), or a 3,19-cyclisation to

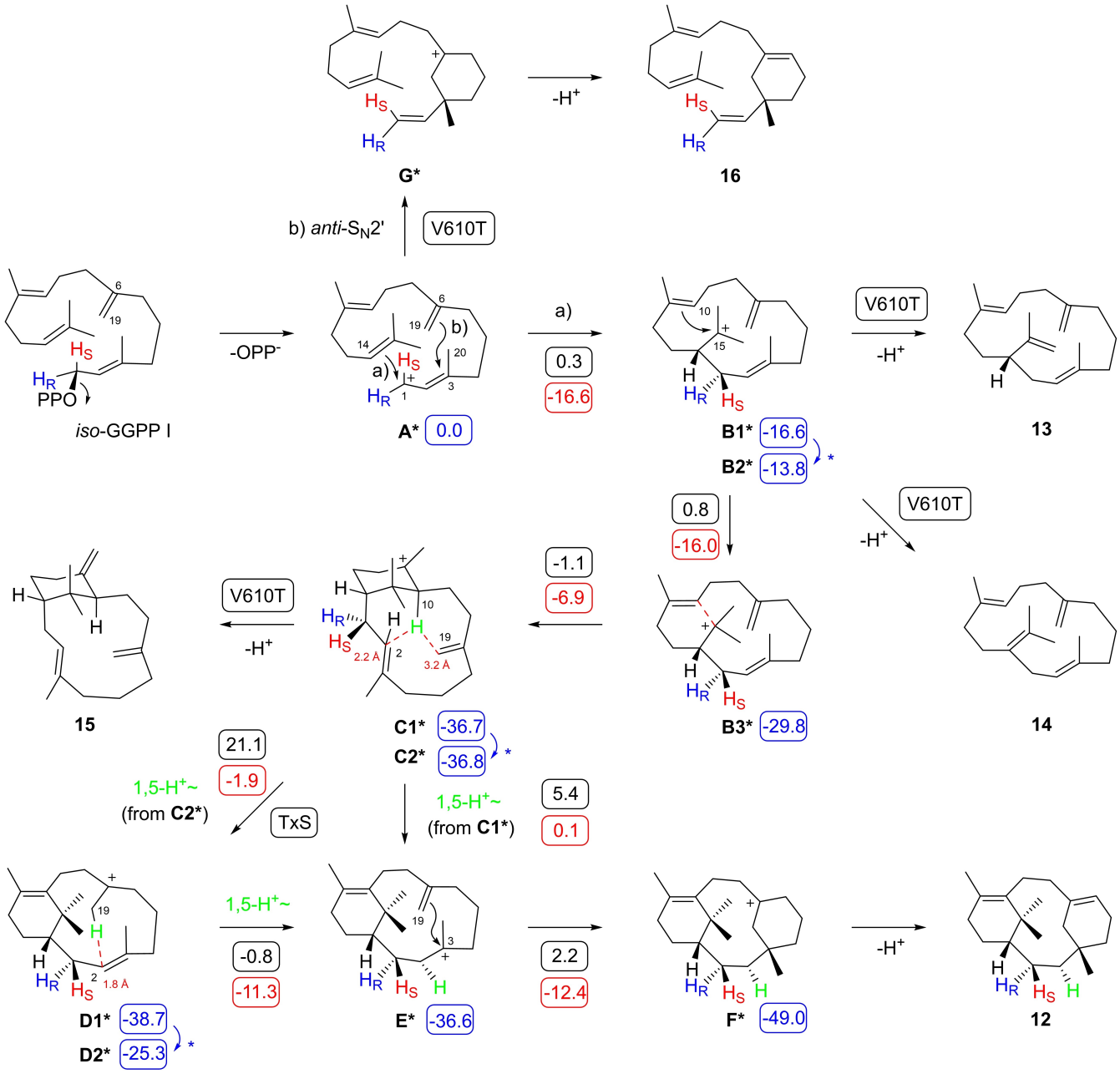

Scheme 5. Mechanism for the cyclisation of *iso*-GGPP I to **12** by TxS. The numbers in boxes are computed energies (in kcal/mol) of intermediates relative to **A*** (set to 0.0 kcal/mol, blue), reaction barriers (Gibbs free energies of activation at 298.15 K, black) and Gibbs free reaction energies (red) relative to each preceeding intermediate. All structures were computed using the mPW1PW91/6-311+G(d,p)//B97D3/6-31 G(d,p) method (298 K). Asterisks indicate conformational changes needed between the product of one transformation and the starting structure of the next step. All carbon numbers follow GGPP numbering (Scheme 1), which is different to the accepted carbon numbering of taxanes.[15]

G* with attack at C3 from the *Re* face (back side, *anti*-S_N2' reaction). This process necessarily turns the 1-*pro*-*R* hydrogen at C1 of *iso*-GGPP I into the (*E*)-position of the vinyl group of **16** and the 1-*pro*-*S* hydrogen into the (*Z*)-position. For a substrate analog a conformational change may be possible, but for the minor structural differences between GGPP and *iso*-GGPP I the overall conformational fold should be similar. Eventually, a conformational change in the C1-C3 portion with Me20 pointing down may be possible (Scheme S3). In this case C3 would be attacked from the *Si* face, leading to the enantiomer of **16**, but such a cyclisation must proceed with the 1-*pro*-*R* hydrogen at C1 of *iso*-GGPP I turning into the (*Z*)-position of the vinyl group of **16** and the 1-*pro*-*S* hydrogen into the (*E*)-position. This analysis demonstrates that the stereochemical fate of the hydrogens at C1 of *iso*-GGPP I can be taken as an indicator for the absolute configuration of **16**, and the experiment demonstrates that **16** has the absolute configuration as shown in Scheme 5 (Figure S82).

Conclusions

Long range proton shifts in the biosynthesis of taxa-4,11-diene (**1**) have extensively been discussed in the literature, first by suggesting a direct transfer from C10 to C6,[21] and later, based on computational data, a two step migration from C10 to C2 and then further to C6 was raised.[23,24] In the present study we have experimentally and computationally uncovered that similar long range hydrogen migrations are also relevant in the high energy process of the mass spectrometric fragmentation reaction towards the base peak ion of **1**, demonstrating that long distance hydrogen shifts are part of the intrinsic reactivity of the unique taxane skeleton. Site-directed mutagenesis experiments resulted in the discovery of a novel product from the G606A variant that was named cyclophomactene (**8**). This compound is formed through an unprecedented concerted process combining a 1,7-proton shift and ring closure that can also be described as the addition of a methylcarbinyl cation to an olefin, again revealing the relevance of long range proton transfers in taxanes and closely related systems. Further insights were obtained through the enzymatic conversion of *iso*-GGPP I with a double bond shifted from C6=C7 to C7=C19. In this substrate analog C6 is unreactive and thus gave first experimental evidence for a migration of H10 to C2, supported through the labelling experiments in conjunction with DFT calculations performed in this study. The downstream steps ultimately lead to taxaxenene (**12**), a compound with a novel skeleton that cannot be formed naturally from GGPP. The V610T substitution in TxS strongly interferes with long distance proton migrations, as not only with GGPP the cyclisation cascade was interrupted at intermediate **C**, resulting only in cembrane and verticillane diterpenes, but – despite the formation of several interesting compounds – also with *iso*-GGPP I no products beyond the analogous intermediate **C*** were obtained.

Long distance proton migrations are not limited to taxa-4,11-diene biosynthesis, but were also invoked for the biosynthesis of trichodiene[58] and asperfumene.[59] Based on DFT calculations two sequential proton shifts have also been proposed for the biosynthesis of fusicocca-2,19(14)-diene.[60] While the results of computational studies are generally trustable, experimental evidence is lacking for fusicocca-2,19(14)-diene biosynthesis, but may be obtained through a similar approach as described here.

Acknowledgements

This work was funded by the Deutsche Forschungsgemeinschaft (DFG, German Research Foundation) – Projektnummer 513548540, and by the computing center of the University of Cologne (RRZK), providing CPU time on the DFG-funded supercomputer CHEOPS. Open Access funding enabled and organized by Projekt DEAL.

Conflict of Interest

The authors declare no conflict of interest.

Data Availability Statement

The data that support the findings of this study are available in the supplementary material of this article.

Keywords: biosynthesis · enzymes · natural products · substrate analogs · terpenoids

[1] M. C. Wani, H. L. Taylor, M. E. Wall, P. Coggon, A. T. McPhail, *J. Am. Chem. Soc.* **1971**, *93*, 2325–2327.
[2] P. B. Schiff, J. Fant, S. B. Horwitz, *Nature* **1979**, *277*, 665–667.
[3] P. K. Ajikumar, W.-H. Xiao, K. E. J. Tyo, Y. Wang, F. Simeon, E. Leonhard, O. Mucha, T. H. Phon, B. Pfeifer, G. Stephanopoulos, *Science* **2010**, *330*, 70–74.
[4] B. Nowrouzi, R. A. Li, L. E. Walls, L. d'Espaux, K. Malci, L. Liang, N. Jonguitud-Borrego, A. I. Lerma-Escalera, J. R. Morones-Ramirez, J. D. Keasling, L. Rios-Solis, *Microb. Cell Fact.* **2020**, *19*, 200.
[5] J. Hefner, S. M. Rubenstein, R. E. B. Ketchum, D. M. Gibson, R. Croteau, *Chem. Biol.* **1996**, *3*, 479–489.
[6] K. Walker, R. E. B. Ketchum, M. Hezari, D. Gatfield, M. Goleniowski, A. Barthol, R. Croteau, *Arch. Biochem. Biophys.* **1999**, *364*, 273–279.
[7] A. Schoendorf, C. Rithner, R. M. Williams, R. B. Croteau, *Proc. Natl. Acad. Sci. USA* **2001**, *98*, 1501–1506.
[8] S. Jennewein, C. Rithner, R. M. Williams, R. B. Croteau, *Proc. Natl. Acad. Sci. USA* **2001**, *98*, 13595–13600.
[9] M. Chau, R. Croteau, *Arch. Biochem. Biophys.* **2004**, *427*, 48–57.
[10] B. Jiang, L. Gao, H. Wang, Y. Sun, X. Zhang, H. Ke, S. Liu, P. Ma, Q. Liao, Y. Wang, H. Wang, Y. Liu, R. Du, T. Rogge, W. Li, Y. Shang, K. N. Houk, X. Xiong, D. Xie, S. Huang, X. Lei, J. Yan, *Science* **2024**, *383*, 622–629.
[11] Y. Zhang, L. Wiese, H. Fang, S. Alseekh, L. Perez de Souza, F. Scossa, J. J. Molloy, M. Christmann, A. R. Fernie, *Mol. Plant Pathol.* **2023**, *16*, 1951–1961.
[12] C. Yang, Y. Wang, Z. Su, L. Xiong, P. Wang, W. Lei, X. Yan, D. Ma, G. Zhao, Z. Zhou, *Nat. Commun.* **2024**, *15*, 2339.
[13] E. Ainoa, J.-B. Nestor, M. Koray, S.-M. Raul, P. Javier, R.-S. Leonardo, M. Elisabeth, *Metab. Eng.* **2024**, *85*, 201–212.
[14] C. Li, X. Yin, S. Wang, S. Sui, J. Liu, X. Sun, J. Di, R. Chen, D. Chen, Y. Han, K. Xie, J. Dai, *Angew. Chem. Int. Ed.* **2024**, *63*, e202407070; *Angew. Chem.* **2024**, *136*, e202407070.
[15] M. Hezari, N. G. Lewis, R. Croteau, *Arch. Biochem. Biophys.* **1995**, *322*, 437–444.
[16] M. R. Wildung, R. Croteau, *J. Biol. Chem.* **1996**, *271*, 9201–9204.
[17] M. Köksal, Y. Jin, R. M. Coates, R. Croteau, D. W. Christianson, *Nature* **2011**, *469*, 116–120.
[18] S. Edgar, F.-S. Li, K. Qiao, J.-K. Weng, G. Stephanopoulos, *ACS Synth. Biol.* **2017**, *6*, 201–205.
[19] P. Schrepfer, A. Buettner, C. Goerner, M. Hertel, J. van Rijn, F. Wallrapp, W. Eisenreich, V. Sieber, R. Kourist, T. Brück, *Proc. Natl. Acad. Sci. USA* **2016**, *113*, E958–E967.
[20] A. E. Koepp, M. Hezari, J. Zajicek, B. Stofer Vogel, R. E. LaFever, N. G. Lewis, R. Croteau, *J. Biol. Chem.* **1995**, *270*, 8686–8690.

[21] D. C. Williams, B. J. Carroll, Q. Jin, C. D. Rithner, S. R. Lenger, H. G. Floss, R. M. Coates, R. M. Williams, R. Croteau, *Chem. Biol.* **2000**, *7*, 969–977.
[22] Q. Jin, D. C. Williams, M. Hezari, R. Croteau, R. B. Coates, *J. Org. Chem.* **2005**, *70*, 4667–4675.
[23] P. Gutta, D. J. Tantillo, *Org. Lett.* **2007**, *9*, 1069–1071.
[24] Y. J. Hong, D. J. Tantillo, *J. Am. Chem. Soc.* **2011**, *133*, 18249–18256.
[25] Y. Freud, T. Ansbacher, D. T. Major, *ACS Catal.* **2017**, *7*, 7653–7657.
[26] T. Ansbacher, Y. Freud, D. T. Major, *Biochemistry* **2018**, *57*, 3773–3779.
[27] A. M. Escorcia, J. P. M. van Rijn, G.-J. Cheng, P. Schrepfer, T. B. Brück, W. Thiel, *J. Comput. Chem.* **2018**, *39*, 1215–1225.
[28] J. P. M. van Rijn, A. M. Escorcia, W. Thiel, *J. Comput. Chem.* **2019**, *40*, 1902–1910.
[29] S. Y. Chow, H. J. Williams, Q. Huang, S. Nanda, A. I. Scott, *J. Org. Chem.* **2005**, *70*, 9997–10003.
[30] Y. Jin, D. C. Williams, R. Croteau, R. M. Coates, *J. Am. Chem. Soc.* **2005**, *127*, 7834–7842.
[31] S. Y. Chow, H. J. Williams, J. D. Pennington, S. Nanda, J. H. Reibenspies, A. I. Scott, *Tetrahedron* **2007**, *63*, 6204–6209.
[32] Q. Huang, H. J. Williams, C. A. Roessner, A. I. Scott, *Tetrahedron Lett.* **2000**, *41*, 9701–9704.
[33] D. C. Williams, M. R. Wildung, A. Q. Jin, D. Dalal, J. S. Oliver, R. M. Coates, R. Croteau, *Arch. Biochem. Biophys.* **2000**, *379*, 137–146.
[34] S. M. Rubenstein, R. M. Williams, *J. Org. Chem.* **1995**, *60*, 7215–7223.
[35] J. Rinkel, J. S. Dickschat, *Org. Lett.* **2019**, *21*, 2426–2429.
[36] L. Lauterbach, J. Rinkel, J. S. Dickschat, *Angew. Chem. Int. Ed.* **2018**, *57*, 8280–8283; *Angew. Chem.* **2018**, *130*, 8412–8415.
[37] F. M. Hahn, A. P. Hurlburt, C. D. Poulter, *J. Bacteriol.* **1999**, *181*, 4499–4504.
[38] P. Rabe, J. Rinkel, E. Dolja, T. Schmitz, B. Nubbemeyer, T. H. Luu, J. S. Dickschat, *Angew. Chem. Int. Ed.* **2017**, *56*, 2776–2779; *Angew. Chem.* **2017**, *129*, 2820–2823.
[39] J. W. Cornforth, R. H. Cornforth, G. Popjak, L. Yengoyan, *J. Biol. Chem.* **1966**, *241*, 3970–3987.
[40] A. Mendoza, Y. Ishihara, Phil S. Baran, *Nat. Chem.* **2012**, *4*, 21–25.
[41] Z. Quan, J. S. Dickschat, *Org. Biomol. Chem.* **2020**, *18*, 6072–6076.
[42] P. Rabe, L. Barra, J. Rinkel, R. Riclea, C. A. Citron, T. A. Klapschinski, A. Janusko, J. S. Dickschat, *Angew. Chem. Int. Ed.* **2015**, *54*, 13448–13451; *Angew. Chem.* **2015**, *127*, 13649–13653.
[43] J. Rinkel, L. Lauterbach, J. S. Dickschat, *Angew. Chem. Int. Ed.* **2019**, *58*, 452–455; *Angew. Chem.* **2019**, *131*, 461–465.
[44] A. Hou, J. S. Dickschat, *Angew. Chem. Int. Ed.* **2020**, *59*, 19961–19965; *Angew. Chem.* **2020**, *132*, 20135–20140.
[45] Z. Quan, J. S. Dickschat, *Org. Lett.* **2020**, *22*, 7552–7555.
[46] S. Basar, A. Koch, W. A. König, *Flavour Fragrance J.* **2001**, *16*, 315–318.
[47] A. J. Birch, W. V. Brown, J. E. R. Corrie, B. P. Moore, *J. Chem. Soc. Perkin Trans. 1* **1972**, 2653–2658.
[48] J. D. Hernandez-Hernandez, L. U. Roman-Marin, C. M. Cerda-Garcia-Rojas, P. Joseph-Nathan, *J. Nat. Prod.* **2005**, *68*, 1598–1602.
[49] H. A. Garcia-Gutierrez, C. M. Cerda-Garcia-Rojas, J. D. Hernandez-Hernadez, L. U. Roman-Marin, P. Joseph-Nathan, *Phytochemistry* **2008**, *69*, 2844–2848.
[50] M. Kobayashi, K. Osabe, *Chem. Pharm. Bull.* **1989**, *37*, 631–636.
[51] A. Meguro, T. Tomita, M. Nishiyama, T. Kuzuyama, *ChemBioChem* **2013**, *14*, 316–321.
[52] T. Tokiwano, E. Fukushi, T. Endo, H. Oikawa, *Chem. Commun.* **2004**, 1324.
[53] L. Zhang, B. Zhang, A. Zhu, S. H. Liu, R. Wu, X. Zhang, Z. Xu, R. X. Tang, H. M. Ge, *Angew. Chem. Int. Ed.* **2023**, *62*, e202312996; *Angew. Chem.* **2023**, *135*, e202312996.
[54] C. Li, S. Wang, X. Yin, A. Guo, K. Xie, D. Chen, S. Sui, Y. Han, J. Liu, R. Chen, J. Dai, *Angew. Chem. Int. Ed.* **2023**, *62*, e202306020; *Angew. Chem.* **2023**, *135*, e202306020.
[55] H. Li, J. S. Dickschat, *Org. Chem. Front.* **2022**, *9*, 795–801.
[56] H. Li, J. S. Dickschat, *Angew. Chem. Int. Ed.* **2022**, *61*, e202211054; *Angew. Chem.* **2022**, *134*, e202211054.
[57] H. Li, J. S. Dickschat, *Chem. Eur. J.* **2024**, *30*, e202303560.
[58] Y. J. Hong, D. J. Tantillo, *Org. Lett.* **2006**, *8*, 4601–4604.
[59] J.-Y. Liu, F.-L. Lin, K. A. Taizoumbe, J.-M. Lv, Y.-H. Wang, G.-Q. Wang, G.-D. Chen, X.-S. Yao, D. Hu, H. Gao, J. S. Dickschat, *Angew. Chem. Int. Ed.* **2024**, *63*, e202407895; *Angew. Chem.* **2024**, *136*, e202407895.
[60] T. Toyomasu, M. Tsukahara, H. Kenmoku, M. Anada, H. Nitta, J. Ohkanda, W. Mitsuhashi, T. Sassa, N. Kato, *Org. Lett.* **2009**, *11*, 3044–3047.

Manuscript received: November 22, 2024
Accepted manuscript online: January 3, 2025
Version of record online: January 10, 2025

Chapter 12

List of Publications

1. H. Li, K. Yang, Z. Yin, B. Goldfuss, J. S. Dickschat, *Angew. Chem. Int. Ed.* **2025**, *64*, e202517373.
2. H. Li, P. Troycke, Z. Yin, M. Groll, J. S. Dickschat, *J. Am. Chem. Soc.* **2025**, *147*, 34901-34909.
3. H. Li, Z. Bai, G. B. Tabekoueng, B. Xing, B. Goldfuss, M. Ma, D.-H. Yang, J. S. Dickschat, *ACS Catal.* **2025**, *15*, 6209-6215.
4. H. Li, B. Goldfuss, J. S. Dickschat, *Chem. Eur. J.* **2025**, *31*, e202500712.
5. H. Li, B. Goldfuss, J. S. Dickschat, *Angew. Chem. Int. Ed.* **2025**, *64*, e202422788.
6. G. B. Tabekoueng, H. Li, B. Goldfuss, G. Schnakenburg, J. S. Dickschat, *Angew. Chem. Int. Ed.* **2024**, *63*, e202413860.
7. H. Xu, H. Li, B. Goldfuss, G. Schnakenburg, J. S. Dickschat, *Angew. Chem. Int. Ed.* **2024**, *63*, e202412040.
8. H. Struwe*, H. Li*, F. Schrödter, L. Höft, J. Fohrer, J. S. Dickschat, A. Kirschning, *Org. Lett.* **2024**, *26*, 5888-5892.
9. H. Li, B. Goldfuss, J. S. Dickschat, *ChemComm.* **2024**, *60*, 7041-7044.
10. H. Li, J. S. Dickschat, *Chem. Eur. J.* **2024**, *30*, e202303560.
11. K. Schell, H. Li, L. Lauterbach, K. A. Taizoumbe, J. S. Dickschat, B. Hauer, *ACS Catal.* **2023**, *13*, 5073-5083.
12. H. Li, J. S. Dickschat, *Angew. Chem. Int. Ed.* **2022**, *61*, e202211054.
13. H. Li, J. S. Dickschat, *Org. Chem. Front.* **2022**, *9*, 795-801.
14. J. Xu, K. Zhang, H. Cao, H. Li, F. Cheng, C. Cao, Y.-P Xue, Y.-G Zheng, *Biocatal. Biotransform.* **2021**, *39*, 190-197.
15. F. Cheng, H. Li, K. Zhang, Q.-H Li, D. Xie, Y.-P Xue, Y.-G Zheng, *J. Biotechnol.* **2020**, *312*, 35-43.
16. F. Cheng, H. Li, D.-Y Wu, J.-M Li, Y.-Fan, Y.-P Xue, Y.-G Zheng, *Green Chem.* **2020**, *22*, 6815-6818.
17. D.-C Wang, H. Li, S.-N Xia, Y.-P Xue, Y.-G Zheng, *Catal. Sci. Technol.* **2019**, *9*, 1961-1969.

Chapter 13

Abstract

This cumulative doctoral dissertation “The Investigations on Diterpene Biosynthesis through Substrate and Protein Engineering” concentrates on diterpene biosynthesis from various aspects, including non-natural biotransformation, genome mining, mechanistic study and enzyme engineering.

First, seven geranylgeranyl diphosphate (GGPP) analogs named *iso*-GGPPs, were synthesized chemically or enzymatically, of which double bonds were replaced by various modified methylene groups, leading to novel reactivities. The subsequent biotransformations with almost 20 characterized diterpene synthases resulted in the isolation of more than 50 non-natural diterpenes featuring novel terpene skeletons. Among them, some compounds can be regarded as the derailment products in the cyclization cascade, while others are generated from distinct cyclization modes in comparison to its natural counterparts. Apart from that, four isotope labelled substrate analogs were stereoselectively synthesized and used in the enzymatic conversions to determine the absolute configurations of isolated non-natural diterpenes. Second, two new fungal terpene synthases were also functionally characterized after bioinformatic analysis, gene cloning and protein expression, whose products were well-investigated for understanding their formations through isotopic labelling experiments. Third, two previously reported diterpenes, benditerpe-2,6,15-triene and venezuelaene A, with tentative biosynthetic proposals presented in the original works, were investigated for the hydride shifts in their biosynthesis through isotopic labelling studies, non-natural biotransformations, product derivations and DFT calculations. In addition, site-directed mutagenesis studies in conjunction with molecular docking on spata-13,17-diene synthase and selina-4(15),7(11)-diene synthase disclosed the function of a specific hydrophobic tunnel in these two enzymes, which enable evolving the second enzyme from a sesquiterpene synthase to a diterpene synthase. Last but not least, the well-known diterpene taxa-4,11-diene was addressed in this thesis. Unique long-proton migrations were observed in the biosynthesis of taxaxenene and cyclophomactene, two compounds generated from a non-natural enzymatic conversion with wild type taxadiene synthase and an enzyme variant, respectively.

All in all, this doctoral dissertation provides novel insights into the terpene field. The combination of various strategies enabled the discovery of novel terpenes and mechanistic investigations of utilized enzymes, which will be described in detail in this thesis.